Life cycle cost optimization of reinforced concrete structures

Lara Saad

N° d'ordre : D.U. : 2692
EDSPIC : 755

Université BLAISE PASCAL – Clermont Ferrand II
École Doctorale
Sciences Pour l'Ingénieur

Université Saint-Joseph
Ecole Supérieure d'Ingénieurs de Beyrouth

Thèse

Présentée par

Lara SAAD

Ingénieur de l'ESIB
en vue d'obtenir le grade de :

Docteur d'Université

Spécialité : Matériaux, Structures, Fiabilité

Optimisation du coût de cycle de vie des structures en béton armé

Soutenue publiquement le 9 Mai 2016 devant le jury :

Rapporteurs :		
	Frank SCHOEFS	Université de Nantes
	André ORCESI	IFSTTAR
Examinateurs :		
	Fadi GEARA	Université Saint-Joseph
	M. Asem ABDUL-MALAK	American University of Beirut
	Fadi HAGE CHEHADE	Université Libanaise
Membres invités :		
	Charles MALEK	Dar al-Handasah
	Rafic FADDOUL	Université Saint-Joseph
Directeurs de thèse :		
	Alaa CHATEAUNEUF	Université Blaise Pascal
	Wassim RAPHAEL	Université Saint-Joseph

This page is intentionally left blank

Life cycle cost optimization of reinforced concrete structures

by

Lara SAAD

A thesis submitted in partial fulfillment
of the requirements for the degree of
Doctor of Philosophy
(Structural Engineering)
2016

Blaise Pascal University
Saint-Joseph University

This page is intentionally left blank

Acknowledgement

First of all, I would like to express my appreciation to my advisor Prof. Alaa Chateauneuf for his guidance, endless patience, continuous support throughout my Ph.D. pursuit and for providing me the opportunity to coauthor two papers for publication in reputable scientific journals. I am thankful for his patience, for his tolerance to my special personal circumstances, and for his frequent guidance that kept me on track.

I would also want to thank my advisor Prof. Wassim Raphael for his assistance, insightful comments, continuous encouragement and trust. Without his precious support, it would not have been possible to conduct this research.

I gratefully acknowledge the support by grants from (a) Conseil national de la recherche scientifique, république libanaise (CNRS), (b) Conseil de la recherche à l'USJ, and (c) Polytech-Clermont Ferrand – Université Blaise Pascal.

I would like to thank my former colleague Dr. Amina Aissani for her contributions to parts of this study. I also thank Dr. Rafic Faddoul for his constructive discussions and comments to improve this study.

Finally and most importantly, I am sincerely grateful to my husband Mohammad Jaber, my parents Abbas and Nawal, and my sisters May and Hala for their love, support, patience, and understanding.

This page is intentionally left blank

Résumé

Les structures de génie civil, en particulier les ponts en béton armé, doivent être conçues et gérées pour assurer les besoins de transport et de communication dans la société. Il est indispensable de garantir un fonctionnement convenable et sécuritaire de ces structures, puisque les défaillances peuvent conduire à des perturbations du transport, des pertes catastrophiques de concessions et des pertes de vies humaines, avec des impacts économiques, sociétaux et environnementaux graves, à court et à long termes. Les gestionnaires entreprennent diverses activités pour maintenir la performance et le fonctionnement adéquat à long terme, tout en satisfaisant les contraintes financières et sécuritaires. Idéalement, ils peuvent recourir à des techniques d'optimisation pour établir les compromis entre la réduction du coût du cycle de vie (LCC) et la maximisation de la durée de vie. Cela nécessite le développement de l'analyse du cycle de vie, de l'analyse de fiabilité et de l'optimisation structurale.

Les approches actuelles pour la conception et la gestion des structures s'appuyant sur l'analyse du coût de cycle de vie, montrent les besoins suivants : (1) une approche intégrée et systématique pour modéliser de façon cohérente les processus de dégradation, les charges de trafic, le vieillissement et les conséquences directes et indirectes de la défaillance, (2) une considération complète des dépendances économiques, structurales et stochastiques entre les différents éléments de l'ouvrage, (3) une approche permettant de modéliser efficacement un système structural formé de plusieurs éléments interdépendants, (4) une évaluation des conséquences de la dégradation et de la redistribution des charges entre les éléments en tenant compte de la redondance du système et de la configuration de l'ouvrage, (5) une méthode d'optimisation de la conception et de la maintenance qui préserve l'exigence de fiabilité tout en considérant la robustesse de la décision.

L'objectif global de cette thèse est de fournir des procédures améliorées qui peuvent être appliquées à la conception et à la gestion fiabilistes et robustes des ouvrages en béton armé, en réduisant les coûts supportés par les gestionnaires et les utilisateurs, tout en tenant compte des dépendances entre les éléments.

Dans la première partie de cette thèse, une synthèse bibliographique concernant les procédures de la conception et de la maintenance basée sur des calculs fiabilistes est présentée, et les différents composants du LCC sont développés.

Ensuite, une approche est proposée pour la conception des ouvrages en tenant compte du coût aux usagers et en intégrant dans la fonction du coût de cycle de vie. Le modèle couplé corrosion-fatigue est aussi considéré dans l'optimisation de la conception.

La planification de la maintenance des ouvrages est ensuite développée, en considérant les différents types d'interaction entre les éléments, en particulier les dépendances économiques, structurales et stochastiques. Ce modèle utilise l'analyse de l'arbre de défaillance et les probabilités conditionnelles pour tenir compte des dépendances dans la planification de la maintenance. Les conséquences de la dégradation et de la redistribution des charges sont prises en compte dans l'approche proposée. Par ailleurs, une méthode pratique de calcul de la fiabilité d'un système formé de plusieurs composantes interdépendantes est proposée, à travers un facteur de redondance calculé par la modélisation mécanique.

Enfin, une nouvelle procédure d'optimisation est proposée, permettant de tenir compte des incertitudes dans le système et la capacité structurale de s'adapter aux variabilités intrinsèques. La procédure proposée tient compte des incertitudes et de la variabilité dans une formulation cohérente, validée au moyen des applications numériques.

Les approches proposées dans ce travail offrent des outils d'aide à la décision pour la conception et la gestion optimales et robustes des structures en béton armé, en tenant compte des incertitudes, de la variabilité et de l'interaction entre les éléments, ainsi que des différentes conséquences directes et indirectes de la défaillance.

Mots-clés : analyse du coût du cycle de vie, coûts aux usagers, dégradation, dépendance économique, dépendance structurale, dépendance stochastique, probabilité de défaillance, conception fiabiliste, conception robuste, optimisation.

Abstract

Civil engineering structures, particularly reinforced concrete bridges, should be designed and managed to ensure the society needs. It is crucial to assure that these structures function properly and safely as damage during the service life can lead to transport disturbance, catastrophic loss of property, causalities, as well as severe economic, social, and environmental impacts, in addition to long term consequences. Decision-makers adopt various activities to maintain adequate long-term performance and functionality while satisfying financial constraints. Ideally, they may employ optimization techniques to identify the trade-offs between minimizing the life-cycle cost (LCC) and maximizing the expected service life. This requires the development of three challenging chores: life cycle analysis, reliability analysis and structural optimization.

The current approaches for the design and management of structures through a Life-cycle cost analysis (LCCA) highlight the following needs: (1) an integrated and systematic approach to model coherently the deterioration processes, the increasing traffic loads, the aging and the direct and indirect consequences of failure, (2) a mutual consideration of economic, structural and stochastic dependencies between the elements of a structural system, (3) an adequate approach for the deterioration dependencies and load redistribution between the elements, (4) an improvement of system reliability computation as a function of the structural redundancy and configuration that can take into account the dependencies between the elements, (5) a consideration of design and maintenance optimization procedures that focus coherently on the robustness of the management decision and on the satisfaction of reliability requirements.

The overall objective of this study is to provide improved LCCA and procedures that can be applied to select optimal and robust design and maintenance decisions regarding new and existing reinforced concrete structures, by minimizing both manager and user costs, while providing the required safety along the structure lifetime, taking into account the most severe degradation processes and the dependencies between structural elements.

In the first part of this thesis, a literature review concerning the current probabilistic design and maintenance procedures is presented, and the LCC components are discussed.

Then, a new approach is developed to evaluate the user delay costs on a reinforced concrete bridge structure, based on direct and indirect costs related to degradation and failure, and to integrate it to the life cycle cost function, in order to allow for probabilistic design. In addition, the coupled corrosion-fatigue model is considered in the design optimization.

Afterward, a structural maintenance planning approach is developed to consider the three types of interactions, namely economic, structural and stochastic dependencies. The proposed model uses fault tree analysis and conditional probabilities to reflect the dependencies in the maintenance planning. The consequences of degradation are evaluated and a method is proposed to account for the load redistribution. Moreover, a practical formulation for quantifying the reliability of a system formed of interrelated components is proposed, by the mean of a redundancy factor that can be computed by finite element analysis.

Finally, a new optimization procedure is proposed, by taking into account the uncertainties in the analysis, and the structural ability to adapt to variability, unforeseen actions or

deterioration mechanisms. The proposed procedure takes account of uncertainties and variability in one consistent formulation, which is shown through numerical applications.

The proposed approaches can provide helpful tools for decision-makers in selecting optimal and robust design and maintenance decisions for civil engineering structures by considering the uncertainty, the variability and the interaction between the elements, as well as the direct and indirect consequences of failure.

Keywords: Life-cycle cost analysis, user cost, degradation, economic dependency, structural dependency, stochastic dependency, probability of failure, reliability-based design, robust design, optimization.

Contents

List of notations

This list is given by order of appearance in the thesis.

R	Resistance
L	Load
$g(\cdot)$	Limit state function
$F_R(\cdot)$	Cumulative distribution function of the resistance
$f_L(\cdot)$	Probability density function of the load
P_{fi}	Cumulative probability of failure for the i^{th} limit state
μ_g	Mean of $g(\cdot)$
σ_g	Standard deviation of $g(\cdot)$
$\Phi(\cdot)$	Cumulative normal distribution function
$\mathscr{R}$	Reliability: probability of survival
β	Reliability index
$P_{f,system}$	System probability of failure
$P_r(E)$	Probability of occurrence of an event E
$E_j \bigcap E_i$	Intersection of failure modes i and j
ρ_{ij}	Correlation coefficient between modes i and j
C_T	Total cost
C_{ini}	Initial cost
C_{QA}	Cost of quality assurance
C_{Ins}	Cost of inspections
C_M	Maintenance cost
C_F	Expected life-cycle failure cost
C_{DC}	Direct failure costs
C_{IC}	Indirect failure costs
C_D	Cost of disposal
C_{PV}	Present value cost
v	discount rate
C_{fi}	Failure cost associated with limit state i
δt_{insp}	Interval of inspections
δ_{Repair}	Interval of maintenance actions
N_{insp}	Number of inspections
L_T	Lifetime
P_f^T	Admissible probability of failure
P_f^R	Predefined threshold for repair
$P_{f_0}^R$	Repair criterion below which repair occurs at every inspection
A_s^*	Optimal reinforcement area
C_U	User cost
C_{DT}	Cost of delay time
C_{VO}	Vehicle operating cost

C_{CR}	Accident costs
S_a	Traffic speed during bridge work activity
S_n	Normal traffic speed
N_{rw}	Number of days of road work
w	Hourly time value of drivers
r	Hourly vehicle operating cost
c_a	Cost per accident
A_a	During-construction accident rate per vehicle-kilometer
A_n	Normal accident rate per vehicle-kilometer
$AvSali$	Average salary of travelers
p_{ij}	Proportion of travelers with profession j in vehicle i
M_{GWj}	Mean gross wage of profession
E_j	Distribution of the actual labor force by employment category
C_{AF}	Cost of additional fuel consumption
C_{AM}	Cost of additional maintenance of the vehicle
P_{CUj}	Probability of occurrence of a user cost scenario j
γ_j	Boolean variable with the value of 1 if scenario j occurs
$C_{U\text{-}D}$	Degradation user cost
$C_{U\text{-}MR}$	Minor rehabilitation user cost
$C_{U\text{-}LR}$	Load rating user cost
$C_{U\text{-}C}$	Collapse user cost
t_{loss}	Time loss due to slowing the traffic flow
N	Number of vehicles
D_{add}	Additional distance of traveling
$V_{average}$	Average travel speed
N_{truck}	Number of trucks
$D_{add\text{-}truck}$	Additional distance traveled by trucks
$V_{average\text{-}truck}$	Average travel speed of trucks
t_{br}	Time needed for bridge replacement
$\mathcal{R}_i$	Reliability level specified by the designer
d_i^L	Lower bound of the design variables
d_i^U	Upper bound of the design variables
M_R	Bending capacity
M_a	Applied moment
M_G	Moment due to a permanent surface load G
f_y	Steel strength
f_c	Concrete Compression
c	Concrete cover
C_{th}	Threshold chloride concentration

C_s	Chloride concentration
D_c	Coefficient of diffusion
d_0	Initial steel bas diameter
n	Number of bars
E_s	Elastic modulus of steel
h^*	Optimal deck height
C_T^*	Optimal total life-cycle cost
d*	Optimal values of the design variables
τ_{ini}	Time to corrosion initiation
τ_{pn}	Time to pit nucleation
τ_{pt}	Time of pit-to-crack transition
τ_{cg}	Time to crack growth
τ_l	Collapse time
a_0	Pit depth at τ_{pt}
a_1	Crack size at critical stress
a_c	Critical crack size at failure
wc	Water/cement ratio
i_{th}	Threshold corrosion rate
f	Traffic frequency
G	Dead Load
Q	Punctual design Load
d_i	Degradation of a component *i*
$d_{ip,k}$	Proper degradation of i^{th} component under k^{th} mechanism
d_{i0}	Initial degradation of component *i*
d_{iF}	Degradation limit before failure
$d_{serv,j,k}$	Service limit degradation of component *j* for k^{th} mechanism
P_{fi}	Probability of failure of component *i* due to the degradation of the component itself
$P_{fi,d}$	Probability of failure of component *i* due to the degradation of the component itself and to all dependent components
$P_{i\|j}$	Probability of failure of component *i* knowing that component *j* has failed
$P_{S,i}$	Probability of survival of component *i*
$L_{i,0}$	Load initially supported by the element *i*
L_i	Load supported by the element *i* after the load redistribution
L_T	Total load supported by all the elements in the system
$\propto_{j,i}$	Coefficient that indicates the amount of the transferred load between elements *i* and *j*
$c_{i,j}$	Geometrical load redistribution coefficient
I_{redund}	Redundancy factor
$P_{f,parallel}$	Probability of failure of a parallel system

$P_{f,series}$	Probability of failure of a series system
G_{pu}	Group of components to be preventively repaired at an optimal scheduled time t_{ku}
C_d^p	Preventive degradation consequence
C_d^c	Corrective degradation consequence
C_{SD}^p	Preventive shutdown cost per unit time
C_{SD}^c	Corrective shutdown cost per unit time *i*
C_{SU}^p	Corrective setup cost
C_{SU}^c	Preventive setup cost
$C_{SI,l}^c$	Corrective setup cost for Setup Iem *l*
$C_{SI,l}^p$	Preventive setup cost for Setup Item *l*
w_i^p	Preventive non-zero maintenance downtimes
w_i^c	Corrective non-zero maintenance downtimes
C_{PM}	Cost of preventive maintenance
C_{CM}	Cost of corrective maintenance
$t_{M,j/i}^{c.AF}$	Time needed to repair an element *j* which has failed as a consequence of the failure of *i* due to stochastic dependency
$t_{M,i}^p$	Downtimes needed to preventively repair component *i*
$t_{M,i}^c$	Downtimes needed to correctively repair component *i*
$\Delta t_{MD,u\|i}$	Downtime needed to dismantle an item *u* which is MD on *i*
M_T	Total moment carried by the whole system
UL	Uniform Load
τ	Basic maintenance time
k_i	Integer multiplier of the basic maintenance time
τ_i	Maintenance time of component *i*
$M_{i\|j}$	Moment applied to *i* knowing that *j* has failed
$inc_{i\|j}$	Increase in the moment of *i* due to the failure of *j*
$f(.)$	Original objective function
$\tilde{f}(.)$	Desirability robustness objective
μ_f	Mean of the objective function
σ_f	Standard deviation of the objective function
μ_f^*	Normalization factors denoting the mean value of the objective function
σ_f^*	Normalization factors denoting the standard deviation of the objective function
α	Weighting factor
λ	Penalty factor
C_{T^*min}	Optimal cost corresponding to the unconstrained formulation

$P_f(d^*)$	Failure probability corresponding to the unconstrained formulation
$C_{T^*_{min}}$	Optimal cost corresponding to the unconstrained formulation
$C_{T,RBDO}$	Optimal cost corresponding to the RBDO formulation
$C_{T,RRBDO}$	Optimal cost corresponding to the RRBDO formulation
μ_{Pf}	Mean of the failure probability
σ_{Pf}	Standard deviation of the failure probability
λ_L	Local buckling factor
λ_G	Global buckling factor
I_U	Moment of inertia of the U-section
I_G	Moment of inertia of the column cross-section
C_{SFL}	Local failure cost
C_{SFG}	Global failure cost

List of abbreviations

This list is given by alphabetical order.

AASHTO	American association of state highway and transportation officials
ADT	Average daily traffic
ADTT	Average daily truck traffic
AF	Associated failure
BMS	Bridge management system
CDF	Cumulative distribution function
COV	Coefficient of variation
DDO	Deterministic design optimization
DOT	Department of transportation
EC2	Eurocode 2
ED	Economic and degradation dependencies
FE	Finite Element
FHWA	Federal highway administration
FORM	First order reliability method
GA	Genetic algorithm
HA	High bond
HL	Hasofer and Lind
ILO	International labor office
IS	Importance sampling
RBDO	Reliability-based design optimization
RC	Reinforced concrete
RDO	Robust design optimization
RRBDO	Robust formulation for reliability-based design optimization
LCC	Life-cycle cost
LCA	Life-cycle assessment
LCCA	Life-cycle cost analysis
LHS	Latin hypercube sampling
LRFD	Load and resistance factor design
MCS	Monte Carlo simulations
MD	Modularly dependent
MPP	Most probable point
PDF	Probability distribution function
PI	Performance Indicator
SD	Stochastic and degradation dependencies
SED	Stochastic, economic and degradation dependencies
SORM	Second order reliability method

UL	Uniformly distributed
WIM	Weight in motion

Synthèse des travaux

1 Contexte

Le développement de méthodes probabilistes pour la conception et la gestion des structures de génie civil implique plusieurs améliorations dans : (1) l'analyse du cycle de vie (LCCA), (2) la modélisation du système en tenant compte de la dépendance entre ses composants, (3) l'analyse de la fiabilité, et (4) l'optimisation structurale.

L'estimation du coût du cycle de vie d'une structure en béton armé est une tâche difficile, à cause de la complexité d'évaluation de ses composants, en particulier le coût de défaillance qui dépend de la dégradation avec le temps. De plus, de nombreuses incertitudes sont liées à la nature stochastique des paramètres de charges et de matériaux. En outre, les conséquences de la défaillance sont considérablement amplifiées par les impacts économiques, sociétaux et environnementaux. Pour cela, il est nécessaire de disposer d'une approche intégrée et systématique pour modéliser de façon cohérente les processus de dégradation, les charges, le vieillissement et les conséquences directes et indirectes de la défaillance.

Les approches actuelles pour la gestion des structures de génie civil s'appuyant sur l'analyse du coût de cycle de vie, ne permettent pas la considération complète et simultanée des dépendances économiques, structurales et stochastiques des éléments de l'ouvrage. La considération efficace de ces dépendances est une tâche très complexe qui dépend des différents chemins de charges possibles, de la configuration et la redondance de la structure. Pour cela, il est essentiel de développer une approche qui permet de modéliser un système formé de plusieurs éléments interdépendants, tout en évaluant les conséquences de la dégradation et de la redistribution des charges entre les éléments. Afin de pouvoir appliquer une optimisation fiabiliste, nous avons également besoin d'une méthode pour calculer la fiabilité d'un système en fonction de son degré de redondance. Par ailleurs, les dépendances doivent être considérées tout en garantissant la fiabilité requise au cours de la durée de vie de la structure dans un environnement de paramètres incertains.

La prise en compte des incertitudes dans l'optimisation de la conception et de la gestion des structures est très importante, mais il faut aussi considérer la variabilité. Dans cette thèse, le terme « variabilité » fait référence à une variation naturelle ou intrinsèque d'une certaine quantité, alors que le terme « incertitude » fait référence au degré de précision avec lequel une certaine quantité est estimée. La conception robuste (RDO) vise à trouver les réglages optimaux pour minimiser les coûts totaux en minimisant la variabilité de la performance ; il s'agit d'une méthode déterministe qui ne peut pas garantir la fiabilité de la structure. A l'opposé, la méthode d'optimisation basée sur la fiabilité (RBDO) ne contrôle pas la variabilité de la performance. Pour cela, une méthode d'optimisation de la conception et de la maintenance qui maintient le niveau de fiabilité tout en considérant la robustesse de la fonction objectif est indispensable.

2 Objectifs de la thèse

L'objectif global de cette thèse est de proposer des procédures cohérentes pour la conception et la gestion fiabilistes, optimales et robustes des structures en béton armé, en particulier les ponts,

en réduisant les coûts supportés par les gestionnaires et les utilisateurs, tout en tenant compte des dépendances entre les éléments.

Le premier objectif de la thèse est de proposer une méthode pour considérer les conséquences directes et indirectes de la défaillance lors de la conception des éléments de pont en béton armé. L'approche proposée a pour but d'analyser et d'évaluer les coûts indirects supportés par les usagers. De plus, la fiabilité des structures en béton armé soumises à un modèle de dégradation couplé corrosion-fatigue est évaluée. L'optimisation basée sur la fiabilité (RBDO) est utilisée pour définir la conception optimale en tenant compte des incertitudes dans les différents paramètres du problème.

Le second objectif est de proposer une évaluation du coût de maintenance des structures qui considère les différents types d'interaction entre les éléments, en particulier les dépendances économiques, structurales et stochastiques. Ce modèle utilise l'analyse de l'arbre de défaillance et les probabilités conditionnelles pour tenir compte des dépendances dans la planification de la maintenance. Les conséquences de la dégradation et de la redistribution des charges sont prises en compte dans l'approche proposée. Cette approche est appliquée à des exemples numériques pour montrer sa validité et sa fonctionnalité dans des cas pratiques.

Le troisième objectif de cette thèse est de proposer une formulation fiabiliste de l'optimisation qui permet de tenir compte de l'incertitude et de la variabilité dans une formulation mathématique cohérente. Une comparaison entre la formulation proposée et les procédures d'optimisation fiabiliste de la conception est effectuée pour la conception de plusieurs problèmes structuraux.

3 Conception probabiliste

La conception optimale d'une structure doit permettre de minimiser le coût du cycle de vie sans compromettre la sécurité. Différents types de coût doivent ainsi être estimés lors de l'évaluation du coût du cycle de vie (LCC) d'une structure. De plus, le couplage des phénomènes de dégradation mécanique et physico-chimique est nécessaire pour l'évaluation de la fiabilité de la structure. Dans ce contexte, l'optimisation de la conception basée sur la fiabilité (RBDO) peut être réalisée pour le LCC de la structure, en considérant les principaux processus de dégradation. Par ailleurs, l'évaluation des coûts totaux peut être améliorée en intégrant le coût aux usagers et les coûts directs et indirects liés à la dégradation et à la défaillance.

Le LCC vise à déterminer l'alternative d'investissement la plus efficace pour atteindre la conception optimale d'une structure. Un modèle général du LCC se compose des coûts suivants :

$$LCC = C_{ini} + C_{ins} + C_M + C_F + C_D \quad (1)$$

où C_{ini} est le coût initial, C_{ins} est le coût d'inspection, C_M est le coût de maintenance, C_F est le coût de défaillance et C_D est le coût de recyclage ou mise au rebut. Pour une certaine période d'analyse, le LCC peut être calculé par la somme de tous les coûts survenus au cours de *t* années, actualisées à la valeur du temps présent. Dans la première partie de la thèse qui se concentre sur l'optimisation de la conception des ouvrages, les coûts d'inspection et de maintenances sont négligés. Pour un temps *t*, le coût de défaillance peut être estimé en fonction des coûts

directs $C_{DC,i}$, et indirects $C_{IC,i}$, associés à l'état limite i. Dans ce document, le coût aux usagers, qui est dû à la fermeture d'une partie ou de l'ensemble du pont lors d'une défaillance ou d'une maintenance, sera considéré comme un coût indirect. Ainsi, $C_{IC,i}$ peut être estimé comme suit :

$$C_{IC,i} = C_{U,i} \times t_{bt,i} \tag{2}$$

où C_U est le coût aux usagers et t_{bt} est la période de blocage de la circulation. Si $P_{CU,i}$ est la probabilité d'occurrence d'un scénario qui requiert un coût aux usagers, le coût total associé à l'état limite *i* durant une période *t* sera :

$$C_T(t) = C_{ini} + C_{DC,i}\, P_{f,i}(t) + C_{IC,i}\, P_{CU,i} \tag{3}$$

Plusieurs scénarios peuvent augmenter le coût aux usagers. Dans ce travail, quatre scénarios sont considérés, à savoir : la dégradation $C_{U\text{-}D}$, la réhabilitation mineure $C_{U\text{-}MR}$, la limitation de tonnage $C_{U\text{-}LR}$ et l'effondrement $C_{U\text{-}C}$.

Les coûts aux usagers sont engagés par les utilisateurs publics du pont, dû à la congestion du trafic normal. Si le trafic augmente, le coût aux usagers peut être important, il est estimé comme suit :

$$C_U = C_{DT} + C_{VO} + C_{CR} \tag{4}$$

où C_U est le coût aux usagers, C_{DT} est le coût du temps de retard, C_{VO} est le coût d'exploitation des véhicules et C_{CR} est le coût des accidents. Le coût d'exploitation des véhicules C_{VO} est associé aux arrêts multiples pendant la conduite dans la file d'attente. Le coût d'exploitation comprend le carburant, l'huile de moteur, l'entretien et l'amortissement du prix des véhicules. C_{VO} peut être estimé comme suit :

$$C_{VO} = C_{AF} + C_{AM} \tag{5}$$

où C_{AF} est le coût de la consommation de carburant supplémentaire et C_{AM} est le coût de maintenance supplémentaire du véhicule.

Deux applications numériques ont été considérées pour optimiser la conception des éléments d'un pont, en tenant compte du coût aux usagers et de l'effet couplé de la corrosion et de la fatigue. Cet effet couplé de dégradation est considéré au moyen du modèle développé par Bastidas et al (2009). La fonction objectif à minimiser est le coût total d'un élément de pont.

L'approche de conception fiabiliste, explicité à la Figure 1, consiste en l'évaluation des coûts initiaux, des coûts aux usagers et des coûts de défaillance. Afin d'estimer le coût de défaillance, une évaluation de la durée de vie probabiliste est effectuée pour chaque application en utilisant la méthode fiabiliste du premier ordre (FORM) pour l'évaluation de la probabilité de défaillance. Après la formulation et l'évaluation du LCC, l'optimisation de la conception basée sur la fiabilité RBDO est appliquée pour obtenir la conception optimale d^* des éléments de la structure, et le coût total optimal C_T^*.

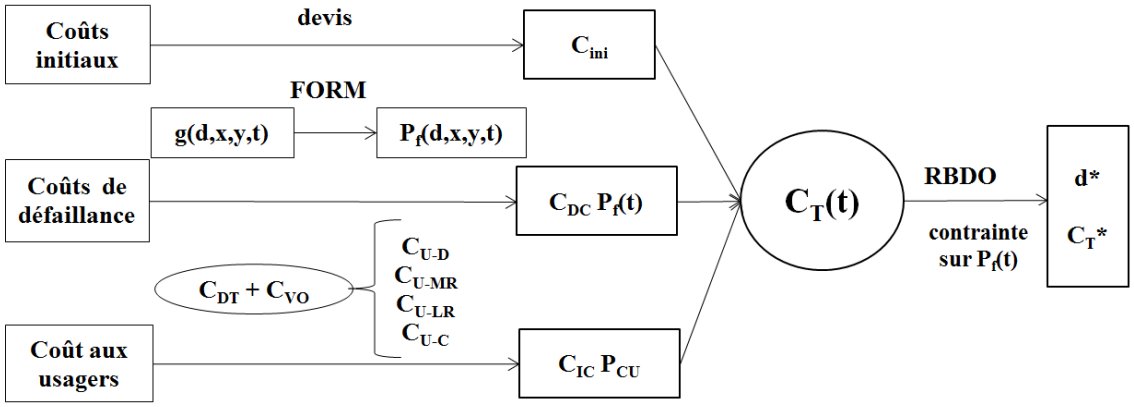

Figure 1 : Conception probabiliste.

Le coût aux usagers est analysé et évalué dans le cas actuel du Liban. Considérer les différents scénarios du coût aux usagers peut donner des résultats très différents. Parmi les résultats de l'exemple numérique, il s'est avéré que choisir de faire une réhabilitation mineure coûte 22% de moins en moyenne que de faire une politique de limitation de la charge autorisée sur le pont à l'ensemble agence-usager. Les résultats numériques ont également montré que la conception optimale d'un pont en béton armé est fortement affectée par les différents modèles de dégradation et par leur agressivité, par les propriétés des matériaux et leur contrôle de qualité, par les différents coûts pris en compte dans le calcul du cycle de vie de la structure, et par le niveau de fiabilité cible. Par conséquent, des améliorations continues apportées aux méthodes d'estimation des coûts et des données contribueront à accroître la précision des résultats dans le futur, où de nouveaux modèles de dégradation peuvent être considérés et des coûts indirects peuvent être mieux évalués.

4 Coût de maintenance des systèmes avec composants dépendants

L'optimisation du plan de maintenance des structures en béton armé est essentielle, puisque celles-ci vieillissent souvent plus rapidement que les fonds permettant leur remise en état. Une difficulté majeure survient du fait que la structure de génie civil est un système complexe composé de nombreux éléments interdépendants. Dans ce contexte, une méthode a été développée dans cette thèse pour la gestion des systèmes multi-composants en tenant compte de la dépendance stochastique, structurale et économique. La prise en compte de la dépendance entre les composants d'un système nécessite la considération simultanée des différents types de dépendance, et l'évaluation des coûts communs qui peuvent induire un groupement des interventions de maintenance. Dans la littérature, très peu de travaux traitent la dépendance structurale. Le système redondant peut être considéré sous la forme de « dépendance horizontale structurale ». Un autre inconvénient des modèles proposés dans la littérature réside dans la limitation aux systèmes en série ou en parallèle lors du calcul de la fiabilité du système, ce qui ne représente pas nécessairement la réalité.

Le coût total de maintenance du système le long d'un cycle est constitué des coûts de maintenance corrective $C^c_{M,T}$ et préventive $C^p_{M,T}$, des coûts de mise en place $C^c_{SU,T}$ et $C^p_{SU,T}$, des coûts d'arrêt du système $C^c_{SD,T}$ et $C^p_{SD,T}$, des conséquences monétaires des dégradations $C_{d,T}$ et du coût de défaillance directs et indirects $C_{F,T}$. Dans ce qui suit, l'indice T est utilisé pour

désigner « total » et l'indice *t* est utilisé pour désigner le « temps ». Nous écrivons ce coût total sous la forme :

$$E[C_T(t)] = C_{d,T}(t) + C^p_{M,T}(t) + C^p_{SU,T}(t) + C^p_{SD,T}(t) + C^c_{M,T}(t) + C^c_{SU,T}(t) + C^c_{SD,T}(t) + C_{F,T}(t) \quad (6)$$

Dans une structure de pont, la défaillance d'un élément peut conduire à la défaillance d'autres éléments. Pour cela, la probabilité de défaillance d'un élément s'écrit sous la forme suivante :

$$P_{fi,d}(t) = P_{fi}(t) + \sum_{j \neq i} P_{i|j}(t)\, P_{fj}(t) \quad (7)$$

où $P_{fi}(t)$ et $P_{fi,d}(t)$ sont respectivement la probabilité de défaillance intrinsèque due à la dégradation de l'élément *i*, et la probabilité de défaillance de l'élément *i* incluant la dépendance aux défaillances des éléments *j*. Cette formule est issue de l'arbre de défaillance tronqué au deuxième niveau $P_{i|j}(t)P_j(t)$. L'approximation définie par la relation ci-dessus est acceptable parce que les probabilités de défaillance sont très faibles en génie civil. De plus, les probabilités conditionnelles sont multipliées par la probabilité de défaillance du composant d'origine, ce qui diminue encore leurs valeurs. Cette probabilité vise à augmenter l'espérance des coûts de défaillance et de maintenance corrective liée aux éléments fortement dépendants. Pour illustrer cette probabilité, la Figure 2 représente un schéma de défaillance d'un système à deux composants b_1 et b_2 stochastiquement dépendants.

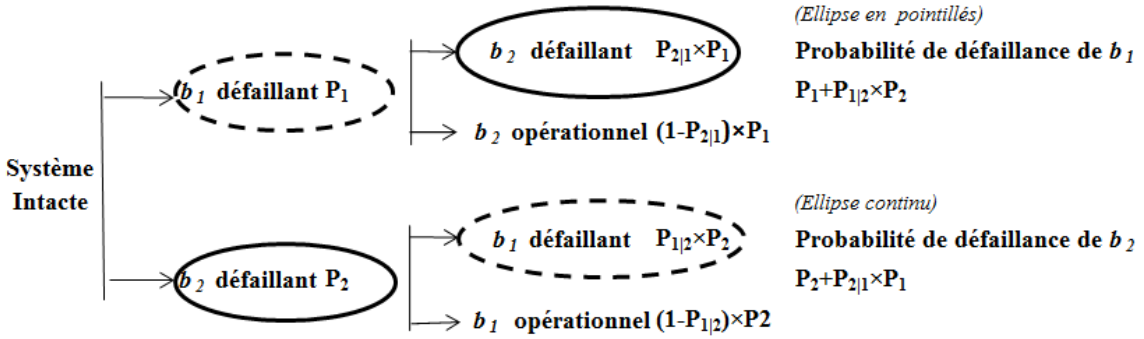

Figure 2 : Diagramme de défaillance pour deux composants.

Le coût total de maintenance corrective $C^c_{M,T}$ des composants du système qui ont subi une défaillance durant un cycle peut alors être formulé comme suit :

$$C^c_{M,T}(t) = \sum_i \left[C^c_{M,i} \left(P_{fi}(t) + \sum_{j \neq i} P_{i|j}(t)\, P_{fj}(t) \right) \right]$$
$$\text{avec} \quad \sum_i \left[\left(P_{fi}(t) + \sum_{j \neq i} P_{i|j}(t)\, P_{fj}(t) \right) \right] \leq 1 \quad (8)$$

où $C_{M,i}^{c}$ est le coût de maintenance corrective du composant *i*, $P_{fi}(t)$ est la probabilité de défaillance de *i* et $P_{i|j}(t)$ est la probabilité de défaillance de l'élément *i* sachant que l'élément *j* est défaillant.

Par ailleurs, la dégradation de l'élément *i* du système peut être accélérée par celle des éléments influents *j*, dû à la redistribution des charges de *j* vers *i*. La charge supportée par *i* sachant que tous les éléments du système sont dégradés peut être estimée par :

$$L_i(t) = L_{i,0}(t) + \sum_{j=1}^{q} \left(\propto_{j,i} L_{j,0}(t) \right) - \sum_{j=1}^{q} \left(\propto_{i,j} L_{i,0}(t) \right)$$

$$\text{avec } \sum_{i=1}^{q} L_i(t) = L_T \tag{9}$$

où $L_{i,0}$ est la charge initialement supportée par l'élément *i* avant le début de la dégradation des éléments du système, $\sum_{j=1}^{q} \left(\propto_{j,i} L_{j,0}(t) \right)$ est la charge supplémentaire supportée par l'élément *i* en raison de la dégradation des l'éléments *j* avec $1 \leq j \leq q \ \ (j \neq i)$, $\sum_{j=1}^{q} \left(\propto_{i,j} L_{i,0}(t) \right)$ est la perte de charge transférée à tous les éléments *j* en raison de la dégradation de l'élément *i* et $\propto_{j,i}$ (ou $\propto_{i,j}$) est une fonction qui indique la quantité de charge transférée de *j* vers *i* (ou de *i* ver *j*).

La dépendance économique peut être considérée par la prise en compte du coût de mise en place, lié aux coûts communs du système, tels que la mobilisation de l'équipe de réparation, les dispositions de sécurité, le transport, les équipements et outils, etc. Ces coûts peuvent être financés une seule fois pour la maintenance de plusieurs éléments si leur maintenance est regroupée en même temps. Une réduction des fonds peut être calculée en fonction de la probabilité que le coût d'un équipement soit inclus dans le coût de mise en place total de l'élément réparé, sachant que ce même équipement peut être utilisé pour la maintenance d'un autre élément. Lors du groupement des actions de maintenance, la réduction des fonds est d'autant plus importante lorsque cette probabilité d'utiliser les mêmes équipements pour la maintenance de plusieurs éléments est importante.

La dépendance structurale peut être horizontale ou modulaire. La dépendance horizontale peut être décrite comme le lien structural entre les différents éléments en série, en parallèle ou en configuration k-parmi-n. La dépendance modulaire signifie que certains composants doivent être démontés afin de réparer d'autres composants, et ils cessent donc de fonctionner pendant toute la durée de la réparation. La dépendance structurale ne peut être modélisée qu'en tenant compte des temps d'arrêt nécessaires pour la réparation ou pour démonter les composants liés entre eux. Les conséquences monétaires de ces arrêts peuvent être obtenues en multipliant le coût unitaire de fermeture de la structure (la suspension du pont ou d'une voie) par le temps d'arrêt nécessaire pour la réparation.

Par ailleurs, l'optimisation de la conception basée sur la fiabilité RBDO est appliquée pour définir la planification optimale de la maintenance tout en minimisant le coût total de maintenance du système le long d'un cycle. Dans le cas d'un système redondant, l'estimation de la probabilité de défaillance du système $P_{f,system}$ est régie entre autres par : (1) les dépendances complexes entre les différents composants et sous-systèmes, (2) les différents chemins de

charge possibles, et (3) le niveau de ductilité de chaque composant. Par conséquent, nous proposons d'introduire un facteur de redondance I_{redund} de telle sorte que :

$$P_{f,system} = (1 - I_{redund})\, P_{f,series} + I_{redund}\, P_{f,parallel} \quad (10)$$

où I_{redund} est fonction de l'architecture du système et de la corrélation entre ses composantes. I_{redund} peut être exprimé en fonction d'un coefficient $c_{i,j}$ qui indique la quantité de charge transférée entre les éléments *i* et *j*, en fonction de la configuration du système, de la ductilité et de la rigidité de chaque composant. Ce même facteur peut être utilisé dans l'estimation de $\propto_{j,i}$ utilisé dans la fonction de redistribution des charges. Par conséquent, le coefficient $c_{i,j}$ peut être estimé par analyse mécanique (e.g théorie des structures, méthode des éléments finis), à l'aide de la méthode d'estimation détaillée dans cette thèse.

Le modèle proposé est validé sur quatre applications numériques, à savoir, deux poutres en parallèle, deux poutres en série, un système formé d'une dalle avec une couche bitumineuse et une superstructure de pont. Les applications numériques ont permis de formuler les observations suivantes :

- la dépendance économique induit le groupement des actions de maintenance ; en conséquence, négliger la dépendance économique conduit à des planifications plus coûteuses allant jusqu'à 25% dans les applications traités ; cette observation a été constatée pour toutes les applications sauf celle du système dalle-bitume, car ces deux éléments ont des probabilités de défaillance intrinsèques très différentes ;
- la dépendance stochastique conduit à des intervalles de maintenance plus petits lorsque la probabilité cible du système est faible ; ainsi, négliger la dépendance stochastique peut conduire à une planification non fiable (e.g. le temps de maintenance optimal est réduit de 4% pour les deux poutres en parallèle et de 2% pour le système dalle-bitume) ; pourtant, ce résultat n'est pas très prononcé lorsque la probabilité cible du système est élevée (e.g. lorsque $P_f^T > 10^{-3}$ pour deux poutres en série, la solution optimale ne change pas avec la dépendance stochastique) ;
- pour des probabilités de défaillance élevées, la dépendance économique a le plus grand effet sur le coût de maintenance (e.g. pour deux poutres en série, la solution optimale coûte 40% de moins à cause du groupement lorsque $P_f^T > 10^{-3}$) ;
- pour les faibles probabilités de défaillance, la dépendance stochastique a le plus grand effet sur le coût de maintenance (e.g. la solution optimale coûte 6% plus cher dans le cas des deux poutres en série et 9% plus cher dans le cas du système dalle-bitume lorsque $P_f^T < 10^{-4}$) ;
- la dépendance stochastique a le plus grand effet sur la planification de la maintenance lorsque la défaillance d'un élément induit automatiquement la défaillance des autres (dans le cas du système dalle-bitume, la défaillance de la dalle induit celle du bitume avec une probabilité conditionnelle $P_{bitume|dalle} = 1$);
- pour une fiabilité cible très élevée, le temps optimal de maintenance devient égal au temps d'initiation de la dégradation pour l'exemple des deux poutres en parallèle.

- considérer simultanément les dépendances stochastiques, économiques et de dégradation dans l'exemple de la superstructure du pont induit au groupement des actions de maintenance, mais à des intervalles de temps plus petits ;
- les conséquences de la dégradation et la dépendance stochastique ont un effet comparable sur les résultats, qui favorise la politique prévention vis-à-vis de la dégradation et de la défaillance en minimisant l'intervalle de maintenance. Pourtant, le coût de dégradation accentue la forme convexe du coût total au cours du temps, ce qui rend la solution indépendante de la contrainte cible lorsque cette contrainte est faible (e.g. pour les deux poutres en parallèle, la solution est indépendante de P_f^T lorsque $P_f^T > 1{,}71 \times 10^{-4}$).

5 Formulation robuste de l'optimisation fiabiliste du LCC

Une formulation robuste de l'optimisation fiabiliste de la conception (RRBDO) est développée, dans le but de combiner les avantages de l'optimisation fiabiliste (RBDO) et de l'optimisation robuste (RDO). La RRBDO proposée tient compte de l'incertitude et de la variabilité simultanément. Dans cette formulation la variabilité fait référence à une variation naturelle ou intrinsèque d'une certaine quantité, et l'incertitude fait référence au degré de précision avec lequel une certaine quantité est évaluée ou mesurée. La formulation RRBDO proposée fournit un cadre général dans lequel le lien entre la RBDO et la RDO est clairement établi, à travers la définition du domaine d'application pour chacune des deux approches et la spécification adaptée des contraintes d'optimisation. L'avantage de la RRBDO par rapport à la formulation actuelle est démontré du point de vue conceptuel et numérique.

En effet, la contrainte de fiabilité dans la formulation RBDO permet de prendre en compte les incertitudes liées aux paramètres structuraux. Cependant, une mauvaise spécification de la probabilité de défaillance admissible conduit à une solution qui satisfait les conditions d'optimalité et les contraintes de fiabilité, mais pas les exigences de robustesse. Cet inconvénient rend la solution très sensible au choix des paramètres probabilistes d'entrée ; elle est donc inappropriée pour une utilisation pratique en ingénierie. La RBDO ne permet pas de garantir une solution robuste, car une grande partie des incertitudes ne peut être prédite ou identifiée dans l'ingénierie pratique. Parmi ces incertitudes, nous pouvons mentionner les coûts de défaillance directs et indirects qui sont souvent très difficiles à estimer avec précision, la probabilité de défaillance admissible qui doit être spécifiée en fonction de la précision des données d'entrée, et les modèles physiques et probabilistes impliqués. Il est donc nécessaire de développer une méthodologie plus cohérente pour la prise de décision optimale en considérant les incertitudes et les variabilités.

La variabilité traduit la variation incontrôlable de la fonction de performance qui peut entrainer la dégradation de la qualité du produit et peut compromettre la faisabilité de la conception. L'effet de ces variables incontrôlables sur la fonction de performance peut être réduit par le choix des variables de conception. Par conséquent, il est nécessaire d'identifier les valeurs des paramètres contrôlables (tels que les dimensions d'une section d'une poutre) qui minimisent les effets négatifs des phénomènes incontrôlables (tels que l'humidité ou la vitesse de corrosion). Dans ce contexte, l'optimisation de la conception robuste (RDO) vise à trouver

les paramètres optimaux pour minimiser les coûts totaux en minimisant la variation de la performance, afin de trouver une conception cohérente et de meilleure qualité.

Bien que l'optimisation robuste permet de réduire la variance de la performance, elle présente de nombreux inconvénients : (1) elle ne permet pas de garantir le niveau de fiabilité souhaité, (2) elle peut présenter des difficultés dans le cas des fonctions objectifs non convexes, (3) la réduction de la variance de la performance structurale est souvent réalisée au détriment de sa valeur moyenne, (4) les résultats obtenus n'indiquent pas exactement quel paramètre a l'effet le plus élevé sur la valeur caractéristique de la performance, (5) la RDO est une méthode déterministe. En effet, les deux paramètres : moyenne et variance peuvent diverger, et le concepteur doit choisir une conception structurale réalisable sur l'ensemble des optima obtenus avec différents facteurs de pondération pour la fonction objectif.

Dans ce contexte, une procédure d'optimisation fiable, qui peut surmonter les inconvénients des deux méthodes d'optimisation est développée dans ce travail. L'augmentation de la valeur moyenne qui est habituellement observée dans la conception robuste est limitée dans cette formulation. Les conditions d'optimalité de la formulation proposée visent à équilibrer, non seulement la moyenne et l'écart-type de la fonction objectif, mais aussi la dispersion de l'espérance du coût de défaillance. En conséquence, la solution obtenue est stable et moins sensible aux variations par rapport aux formulations classiques. Les avantages de la méthode d'optimisation proposée sont les suivants : (1) la sensibilité de la fonction objectif est réduite par rapport à la formulation RBDO classique, (2) l'effet des variables aléatoires incontrôlables sur la performance structurale est réduit, (3) la tolérance de se conformer aux actions imprévues ou à des mécanismes de dégradation est contrôlée, (4) le niveau de fiabilité prescrit est assurée.

La formulation robuste de l'optimisation fiabiliste de la conception (RRBDO) est exprimée pour le coût total de la structure comme suit :

$$
\begin{aligned}
&\text{Trouver} && \boldsymbol{d}, && \\
&\text{minimisant} && \tilde{f} = \frac{(1-\alpha)\mu(C_T(X,d))}{\mu^*_{C_T}} + \frac{\alpha\sigma(C_T(X,d))}{\sigma^*_{C_T}}, && (0 < \alpha < 1) \\
&\text{avec} && C_T(X,d) = C_{\text{ini}}(X,d) + \textstyle\sum_{j=1}^{m} C_{fj}\, P\left[g_j\,(X,d) \le 0\right], && \\
&\text{soumis à} && \frac{\mu(g_j(X,d))}{\sigma(g_j(X,d))} \le -\lambda_j && j = 1, \cdots, m \\
& && d_L \le d \le d_U && (11)
\end{aligned}
$$

où $\tilde{f}(.)$ est la fonction objectif du problème RRBDO, C_T est le coût total, *X* et *d* sont les vecteurs des variables aléatoires et de conception, respectivement, $\mu(\cdot)$ et $\sigma(\cdot)$ sont respectivement la moyenne et l'écart-type de la fonction objectif, $\mu^*_{C_T}$ et $\sigma^*_{C_T}$ sont des facteurs de normalisation pour la moyenne et l'écart-type de la fonction objectif, respectivement, *m* est le nombre d'états limites $(1 \le j \le m)$, C_{fj} et $P\left[g_j\,(X,d) \le 0\right]$ sont respectivement le coût et la probabilité associés à la fonction d'état limite g_j, d_L et d_U sont respectivement les bornes inférieures et supérieures des variables de conception, α est un facteur de pondération, et λ_j est un facteur de pénalité. La valeur du facteur de pondération α est définie pour spécifier les poids relatifs des différentes fonctions objectifs et permet donc à l'utilisateur d'établir le compromis entre les objectifs d'une manière simple, selon ses préférences.

Une procédure de résolution est proposée de telle sorte que les problèmes pratiques d'ingénierie puissent être traités dans un temps de calcul raisonnable. Cette procédure permet également de comparer la RDO et la RRBDO. Elle est illustrée sur la Figure 3, où MCS est la méthode de simulations de Monte Carlo, FORM est la méthode de fiabilité du premier ordre, d^* est la solution optimale des variables de conception et C_T^* est le coût optimal.

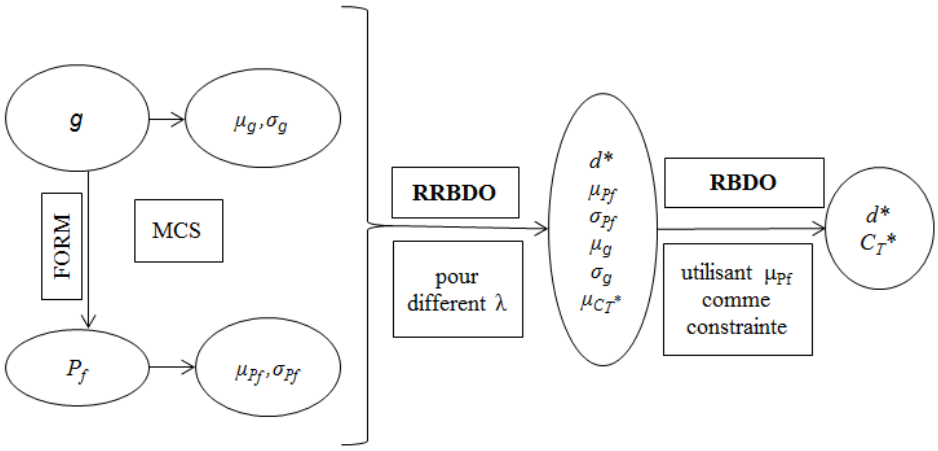

Figure 3: Formulation robuste pour l'optimisation fiabiliste de la conception.

Quatre applications numériques sont considérées pour montrer la performance de la formulation proposée et la comparer aux autres formulations. Le premier exemple illustre en détail la procédure proposée et décrit le comportement des différentes méthodes. Dans la seconde application, le comportement du RRBDO vis-à-vis de la dégradation de la structure avec le temps est étudié. Le troisième exemple montre l'intérêt du cadre RRBDO pour l'analyse d'un système à plusieurs composants. La quatrième application étudie les effets de la RRBDO sur la topologie structurale, où plusieurs modes de défaillance sont considérés. Les résultats montrent que la topologie joue un rôle très important pour la préservation de la robustesse. De plus, la RRBDO a un meilleur comportement que la RBDO quel que soit l'objectif de fiabilité, parce qu'elle offre des solutions optimales plus robustes et moins coûteuses pour des niveaux de fiabilité élevée, et elle continue à fonctionner convenablement pour les niveaux de fiabilité plus faible. Par ailleurs, la RRBDO propose des solutions qui sont moins sensibles aux variations, tout en conservant le même niveau de fiabilité que la RBDO. De plus, la RRBDO proposée est capable de gérer correctement l'effet système dans le cadre de l'optimisation de la structure.

6 Conclusion

L'objectif de cette thèse est de proposer des procédures améliorées qui peuvent être appliquées pour la conception et la gestion fiabilistes, optimales et robustes des structures en béton armé, en réduisant les coûts supportés par les gestionnaires et les utilisateurs, tout en tenant compte des dépendances entre les éléments.

Une méthode de conception probabiliste est proposée au Chapitre 2 pour la modélisation de manière cohérente des processus de dégradation, de l'augmentation des charges de trafic, du vieillissement, des conséquences directes et indirectes de la défaillance lors de la conception d'une nouvelle structure. Une discussion autour des différents composants du LCC est aussi

présentée au chapitre 2. L'originalité de cette méthode réside dans : (1) le développement d'une nouvelle approche pour évaluer le coût aux usagers et pour l'intégrer dans la fonction de coût du cycle de vie, (2) la considération du modèle de dégradation couplé corrosion-fatigue dans l'optimisation de la conception des structures en béton armé. Par ailleurs, plusieurs scénarios de perturbation de la circulation sont considérés. Une étude de cas au Liban est présentée, où le modèle est appliqué pour la conception des éléments situés dans divers environnements correspondant à différents degrés de contamination en chlorure et soumis à différentes fréquences de trafic. Les résultats ont montré l'effet considérable des modèles de dégradation, des coûts directs, indirects et des probabilités de défaillance sur les variables de conception.

Les différents types de dépendance entre les éléments structuraux : économique, structurale et stochastique, sont considérés au chapitre 3 dans le but d'optimiser le plan de maintenance d'une structure de pont. L'originalité de cette partie réside dans l'étude simultanée de ces dépendances, ce qui nécessite la considération des différents chemins de charges possibles, en plus de la configuration et la redondance de la structure. Ces dépendances sont considérées tout en offrant la fiabilité requise au cours de la durée de vie de la structure dans un environnement de paramètres incertains. L'absence d'approches de modélisation des systèmes qui prennent en compte les dépendances entre les éléments nous a motivés pour développer une nouvelle approche de calcul de la fiabilité du système en fonction de la redondance. La dépendance stochastique est intégrée dans la fonction de coût au moyen des probabilités conditionnelles ; un processus visant à quantifier les conséquences de la dégradation est présenté. Ce processus requière le calcul de la redistribution des charges aux éléments non-défaillants, qui est également proposée et intégrée dans la formule des coûts totaux. La dépendance structurale tient compte des temps d'arrêt nécessaires pour démonter les éléments modulairement liés, et de réparer les éléments dont la défaillance est associée (c'est-à-dire la défaillance d'un élément qui est induite par la défaillance d'un autre). La dépendance économique est intégrée au moyen des probabilités d'avoir des coûts de mise en place communs à plusieurs éléments. La méthodologie proposée est appliquée à quatre exemples numériques de validation.

Une nouvelle procédure d'optimisation fiabiliste et robuste est proposée dans le chapitre 4. Cette méthode prend en compte les incertitudes dans l'analyse, la capacité de la structure à s'adapter à la variabilité et aux évènements imprévus. Les applications numériques montrent que la formulation proposée se comporte mieux que les méthodes actuelles quel que soit l'objectif de fiabilité. Elle fournit des solutions optimales plus robustes pour les niveaux de fiabilité élevés, et continue à fonctionner convenablement pour les niveaux de fiabilité faible.

7 Perspectives

A l'issue de cette thèse, des améliorations peuvent être appliquées à l'approche de conception proposée pour représenter d'autres conséquences de défaillances indirectes, en particulier les conséquences sociales et environnementales. D'autres processus de dégradation devraient également être envisagés.

De plus, les procédures proposées dans les chapitres 3 et 4 sont coûteuses en temps de calcul, et plusieurs approximations sont nécessaires pour obtenir des résultats dans des délais raisonnables. Des efforts devraient être réalisés pour améliorer les procédures de solution pour les approches proposées.

Les approches et les formulations proposées offrent des outils d'aide à la décision pour la conception et la gestion optimale et robuste des structures en béton armé, en tenant compte des incertitudes, de la variabilité, de l'interaction entre les éléments et des différentes conséquences directes et indirectes de la dégradation, de la défaillance et de la maintenance. Il conviendrait donc de développer un outil intégré de gestion des structures en s'appuyant sur les développements effectués dans cette thèse.

General Introduction

Overview

The early design methods proposed by regulations are based on the principle of allowable stresses. Given the scattered nature of data, designers started using, since the 1960's, semi-probabilistic approaches based on safety factors that are supposed to deal with variability. This approach is nowadays used in most of the codes of practice, as it allows us to cover a large number of uncertainties. The probabilistic methods constitute an improvement of the semi-probabilistic approaches and allow for optimization procedures. These methods have been successfully used in reliability-based code calibration procedures for design and assessment of buildings and bridges (Ellingwood et al. 1982; Nowak 1995) and also in life-cycle maintenance procedures for existing structures as indicated by Frangopol and Maute (2003). However, their application as a tool for day-to-day design is still under consideration. The development of probabilistic methods for the design and management structures requires several enhancements in life-cycle analysis, system modeling, reliability analysis and structural optimization.

The Life-Cycle Cost Analysis (LCCA) is a methodology to evaluate the Life-Cycle Cost (LCC) over a specific period of time. The estimation of the life cycle cost of a structure is a challenging issue, due to its complex components, particularly failure cost which depends on degrading resistance with time. As many uncertainties are related to the stochastic nature of load and material parameters, the developments are still needed to accurately estimate the deteriorating structural performance and the life-cycle cost under uncertainties and to optimally plan maintenance actions along the service life of a structure. In addition, the consequences of failure are significantly amplified by environmental and social impacts.

Moreover, system modeling approaches have not been successfully applied for structural deterioration modeling (Wang, 2012). Approaches better than the currently used series and/or parallel logical relationships for modeling of a structural system components are to be founded, as a civil engineering structure is a complex system composed of many inter-related elements. A model has to be developed to consider the multiple deterioration dependencies among the elements. Although the deterioration of the structure is largely dependent on the deterioration of each element, the deterioration of one element can accelerate that of the others. For example, if a bridge bearing freezes due to corrosion, the bridge deck will be subjected to expansion and contraction stresses that cause cracking (Sianipar and Adams 1997).

Decision-makers can employ optimization tools to specify the most efficient LCC alternative. For this purpose, probabilistic optimization tools involving appropriate modeling of uncertainties can be used. These tools should reflect the ability of the structure to comply with data variations, unforeseen actions or deterioration mechanisms.

Contribution

This work provides several contributions to overcome the above explained limitations:

An integrated and systematic approach to model coherently the deterioration processes, the increasing traffic loads, the aging, and the direct and indirect consequences of failure is proposed. The design optimization of reinforced concrete structural elements is performed with coupled corrosion and fatigue degradation models. Moreover, a new approach to evaluate the user delay costs on a bridge structure is developed, based on direct and indirect costs related to degradation and failure.

For the moment, there is no research consideration of economic, structural and stochastic dependencies among structural elements. A procedure to model all types of failure interactions is suggested herein, using failure tree analysis and conditional probabilities. Economic dependency is taken into account through several interdependent common costs. Horizontal structural dependency is considered by the mean of a proposed redundancy factor, for which a sensitivity analysis is performed. Modular or vertical structural dependency is modeled through the consideration of downtimes needed to dismantle modularly dependent units, and/or to repair associated failed units. Moreover, the load redistribution to non-failed elements in case of failure of an adjacent structural element is considered in the formulated model. Also, for evaluating the system reliability, a new approach different than the currently used series and/or parallel logical relationship is suggested. A solution procedure is also proposed for the life-cycle maintenance planning of interrelated multi-component structural system. Several numerical examples are treated to verify the validity of the proposed approach.

Design and maintenance optimization procedures focus either on the robustness of the objective function or on the satisfaction of a prescribed reliability level. A new formulation is proposed to combine the benefits of robust and reliability design by considering both; the objective function robustness and the reliability level. Moreover, it takes account for uncertainty and variability in one mathematical formulation. A numerical procedure to solve the proposed optimization formulation is developed. A comparison between the proposed formulation and the reliability based design optimization procedures is held for the design of several structural concrete and steel problems, proving the applicability of the proposed methodologies on a large range of civil engineering problems.

Thesis Outline

This thesis is divided into four chapters. Each chapter aims at meeting one of the objectives listed above.

Chapter 1 presents a literature review on the procurement and the maintenance planning of civil engineering structures based on reliability concepts. The formulations of direct and indirect failure costs are summarized. Probabilistic and reliability concepts for performance evaluation of components and systems are presented. The existing maintenance models and management systems are then described by considering the above costs and reliability. Furthermore, the different types of dependencies between the components of a system and the main advances concerning each type are discussed. Finally, each component of the life-cycle cost formulation is detailed.

In chapter 2, a consistent approach is proposed for a probabilistic design that can account for the indirect consequences of failure within the life cycle cost formulation. An approach to evaluate the user costs on a bridge structure is developed. The proposed user costs takes into account the vehicle operating costs and the user delay costs. Various scenarios that may lead to user costs are considered, namely the degradation of a bridge element, the rehabilitation, the traffic congestion and the bridge collapse. The developed model is applied to bridge elements subjected to chloride-contaminated environments and various traffic frequencies. The different components of the life cycle cost are estimated, and their effect on the design variables is studied and analyzed through numerical applications.

Chapter 3 aims at developing a procedure for the maintenance planning of a multi-component structural system by jointly taking into account stochastic, structural and economic dependencies. These dependencies can be only modeled by the consideration of structural redundancy and possible load paths. Therefore, a procedure to calculate the load redistribution to non-failed elements is proposed and integrated in the cost function. Also, stochastic dependency for all the elements is integrated in the cost function by the mean of conditional failure probabilities. The approach also accounts for downtimes needed to dismantle modularly dependent elements, and/or to repair associated failed elements. The proposed methodology is applied to four numerical examples to show its validity and functionality.

In chapter 4, the behavior of two utilized optimization procedures is assessed, namely the reliability-based design optimization (RBDO) and the robust design optimization (RDO). In this framework, a robust formulation for reliability-based design optimization (RRBDO) is proposed, in order to combine the advantages of RBDO and RDO procedures. The results of the proposed formulation are analyzed and compared with usual RBDO for several examples of reinforced concrete and steel structures.

The conclusions highlight the improvements that can be achieved by the proposed approaches to help the decision-makers in selecting the best design and maintenance solutions.

Chapter 1: Literature Review: Probabilistic design and maintenance

1.1 Introduction

The aim of this chapter is to provide an overview of the state-of-the-art concerning the life cycle analysis of structural reliability in design and maintenance. These analyses are necessary for improving and rationalizing the design, the evaluation, the repair and the management of civil engineering structures in order to balance lifetime cost and life cycle reliability. This chapter starts by summarizing the benefits of considering reliability approaches for structural design and evaluation. Then, it discusses how to model the applied loads and deteriorating capacity in order to account for uncertainties within the safety assessment. The management of existing structures is also explained, and the applicability of reliability methods to safety assessment of structural systems and components is discussed. The recent developments on modeling the capacity of a structural system based on redundancy of interrelated component are presented. The former assessment is crucial for the evaluation and the maintenance decision. Finally, the methods for cost-effective management incorporating lifetime reliability and life cycle cost are detailed.

1.2 Structural reliability concepts

Structural failure and damage involves, among other catastrophic consequences, loss of human lives and user delays, leading to massive economic and social losses. Therefore, a lot of investments in inspection, maintenance and inadequate strength reserves are anticipated.

Historically, high degree of structural performance reliability against failure was observed. This situation is caused by the conservative models that were used due to limited capabilities back in time. Moreover, system performance was generally neglected, and the design checks were mostly done on components. This conservative situation has changed, mainly because of available computer software and optimization methods that push the design closer to their failure limits. In addition, transport agencies are exerting economic pressure to increase truck weight and volume.

Research efforts in structural reliability have led to new design methods and specifications, considering explicitly the system uncertainties.

The first step in developing a reliability-based structural specification is to identify the basic random variables; i.e. resistance R and load L. Then, a limit state expression g can be written as function of these random variables as follows:

$$g = R - L \tag{1.1}$$

The next step in the reliability assessment is to identify the appropriate distribution for each random variable by considering available database and expert analyses. This step involves expressing the bias (i.e. mean over nominal value), the coefficient of variation (i.e. COV, equal to the ratio of the standard deviation to the mean value), and the distribution function (e.g. normal, lognormal, exponential, etc ...) of each random variable. For example, the main uncertainty governing the reliability analysis of short and medium span bridges is live load due

to traffic. The maximum traffic load is a function of the highway class, the truck volume, the legal weight laws and the exposure life.

The probability of failure may then be expressed as:

$$P_f = P[g < 0] = \int_{-\infty}^{+\infty} F_R(x) f_L(x) dx \tag{1.2}$$

where $F_R(x)$ is the cumulative distribution function of the resistance, $f_L(x)$ is the probability density function of the load and x is the vector of random variables.

Determining the failure probability is usually a difficult task, requiring the evaluation of multiple integrals whose dimension increases with the number of random variables. Numerical integrations can be used when the failure function g is not highly nonlinear and the tail distributions of the functions do not deviate too far from the normal one. For normal and lognormal load and resistance distributions, exact expressions are formulated for the calculation of the probability of failure (Ditlevsen and Madsen 1996). Otherwise, numerical models can be employed for all kinds of distributions, such as Monte Carlo simulation methods (MCS). The MCS is statistical trial method that makes realizations based on randomly generated sampling sets for uncertain variables. However, it requires a very large number of samples to give acceptable approximations, especially in case of engineering structures where the probability of failure is usually very low. To improve the rate of convergence, several improvements can be introduced to MCS using approaches in variance reduction methods; e.g. Importance sampling (IS), Latin Hypercube Sampling (LHS) and subset simulations.

The most used approximation methods are First Order Reliability Method (FORM) and Second Order Reliability Method (SORM). Considering a quasi-linearity approximation around the design point, the failure probability P_f is estimated as a function of the mean and the standard deviation of g as follow:

$$P_f \approx \Phi\left(-\frac{\mu_g}{\sigma_g}\right) \tag{1.3}$$

where μ_g and σ_g are respectively the mean and the standard deviation of g and $\Phi(\cdot)$ denotes the cumulative normal distribution function. The reliability, also called probability of survival, is the complement of the probability of failure; $\mathcal{R} = 1 - P_f$. The associated reliability index β can be determined in approximate form as:

$$\beta = \frac{\mu_g}{\sigma_g} \tag{1.4}$$

In the case of normal random variables, the mean and standard deviation of the limit-state, $g(\cdot)$, can be determined as follows:

$$\mu_g = \mu_R - \mu_S \tag{1.5}$$

$$\sigma_g = \sqrt{{\sigma_R}^2 + {\sigma_S}^2 + 2\,\rho_{RS}\,\sigma_R\,\sigma_S} \tag{1.6}$$

where ρ_{RS} is the correlation coefficient between R and S, and σ_R and σ_S are the standard deviations of R and S, respectively.

The reliability index gives the number of standard deviations that the mean safety margin falls on the safe side, as shown in Figure 1.1. The shaded area identifies the probability of failure.

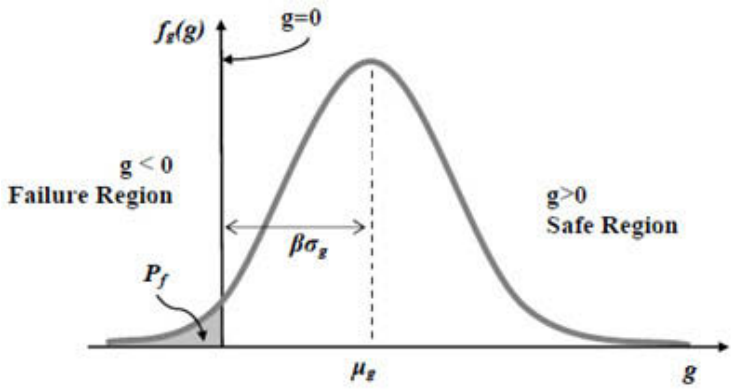

Figure 1.1: Probability density function for limit state $g(\cdot)$

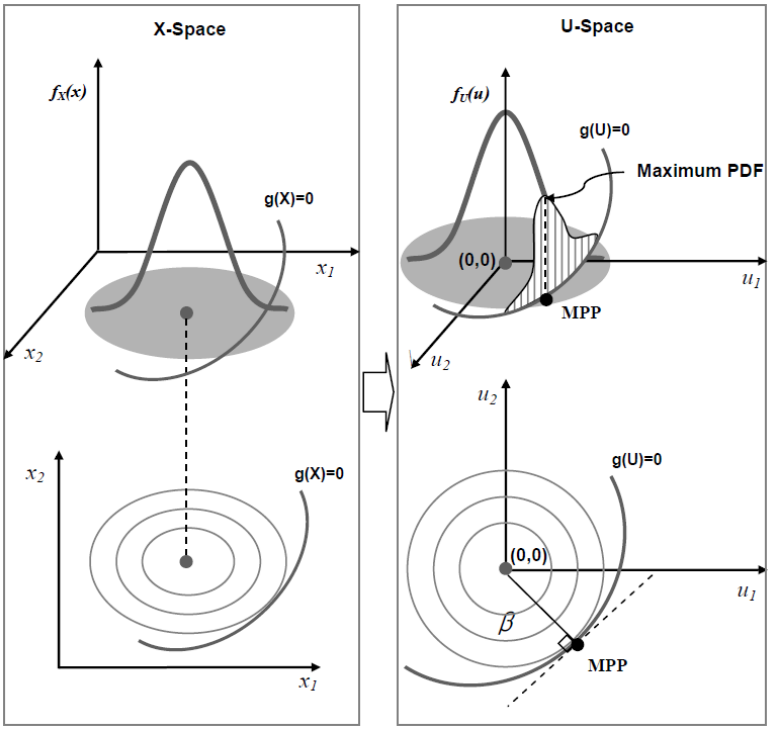

Figure 1.2: Transformation and MPP.

Finding β comes down to find the distance between the mean point and the surface that divides the limit into safe and unsafe regions. Different types of response surfaces correspond to different approximation methods for failure probability calculations. If the mechanical response is approximated by a first-order approximation at the MPP, the method is called the first-order reliability method (FORM); if the mechanical response is approximated by a second order approximation at the MPP, the method is called the second-order reliability method

(SORM). Furthermore, if the mechanical response is approximated by a higher order approximation at the MPP, the method is called the higher-order reliability Method (HORM). FORM gives inaccurate results when the failure surface is highly nonlinear. Thus, FORM sometimes oscillates and converges on unreasonable values for probability of failure.

The Taylor series can be used to linearize the limit state $g(\cdot) = 0$ in FORM and SORM. The reliability analysis is considered as a mathematical optimization problem for finding the point on the structural surface that has the shortest distance from the origin to the failure surface in the standard normal space. Hasofer and Lind (1974) provided a geometric interpretation of the reliability index and improved the method by introducing the Hasofer and Lind (HL) transformation, where $g(\cdot)$ is transformed into a set of normal variables with zero mean and unit standard deviation. In the transformation procedure, the design vector *X* is transformed into a vector of standardized, independent Gaussian variables, *U*. Because of rotational symmetry of the HL transformation, the design point in *U*-space represents the point of greatest probability density or maximum likelihood as shown in Figure 1.2.

Typical values of engineering structural reliability index β are in the range of 2 to 5. Note that a β of 3.5 corresponds to a probability of failure of 2.33×10^{-4} . β is used by many code groups nowadays to calibrate the safety factors. A value equal to 3.5 has been used to calibrate the AASHTO LRFD. The implicit design goal is to achieve a uniform β for all structures constructed by the code. The value of the safety index targeted by design codes is based on existing designs that were found to be satisfactory. This commonly used calibration with past performance helps minimizing any inadequacies in the database (Moses and Ghosn 1985). However, higher β are imposed for gravity load cases than for environmental limit states. This need arises because of the greater psychological impact of failure in the absence of a corresponding act of nature. Also, higher β are imposed in design than used in evaluation. It costs more to strengthen an existing structure than to provide strength initially in a construction. It is worth noting that the values of β are notional rather than actuarial values since only specified limit sate functions are examined (Moses 1999). Moreover, further accidents, human errors and construction failures are not included in the safety index approximation.

Other commonly used lifetime performance evaluation functions are the survivor, the hazard and the risk functions. Several time-variant performances can be related to the possible occurrence of local and global failures, including system redundancy, elapsed time between failures, and robustness. Redundancy is defined by Frangopol et al. (1987, 1992) as the ability of the system to redistribute among its members the load which can no longer be sustained by some other damaged members after the occurrence of local failures. An effective indicator of the damage tolerance of the system and its ability to be repaired after local failures is the elapsed time between local and structural collapse (Biondini and Frangopol 2008). Robustness is the ability of the system to suffer an amount of damage without presenting a disproportionate response with respect to the causes of damage itself. Thus it is very important to measure the impact of a localized damage on the structural global damage. Robustness is related to the capacity of the system to operate when there is a localized damage. Many authors proposed measures for the quantification of the structural robustness, which can be globally divided into two approaches (Kagho-Gouadjio et al. 2015). The first approach compares the system probability of failure of the intact structure to the damaged structure. The second approach

compares the consequences of a local failure to the consequences of global failure. Kagho-Gouadjio et al. (2015) proposed a probabilistic approach for quantifying structural robustness as the impact of local failure on global failure. Their approach requires the computation of local and global failure probabilities; a low impact characterizes a robust structure.

Barone and Frangopol (2014) investigated the effect of four different performance indicators (PI) related to the optimization of maintenance schedules of deteriorating structures. The use of two annual performance indicators (reliability index and annual risk), and two lifetime performance indicators (availability and hazard functions) were compared. The solutions provided by annual PI in their study required more computational effort, but were considered more reliable by the authors. Usually, annual basis approaches are appropriate for life risk, and lifetime basis approaches are appropriate for economic loses.

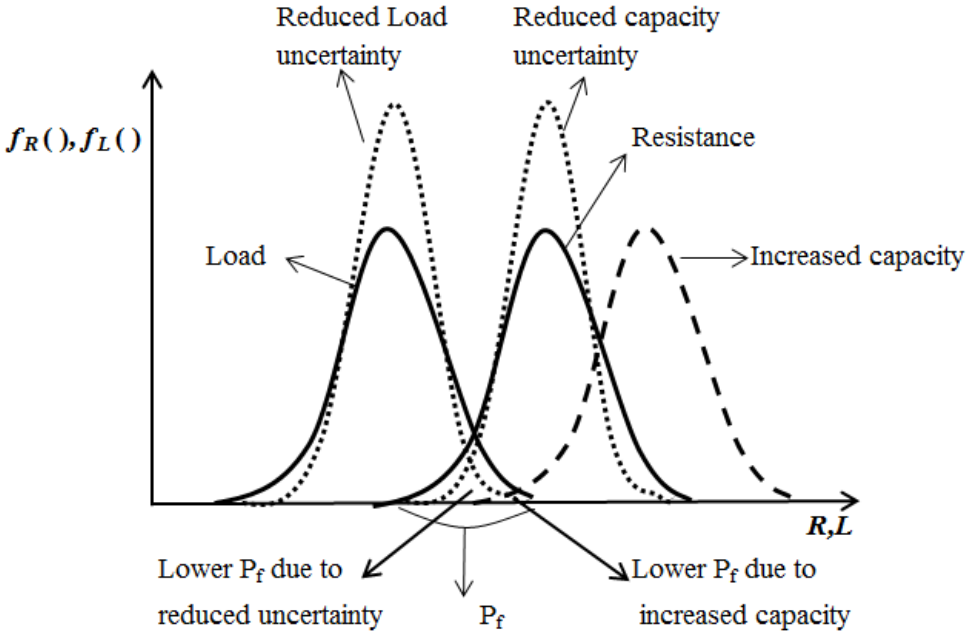

Figure 1.3: Different ways to achieve higher reliability with load and capacity distributions (Moses 1999).

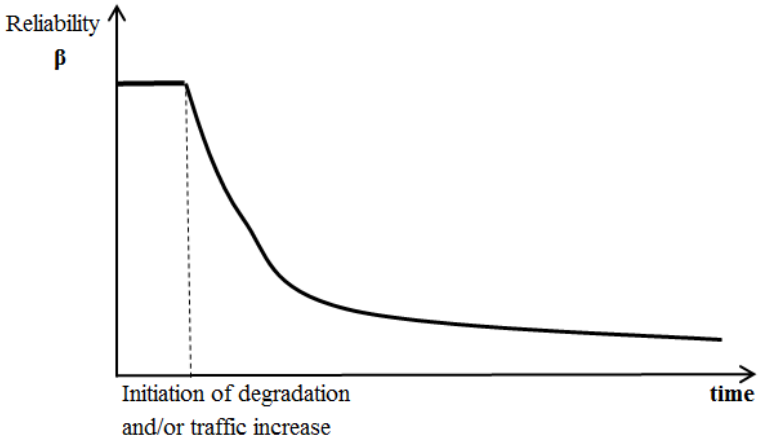

Figure 1.4: Reliability evolution as a function of time.

The probability of failure depends on the degree of overlap between the load distribution $f_L(\cdot)$ and the resistance distribution $f_R(\cdot)$ (Figure 1.3). Higher reliability may be achieved by increasing the resistance, or by reducing the uncertainty in either load or capacity (Moses 1999), as shown in Figure 1.3. The inspections and observations can be performed to reduce the levels of uncertainty. In fact, truck loads increase with time due to new regulations and increases in truck volume and weight. Meanwhile member capacity is decreasing due, besides aging, to inadequate maintenance and environmental effects. Therefore reliability is assumed to be constant with time until the initiation of degradation, and/or the increase in traffic volume, afterward β is reduced with time as shown in Figure 1.4.

1.3 Definition of uncertainties

Uncertainties can belong to different categories. Ang and Tang (1984) sorted the uncertainties into two groups, namely: inherent variability and epistemic uncertainties.

Inherent variability is irreducible, like the wind, the material properties after casting, the loads, the geometry and the degradation. They result from variations in the physical properties of components and interfaces, and correspond to the parameters entering into mechanical modeling that are intrinsically random. It is referred as "non-cognitive" by Pendola et al. (2000) , "inherent uncertainties" by Tovo (2001), aleatory by Guedri et al. (2012), or simply as variability by Van Belle (2011). These are the only uncertainties covered by structural design approaches.

Epistemic uncertainties are related to the fabrication measures, the errors of the numerical model as well as in the estimation of the parameters. They are due to a lack of accurate knowledge concerning the physical laws governing the behavior of a component or interface and can generally be reduced with a combination of more detailed modeling and experimental investigations. Epistemic uncertainties can be difficult to characterize due to simplifications in geometric and material field properties, and as such are rarely taken into account explicitly in reliability analysis.

It is important to note that Van Belle (2011) terminologies will be used in this study, where 'variability' refers to natural or intrinsic variation in some quantity and 'uncertainty' refers to the degree of precision with which a quantity is measured.

Statistical distributions are used to model variability and uncertainty. In terms of design, partial safety factors attempts to cover the variability in deterministic approaches. The main drawback in this approach is that the safety factors often lead to over or under-design since they do not account for uncertainty and for site to site variation.

Probabilistic design approaches studied in chapter 2 inquire the estimation of failure probabilities that are extremely sensitive to the assumptions made on the distribution of random variables. In practice, only limited data is available to build the probabilistic representations of these variables. Pendola (2000) proposed a methodology to characterize the statistical uncertainties due to the limited number of data in order to take them into account in the reliability analysis. He also proposed partial safety factors that are evolving as a function of the number of statistical data available and as a function of the sophistication level of the mechanical modeling. Echard (2012) proposed a general probabilistic approach that can overcome the design dependency on variability. His approach is an alternative to calculate an

accurate estimate of the failure probability as well as the influent parameters on structural reliability.

Variability can be controllable when the geometrical and material parameters can be set by engineers, or uncontrollable as for environmental parameters related to the deterioration mechanisms. The transmitted variation from uncontrollable variability to the objective function can result in the deterioration of product quality and can compromise the design feasibility. The effect of variability on the objective function can be properly reduced by adjusting the design values. Therefore, the need to find values for controllable settings (such as concrete dimensions of a structural element cross-section) that minimize the negative effects of the uncontrollable settings (such as humidity or corrosion rate) has submerged.

1.4 Structural loading

Structural loading is a complex phenomenon that requires many assumptions in order to obtain fine numerical estimates. In case of bridges, most of the loads are time-varying quantities in magnitude, position, and type of structural response (static or dynamic) (Thoft-Christensen 1998). Even permanent values that do not change with time are random variables, because their magnitudes are not precisely known. For example, there are a lot of uncertainties in predicting the magnitude of the dead load due to the weight of reinforced concrete. Variations can subsist in the material density, the component dimensions, the steel reinforcement area, and in the distribution of aggregates in concrete. However, the effect of these factors on the bridge reliability estimate is low compared to the effect of vehicle live load.

Transient loads include all moving loads such as traffic load, temperature effect and wind. Though, the most important loads in typical short to medium span bridges are vehicle traffic loads (Ghosn and Frangopol 1999). Expected load models are based on data gathered on site for the Average Daily Truck Traffic (ADTT). Truck weight data is either taken from highly static scales, or from moving vehicles using weight in motion (WIM). Unfortunately, static weighting may be avoided by heavy truck drivers to avoid penalties imposed by the government on overweighed trucks. Also, pavement embedded scales can be detected and intentionally missed by drivers. Such factors can reduce the accuracy of the gathered data. These data can then be adjusted, and may be used to fit a distribution so that the tail can be extended with normal or lognormal assumptions.

Some reduction is observed in the influence of the extreme truck weight distribution results, because the critical load event for many spans is usually a multiple presence event. Failure of a bridge member can be due to the occurrence of one set of load that causes stresses in the bridge component to exceed its capacity. Failure can also be due to repeated crossings of a large number of trucks that produce fatigue fracture of the component.

As a matter of fact, the traffic loading effect on a bridge is a multidimensional stochastic process and has been studied as a Markov Renewal process and also by filtered Poisson models. There are several methods to study these problems, including simulation and convolution approaches. Ghosn and Frangopol (1999) described how these methods can be used to study the extreme load event problem. These reliability methods were used to develop empirical live load models for design codes that can be applied by civil engineers. The maximum load is the maximum expected event based on a 50-75 years exposure for design, and two year exposure

for evaluation. Code calibration procedure was developed by Nowak (1989). It basically includes the following steps:

- Selection of representative structures
- Establishment of the statistical database for load and resistance parameters
- Development of load and resistance models
- Development of reliability analysis procedures
- Selection of the target reliability index
- Calculation of the load and resistance factors

The calculated load and resistance factors may provide rational basis for the design of civil engineering structures. However, further researches are needed in different areas. A whole life cycle approach to structural design and evaluation needs to be developed, including various forms of deterioration (corrosion, fatigue, cracking), and considering the entire system with all the interactions between different components.

1.5 Structural capacity and deterioration

The capacity of a structure depends on the resistance of its components and connections. The component resistance is a random variable depending on material, fabrication and analysis uncertainties. Typical coefficients of variation for structural engineering applications range from 5 to 15% for material strength, 5 to 10% for deal load, and 15 to 30% for live load, and even higher for seismic and wind loads (Ghosn and Frangopol 1999).

Moreover, structural capacity is degrading with time. The deterioration is usually caused by a combination of (Das 2000): (1) traffic related effects, e.g. surface/joint damage, fatigue effects, deformation; (2) environmental factors both natural and man-made, e.g. de-icing effect, freeze thaw cycles; (3) material degradation, e.g. loss of ductility, corrosion, cracking.

In addition to the reliability index, other performance indicators, as explained in section 2.2, can be used to properly specify the structural performance of deteriorating structures; e.g. structural ductility, redundancy, robustness, resilience and elapsed times between failure. Discussions of these indicators can be found in (Biondini et al. 2014; Frangopol and Soliman 2016).The performance indicator for the structural system is schematically shown in Figure 1.5 (Das 2000). The unacceptable elements such as those with severe deterioration are likely to be located towards the left. Without any maintenance, the overall distribution will tend to move leftwards.

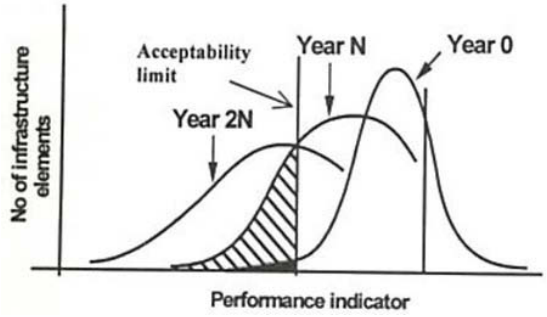

Figure 1.5: Structural deterioration (Das 2000).

The degradation process leading to failure is a complex process. Figure 1.6 shows examples of three general degradation curves in arbitrary units of degradation and time: linear, convex and concave (Meeker et al. 1998).

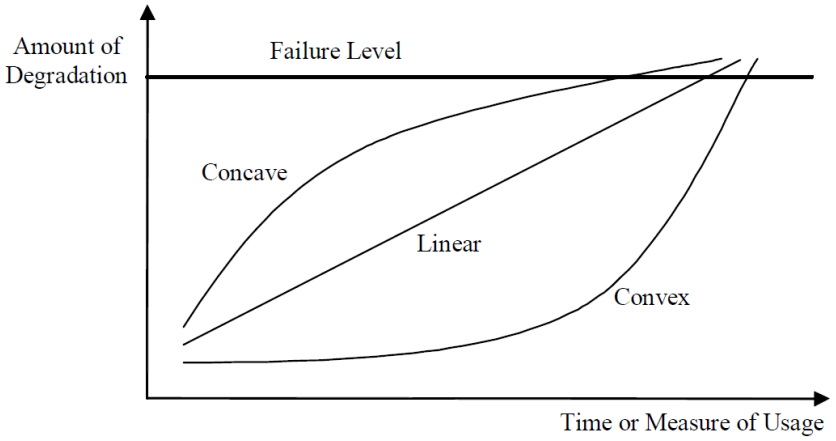

Figure 1.6: Possible shapes for univariate degradation curves (Meeker et al. 1998).

Dasgupta and Pecht (1991) divided the failure mechanisms into two broad categories: overstress failure and wear-out failure. Overstress failures are those due to brittle fracture, ductile fracture, yield, buckling, large elastic deformation, and interfacial de-adhesion. Wear-out failures are those due to wear, corrosion, inter-diffusion, fatigue crack propagation, diffusion, radiation, fatigue crack initiation, and creep. Variation in the degradation process can be due to operating conditions, variability in environmental conditions, manufacturing variability, and material variability. Modeling degradation with time provides necessary information to assess reliability and to estimate the time to failure.

Time-dependent structural deterioration processes such as corrosion and fatigue impose continuous aging effects on structures. Corrosion is the main cause of damage in reinforced concrete structures (Deby et al. 2009). Severe cracking of the concrete cover may be caused by corrosion in aggressive environment. Also, fatigue damage may occur in a bridge member due to the accumulation of damage following the application of a large number of stress cycles. A reinforced concrete bridge may experience up to 7×10^8 stress cycles during the course of its lifespan (Rocha and Brühwiler 2012). It is thus important to be able to assess the corrosion and fatigue performance of such structures.

Several published studies are related to modeling the probabilistic corrosion initiation and propagation (Vidal et al. 2004; Vu et al. 2005; Chen and Mahadevan 2008) and to assessing the influence of reinforcement corrosion on reliability (Stewart 2004; Vu et al. 2005; Bastidas-Arteaga et al. 2008; Bastidas-Arteaga et al. 2009; Bastidas-Arteaga et al. 2011; Liberati et al. 2014; Soliman 2015), Methods for reliability assessment of reinforced concrete (RC) slab with corroded reinforcement have also been developed (Coronelli and Gambarova 2004; Stewart and Al-Harthy 2008). The procedure proposed by Val et al. (1998) for time-dependent reliability analysis had important repercussions for the optimal allocation of resources for structural design and maintenance. Improved corrosion models were later developed by Vu and Stewart (2000) in the aim of calculating the failure probabilities. Stewart (2004) developed a stochastic process for assessing the effect of spatial variability of pitting corrosion on structural reliability and

fragility for reinforced concrete *(RC)* beams in flexure. Deby et al. (2009) presented a complete methodology for the durability design of cover depth for a concrete immersed in sea water by quantifying the service life of concrete through the reliability index. El Hassan et al. (2010) proposed a reliability model to determine the probability distributions of the time to corrosion initiation and the time to failure of *RC* members subjected to chloride ingress. Bastidas-Arteaga et al. (2008; 2009; 2011) presented a model of *RC* deterioration by coupling deterioration due to corrosion and cracking. Bastidas' model computes the reduction of the concrete section and the area of steel reinforcement in order to assess the change of structural capacity with time. Their coupled corrosion-fatigue deterioration process is detailed in Appendix 2.

Damage mechanisms, including uniform corrosion in steel structures, as well as crushing, cracking, abrasion and erosion in concrete structures, can be effectively represented at the member level by a progressive reduction of the cross-section resistance and used to evaluate the corresponding performance at the global level (Biondini et al. 2014). Available empirical deterioration models are used for this purpose. Two corrosion and fatigue models are explained in Appendixes 1 and 2, and they will be used in the numerical applications in the following chapters.

1.6 Structural reliability: components and systems

Civil engineering systems are complex structures formed by several individual components. The reliability analysis of such systems is only possible when all failure modes are identified. This analysis has to include the interaction between potential failure modes. The effects of structural deterioration due to mechanical loadings and environmental stressors on system reliability should also be accounted for.

The reliability indexes of individual members assuming linear elastic behavior differ from the system reliability accounting for load redistribution. Material nonlinearity has large influence on the redistribution of forces in a structural system. When there is adequate redundancy, the overall system safety will be higher for systems with passive components. System reliability is affected by the way in which the components are joined together: in series, in parallel, or in a combination of series and parallel sub-systems. Component ductility and the correlations between member capacities also affect significantly the system reliability. The system probability of failure may be obtained for both statistically independent and perfectly correlated components, by considering the system configuration (series, parallel or series-parallel).

The failure of any member in a series system will produce the failure of the complete system. If the members of a series system are independent, then the system probability of failure is:

$$P_{f,system} = 1 - \prod_i (1 - P_{fi}) \tag{1.7}$$

The failure of a parallel system requires the failure of all the components. If the members of a parallel system are independent, then the system probability of failure is:

$$P_{f,system} = \prod_i P_{fi} \tag{1.8}$$

In reality, the members of a structure are usually correlated. In fact, the performance functions of different members have common variables, while the other variables have various degrees of correlation. For correlated systems, many authors proposed upper and lower bounds.

Bounds on system failure probability have been proposed by Ang and Tang (1984) for series and parallel systems, as follows:

Series systems: $$\max_i P_{fi} \le P_{f,system} \le 1 - \prod_i \left(1 - P_{fi}\right) \tag{1.9}$$

Parallel systems: $$\prod_i P_{fi_i} \le P_{f,system} \le \min_i P_{fi} \tag{1.10}$$

Ditlevsen (1979) proposed bounds for the system probability of failure of series system, based on individual failure modes and their correlation, as follows:

$$P_r[F_1] + \sum_{i=2}^{n} max\left\{\left[P_r(E_i) - \sum_{j=1}^{i-1} P_r\left(E_j \cap E_i\right)\right]; 0\right\} \le P_{f,system} \le \sum_{i=1}^{n} P_r(E_i) - \sum_{j=2}^{n} \max[P_r\left(E_j \cap E_i\right)] \tag{1.11}$$

where n is the total number of failure modes, $P_r(E_i)$ is the probability of occurrence of failure mode i, and $P_r\left(E_j \cap E_i\right)$ is the probability of occurrence of the intersections of failure modes i and j. The probability of occurrence of the intersection of two events can also be expressed by its lower and upper bounds as follows:

$$\max[\phi(-b) \times \phi(-\beta_i); \phi(-a) \times \phi\left(-\beta_j\right)] \le P_r\left(F_j \cap F_i\right) \le \phi(-b) \times \phi(-\beta_i) + \phi(-a) \times \phi\left(-\beta_j\right)$$

$$\text{with } a = \frac{\beta_i - \rho_{ij} \times \beta_j}{\sqrt{1 - {\rho_{ij}}^2}} \quad \text{and} \quad b = \frac{\beta_j - \rho_{ij} \times \beta_i}{\sqrt{1 - {\rho_{ij}}^2}} \tag{1.12}$$

where ρ_{ij} is the correlation coefficient between modes i and j.

The above bounds are compatible with the fact that for series systems, if all components are fully correlated, the system probability of failure is that of the less safe component (i.e. higher P_{fi}). The upper bound corresponds to the failure of uncorrelated series system. For parallel systems, if all components are fully correlated, the probability of failure is that of the safer component (i.e. lower P_{fi}). The lower bound corresponds to the failure of uncorrelated parallel system.

Such calculations show that for series systems, the reliability of the system decreases when the correlation decreases, and when the number of elements decreases. Inversely, the reliability of parallel systems decreases when the correlation increases and the number of elements increases.

The level of member ductility does not influence the series system reliability. A series system will totally fail whether a member fails in a brittle or a ductile mode. However, the

member ductility affects the parallel system reliability. A parallel system formed of two perfectly ductile members will only fail if the two members fail. However, if a parallel system is formed of brittle members, the system reliability will depend on the level of reserve strength in each member. When a ductile member reaches its limit capacity, it continues to carry its limit load and redistribute all other additional loads. Otherwise, if a brittle member reaches its limit capacity, it will shed its limit load plus any additional load. This behavior is explained in Ghosn and Frangopol (1999).

Yang et al. (2004) proposed a model to evaluate the overall system reliability for independent or correlated components of existing bridges modeled as series and parallel systems. They demonstrated that correlation has a significant influence on the system reliability; an increase in the positive correlation between the safety margins of components increases the safety of the system for series systems and decreases it for parallel systems.

The system reliability is required to be accounted for in life-cycle optimization as the overall performance indicator for new and existing structures. Recently, Sabatino et al. (2015a) shared the importance of the effect of system modeling (series or parallel) and of the way the system reliability is calculated (annual or cumulative) on optimum structural maintenance planning.

1.7 Management Practice

Civil engineering structures, particularly bridge infrastructures, are often aging faster than funds allowing reconditioning to meet current loading requirements. In management practice, a structure that does not meet satisfactory ratings must be posted or replaced. Posting causes travel inconveniences and costs to the economy. Ideally for heavily trafficked roads, life cycle costs of a bridge repair and damage are balanced by increased productivity with higher vehicle weights by the mean of fees assigned to heavy vehicles by some agencies. In order to be consistent in applying user fees, a concept of uniform risk must be maintained. Therefore, any reduction in reliability created by heavier truck weights can be translated to cost factors.

Rising highway productivity causes more problems to existing bridges, compared to new ones. In fact, the costs for increasing the capacity of a new structure are low compared to existing ones. When designing, the structural capacity can be increased by simply enlarging a cross-section size. However, if an existing structure is deteriorating, expensive maintenance is necessary to allow the bridge to continue carrying legal traffic, otherwise, the bridge must be load posted by weight restrictions or replaced.

1.7.1 Management system

The Bridge Management System (BMS) provides data, models and analyses that support decisions in design, in maintenance, in hazard mitigation, and in anticipated obsolescence of structures (Hearn 1998). The decision supports in design aims at finding a balance between a greater durability that offers an increased service life under normal service, and a lower initial cost of material and components. In maintenance, it balances between longevity and the costs of repairs and replacements. Facing natural hazards, the BMS considers the return period of the extreme event, the probability that the bridge will withstand the event, the cost options for design and reconstruction required to strengthen bridges for the events, and the cost of loss of

service if the bridge fails. The BMS for obsolescence compares the expected increase in traffic volume and requirements to the costs of providing superior bridges. The management is needed because resources for improvement are limited. The economic analysis considering user costs of deficient service becomes the basis for management of deficient bridges.

The first step in bridge management is to separate the elements into groups of similar characteristics, for example by construction type. For each group, it is necessary to establish an optimum maintenance regime, which is based on whole life cost considerations. The next step is to consider the maintenance planning from the project and network point of views. At the project level, the condition measurements and evaluations are used to carry out the assessments that form the basis for any bid for funding. Then, the project level programs are adjusted to reflect the network strategic plan. User delay cost must be considered as a consequence of not funding part of the bids. Traffic disruptions are likely to take place due to weight restrictions or load posting, which would be necessary for maintaining safety if the full bid is not funded.

The evaluation of bridge structures is needed periodically because of increasing loading and decreasing capacity. The final computation of a bridge evaluation is often the rating factor which leads to active decisions (e.g. load posting, repair, replacement or permit).

The life-cycle management framework is shown in Figure 1.7 (Frangopol and Soliman 2016). Different modules of the life cycle framework have to be combined to obtain the optimum life cycle decisions.

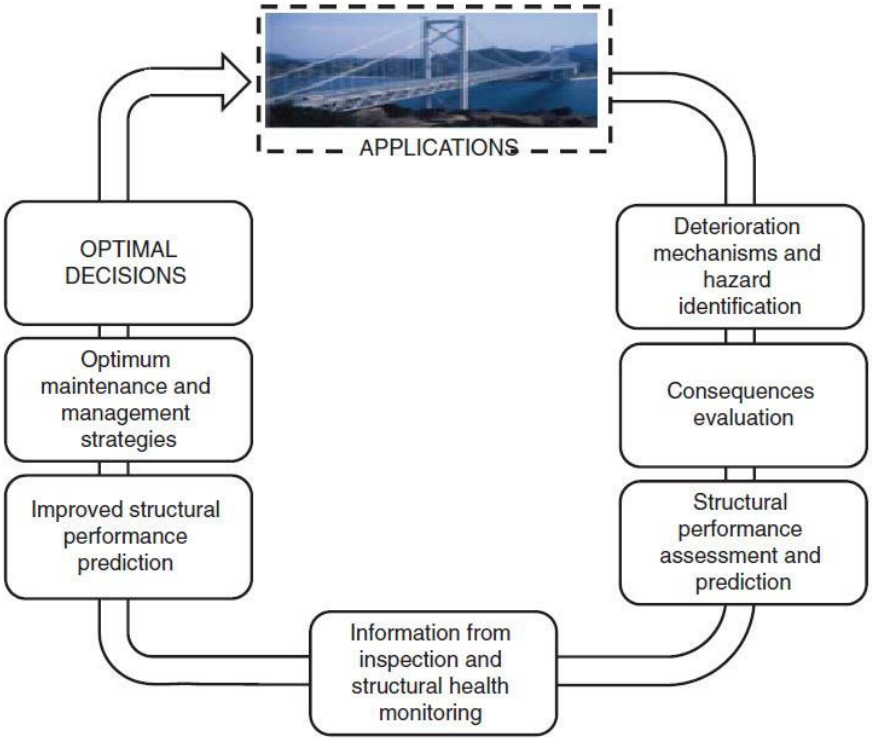

Figure 1.7: General life-cycle management procedure (Frangopol and Soliman 2016).

1.7.2 Reliability versus Condition based models

Currently, two methods are used to evaluate existing structures: reliability-based rating (Mori and Ellingwood 1993) and condition-based rating (Hudson et al. 1987).

Condition rating models are extensively used in structural management systems. Condition ratings are numerical codes estimated from visual inspection, which have been commonly used as an indicator of structural deterioration describing the extent and severity of damage. The dominant BMS that uses condition-based models in the US are BrM (formerly Pontis BMS (Thompson and Shepard 1994) for the Federal Highway Administration (FHWA) and BRIDGIT (Hawk and Small 1998) for the National corporative highway research program (NCHRP). Similar BMS have also been developed in other countries, as for example Denmark (Lauridsen et al. 1998), Finland (Söderqvist and Veijola 1998) and the UK. They all include the use of condition ratings as indicators of repair needs and use Markovian deterioration predictors for elements (Hearn 1998). Explicit evaluation and updating of structural safety are not parts of BMS.

Reliability-based rating models are more recent and its current application to the codes of practice is either shy or implicit. The structural reliability of bridge systems is estimated from bridge elements to the entire bridge. The structural reliability of each structural element is evaluated from their limit state functions, considering the probability distributions of resistance and loading. The interaction between rating and reliability of a group of 14 bridges in an existing network was investigated by Frangopol and Maute (2003). The bridge rating factor and the reliability index are evaluated for various limit states belonging to different member types within the bridge network.

Reliability-based evaluation model contributed to further developments of the structural maintenance methodology that has been set up by the UK Highways Agency, whereas condition-based model has been applied in the Netherlands. A comparison between the two maintenance models was held by Van Noortwijk and Frangopol (2004). While the reliability-based models treat the multicomponent, multi-failure mode and multi-uncertainty case, the condition-based model treats only one component, one failure mode and one uncertainty. Another difference is that reliability-based model uses Monte Carlo simulations, whereas condition-based model is analytical and deterministic. Furthermore, the maintenance models differ in the way the uncertainty in the deterioration is modeled; that is, uncertain parameter as opposed to stochastic processes, respectively. Due to the difference between the condition-based and reliability-based concepts, the management decisions associated with each of these concepts will in general be different.

Reliability and condition based models were also compared by Wang et al. (2012). One of the main disadvantages of reliability-based models when predicting structural health is the low ability to address the interactions between the elements. Redundancy and load redistributions are not adequately considered in reliability-based rating models. Therefore, condition rating may exceed reliability rating for spans with redundant load paths. However, if data is unavailable, then load rating based on AASHTO specifications yields conservative assumptions.

Reliability applications for structural evaluation differ from design because there is more information available from inspection, observation and field testing. Moreover, site-specific information on loading may be incorporated, and therefore, more accurate predictive models can be developed. Site-specific information incorporated in the reliability-based criteria provides useful benefits to the evaluation and the economy of bridge expenditures. This

methodology is used in the Canadian S-6 code (CSA), where the site specific risks are computed and compared to allowable risk values. In the United Kingdom, a bridge assessment standard (BD21/01 volume 3 section 4, The Assessment of Highway bridges and Structures) recommends the minimum acceptable safety levels in terms of load carrying capacity. Nevertheless, bridge engineers are unfamiliar with risk analysis methods. Therefore, the LRDF format of the AASHTO specification can be more familiar to bridge engineers because it works with terminology that makes the risk analysis transparent to the user (AASHTO 2014). The basic methodology is to relate the required safety margins to the level of uncertainty and the target reliability. However, the target safety in the evaluation does not need to be as stringent as in new designs, mainly because of economic factors. AASHTO uses a β value of 3.5 for the design and 2.3 for the evaluation of redundant spans. Moreover, uncertainties for existing structures are often smaller than for new designs when field tests can be performed and additional information can be gathered. Any reduction in uncertainty raises the value of β, and therefore the associated bridge rating. The rating engineer must use judgment to adjust the input uncertainties according to the quantity and quality of available information.

Although probability theory has been successfully applied to deal with uncertainties, practical engineers, inspectors and maintenance workers are not familiar with probability and statistic concepts. Some authors proposed maintenance models that consider uncertainties and/or life cycle user and environmental costs, without having to deal with probabilistic methods. Tamaki et al. (1998) provided some approximate solutions for the uncertain situations without using direct probability methods, by introducing the concept of age into the evolutionary process of a Genetic Algortithm (GA).

Recently, the increase in computational capabilities have made it possible to conduct complex, large-scale simulations, and paved the road for sophisticated probabilistic techniques to be applied to infrastructure management problems (Frangopol and Soliman 2016).

1.8 Reliability-based Maintenance Planning

The evaluation of strength and safety, the modeling of deterioration and the explicit consideration of uncertainties are the main advantages of reliability models over condition rating models. A measure of the time-variant structural performance is realistically possible only in probabilistic terms (Ang and Tang 2007). In order to establish a rational maintenance program, it is necessary to evaluate the structural performance of existing structures. Life cycle cost (LCC) is a useful measure for evaluating structural performance from economic and social points of view. LCC involves the costs of design, construction, maintenance and failure, which are explained in section 1.9. The optimal maintenance strategy obtained by LCC optimization can be different according to the prescribed level of structural performance and required service life.

The basic replacement and maintenance models *are "Control limit rule", "Minimal repair rule" and "Shock models"*. Derman and Veinott Jr (1972) were the first to show that a "control limit rule" is an optimal rule when the probability of deterioration is increasing with time. The idea is: if the probability of deterioration increases in the next period with respect to the present state *i*, then a "*control limit"* rule is optimal, so that one should repair or replace when the observed state *i* is greater than some limit *i**. "*Minimal repair variant models*" are fixed time

repair models (Barlow and Hunter 1960). The repair of a failed unit restores it to a working state but without changing its failure rate from what it was just before it failed. "*Shock models*", firstly introduced by Taylor (1975), suggest that the unit is subject to external random shocks, each of which damage the unit to some degree. The probability that the unit will fail is a function of the accumulated shock damage it has received, but again the optimal policy for preventive repair or replacement is to replace when the amount of damage exceeds a *control limit*.

Optimizing the maintenance planning schedules of deteriorating concrete structures is crucial for maximizing the service life. Nevertheless, engineers have to decide between alternatives that concern different levels of expenditure and different probabilities of success. It is very difficult to decide an appropriate order for repairing some structures among many deteriorating ones within an annual budget, because there are many combinations of repairing times and repairing methods. Moreover, the traffic characteristics of road network and the concept of life cycle cost must be considered.

Several authors applied Genetic algorithms (GA) for the establishment of optimal maintenance planning of existing structures. GA is inspired by the biological evolution. Solution candidates are initially randomly generated. Then crossover, mutation, natural selection and reproduction are repeatedly implemented until a termination condition is fulfilled. Each individual has a fitness value to the environment. The environment corresponds to the problem space and the fitness value corresponds to the evaluation of the objective function. GA can provide useful solutions for large and complex combinatorial scheduling problems with discontinuous objective functions. The concept of Pareto optimum is important to balance the trade-off relations, where an optimal solution cannot improve an objective function without sacrificing other functions. A decision supporting system for the maintenance program of reinforced concrete bridges is developed by Dogaki et al. (2000) using GA. The optimization problem is formulated with two objective functions: maximize the fitness of repair method and minimize user, environmental and maintenance costs. GA was also used by Furuta et al. (2006) to develop a maintenance program of infrastructure systems, considering uncertainties regarding future environmental and deterioration predictions.

There are mainly two types of maintenance interventions: corrective and preventive (Das 1998). Corrective maintenance is required in order to bring the element to the safe condition. Preventive maintenance is carried out before the critical level is reached, in order to postpone the beginning of the critical condition. In general, a performance indicator is used to specify when any work or investigation is deemed necessary. Maintenance interventions can be planned to achieve a prescribed value of the structural lifetime.

The effect of deterioration on the performance level (e.g. reliability index, structural capacity) is schematically shown in Figure 1.8 (Frangopol et al. 2001). The performance level decreases with time due to deterioration. If the calculated performance level is below a target level, the structure has to be strengthened by corrective maintenance. If the performance is above the target level, and yet some work is deemed to be justified, such a work is considered as preventive maintenance. The propagation of uncertainties during the whole life of a bridge is also indicated in this Figure. The probability density functions in Figure 1.8 remind the fact that similar bridges under similar environments have different performance levels at the same point in time.

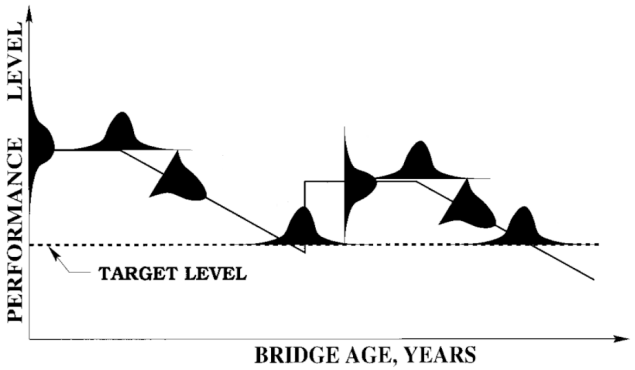

Figure 1.8: Uncertainty propagation during the whole life of a bridge (Frangopol 2001).

The time of application of inspection and maintenance depends on several parameters and randomness. Kong and Frangopol (2003) proposed a method to evaluate the expected probability of maintenance at a certain time of a deteriorating structure and the expected maintenance cost due to the application of subsequent maintenances. Associated costs are predicted by the mean of conditional joint distributions. Decision tree model (Ang and Tang 1984) is used for the evaluation of the expected annual probability of maintenance, where independent reliability cycles are assumed. Maintenance cost estimation is discussed in section 1.9.

Many authors represented the maintenance decisions and related outcomes during a structure lifetime by a decision tree model (Nielsen and Sørensen 2015; Sahraoui et al. 2013), such as in Figure 1.9. To rank a set of design alternatives, the potential risk associated with a given alternative should be considered, as well as the capital cost of the alternative. The procedure identifies first the available alternatives of action and the possible outcomes, or sequence events, associated with each alternative. Then, the respective consequences for each scenario or path can be assessed. The probability of each branch of outcome can be determined either from probabilistic models or by the engineer's judgment based on the available information. The probability of a path is simply the product of the respective probabilities. The expected cost of each alternative is the summation of the path probability multiplied by the path consequence over all outcome scenarios for that alternative. The alternative with the least expected cost is considered optimal if the commonly used “expected value criteria” are adopted for the decision.

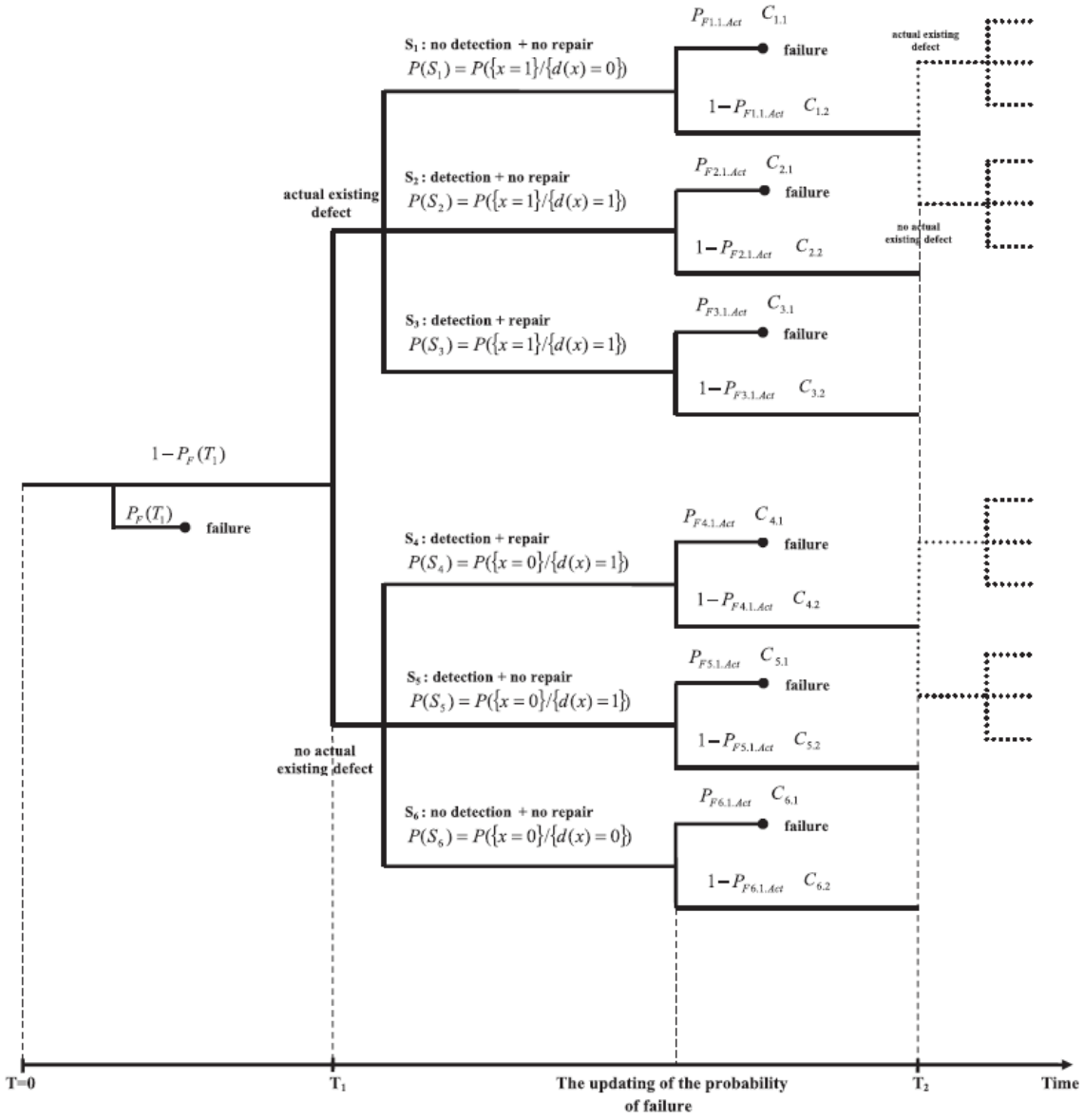

Figure 1.9: Idealized decision tree example for reliability-based maintenance models (Sahraoui et al. 2013).

In addition, structural failure probabilities are calculated based on several limit state functions. Orcesi et al. (2010) presented a global approach to determine the optimal maintenance strategies associated with several limit states. They showed that optimal solutions cannot be seen as a juxtaposition of optimal results for different limit states taken individually. Moreover, some limit states contribute more than the others when considered simultaneously. This contribution can change when different or additional constraints are applied. A series system is considered in Orcesi's approach, and structural health monitoring *(SHM)* is included to determine the optimal maintenance strategies (Orcesi and Frangopol 2011).

Recently, many algorithms were used to provide solutions for the maintenance scheduling with reasonable time; e.g. Genetic Algorithm (Sabatino et al. 2015a), Simulated Annealing Algorithm (Doostparast et al. 2014). The results of recent works showed that the cost

reduction yielded by the maintenance optimization is very dependent on the system configuration, the number of components, the planning horizon and the reliability threshold.

It is however observed that many studies proposed approaches to optimize the maintenance planning of systems with independent components, but few considered dependencies. In the following section, the different types of dependencies and the main advances concerning each type are discussed.

1.9 Correlation of the components of a structural system

The interactions between the components in a system should be taken into account in maintenance and replacement policy. Many of the multi-unit systems are designed so that their structural dependency improves the system reliability through redundancy. However, the structural dependency may also decrease the system reliability (as discussed in section 1.5). This dependency between the elements means, however, that the net optimal operating policies for the single element rarely remain optimal for multi-unit systems. Thomas (1986) defined three types of interactions in a multi-unit system: economic, structural and stochastic. Each of these interactions was studied to some extent by several authors, but very rarely several types were considered in a single study. Though, we will review the main works in this field in the following subsections.

1.9.1 Economic dependency

The cost of replacement and maintenance has interdependencies between the elements. The simplest of such case is when the replacement or repair cost of several components is less than the sum of their individual replacement or repair costs.

Opportunistic replacement introduced by Radner and Jorgenson (1962) is one of the first examples of economic dependency. When the cost or time of replacing two or more units in the system is less than the sum of their individual replacement costs or times, it may be worthwhile to replace a working unit when one is replacing other failed units. Many opportunistic models were introduced, e.g. the (n, N) strategies (Sasieni 1956), and preparedness problem (Radner and Jorgenson 1962), where the costs of inspection and repair when emergency occurs costs more than when the same inspection and repair occurs under non-emergency condition. Laggoune et al. (2009) developed a preventive/ corrective/ opportunistic maintenance plan for a multi-component system subject to high production loss and economic dependency. Grouping maintenance is considered in many studies by the means of a penalty cost caused by shifting from the component optimal cost. Laggoune considered a series system, given by the arrangement of components, and described all the possible “operation” or “failure” scenarios. When a component fails, it is replaced by a new one and the whole system is down during the replacement operation. A non-failed component can also be replaced during preventive maintenance. The economic dependency is due to the production loss when the system is down for corrective or preventive replacement of components. The cost model is divided into a first part related to common costs and a second part related to the specific component. However, in Laggoune’s study, there was no consideration of structural failure interaction. Among the very rare studies considering at the same time several dependencies, economic and structural dependencies are considered simultaneously by Van Horenbeek and Pintelon (2013) by the

mean of a partial dependent parameter α_d multiplied by the set-up cost. The set-up cost illustrates economic dependency, and the non-zero times illustrate structural dependency. However, the structural dependency is defined by the fact that the downtime affects all failed and non-failed components. Other aspects of structural dependency may have stronger effect on the optimal planning, namely; horizontal dependency due to the system structure, and vertical dependency due to the system modular subunits (Thomas 1986).

Many authors considered series systems (Laggoune et al. 2009; Van Horenbeek and Pintelon 2013), which may not be adequately applicable in the case of redundant structures formed by interrelated components with many possible load paths. Several combinations of basic structures were investigated by Vu et al. (2014) (series, parallel, k-out-of-n structures) via the criticality of components, where the system fails if a critical component fails, but can still be functioning if a non-critical component fails.

1.9.2 Socio-economic dependency

As infrastructures also involve risk to human life and limb, a socio-economic acceptability criterion is to be added as a constraint to the cost-benefit analyses. Civil engineering structures should be optimal not only from a technological point of view but also from a sustainability point of view. The cost as well as the benefits may differ for the different involved parties; e.g. the owner, the builder, the user and the society, which may also have different economic objectives. In view of sustainability, one has to distinguish between at least four replacement strategies:

- the facility is given up after service or failure
- the facility is systematically replaced after failure
- the facility is repaired after deterioration
- the facility is renewed due to obsolescence

Rackwitz et al. (2005) proposed renewal models that considers the monetary loss in case of failure including direct failure cost, demolition cost, cost of removal of debris, loss of business and other indirect costs and, of course, the cost to reduce the risk to human life and limb. He further decomposed the losses into physical losses and losses associated with human life and limb. Social dependencies can only be modeled by the quantification of indirect failure cost such as loss of use by the public, loss of business, and the assessment of the benefit derived from a civil engineering infrastructure, which are very difficult tasks.

A modular framework for assessing the economic, environmental and social impacts of structural durability has been proposed by Flint et al. (2014) and applied to concrete structures expected to undergo climate changes accelerated chloride induced reinforcement corrosion. The analysis has been divided into three stages: exposure, deterioration/repair, and impact. At each stage, the distribution of the probability of exceeding a specified threshold is computed. These distributions are conditioned by the output value of the previous state. Convolving a series of conditional distributions yields a final distribution for lifetime decision information. However, in Flint's study, the frequent repairs were responsible of high costs and downtimes, therefore, concurrent maintenance may have been considered.

1.9.3 Structural dependency

Whereas with economic dependencies it may be useful to replace the working units at the same time as the failed ones, structural dependencies mean that one has to replace or at least dismantle some working units in order to replace or repair the failed ones (Thomas 1986). There are two types of dependency: horizontal and vertical. Horizontal dependency is the connection between the units of the system that affects the system reliability. The vertical dependency is the system modular structure that affects the maintenance and replacement policies of the system. Many models consider the items in a multi-item system as being on different levels or echelons. If the system is built in modular form then when replacing any module, it is necessary to question whether to replace all the sub-modules attached to it or not. Many suboptimal policies have been suggested for this problem, such as the minimum replacement, the replacement of the whole system when a unit fails, or by linking the replacement policy to a defined limit age for every unit.

Another type of structural dependency that has been studied recently is the bridge-vehicle interaction (VBI). The fundamental problem in VBI modeling is that the contact points move with time and for each point in time, the displacements of the vehicle are influenced by the displacements of the bridge, which affect the vehicle forces applied to the bridge which in turn again alter the bridge displacements and interaction forces. Vehicle-Bridge Interaction (VBI) problems were initially addressed by railway engineers. VBI modeling offers a mean to extend the analysis to a wide range of scenarios, namely the effect of road roughness or expansion joints, the effect of vehicle characteristics such as suspension, tyres, speed, axle spacing, weights, breaking, or the effect of bridge structural form, dimensions and dynamic properties (González 2010).

A framework to determine optimum maintenance strategies by considering the risk attitude, structural correlation among components and the number of maintenance interventions on the optimum maintenance strategies was presented by Sabatino et al. (2015a), where lifetime functions and correlation effects are directly incorporated within risk calculations. However, only perfect or nil correlations were considered.

1.9.4 Stochastic dependency

In practice, civil engineering structures consist of multiple components and the failure of one component affects the other components. This means that failures in multi-component systems are stochastically correlated. Failure interaction occurs either due to system mechanism or design problem, which decreases the system reliability. Therefore, the failure dependency among component should be taken into account in the design and maintenance of a multi-component system.

Thomas (1986) defined the following failure interactions:

- The sudden failure of an item potentially produces failure to the subsequent downstream items; which may be the modular components attached to the failed item.
- The failure of some items causes an increased load to be carried by the working items; this may be the case of the load redistribution that occurs in case of a bearing component failure.

- There is a common cause of failure effect produced by external sources, such as earthquakes or hurricanes, etc...

Failure interactions are divided into three types by Lai and Chen (2008):

- Type I failure interaction: when a unit fails, other units will immediately fail at a certain probability.
- Type II failure interaction: a failure of a unit is regarded as an internal shock that increases failure rates of other units.
- Type III failure interaction: a failure of one unit causes a random amount of damage to the other units.

Such interdependencies occur commonly in practice, but they are difficult to model because the probabilistic dependencies are hard to estimate.

Murthy and Nguyen (1985) were the first to derive expressions for the expected cost of operating two-component system with failure interactions. In their study, the failure of a component induces the failure of the other component with probability p, and has no effect on the other component with probability $1 - p$.

Some authors proposed inspection and/or maintenance optimization models for a two-unit system subject to failure interactions (Golmakani and Moakedi 2012). Nevertheless, their models are limited to two components and to a specific type of failure interactions.

Few researches extended the modeling of failure interaction to more than two-unit systems. “Common cause” failure interaction for several-units system is considered in Khodakarami and Abdi (2014). They proposed a Bayesian network approach to model dependencies between cost items. However, the authors only consider project cost from permit to construction. Moreover, their model needs the knowledge of the probabilities of common causes which are obtained by expert questionnaires and thus may be subjective. Only “common cause” correlation is modeled, which is a failure effect produced by external sources like organizational issues, technologies, material, etc…Though, there is other failure correlation types that may occur like “cascade” or “compound” consequence correlation.

1.9.5 Interaction between deterioration models

In general, the deterioration caused by the combined mechanisms is more harmful than the ageing induced by a single mechanism. Kari (2011) developed a model to combine different damage models to one service life model. Kari’s model was used to determine the interactive effects between the penetrating chlorides and the carbonation of the concrete and freezing of concrete (Kari 2011). A challenge in the modeling is to combine the mechanisms of varying humidity and temperature, taking into account the concrete freezing. In addition, the external concentrations of the chlorides are not constant during the exposure period. The mechanisms identified and included in the mathematical model are: the carbonation of concrete, moisture ingress, chloride penetration and internal and external frost damage. The deterioration caused by the combined mechanisms is significantly more damaging than the ageing induced by a single mechanism. The mathematical methods based on a group of differential equations can be used to simulate the interaction of different deterioration mechanisms. The obtained results emphasize the importance of considering the interaction between different deterioration mechanisms of reinforced concrete.

Even in case where only one deterioration mechanism is considered, the performance functions of the different members in a system have common variables, and the other variables have various degrees of correlation.

Nicolai and Dekker (2008) published a review report on the literature works on multi-component maintenance optimization, focusing on the dependency between components. The articles were classified on the basis of dependency (stochastic, structural and economic). Planning is also discussed (Finite and infinite horizon). The type of optimization is apprehended (exact, heuristic or policies). Their conclusion is that more researches are needed to model the combinations of dependencies, the multiple set-up activities, and more case studies are to be intended. In addition to Nicolai and Dekker's conclusions, in our opinion, many weaknesses must be addressed, particularly the fact that most works dealing with stochastic dependency only considers two components. Moreover, very few articles deal with structural dependency.

1.10 Life cycle cost analysis

Structural design and management must ensure adequate level of reliability at the lowest possible life-cycle cost. Many authors proposed methods to evaluate the life-cycle cost of concrete structures. A life-cycle cost analysis (LCCA) can lead to a more economic long term decision making, like the use of costly materials and systems or the adoption of a structural conception that has a higher initial cost but requires less maintenance or is less susceptible to fail. For example, Val and Stewart (2003) justified the use of stainless steel reinforcing bars in RC structures in marine environment, even though they are six to nine times more expensive than carbon steel. For this purpose, they proposed a time-variant probabilistic model to predict the LCC under different exposure to corrosion conditions. A brief review of the life-cycle reliability-based optimization field was presented by Frangopol and Maute (2003). One of the paper broad conclusions is that the life-cycle optimization criterion in the design of new structures is the minimum expected total cost. Alternatively, for planning maintenance interventions on existing structures, the expected total intervention cost has to be used as the optimization criterion.

A general LCC model consists of initial costs and direct and indirect rehabilitation costs, including repair/replacement costs, loss of contents or fatality and injury losses, road user costs, and indirect socio-economic losses (Lee et al. 2004). Many formulas for the expected life-cycle cost can be found in the literature, sharing the same basic components (Frangopol and Maute 2003; Val and Stewart 2003; Yang et al. 2004):

$$LCC(t) = C_{ini} + C_{QA} + C_{Ins}(t) + C_M(t) + C_{DC}(t) + C_{IC}(t) + C_D(t) \tag{1.13}$$

where C_{ini} is the initial cost, C_{QA} is the cost of quality assurance, $C_{Ins}(t)$ is the cost of inspections, C_M is the maintenance cost, $C_{DC}(t)$ and $C_{IC}(t)$ are respectively the direct and indirect failure costs, $C_D(t)$ is the cost of disposal, and t is the analysis period. Each future cost $C(t)$ is then converted to the present value $C_{PV}(t)$ via the discount rate v at time t as follows;

$$C_{PV}(t) = \frac{C}{(1+v)^t} \tag{1.14}$$

The current value of the discount rate used in different countries varies from 2% to 10% (Frangopol 1999). These values have significant implications on structural management and maintenance planning. This is due to the fact that including the discount rate gives the opportunity of performing the same maintenance option at different times in the future where each one has different calculated present cost (Soliman 2015). Choosing a higher discount rate may promote management strategies with low initial costs but high future costs (Orcesi 2015). Therefore, including a realistic discount rate allows the manager to select the best maintenance planning which fits the management constraints.

1.10.1 Initial Costs

Woodward (1997) defined the initial cost as "the capital cost category that includes all the costs of buying the physical asset and bringing it into operation". The importance of minimizing the initial cost has been recognized long time ago. For example, in case of RC structures, an owner may prefer the use of more volumetric concrete in the aim of decreasing the weight of steel (if the decrease in steel volume is more cost-effective than a decrease in concrete volume). The initial cost is related to the material and the labor cost for the construction of the structure which includes, in the case of reinforced concrete structures: concrete, steel reinforcement, labor cost for construction and material transportation, as well as the non-structural cost components such as project management, overhead, tool locations, etc…(Mitropoulou et al. 2011).

1.10.2 Inspection and Maintenance costs

Effective cost evaluation methods are needed to assess reasonable expenditures for managing structures during their service lives, where structures can experience various types of inspection and maintenance actions at different times. The associated costs of these actions can only be predicted by the mean of conditional joint distribution. The method of evaluating the probability distributions of associated maintenance actions is described in Frangopol et al. (2001) and Kong et al. (2000, 2001). Let us assume the case where *n* rehabilitations occur at relative time scales $t_1, \dots, t_n$. The origin of the relative time scale is the time of occurrence of the previous rehabilitation. The absolute application time of the n^{th} rehabilitation is:

$$T = t_1 + t_2 + \cdots + t_n \tag{1.15}$$

The total expected rehabilitation cost at time T associated with all possible rehabilitation cycles is:

$$C_M(t) = \sum_{i=1}^{n} \sum_{j=0}^{t} \frac{P_i(j) \times C_{M,i}}{(1+\nu)^j} \tag{1.16}$$

where $C_{M,i}$ is the undiscounted cost of the i^{th} rehabilitation, $P_i(j)$ is the probability mass function at time *j* associated with the i^{th} rehabilitation cycle, and ν is the discount rate.

It is difficult to obtain the probability mass functions associated with all rehabilitation cycles. The correlations between various rehabilitations may be obtained if the time-dependent behavior of a deteriorating system is known. Therefore, statistically independent rehabilitations

are usually considered. Using this assumption, the expected probability of rehabilitation at time j can be obtained from the product of all probability mass functions of rehabilitations at this time.

Joint probability calculation requires expensive multiple integrals. To reduce the computational time, decision tree method applicable to all rehabilitation scenarios can be applied for discrete probability mass functions. A decision tree example showing all possible paths after applying two rehabilitations is drawn from Frangopol and Kong (2001) and shown in Figure 1.10. Subscripts A and R are used to indicate that the rehabilitation is based on the absolute and relative times respectively. $P_{i,A}$ represents the probability of the i^{th} rehabilitation with respect to the absolute time scale. The probability that rehabilitation will occur at a specific time can be obtained from the decision tree by selecting all paths ending at the same time and adding all probabilities associated with these paths.

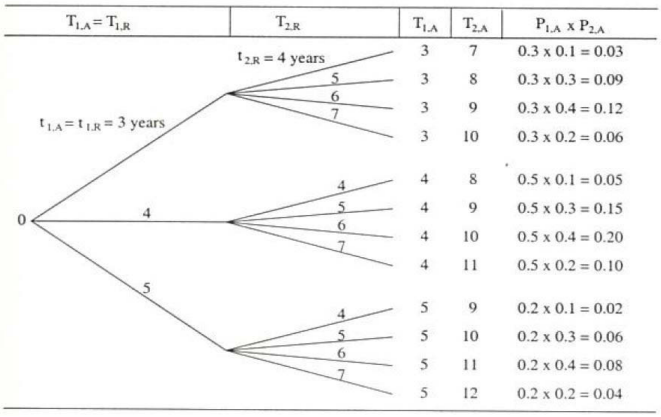

Figure 1.10: Example of a decision tree after applying two rehabilitations (Frangopol and Kong 2001).

1.10.3 Direct and Indirect Failure costs

The failure cost corresponds to the monetary consequences associated with system or component failure. It is referred as "risk" in many papers (Sabatino et al. 2015b; Barone and Frangopol 2014) and defined as the product of the failure probability by the consequences due to failure in monetary equivalence (Ang and Tang 1984).

Failure cost is a result of violating a critical limit state of failure or serviceability. The complexity of evaluating the failure cost is mainly due to: (1) the decrease of structural resistance with time; (2) the uncertainties related to the stochastic nature of load and material parameters; and (3) the indirect consequences of failure. It is very important to wisely evaluate the probabilistic lifetime of concrete structures subject to degradation with time. The present value of the expected life-cycle failure cost at time t can be estimated as follows:

$$C_F(t) = \sum_{i=1}^{M} \sum_{j=0}^{t} \frac{P_{fi}(j) \times C_{fi}}{(1+v)^j} \tag{1.17}$$

where M is the number of limit states (i.e., flexure, shear, crack width), $P_{fi}(j)$ is the annual probability of failure for limit state i at the j^{th} year, v is the discount rate and C_{fi} is the failure cost associated with limit state i.

These monetary consequences cover the direct costs related to failure, which can be the cost of rebuilding (material and labor, etc...). The direct costs are usually suffered by the owner, but other indirect costs related to failure may be suffered by the users, the society or by the environment. Therefore, the failure cost can be estimated as the sum of direct and indirect costs for the limit state i (Lee et al. 2004):

$$C_{fi} = C_{DCi} + C_{ICi} \tag{1.18}$$

where C_{DCi} is the direct cost and C_{ICi} is the indirect cost. Several models have been proposed to estimate the effect of indirect economic, social and environmental costs arising from structural failure or from maintenance activities on the life-cycle cost. In the aim of quantifying the user delay costs suffered by motorists in case of bridge failure or maintenance, a model to estimate the vehicle operating cost was proposed by Berthelot et al. (1996).

Ehlen (1999) divided the total project cost into agency, user, and third-party costs; where examples of third-party costs are lost business revenues for establishments whose customers are blocked by project activity and environmental damage and costs that result from toxic runoff. Ehlen did not quantify the third party costs; however he proposed equations for different components of user delay cost to examine the life-cycle cost-effectiveness of three fiber reinforced polymer bridge decks.

Equations were also developed for calculating traffic disruptions based on typical traffic control plans by Tighe et al. (1999). User and environmental costs were also evaluated by Dogaki et al. (2001) in the aim of developing a decision support system for maintenance planning of bridge decks. User costs are usually dependent on the traffic volume and speed, the number of lanes, the number of days the road is closed and the unit requirements for driving cost and time. Later, the computation of road user delay costs was established by the New Jersey department of transportation who issued a road user delay manual (DOT 2001).

Lee et al. (2004) proposed a newer road user cost model and regional socio-economic losses model for steel bridges. The costs resulting from the traffic, environmental, and commercial impacts of construction are defined as social costs by Yu and Lo (2005) who estimated them as 5.52 times the total construction cost.

Kendall et al. (2008) compared the life cycle costs of two bridge deck systems, including agency, user and environmental costs. As in Kendall's study, user costs dominate other costs, and comprise more than 90% of the total life cycle costs for both systems, while environmental costs did not exceed 0.5% of the total costs.

Orcesi and Cremona (2010) evaluated the user delay cost based on a method provided by QUADRO (Queues and delays at road works) for the aim of proposing an advanced bridge management system.

The Federal Highway administration (FHWA) issued a final report on work zone road user cost concepts and applications (Sadasivam and Mallela 2015), where the user delay cost is defined as the additional costs carried by motorists and the community as a result of work zone activity.

Many authors used the bridge user cost formulations to compare new materials/systems (Kendall et al. 2008), or to propose new bridge maintenance planning (Sabatino et al. 2015a).

The direct loss is measured by Sabatino et al. (2015a) in terms of the risk associated with the rebuilding cost during a certain year, while the indirect consequences of bridge failure include the extra travel time and distance experienced by vehicle operators, in addition to any fatalities that may occur. The environmental impacts were quantified by accounting for the carbon dioxide emissions and the energy consumption associated with detour and bridge repair.

In general, indirect risks integrate the effects of both social and environmental consequences of structural failure. Recently, more sustainable decision making are urged by combining the life cycle assessment (LCA) with life cycle costs. Islam et al. (2015) suggested a life cycle management perspective by integrating life cycle environmental impacts (LCEI) and life cycle costs (LCC) components to identify optimal trade-off between different roofing and floor designs for typical Australian houses. However, risk attitude via failure costs were not considered in their study.

1.11 Conclusion

This literature review focuses on reliability techniques and formulations used to optimally design and maintain a structure during its lifetime.

Structural reliability models are the basis of many design codes including load and resistance factor design (LRFD) which deals with load-carrying capacity and safety. The reliability-based design and maintenance implies the assessment of the life-cycle and the evaluation of the structural failure probabilities, which are calculated objectively based on several explicit limit state functions. Life-cycle assessment requires the knowledge of the general methods for the computation of direct and indirect cost components, which are discussed in this chapter. The structural safety assessment entails the understanding of methodologies for predicting the degradation processes, taking into account uncertainty and variability through time-variant probabilistic assessment.

The general concepts of maintenance scheduling are also discussed with emphasis on the condition-based and the reliability-based maintenance planning. In this framework, we review the state-of-art that shows low consideration of various types of interaction between components of a system.

From this literature review, it comes that existing procedures concerning the reliability-based design and maintenance procedures undergo many limitations: (1) indirect consequences of failure are poorly exhibited, (2) the interactions between structural elements are not explicitly addressed, (3) the system is not properly approached to consider interdependent elements, (4) the representation of a system as a parallel and/or series structural elements does not account for the real structural redundancy and configuration, (5) the reliability and robustness of optimization procedures are not simultaneously addressed .

The procedures to overcome the above cited disadvantages are proposed in the following chapters.

Chapter 2 : Cost-effective Probabilistic Design

2.1 Overview

The traditional structural design methods focused on minimizing the structural weight while ensuring that the loading effect is less than the resistance. Afterwards, the structural weight is replaced by the initial construction cost, which can better reflect the contractor's objective of favoring the use of less costly materials. Minimizing the construction cost may seem appealing to designers; however, this method does necessarily not ensure structural durability. For this reason, recent researches aimed at designing structures that minimize the total expected cost of the structure during its service lifetime, by including the monetary expectation of the consequences of failure. However, these failure consequences are significantly amplified by social and environmental impacts, which should be included in the total cost when designing structures.

Conservative empirical partial safety factors were used to cover the lack of knowledge concerning the uncertainties related to material parameters and loads. This traditional procedure produced conservative and safe designs. The situation has changed mainly due to economic pressure and increased traffic weight, combined with the availability of computer analysis methods that are pushing the designs closer to their failure limits (Moses 1999). Lately, research efforts have led to new probabilistic design methods based on structural reliability which explicitly deals with criteria based on uncertainty effects. The probabilistic methods require the performance prediction of the structure, which deteriorates due to the effect of excessive loading and harsh environment. Degradation models may be often successfully adopted for an overall evaluation of the life-cycle structural performance (Biondini et al. 2006). Therefore, deterioration models have been developed to describe the time-variant behavior of the structure and its environment. In aggressive environments where concrete bridge structures support high traffic frequencies, the two main degradation models are corrosion and fatigue. A coupled deterioration model of fatigue and corrosion has been developed by Bastidas-Arteaga et al. (2009) and is used herein to assess the structural performance of the RC elements.

The aim of this chapter is to optimize the design parameters of the structural elements, and not the maintenance planning of the structural system, which will be studied in the next chapter. In the following sections, a LCC model for structural design is detailed and improved, and a method to estimate more precisely the indirect consequences of failure is proposed. Then, the degradation processes of fatigue and corrosion are considered. Finally, a procedure that allows integrating indirect failure consequences and considering the coupled deterioration mechanism is proposed and verified through the optimization of the design of structural elements.

2.2 Life-cycle costing

A general life-cycle cost (LCC) model for new structures consists of initial costs and direct and indirect rehabilitation costs, including repair and replacement costs, loss of contents or fatality and injury losses, road user costs, and indirect socio-economic losses (Lee et al. 2004). Most phenomena involved in the total cost are time-variant, because loading fluctuates over the lifetime of a structure, and resistance degrades with time. When designing a new structure, the ideal scheme consists of considering the whole lifetime of the structure in a time-variant

reliability-based design optimization framework. Considering that all parameters related to design are uncertain and need to be modeled by random variables, the corresponding life-cycle cost is itself a random variable. Therefore, designers should use the expectation of the life-cycle cost function in order to take into account the probabilistic events. Many formulas for the time-dependent expected life-cycle cost can be found in the literature, sharing the same basic components (Val and Stewart 2003):

$$LCC = C_{ini} + C_{Ins} + C_M + C_F \tag{2.1}$$

where C_{ini} is the initial cost, C_{Ins} is the cost of inspections, C_M is the maintenance cost, and C_F is the failure cost. Each future cost C is converted to its present value C_{PV} using the discount rate ν at time t as follows:

$$C_{PV} = \frac{C}{(1+\nu)^t} \tag{2.2}$$

The current value of the discount rate used in different countries varies from 2% to 10% (Frangopol 1999). These values have significant implications on management and maintenance planning. This is due to the fact that including the discount rate gives the opportunity of performing the same maintenance option at different times in the future where each one has different calculated present cost (Soliman 2015). Choosing a higher discount rate may promote management strategies with low initial costs but high future costs (Orcesi 2015). Therefore, including a realistic discount rate allows the manager to select the best maintenance planning which fits the management constraints.

The different cost items in the expected life-cycle cost function have been described in chapter 1.

2.2.1 Why neglecting maintenance costs during design optimization?

Dealing with maintenance and design uncertainties simultaneously is a very difficult task due to the high complexity of engineering structures.

Many researchers such as Kang and Wen (2000) and Lee et al. (2004) stated that although the maintenance costs over a lifetime may be high, their dependence on the design variables under consideration were generally weak. Moreover, Gomes et al. (2013) showed that optimum expected total costs are not highly sensitive to the assumed costs of inspection. The above statements may be debatable; therefore, the following example is developed in order to observe the influence of maintenance planning on design variables.

In this example, the steel cross-section of a deteriorating reinforced concrete (RC) beam is optimized considering the number of inspections and maintenance actions during the lifetime of the structure. The beam is located in an extreme corrosive environment. The corrosion model detailed in Appendix 2 is used in this example to predict the service life of the structure. The model considers that the steel reinforcement cross-section is reducing with time due to uniform corrosion. With no loss of generality, the bending limit state function is considered in this example. The random variables are defined by statistical distributions. Classically, the parameters of the density functions are adjusted by maximum likelihood estimations and goodness-of-fit tests are conducted to determine the validity of the assumed distributions. In

this example, the statistical descriptions are shown in Table 2.1, where data are taken from literature (El Hassan et al. 2010; Bastidas-Arteaga et al. 2011). The initial value of the design variable A_s^* is 8 cm^2.

Variable	Symbol	Average	COV	Distribution
Random Variables				
Concrete Compression	f_c	30 MPa	0.15	Lognormal
Steel strength	f_y	500 MPa	0.07	Lognormal
Concrete cover	c	0.05 m	0.2	Lognormal
Chloride concentration	C_{th}	0.9 kg/m^3	0.19	Lognormal
Chloride concentration	C_s	7.35 kg/m^3	0.7	Lognormal
Coefficient of diffusion	D_c	6.10^{-12} m^2/s	0.2	Lognormal
Dead Load	G	26 kN/m	0.15	Normal
Punctual design Load	Q	90 kN	0.25	Normal
Deterministic Variables				
Beam length	l	10 m		
Beam width	b	0.4 m		
Beam height	h	0.7 m		
Water/cement ratio	wc	55 mm		
Elastic modulus of steel	Es	210000 MPa		

Table 2.1. Statistical Description of variables.

The probability of failure is approximated by the first order reliability method (FORM) at every inspection interval. The number of inspections is considered as known a priori. The number of maintenance actions depends on a repair criteria linked to the reliability index of the structure at the time of inspection. Maintenance is considered to take place when the failure probability at the time of inspections exceeds a predefined threshold P_f^R.

Let δt_{insp} be the interval of inspections fixed a priori. The number of inspections N_{insp} during the lifetime L_T is $N_{insp} = \frac{L_T}{\delta t_{insp}}$. Let δ_{Repair} be the maintenance interval, which is calculated such that the failure probability at the time of inspections exceeds the repair threshold. Perfect repair is considered, therefore the number of maintenance during the structural lifetime L_T is $\frac{L_T}{\delta t_{Repair}}$.

A reliability-based optimization formulation is used as follows:

Find d

Minimizing $C_T(x,d,t) = C_{ini} + C_{Ins}(t)\ \frac{t}{\delta t_{insp}} + C_M(t)\ \frac{t}{\delta t_{Repair}} + C_f(t)\ P[g(x,d,t) \le 0]$

Such that

$$P[g(x,d,t) \le 0] \le P_f^T$$

$$d_L \le d \le d_U$$

$$\delta t_{Repair} = n\,\delta t_{insp} \quad if \quad P\left[g\left(x,d,(n\,\delta t_{insp})\right) \le 0\right] \ge P_f^R \qquad n = 1,\cdots,N_{insp} \quad (2.3)$$

where x and d are random and design variables respectively, L_T is the studied timespan of the structure, $C_T(x,d,t)$ is the total cost, P_f^T is the admissible probability of failure, P_f^R denotes the repair criterion which is a threshold failure probability for repair.

The associated costs of inspection, maintenance and failure are defined as functions of the initial cost C_{ini} such that :

$$C_\eta^\nu = \frac{f_\eta \times C_{ini}}{(1+\nu)^t} \tag{2.4}$$

where ν is a discount rate taken equal to 0.05, η is an event of inspection, repair or failure occurring at time t. f_η is taken equal to 0.0177 for inspection, 0.4 for maintenance and 25 for failure (Gomes et al. 2013).

The design value A_s^* is optimized for different values of P_f^T and P_f^R using the optimization module in Matlab software (Figure 2.1).

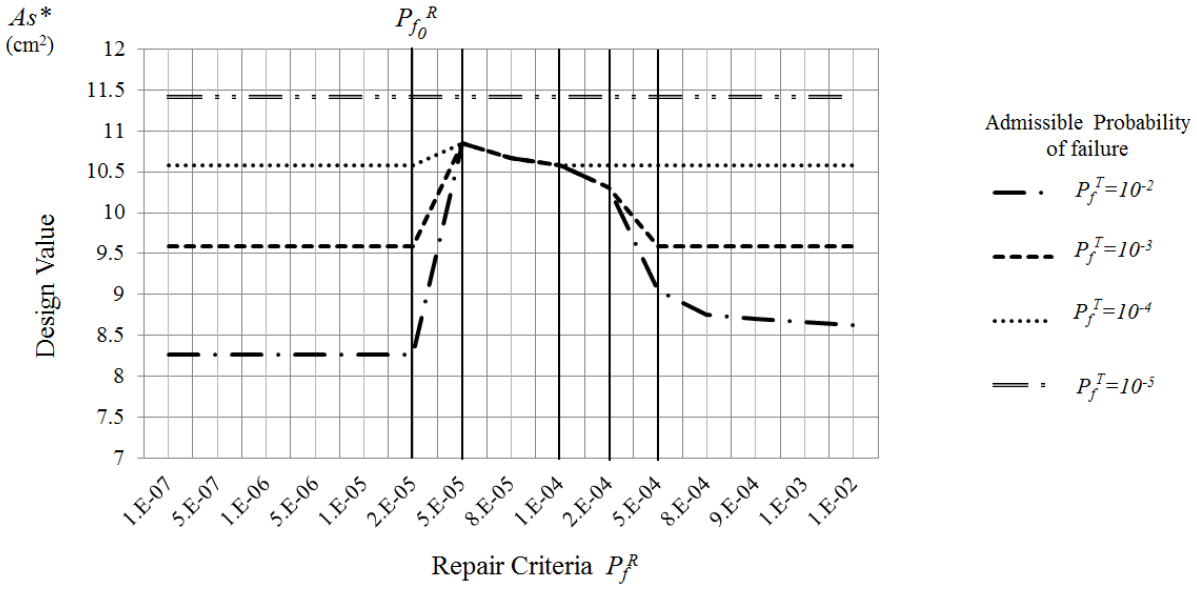

Figure 2.1. Optimization results for different values of repair criterion and admissible probability of failure.

As explained above, P_f^T is the admissible probability of failure and P_f^R denotes the repair criterion which is an admissible probability of failure before repair.

Let $P_{f_0}^R$ be a repair criterion below which repair has to take place at every inspection, i.e. $\delta t_{insp} \geq \delta t_{Repair}$. Since the probability of failure is only estimated at time of inspections, then $\delta t_{insp} = \delta t_{Repair}$. Thus the maintenance cost is constant for all repair criterion below the value of $P_{f_0}^R$. This is caused either by very stringent repair criterion, or by very large inspection intervals. Hence at every inspection the structural probability of failure is higher than $P_{f_0}^R$. For this example the value of $P_{f_0}^R$ is equal to 2×10^{-5}. From Figure 2.1, three failure domains can be distinguished:

Domain 1: $P_f^R \leq P_{f_0}^R$

As shown in Figure 2.1, a repair criterion below the value of $P_{f_0}^R = 2 \times 10^{-5}$ has no influence on the design value for all admissible probability of failures $P_f^T = [10^{-5}, 10^{-2}]$. This may be caused by the stringent value of the repair criterion which requires maintenance at every inspection time, and thus the maintenance cost becomes constant and irreducible. In this case, the probabilistic constraint is the dominant design factor, and the inclusion of the maintenance planning in the optimization has no influence. The design value can be obtained by minimizing only the initial and failure costs, since in this case the inspection and maintenance costs have no influence on the optimal solution:

$$d^* = argmin\left(C_{ini} + C_F(t)\right) \qquad \forall\, P_f^R \leq P_{f_0}^R \tag{2.5}$$

Domain 2: $Pf_0^R < P_f^R < P_f^T$

In this case, the repair criterion requires a design value higher than the value imposed by the admissible failure probability in order to reduce the maintenance cost. The design value in this case is independent of P_f^T, i.e. the same design value is imposed by P_f^R for all values of the admissible failure probability. For example, as shown in Figure 2.1, for a repair criterion of $P_f^R = 2 \times 10^{-4}$, the same design value $A_s^* = 10.3\, cm^2$ is obtained for P_f^T equal to 10^{-2} or 10^{-3} because P_f^T is higher than P_f^R . However, if $\left(P_f^T = 10^{-4}\right) < \left(P_f^R = 2 \times 10^{-4}\right)$, then a different design value is obtained $A_s^* = 10.51\, cm^2$. Also, for a repair criterion of $P_f^R = 5 \times 10^{-5}$, the same design value $A_s^* = 10.58\, cm^2$ is obtained for P_f^T equal to 10^{-2} or 10^{-3} or 10^{-4}, but another design value is obtained for P_f^T equal to $10^{-5} < P_f^R$. Nevertheless, domain 2 is very improbable practically because it is not likely to set a repair criterion P_f^R more stringent than the admissible failure probabilityP_f^T.

Domain 3: $P_f^T \leq P_f^R$

In reality, managers will set a repair criterion P_f^R smaller than the admissible probability of failure. It is irrelevant to repair the beam for any failure probability higher than the admissible target during the service life of the structural element, because the element is considered as failed when its probability of failure reaches P_f^T. Figure 2.1 shows that the repair criterion does not have an impact on the design value beyond the target reliability. For example, when the admissible probability of failure is 10^{-3}, only a repair criterion between 5×10^{-5} and 2×10^{-4} can modify the design value, which is a more severe value than the targeted admissible probability of failure itself. Also, when the admissible failure probability is 10^{-5}, even a repair threshold of 10^{-7} cannot modify the design value.

As shown above, including the maintenance planning when designing a structure may influence in some cases the optimum design values. However, a common approach which is widely accepted in engineering practice consists in separating the design into two steps (Chateauneuf 2008). In the first step, the structure is designed to avoid failure, hence the total cost minimization is carried out for initial and failure costs. In the second step, the maintenance planning is optimized for the structure designed in the first step; therefore the total cost corresponds to the maintenance cost. This approach has the practical advantage of designing

structures that are independent of the maintenance policy which may vary over the lifespan due to environmental or political considerations. However, it presents the drawbacks of neglecting any conflicting influence of the variation of some design variables on failure and maintenance costs. In the remaining of the present chapter, only initial and failure costs are considered. Therefore, the total expected cost to minimize when designing a new structure $C_T(t)$ is simplified to (Ditlevsen and Madsen 1996) :

$$C_T(t) = C_{ini} + C_F(t) \tag{2.6}$$

Note that a more rigorous mathematical notation consists in writing $E[C_T(t)]$ instead of $C_T(t)$ because what is optimized is the expectation, not the cost itself which is a random function (Chateauneuf 2008). However, we will proceed with the notation in equation (2.6) for simplicity.

In the following subsection, a discussion is held concerning failure costs purposes and developments.

2.2.2 Direct and indirect failure costs

Several models have been proposed to estimate the effect of direct and indirect economic, social and environmental costs arising from structural failure or from maintenance activities on the life-cycle cost. The cost formulations and an overview of the related researches are provided in Chapter 1 section 10. The contribution of this chapter is focused on assessing the road user costs, which is believed to dominate other indirect costs in case of bridge structures (Kendall et al. 2008). The Road User Costs are incurred by the public users of the bridge due to the blocking of normal traffic flow. When traffic level increases, the road user costs can be significant. For example, the New Jersey department of transportation has constructed a 1 million dollars full width shoulder to reduce road user costs by 2 million dollars. Therefore, designers should consider road user costs when determining the most appropriate construction design.

User costs include those caused by traffic control and detours, in the form of vehicle operating costs and costs from delays and accidents. The indirect user costs from delay and detours may be due to inadequate load capacity, environmental damage, traffic congestion, or work zone impacts during construction. The amount of delay is related to the traffic flow on the road, the closure time, the detour length, the vehicles speed and the type of used traffic management (Gould et al. 2013)

The road user cost is estimated as follows (Ehlen 1999):

$$C_U = C_{DT} + C_{VO} + C_{CR} \tag{2.7}$$

where C_U is the user cost, C_{DT} is the cost of delay time, C_{VO} is the vehicle operating cost, and C_{CR} is the accident costs.

Driver delay costs and vehicle operating costs are based on the additional time that drivers and vehicles spend in traffic when there is road construction or maintenance. They are formulated by Ehlen (1999) as follows:

$$C_{DT} = \left(\frac{L}{S_a} - \frac{L}{S_n}\right) ADT\ N_{rw}\ w \tag{2.8}$$

$$C_{VO} = \left(\frac{L}{S_a} - \frac{L}{S_n}\right) ADT\ N_{rw}\ r \tag{2.9}$$

where L is the length of affected roadway, S_a is the traffic speed during bridge work activity, S_n is the normal traffic speed, ADT is the average daily traffic measured in number of cars per day, N_{rw} is the number of days of road work, w is the hourly time value of drivers, r is the hourly vehicle operating cost. Ehlen's Formulas were extensively used in the literature (Huang and Huang 2012). However, the drawback of these formulations is that the user costs are calculated based on the traffic delay caused by slowing the average speed, but detour and other scenarios that have negative impacts on bridge users are not considered. For this reason, several scenarios that may adversely affect bridge users are investigated herein. All user cost assessments below are applied to Lebanon's traffic criteria and roads.

Accident costs are related to damage for drivers caused by higher probability of highway accidents during bridge construction. In Lebanon, road accidents cause on average one death per day and over 3,000 injuries per year (Hmaidan 2002). These numbers are very high for a country like Lebanon where traveled distances are relatively short. Accident cost is expressed as follows:

$$C_{CR} = (A_a - A_n) \times ADT \times N_{rw} \times L \times c_a \tag{2.10}$$

where c_a is the cost per accident, and A_a and A_n are during-construction and normal accident rates per vehicle-kilometer, respectively.

Liu and Frangopol (2006) assumed that user delay cost is proportional to the total increase in travel time and distance. The value of time was based on data reported by Schrank and Lomax (2003) from the perspective of the individual's value of their time, rather than being based on the wage rate. However, the computation of user delay cost based on some percentage of their wages has been outlined in the FHWA report in 2011 (FHWA 2011), and has been extensively used by several authors (Hansen 2001; Yu and Lo 2005; Kendall et al. 2008; Wang et al. 2012; Huang and Huang 2012). In this study, the hourly time value of drivers is estimated based on the average salary *AvSali* of travelers using each type of vehicle (Singh and Tiong 2005).

$$AvSal_i = \frac{\sum_j p_{ij} E_j M_{GWj}}{\sum_j p_{ij} E_j} \tag{2.11}$$

where E_j is the distribution of the actual labor force by employment category, p_{ij} represents the proportion of travelers with profession j in vehicle i and M_{GWj} represents the mean gross wage of profession j. M_{GWj} is calculated based on the median annual income for each profession j of all Lebanese household (Byblos bank economic research 2014). The labor forces E_j are quoted from IDAL (2015). The jobs and professions are categorized according to the international categorization of jobs and professions adopted and applied by the ILO (International Labor Office, 1996). The cost of delay time C_{DT} is obtained by multiplying the average salary per unit time by the occupancy rate. The occupancy rates are quoted from (FHWA 2011).

The vehicle operating cost C_{VO} is associated with "stop and go" driving in the queue. The operating cost includes fuel, engine oil, maintenance and depreciation. It can be estimated as follows:

$$C_{VO} = C_{AF} + C_{AM} \quad (2.12)$$

where C_{AF} is the cost of additional fuel consumption and C_{AM} is the cost of additional maintenance of the vehicle.

The authority may apply several bridge management solutions during the lifetime of a bridge to maintain its functionality; each of the solutions may cause a different user delay cost scenario (loss of average speed, lane closure, detour for large vehicles, rehabilitation, replacement, etc...). The occurrence of a scenario is dependent on the bridge condition. Each of these scenarios can be associated with a probability of occurrence that depends on the severity of the scenario and the likelihood of its occurrence. Let P_{CUj} be the probability of occurrence of a scenario *j*. The user cost scenarios corresponding to the different decisions taken during the bridge lifetime may thus be added to the total cost formula. For a limit state *i*, the total cost become:

$$C_T(t) = = C_{Ini} + C_{DC,i}P_{fi}(t) + \sum_j[\gamma_j\, C_{IC,i,j}P_{CUi,j}] \quad (2.13)$$

where γ_j is a Boolean variable with the value of 1 if scenario *j* occurs during the bridge lifetime, $P_{fi}(t)$ is the cumulative probability of failure, $C_{DC,i}$ is the direct cost of failure, and $C_{IC,i,j}$ is the indirect user cost related to the occurrence of the scenario *j*. Four specific scenarios will be herein considered and explained below, namely: degradation $C_{U\text{-}D}$, minor rehabilitation $C_{U\text{-}MR}$, load rating $C_{U\text{-}LR}$ and collapse $C_{U\text{-}C}$.

2.2.2.1- $C_{U\text{-}D}$ due to Degradation

Degradation user delay cost is caused by the loss of the average speed of vehicles due to the degradation of some bridge elements. As degradation does not necessarily imply congestion or blocking the traffic flow, the probability of occurrence $P_{CU\text{-}D}$ of 10^{-2} can be accepted for a 50 years timespan. This may be the case of a deflection that induces some discomfort, leading to slowing the traffic. Considering that C_U in equation (2.9) is calculated per vehicle per unit time, $C_{U\text{-}D}$ is estimated by multiplying C_U by the time loss t_{loss} due to slowing the traffic flow multiplied by the number of vehicles *N* affected by this loss.

$$C_{U-D} = C_U\, t_{loss}\, N \quad (2.14)$$

2.2.2.2- $C_{U\text{-}MR}$ due to Minor Rehabilitation

This user delay cost is caused by detours of vehicles due to the bridge or a lane suspension over the period of minor rehabilitations. $C_{U\text{-}MR}$ is estimated by multiplying C_U by the additional distance D_{add} of traveling at the average speed $V_{average}$ by the number of vehicles *N* making the detours.

$$C_{U-MR} = C_U\, \frac{D_{add}}{V_{average}}\, N \quad (2.15)$$

where $C_{U\text{-}MR}$ is sustained during the period of rehabilitation.

2.2.2.3- $C_{U\text{-}LR}$ due to Load rating

The cost of load rating $C_{U\text{-}LR}$ (or traffic distribution) is the user delay cost induced by the detours of trucks only due to the necessity of limiting the loading on the bridge. One implication of $C_{U\text{-}LR}$ may be when the steel reinforcement cross-section of a bridge element is corroded, and no rehabilitation is planned for a given timespan.

$$C_{U-LR} = C_U \frac{D_{add-truck}}{V_{average-truck}} N_{truck} \tag{2.16}$$

where $D_{add\text{-}truck}$ is the additional distance traveled by trucks during a detour, $V_{average\text{-}truck}$ is the average speed and N_{truck} is the number of trucks making the detours.

2.2.2.4- $C_{U\text{-}C}$ due to Collapse

In case of collapse of the bridge, detours of all vehicles are lasting until bridge replacement. This is the most severe user delay cost; the admissible probability associated with $C_{U\text{-}C}$ is very low. The cost $C_{U\text{-}C}$ is estimated by multiplying the road user cost by the time needed for bridge replacement t_{br}, by the number of vehicles N.

$$C_{U-C} = C_U \, t_{br} \, N \tag{2.17}$$

Figure 2.2 shows the costs involved in the user cost computation, as explained in this section.

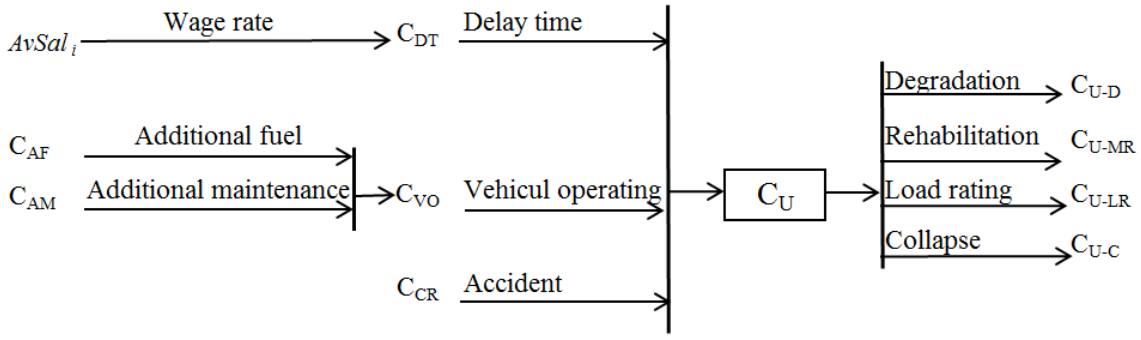

Figure 2.2: User cost computation.

The above developed methodology for the computation of user delay costs in Lebanon is illustrated in the example below. The proposed methodology is applied to Lebanon's traffic criteria in the following section.

2.2.3 Application: the indirect user cost computation in Lebanon

The user costs currently applicable in Lebanon with the mean gross wage (MGW) and the proportion of travelers with profession *j* in vehicle *i* are given in Table 2.2.

Vehicle Type (MGW) $/month	Type of professions, *j*								
	Number	1*	2*	3*	4*	5*	6*	7*	8*
	Type	Managers	Professionals	Technicians	Craftsmen	Clerks	Service workers	Operators	Laborers
Car (2500)		0.9	0.8	0.7	0.5	0.4	0.3	0.2	0.1
Truck (1000)		0.1	0.2	0.3	0.5	0.6	0.7	0.8	0.9

Table 2.2. Estimated proportion professions.

Road user cost analysis based on various vehicle classifications requires extensive traffic data. They include commercial and non-commercial vehicles ranging from motorcycles and passenger cars through the heaviest trucks. For simplification of vehicle classifications and consistency with available traffic data, it is recommended to use *Car* and *Truck* classifications only. The value of time lost is obtained by multiplying the average salary per unit time by the occupancy rate for different types of vehicles (Table 2.3). Prices have been converted from the local currency to U.S. dollars.

Vehicle Type	**Occupancy** Rate	**AvSal** $/month	**AvSal** $/mn	$\mathbf{C_{DT}}$ $/mn
Car	1.51	1868.4	0.1769	0.2672
Truck	1.4	974.46	0.0923	0.1292

Table 2.3. Cost of delay time C_{DT}.

To calculate the cost of additional fuel consumption C_{AF}, the following factors are required:

- The cost per liter of fuel is $1.85 in Lebanon.
- The efficiency factor of fuel consumption is 10km/l for cars and 4 km/l for trucks.
- The cost of travel per km is $0.185 for cars and $0.46 for trucks, which is the cost of additional fuel consumption C_{AF}.
- The additional cost of maintenance C_{AM} is calculated in Table 2.5. It covers the costs of spare parts, oil and tires.
- The vehicle-kilometers per year are quoted from the workshop on transport policies in Lebanon (Darwish and Timberlake 1999).

Vehicle Type	**Maintenance** $/year	**Mileage** km/year	$\mathbf{C_{AM}}$ $/km
Car	1525.13	12000	0.127
Truck	3474.85	187000	0.018

Table 2.4. Maintenance Cost C_{AM}.

Vehicle Type	C_{AF} $/km(a)	C_{AM} $/km(b)	C_{VO} $/mn (a+b)*0.917
Car	0.185	0.127	0.286
Truck	0.46	0.018	0.438

Table 2.5. Vehicle Operating Cost C_{VO}.

The vehicle operating cost C_{VO} per unit time for different types of vehicles is presented in Table 2.6. The distance travelled by each vehicle in one minute is approximated by 0.917 km, considering an average speed of 55 km/h. Due to the limited availability of work zone accident cost data, the inclusion of accident costs as part of the road user costs will not be considered in this work. The user costs for different types of vehicles are given in Table 2.7.

Vehicle Type	C_{DT} $/mn (a)	C_{VO} $/mn (b)	C_U $/mn (a+b)
Car	0.267	0.286	0.553
Truck	0.129	0.438	0.567

Table 2.6. User Cost for C_U.

Based on Kaysi and Salvucci (1993), 88% of the Lebanese fleet consists of passenger cars while the remaining 12% consists of buses, heavy trucks and pickups. The user cost per vehicle per hour per km for the *car* category can be taken as 33$ (which equals 0.553×60 min), and the *truck* category as 35$ (which equals 0.567×60min).

The four user delay costs corresponding to the scenarios explained in section 2.3 are estimated and applied to the bridge. The assumptions in Table 2.7 will be considered.

Variable	value	Units
Bridge length (L_b)	1	km
Number of travelers (N)	1000	vehicle/hour
Detour length (L_{bnew})	3	km
Average speed ($V_{average}$)	55	km/hour

Table 2.7. Assumptions for estimating C_U.

2.2.3.1- $C_{U\text{-}D}$ due to Degradation

A 10 km/h loss of the average speed of vehicles is considered. The new average speed due to the degradation is 45 km/h. The time loss t_{loss} is 14.5 seconds per vehicle. After 2 years of user delay costs uphold, $C_{U\text{-}D}$ is estimated by $2 320 756.

2.2.3.2- $C_{U\text{-}MR}$ due to Minor Rehabilitation

Considering the assumptions in Table 2.6, each vehicle loses 2.2 minutes to make a detour. Considering a minor rehabilitation of 2 months, $C_{U\text{-}MR}$ is estimated by \$5 221 702.

2.2.3.3- $C_{U\text{-}LR}$ due to Load rating

For the load rating user delay cost, the 2.2 minutes loss per vehicle concerns the truck category only. After 2 years of user delay costs uphold, $C_{U\text{-}LR}$ is estimated by \$11 762 967.

2.2.3.4- $C_{U\text{-}C}$ due to Collapse

When the bridge collapses, all vehicles must make detours until the replacement of the bridge. Considering a bridge replacement period of 2 years, $C_{U\text{-}C}$ is estimated by \$20 886 807.

The four scenarios of user delay costs estimated above will be used in section 2.4 for the design optimization of a bridge deck example. A detailed comparison between the scenarios will be also held.

The design of new structures must fulfill the total cost criteria studied in section 2.2. However, another criterion must also be satisfied, which is a target safety level. The two conflicting criteria can only be met by the mean of an optimization procedure that can minimize the cost without affecting the reliability level, such as the reliability-based design optimization (RBDO). This necessitates the estimation of the probability of failure of a degrading structure in a time dependent stochastic manner. The targeted task is made possible by the existence of explicit degradation models for the most influential deterioration processes like corrosion and fatigue, and also by the development of numerical procedures that can evaluate the probability of failure of complex nonlinear problems. A design method that can target all these difficulties is explored in section 2.3 below.

2.3 Design Methodology

In order to design a structure considering all related uncertainties, the reliability-based design optimization is widely used to balance the lifetime reliability and life-cycle cost. In the present work, the design parameters are the dimensions of structural members. The objective function is the total cost of the elements which is subject to deterioration processes. The design constraint is represented by an admissible probability of failure.

2.3.1 Reliability-based design optimization

The *RBDO* is formulated as follows (Ditlevsen and Madsen 1996)

$$\begin{aligned} &\text{Find} && d \\ &\text{Minimizing} && E[C_T(d, X, y, t)] \\ &\text{Such that} && 1 - P_{fi}[g_i(d, X, y, t)] \geq \mathcal{R}_i \quad , \quad i=1,\ldots,m, \\ & && d_i^L \leq d_i \leq d_i^U \quad , \quad i=1,\ldots,n, \end{aligned} \tag{2.18}$$

where d, X and y are the vectors of design, random and deterministic variables respectively, t is the time, P_{fi} is the probability of failure for the limit state function g_i, $\mathcal{R}_i$ is the reliability level specified by the designer, d_i^L and d_i^U are respectively the lower and upper bounds of the design variables, m is the number of limit states and n is the number of design variables.

The vector of random variables X represents geometrical, material or loading uncertainties. Each random variable is defined by a statistical distribution. The probability density functions (PDF), such as normal, lognormal and Weibull distributions, can be used to stochastically model the uncertainties. The PDFs are inferred from data sets that may be acquired by quality controls for geometrical and material parameters, experience feedback and field measurements for the load uncertainties. Classically, the parameters of PDF are adjusted by maximum likelihood estimations and goodness-of-fit tests are conducted to determine whether the assumed distribution is valid or not (Echard 2012). Nevertheless, if no data are available, distributions can be assumed based on empirical knowledge and expert judgment.

The design variables are deterministic parameters that should be optimized; however they can be the mean values of the probabilistic variable distributions. For a given random vector X, the *RBDO* yields a realization of a design variable d.

The RBDO aims at minimizing the objective function $C_T(d, X, y, t)$ which refers to the time-variant stochastic total cost explained in section 2.2:

$$C_T(d, X, y, t) = C_{ini} + C_{DCi} \times P_{fi}[g_i(d, x, y, t) \leq 0] + \sum_j [\gamma_j \, C_{ICi,j} \, P_{CUi,j}] \tag{2.19}$$

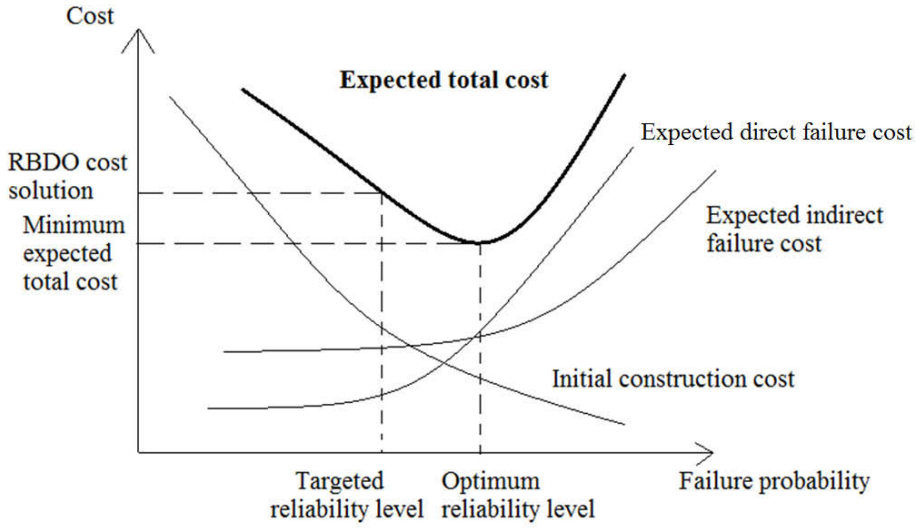

Figure 2.3: Evolution of the costs in function of the failure probability.

It is worth noting from Figure 2.3 that the optimal solution that can be found by considering the total cost in equation (2.2) may be different from the optimal one found by the consideration of direct costs only (i.e. $C_{ini} + C_{DCi} \times P_{fi}$). This is mainly due to:

(1) the high values of user costs; in some applications, these costs have been estimated by some authors as 5.52 times the construction costs (Yu and Lo 2005), or 90% of the total life-cycle costs (Kendall et al. 2008);

(2) the direct failure costs take place only at time of failure, which is usually at the end of the structural service life. Even though the direct costs may be higher than the indirect costs at the end of the service life, their present value at time of conception is a severely discounted value. However, the indirect costs are adept at every management decision that causes the closure or the suspension of some lanes. The user costs are paid during the whole lifespan of the structure.

2.3.2 Performance function

The limit state of bending is considered herein without loss of generality, its performance function can be written as:

$$g(d, X, y, t) = M_R(d, X, y, t) - M_a(d, X, y) \tag{2.20}$$

where M_R is the bending capacity and M_a is the applied moment. The resisting bending moment decreases with time due to the deterioration of the concrete member. The time dependent moment M_R can be estimated by introducing appropriate degradation models. Damage mechanisms of reinforced concrete structures can be effectively represented by a progressive reduction of the cross-sectional resistance and used to evaluate the corresponding performance function. Many degradation models were successfully adopted for this purpose; two of them are detailed in Appendixes 1 and 2. As explained in chapter 1, the performance function decreases with time due to the combination load increase and capacity decrease. However, in the remaining of this chapter, the applied loading is considered time invariant.

2.3.3 Probability of failure

The failure probability increases with time which is generally a result of the decrease of the safety margin. It can be estimated by integrating the joint probability density $f_g(d, X, y)$ over the failure domain:

$$P_f(d, X, y, t) = F_g(0) = \int_{g(d,x,y,t)\leq 0} f_g(d, X, y)dx \tag{2.21}$$

where $F_g(0)$ is the cumulative distribution function (CDF) at $g = 0$. For normal and log-normal distributions, exact expressions are formulated for the calculation of the probability of failure (Ditlevsen and Madsen 1996). For example, if M_R and M_a follow independent normal distributions, then:

$$P_f = F_g(0) = \phi\left(\frac{0-\mu_g}{\sigma_g}\right) = \phi\left(\frac{\mu_{M_R}-\mu_{M_a}}{\sqrt{{\sigma_{M_R}}^2+{\sigma_{M_a}}^2}}\right) \tag{2.22}$$

where μ_g is the mean safety margin, σ_g is the standard deviation of the safety margin, $\phi(\cdot)$ is the normal cumulated probability function that gives the probability that the normalized random variable g is below a given value (here the value is 0).

In this chapter, the First order reliability method (FORM) is used to estimate the probability of failure. FORM employs a linear approximation of the limit state function at the most probable failure point (MPP or P*) in the standard normal space. The MPP is the nearest failure point to

the origin O in the normalized space, and it is found by applying an optimization algorithm. The distance between the origin O and the MPP is the Hasofer-Lind reliability index noted β (Hasofer and Lind 1974).

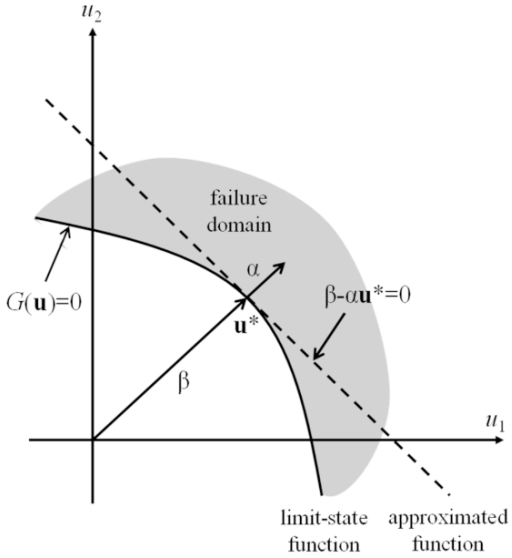

Figure 2.4: FORM liner approximation of the limit state function at the MPP (P*).

One of the main advantages of FORM in the RBDO context is that it allows the computation of the importance factors. The knowledge of the most influencing variables represents valuable information for the optimization process. However, this gradient-based advantage can be mischievous in high dimensional problems for highly non-linear limit states. Nevertheless, FORM requires less computational time than the other procedures such as MCS while providing high efficiency even for small probabilities.

Many uncertainties are associated with the degradation processes, the resistance and the loads. To properly address the capacity of deteriorating structural elements, a time-dependent structural reliability study has to be performed under various sources of uncertainty associated with environmental aggressiveness and increasing traffic loads. These uncertainties can be integrated through the performance assessment of concrete structures.

2.3.4 Analysis Procedure

The steps of the design methodology are as following:

Step 1: Initial costs are estimated by the mean of a priced bill of quantity.

Step 2: The bridge user delay cost is evaluated as illustrated in section 2.2.

Step 3: Suitable distributions are assessed for different material, geometric and loading random variables of the structure.

Step 4: Time-variant stochastic resistance of the structure is calculated based on appropriate degradation model.

Step 5: FORM is applied to the limit state function to evaluate the probability of failure.

Step 6: the RBDO is applied to find the optimal design of the bridge member.

Figure 2.5 shows a diagram that explains the above procedure, where d^* refers to the optimal solutions of the problem and C_T^* refers to the optimal total life-cycle cost of the structure formed by the initial costs, the user costs and the failure costs.

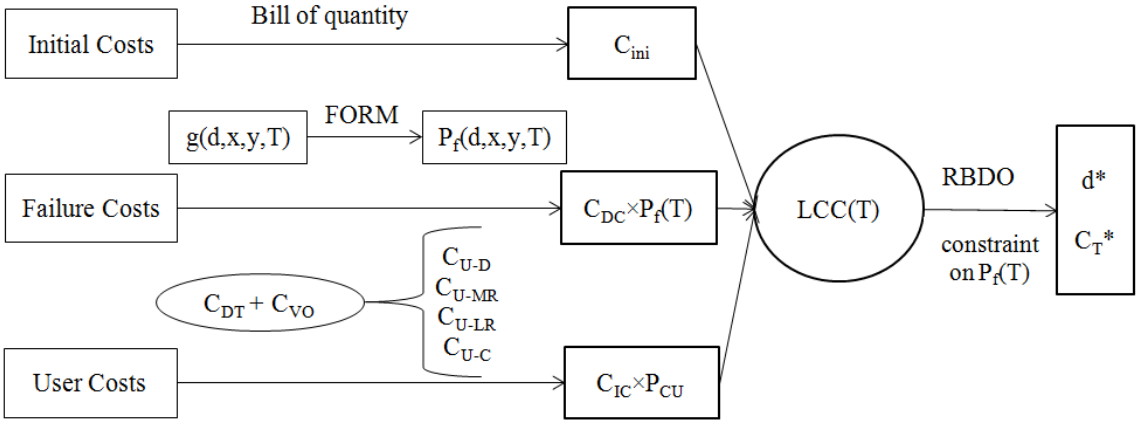

Figure 2.5. Sequence of analysis diagram.

2.4 Numerical application

The numerical application in this section aims at optimizing the design of bridge elements, considering mechanical degradation and user delay costs. The objective function corresponds to the total cost of the bridge member composed of the initial cost and the failure direct and indirect costs, as explained in section 2.2.

In the first application, a deck slab supported on four bridge girders is optimally designed, considering deterioration due to only steel corrosion. In the second application, the coupled effect of corrosion and fatigue detailed in Appendix 1 will be considered on a simply supported bridge girder.

2.4.1 Bridge Deck

The aim of this application is to optimize the dimensions of a reinforced concrete bridge deck, by minimizing the life-cycle cost in corrosive environment, considering the direct and indirect failure costs. The bridge deck is made of reinforced concrete with 100 m^2 area, simply supported on its four sides by girders. The deck has been designed according to the EC2 (EuroCode 2005). The user delay cost is computed as explained in section 2.2. The moment M_G due to a permanent surface load G, is given for $a=b=10m$, where a and b are the deck dimensions, by:

$$M_G = \theta \; G \; a^2 \qquad \text{with } \theta=0.0479 \tag{2.23}$$

First, the evolution of the reliability index with time under environmental aggressiveness is computed, and a sensitivity analysis is held. Then, the effect of concrete parameters and environmental aggressiveness on the optimization variables is analyzed. Finally, the impact of different scenarios that may lead to user delay costs on the LCC optimization is studied.

The effect of environmental aggressiveness on structural reliability is considered by accounting for three levels of aggressiveness: moderate, high and extreme. They differ by the distance between the structure site and the coast, and by the degree of exposure to seawater.

The random variables in this example are the steel strength f_y and the uniform permanent load G. Table 2.8 presents the loads and the material properties used in design and analysis.

Variable	Symbol	Average	Units	COV	Distribution
Random Variables					
Steel strength	f_y	500	MPa	0.07	Lognormal
Dead Load	G	12	kN/m^2	0.15	Normal
Design Variable					
Deck height	h*		m		
Deterministic Variables					
Concrete Compression	f_c	30	MPa		
Concrete cover	c	0.05	m		
Chloride concentration	C_{th}	0.9	kg/m^3		
Chloride concentration	C_s				
Moderate		1.15	kg/m^3		
High		2.95	kg/m^3		
Extreme		7.35	kg/m^3		
Coefficient of diffusion	D_c	6.10^{-12}	m^2/s		
Steel bas diameter	d_0	12	mm		
Number of bars	n	7	bars /m		
Elastic modulus of steel	E_s	210000	MPa		
Dimensions of the deck	a,b	10	m		

Table 2.8. Bridge deck example - Input data.

2.4.1.1- Probabilistic lifetime analysis

Figure 2.6 shows the importance of considering environmental aggressiveness when assessing the reliability index of a structure in a corrosive environment. We note that for high or extreme levels of aggressiveness, the reliability index of the concrete structure subject to corrosion decreases within 30 years by 17%. However, the structural reliability in a moderate environment does not change with time. This is expected because the concrete cover is taken as 50 mm, which is the value recommended in an aggressive environment by the code. Consequently the time to corrosion initiation is not reached in a moderate environment. The time to corrosion initiation is calculated as per equation A.2 in Appendix 1. Also, the reliability index decreases by 2.2% when going from highly to extremely corrosive environment. When going from a moderate to extremely corrosive environment, the reliability index decreases by 20% at the first 30 years, by 30% at 50 years, and by 40% at 80 years.

The importance factors allow us to assess the relative weights of random variables. These factors are computed by the direction cosines at the most probable failure point (MPP). The results of *FORM* at 50 years are shown in Table 2.9. The reliability is affected by the applied load with 66%, and by the yield strength with 34%. Moreover, the evolution of the importance factors with time in terms of environmental aggressiveness is shown in Figure 2.7. Similar to the reliability index, the importance factors are time-invariant in a moderate environment. In

highly and extremely aggressive environments, the effect of the applied load on the reliability index increases with time, and the effect of the yield strength decreases with time.

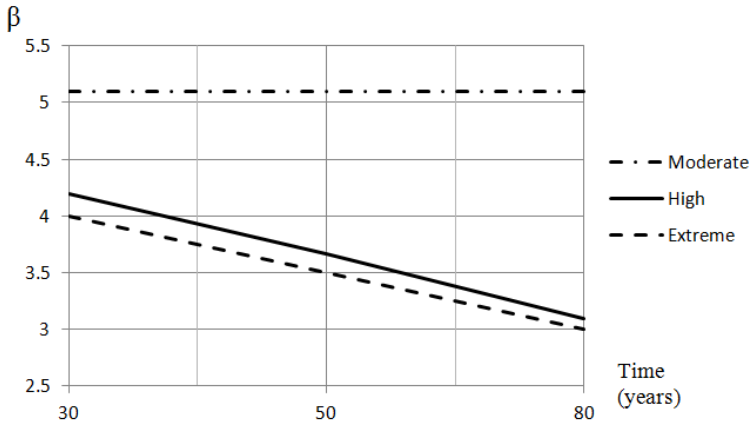

Figure 2.6. Evolution of the reliability index, in terms of environmental aggressiveness.

Environment	Reliability index β	Failure probability	Importance factor		MPP P*	Units
Moderate	5.08	1.92×10^{-7}	f_y	36.7%	402.2	MPa
			G	63.2%	19.2	kN/m^2
High	3.68	1.18×10^{-4}	f_y	32.5%	430.8	MPa
			G	67.5%	17.4	kN/m^2
Extreme	3.59	1.60×10^{-4}	f_y	32.2%	432.4	MPa
			G	67.7%	17.3	kN/m^2

Table 2.9. Reliability results for a lifetime of 50 years in different environmental aggressiveness.

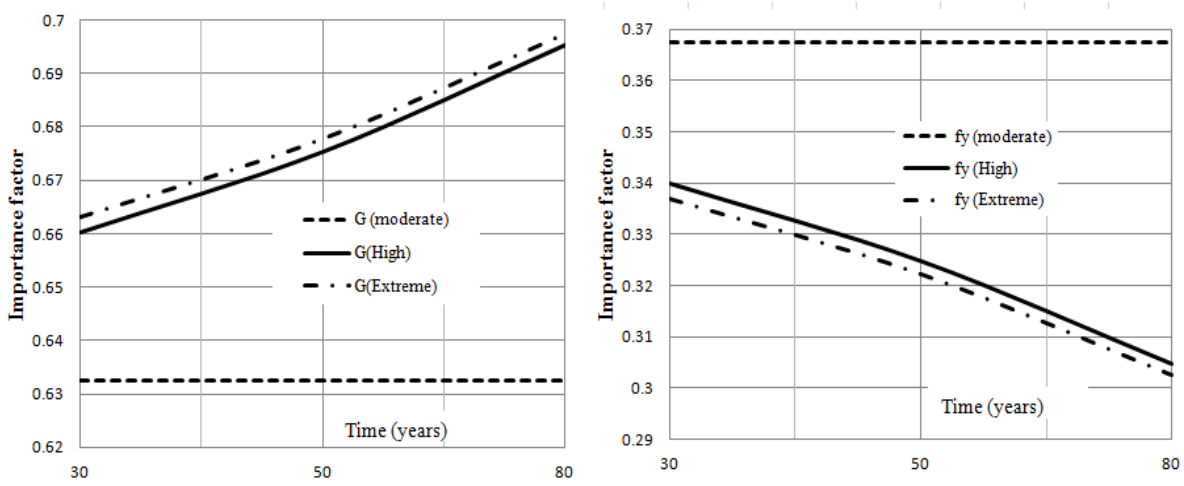

Figure 2.7. Evolution of the importance factors with time, in terms of environmental aggressiveness.

2.4.1.2- Optimization

In this example, the design variable is the thickness of the concrete deck h. The objective function is the life-cycle cost, and the constraint is the admissible failure probability. The optimal dimensions are found for different target reliabilities, different environmental aggressiveness, and at different timespan. The initial value of the design variable h is 0.4 m. The upper and lower bounds are 0.3 m and 0.6 m respectively.

As shown in Figures 2.8 and 2.9, the optimal deck thickness and cost increase by 11% and 5% respectively, if the studied timespan goes from 50 to 100 years. This is expected because the reinforcement cross-section is reduced with time due to corrosion. Furthermore, the optimal deck thickness and cost increase by 16% and 6% respectively, when the admissible probability of failure goes from 10^{-7} to 10^{-4}. It is thus very important to wisely define the lifetime of the structure and the admissible probability of failure.

For a 100-years timespan, Figures 2.8 and 2.9 show an increase of 25% and 11% in the optimal thickness and cost respectively, between moderate and extreme environments. As explained before, the structure in this example is not subjected to a moderate environment. Therefore this increase in the optimal thickness and cost is due to the effect of degradation on the structure. Consequently, all degradation processes must be wisely modeled when designing a concrete structure.

It is also interesting to study the influence of the average value of concrete cover on the optimization variable and cost. It is noted that when the average value of concrete cover is low, the corrosion reaches the steel bar quickly. Thus, to fit the target reliability, we need a larger depth, because the loss of steel area by corrosion is balanced by more concrete thickness to increase the internal moment capacity. In this application, a decrease of the average value of the concrete cover by 2 cm leads to 12% increase of the optimal concrete thickness and 5% increase of the optimal cost. Contrariwise, an increase of the average value of the concrete cover by 2 cm leads to 7% decrease of the optimal concrete thickness and 3% decrease of the optimal cost.

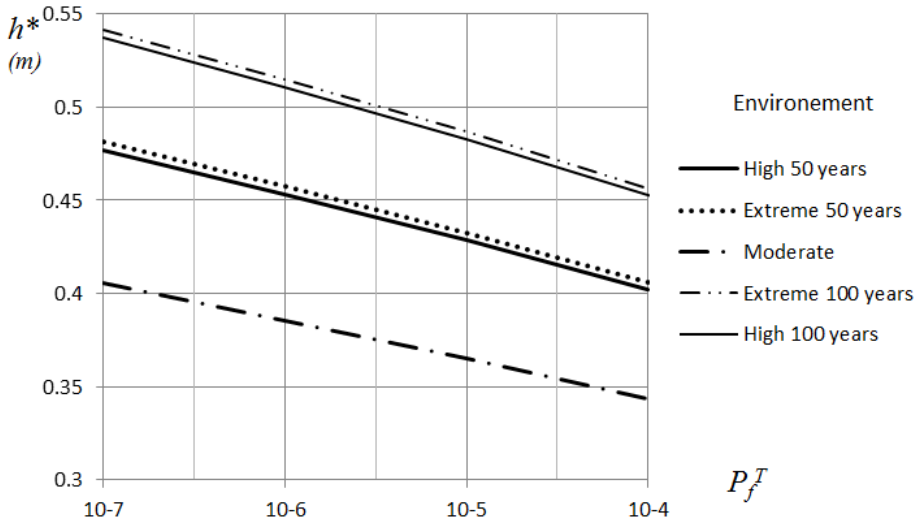

Figure 2.8. Variation of the optimal thickness as function of threshold probability of failure under various environmental aggressiveness.

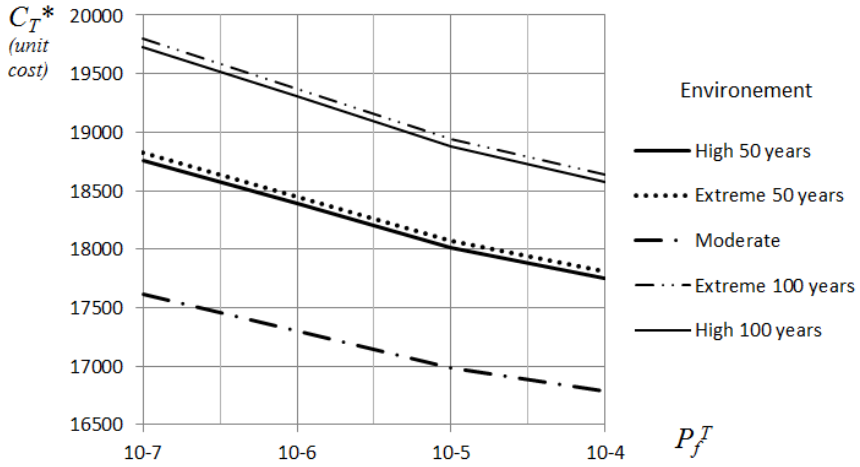

Figure 2.9. Variation of the optimal cost as a function of threshold probability of failure under various environmental aggressiveness.

2.4.1.3- User cost

Finally, the optimization of the bridge deck is performed for the four scenarios of the user delay costs explained in section 2.2. In order to investigate the sensitivity of design parameters and optimal costs on each scenario, only one scenario is considered in each run. The threshold reliability for each user delay cost scenario is given in Table 2.10.

	$P_{CU\text{-}D}$	$P_{CU\text{-}MR}$	$P_{CU\text{-}LR}$	$P_{CU\text{-}C}$
P_{CU}	10^{-2}	10^{-3}	10^{-3}	10^{-6}

Table 2.10. Admissible probability P_{CU}.

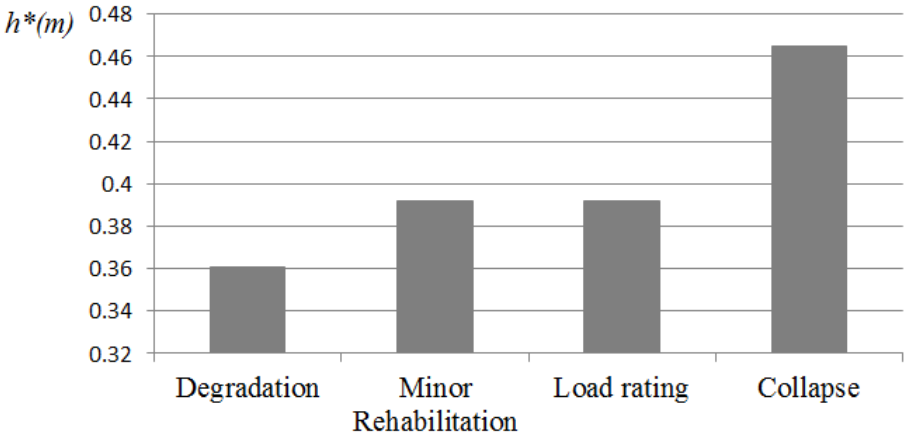

Figure 2.10. Optimal thickness considering different scenarios of C_U.

Figure 2.10 shows the optimal thickness of the bridge deck for each user delay cost scenario. If the considered user delay cost is caused by the loss of the average speed due to degradation, an optimal deck thickness of 36 cm is sufficient. However, if the user delay cost is caused by the

bridge collapse, then the optimal deck thickness is 46 cm. The optimal design of the deck can vary by 25% depending on the reasons that lie behind the user delay cost acquirement.

As shown in Table 2.10, the minor rehabilitation and the load rating user delay costs have the same admissible probability of failure of 10^{-3}. The two scenarios may have the same optimal thickness of 39 cm (Figure 2.10), therefore the same initial cost, although total cost varies between the two scenarios. It is noted that a minor rehabilitation costs 22% less than a traffic disruption in this example. Therefore the computation of different scenarios of user delay costs is crucial to make the best remedial decisions in case of bridge degradation.

2.4.2 Simply supported bridge Girder

The purpose of this application is to optimize the design of a reinforced concrete simply supported bridge girder under corrosion and fatigue according to the degradation model developed by Bastidas-Arteaga et al. (2008; 2009; 2011). Bastidas model computes the reduction of the concrete section and the area of steel reinforcement in order to assess the change of structural capacity with time, this model is detailed in Appendix 1. In addition to dead load, a truck wheel load is applied and located at the middle of the span. The initial design is made according to the EC2. Table 2.11 presents the load and material properties used in the analysis. All the values are based on data taken from literature (El Hassan et al. 2010; Bastidas-Arteaga et al. 2011).

By considering the mean values in Table 2.11, and for a 1 m beam height, the prediction of the bending capacity in a highly aggressive environment, subject to f = 2000 cycles per day, is shown in Figure 2.11, with the parameters related to coupled corrosion-fatigue deterioration model in Table 2.12. The definitions and equations of these parameters are explained in Appendix 1. From the curves in Figures 2.11 and 2.12, we can distinguish four stages:

1- The first stage corresponds to corrosion initiation $t \in [0, \tau_{ini}]$. The bending moment remains constant because the steel cross-section does not change.

2- When the girder goes into the propagation stage, the moment resistance decreases. In the first year after the time of corrosion initiation, the corrosion rate is constant, which explains the fact that just after τ_{ini}, the resistant moment M_r drops suddenly.

3- In the stage of propagation, we can see clearly that after $\tau_{ini} + 1$, the resisting moment decreases monotonically until the transformation from pit to crack at τ_{pt}.

4- Afterward, the moment continues to decrease during the crack growth time τ_{cg}, for $t \in [\tau_{pt}, \tau_l]$. The last point corresponds to the collapse time τ_l.

In a moderate environment, the time to corrosion initiation is greater than t_{max}. So the steel cross-section remains intact throughout the life of the structure and the bending moment remains constant. The bridge girder probabilistic study shows that for a given level of aggressiveness and traffic frequency, the reliability index of the concrete structure subject to coupled corrosion-fatigue deterioration process decreases within 10 years by nearly 10%. Furthermore, at a given time and for a certain level of aggressiveness, the reliability index decreases by nearly 50% when the traffic frequency increases from 500 to 2000 cycles per day. In addition, the reliability index decreases between high and extreme corrosive environments by 6.7% in early years (t=10 years), and by 33.8% in later years (t=20years).

Variable	Symbol	Average	Units	COV	Distribution
Random Variables					
Concrete Compression	f_c	30	MPa	0.15	Lognormal
Steel strength	f_v	500	MPa	0.07	Lognormal
Concrete cover	c	0.05	m	0.2	Lognormal
Chloride concentration	C_{th}	0.9	kg/m^3	0.19	Lognormal
Chloride concentration	C_s				
Moderate		1.15	kg/m^3	0.5	Lognormal
High		2.95	kg/m^3	0.5	Lognormal
Extreme		7.35	kg/m^3	0.7	Lognormal
Coefficient of diffusion	D_c	6.10^{-12}	m^2/s	0.2	Lognormal
Dead Load	G	26	kN/m	0.15	Normal
Punctual design Load	Q	115	kN	0.25	Normal
Design variables					
Beam height	h^*		m		
Reinforcement Area	As^*		cm^2		
Deterministic Variables					
Beam length	l	10	m		
Beam width	b	0.8	m		
Steel bar diameter	d_0	25	mm		
Elastic modulus of steel	E_s	210000	MPa		
Water/cement ratio	wc				
Moderate		45	mm		
High		50	mm		
Extreme		55	mm		
Threshold corrosion rate	i_{th}				
Moderate		2	μA/cm^2		
High		5	μA/cm^2		
Extreme		10	μA/cm^2		
Traffic frequency	f	500	cycles/day		
		1000	cycles/day		
		2000	cycles/day		

Table 2.11. Input data for the bridge girder.

Environment	Symbol	High	Extreme	Units
Time to corrosion initiation	τ_{ini}	6.280	2.770	years
Time to pit nucleation	τ_{pn}	0.037	0.036	days
Time of pit to crack transition	τ_{pt}	38.00	20.00	years
Time to crack growth	τ_{cg}	6.680	3.200	years
Collapse time	τ_l	51.00	26.00	years
Pit depth at τ_{pt}	a_0	12.46	13.20	cm
Crack size at critical stress	a_1	6.200	6.200	cm
Critical crack size at failure	a_c	15.00	15.00	cm

Table 2.12. Coupled deterioration model results.

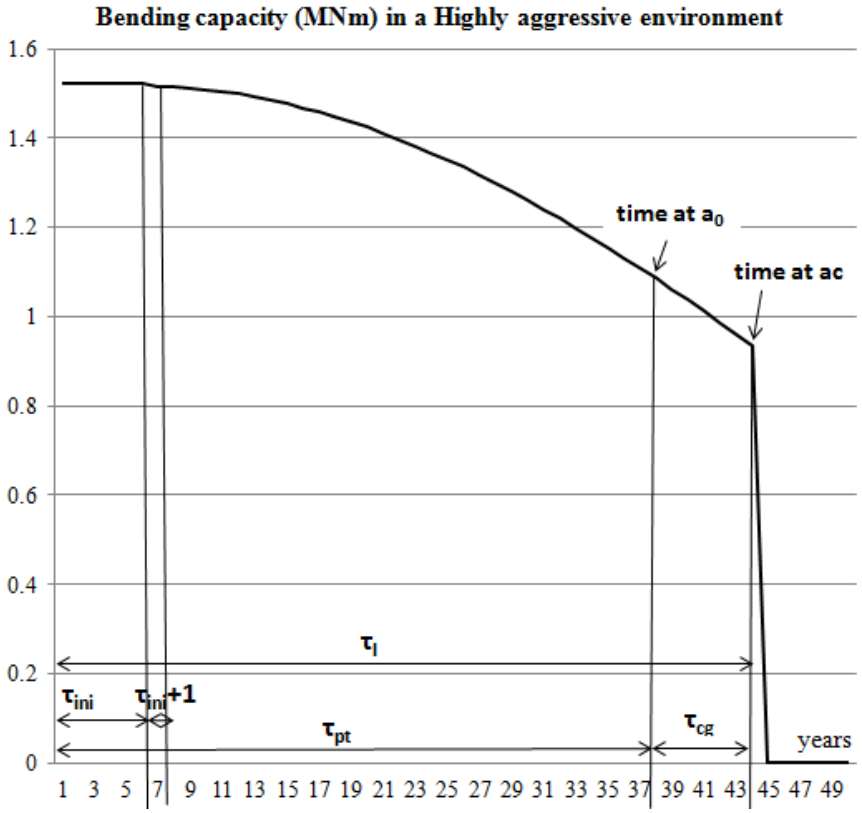

Figure 2.11. Evolution of the bending capacity in a highly aggressive environment (f=2000 cycles/day).

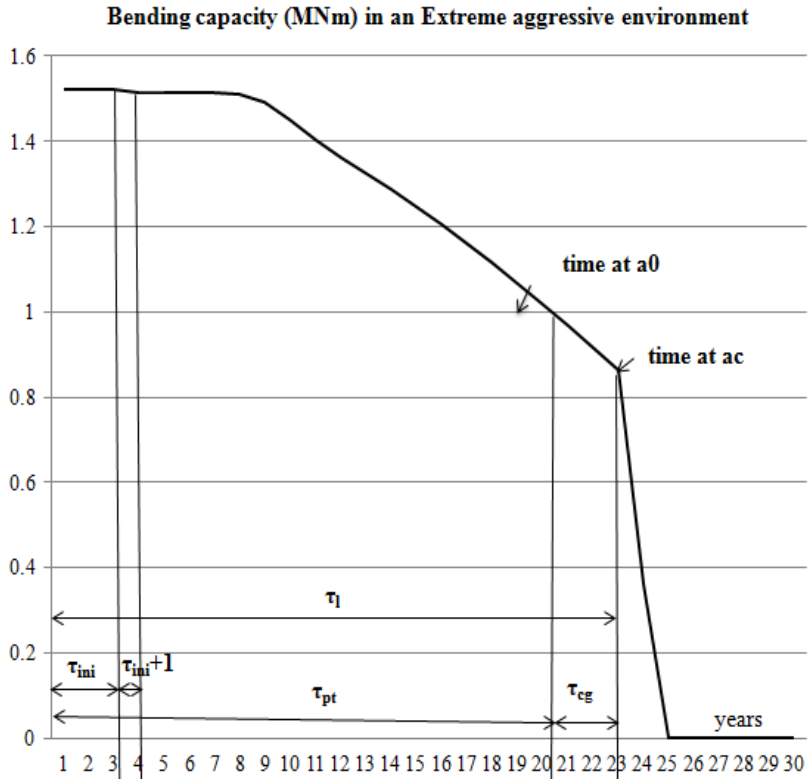

Figure 2.12. Evolution of the bending capacity in an extremely aggressive environment (f=2000 cycles/day).

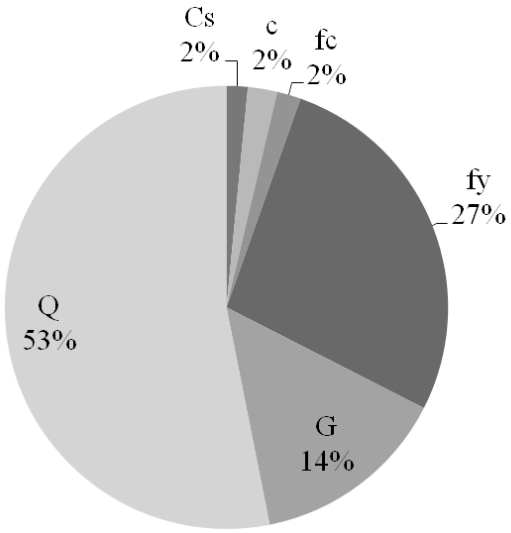

Figure 2.13. Bridge girder example – Importance Factors.

As shown in Figure 2.13, the importance factors show that the parameters that mostly affect the reliability are dead and live loads (G and Q), the compressive concrete strength f_c, the steel yield strength f_y and the concrete cover c. It is also noted that c, f_y and f_c lead to an increase in reliability, while the influence of G and Q is to decrease the reliability. The results of FORM are shown in Tables 2.13 and 2.14. The MPP for c, f_y and f_c are below the mean values, and the MPP for G and Q are above the mean values.

The results given in Table 2.13 indicate that the reliability of the structure in a moderate and high environment is respected for 25 years in contrast with the extreme environment which fails even before 20 years (Table 2.14). Furthermore, the reliability index decreases by 15% between moderate and high corrosive environments at 25 years.

Environment	**Reliability β**	**Failure probability**		**Importance factor**	**MPP P***	**Units**
Moderate	4.93	3.91×10^{-7}	C_s	1.38%	1.028	kg/m^3
			c	3.22%	0.047	m
			f_c	1.69%	26.82	MPa
			f_y	25.7%	412.3	MPa
			G	14.4%	0.033	kN/m
			Q	53.4%	0.285	kN
High	4.28	9.26×10^{-6}	C_s	1.54%	1.028	kg/m^3
			c	2.13%	0.039	m
			f_c	1.74%	27.27	MPa
			f_y	27.0%	426.9	MPa
			G	14.3%	0.032	kN/m
			Q	53.0%	0.266	kN

Table 2.13. Reliability of bridge girder at 25 years age in moderate and high environmental aggressiveness, with f = 2000 cycles/day.

Environment	Reliability β	Failure probability		Importance factor	MPP P*	Units
Extreme	3.22	6.36×10^{-4}	C_s	0.16%	6.991	kg/m^3
			c	0.57%	0.044	m
			f_c	1.56%	27.94	MPa
			f_y	22.9%	447.9	MPa
			G	17.1%	0.031	kN/m
			Q	57.7%	0.241	kN

Table 2.14. Reliability of bridge girder at 20 years age in extreme environmental aggressiveness, with f = 2000 cycles/day.

Environment	Higher frequency	Higher environmental aggressiveness
τ_{ini}	Independent	↘ (55%)
τ_{pt}	↘ (15%)	↘ (49%)
τ_{cg}	↘ (50%)	↘ (52%)
a_0	↘ (15%)	↗ (5%)
a_c	Independent	Independent
τ_l	↘ (2%)	↘ (49%)

Table 2.15. Behavior of time lengths and pit depths.

Furthermore, the timespan and the pit depths of each stage are examined for different levels of aggressiveness (moderate, high and extreme), and different frequencies (500, 1000 and 2000 cycles/day). The behavior is summarized in Table 2.15.

The time to corrosion initiation decreases by 55% when the environmental aggressiveness increases. However, τ_{ini} is independent of the traffic frequency. In fact, τ_{ini} depends on the chloride concentration, the concrete cover and the coefficient of diffusion, as shown in equation (A.1).

The time for transition from pit-to-crack decreases by 15% for higher values of traffic frequency and it decreases by 49% in corrosive environments.

The time to failure τ_l decreases by 2% for higher values of traffic frequency and decreases by 49% in corrosive environments. This is expected because the failure occurs in a shorter period when the frequency is high or the environment is more corrosive.

μ_d	μ_d^0	μ_d^{LB}	μ_d^{UB}
μ_{As} (cm^2)	39.25	19.6	73.6
μ_h (m^2)	1	0.6	3

Table 2.16. Description of optimization variables for the bridge girder example.

In this application, the optimization parameters are the initial cross-section of steel reinforcement A_s and the height of the concrete section h. The initial values μ_d^0 and the upper and lower bounds respectively μ_d^{UB} and μ_d^{LB} of the optimization variables are summarized in Table 2.16.

Figure 2.14 shows the influence of the mean value of concrete cover on the optimization variables, in high environmental aggressiveness for 50 years of timespan. It appears that when the average value of the concrete cover is low, the corrosion reaches the steel bar quickly. Thus, to fit the target reliability, we need a larger steel cross-section or a larger concrete depth, therefore a higher optimal cost, as can be shown in Figure 2.14. In fact, the optimal cost increases by 2.5% when the concrete cover decreases from 7 cm to 5 cm. Also, the optimal cost increases by 8% when the concrete cover decreases from 5 cm to 3 cm. As a result, choosing the design values of concrete parameters has a big influence on the optimum dimensions.

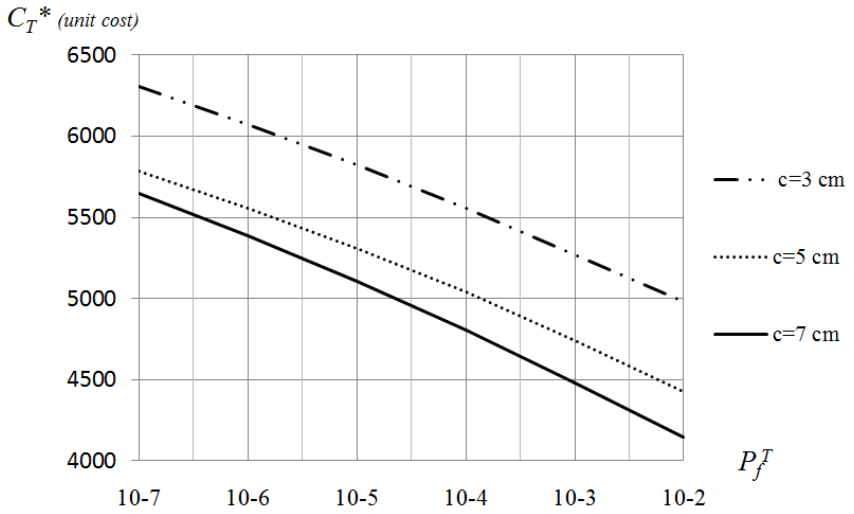

Figure 2.14. Effect of the concrete cover on the optimal cost of the bridge girder example.

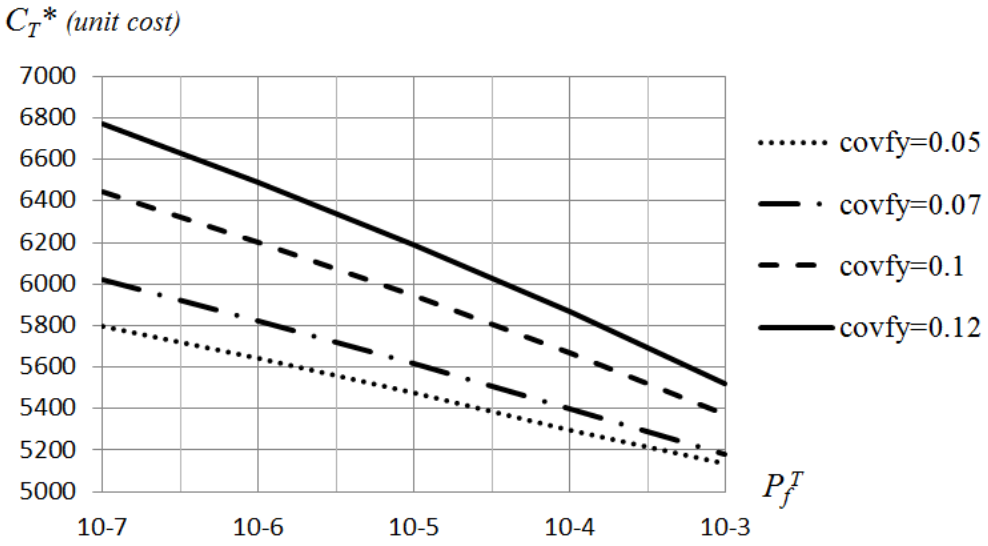

Figure 2.15. Effect of the coefficient of variation of f_y on the optimal cost.

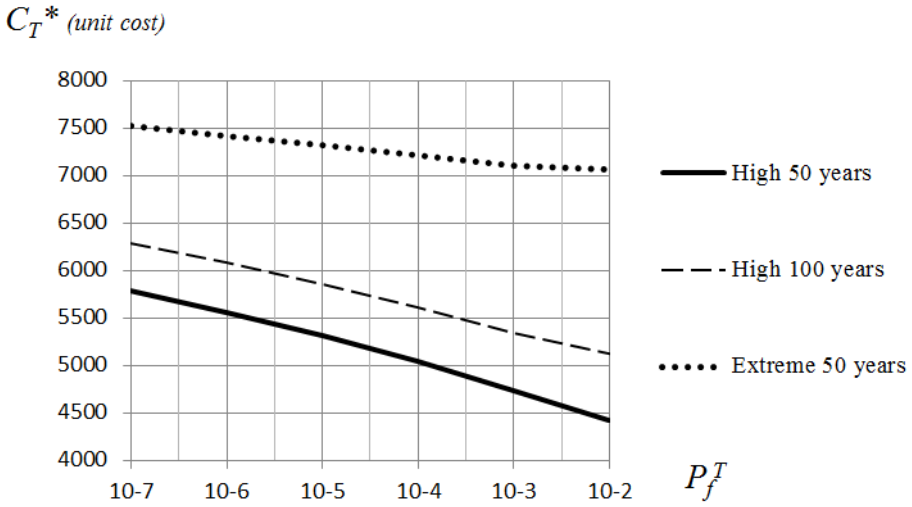

Figure 2.16. Variation of the optimal cost for the bridge girder example.

In addition, the coefficient of variation contributes largely to the optimal life-cycle dimensions. Figure 2.15 shows the effect of the coefficient of variation of steel yield strength f_y on the optimal life-cycle cost. The study is made for coefficient of variation of f_y equals 0.05, 0.07 and 0.12. It appears that when the target reliability is high (P_f^T=10^{-7}), the optimal cost decreases by nearly 15% when the coefficient of variation of f_y goes from 0.12 to 0.05. However, it decreases by 7.5% only when the target reliability is low (P_f^T=10^{-3}). Therefore, the coefficient of variation has a bigger impact on the life-cycle design when the target reliability is high.

Figure 2.16 shows the influence of the environment and the studied timespan on the optimal cost. In fact, the optimal cost increases by 10% when the timespan goes from 50 to 100 years. Also, the optimal cost increases by 30% when going from high to extreme corrosive environment. Furthermore, the optimal cost is increased by 25% in high environments, and by 6.5% in extreme environments, when the target probability of failure goes from 10^{-2} to 10^{-7}.

Another comparison is held between the optimal results for the bridge girder subject to corrosion only, or to the coupled corrosion-fatigue deterioration process. In fact, applying the same dead and live load, concrete characteristics, target reliability and corrosion aggressiveness, to the same girder, shows an increase of 8.3% in the optimal height, when the coupled effect of fatigue and corrosion is considered with a traffic frequency of 2000 cycles/day. Thus, the degradation models considered in the lifetime assessment influences significantly the optimal design of a concrete bridge structures.

2.5 Conclusion

This chapter has two main purposes. First, it aims at improving the life-cycle cost evaluation in order to better design civil engineering structures. Second, it aims at studying the effect of each component of the life-cycle cost formulation on the optimum design of structural elements.

We have discussed the various cost components that come into the calculation of the LCC of a degrading structural component when designing new structures, considering direct and indirect costs related to failure. A probabilistic approach has been used to assess the reliability

of reinforced concrete structures subject to corrosion and fatigue. A new approach is also proposed for the evaluation and analysis of user delay costs, and is applied to the current state of Lebanon. As shown, the optimal design of a reinforced concrete bridge elemtn is strongly affected by the two degradation models considered herein (corrosion and fatigue), by the different scenarios of user delay costs, by the concrete cover and parameters, by the failure costs considered in the LCC, and by the admissible probability of failure. Therefore, continuous refinements to the cost estimation methods and data used in the life-cycle cost assessment will contribute to increase the accuracy of results in the future, where more degradation models can be considered, and more indirect costs can be evaluated. Moreover, the improved life-cycle cost formulation may be applied in the future to the whole structural system instead of components.

Chapter 3: Maintenance cost of systems with dependent components

3.1 Overview

Optimizing the maintenance planning of deteriorating civil engineering structures is crucial for maximizing their service life. The major difficulties come from the fact that a structure is a complex system composed of many inter-related elements. Nicolai and Dekker (2008) published a review-report on multi-component maintenance optimization, focusing on the dependency between components. The articles were classified on the basis of different types of dependency: stochastic, structural and economic. Planning is also discussed for finite and infinite horizons. The type of optimization can be apprehended according to exact or heuristic policies. Their conclusion was that more researches are needed to model the combination of dependencies and the multiple setup activities, in addition to more case studies to be intended. A review for the most recent work on component dependencies of a system is held in chapter 1. Many weaknesses must be addressed, particularly the fact that most of the researches, even recent ones, dealing with stochastic dependency only consider two-component systems and a specific type of failure interaction. Also, only "common cause" correlation is modeled, which is a failure effect produced by external sources. However, there are other failure scenarios that may occur like "cascade" or "compound" consequence correlations. Moreover, very few works deal with structural dependency. However, the redundant system can be considered as "structural horizontal dependency" as defined by Thomas (1986). Another drawback of the proposed models in the literature lies in the consideration of series system, which does not necessarily represent reality and leads to very conservative computation of system reliability. System modeling approaches have not been successfully applied to structural deterioration modeling (Wang et al. 2012), although simpler approaches for modeling the structural system are to be founded. In addition, the maintenance model has to consider the multiple deterioration dependencies among elements.

In this chapter, a procedure is developed for the maintenance planning of multi-component structural systems taking into account stochastic, structural and economic dependency. An approach for grouping the dependent components is presented, where the redundancy of the structural elements is accounted for. A procedure to calculate the load redistribution for non-failed elements is also proposed and integrated in the cost formulation. Stochastic dependency of elements is integrated in the cost function by the mean of conditional probabilities of failure. The approach also accounts for downtimes needed to dismantle modularly dependent elements and/or to repair associated failed elements. A new method to compute structural system reliability is also suggested in this chapter. The proposed methodology is applied to numerical examples to show its validity and functionality in practical cases.

3.2 Degradation and failure conditions

The first step in evaluating a reliability-based maintenance cost is the prediction of the components degradation and failure. Some empirical degradation models in literature can fairly predict the intrinsic degradation of an element under a certain deterioration mechanism. However, the task becomes significantly more complex when the failure dependency and the interaction between deterioration mechanisms are to be considered.

3.2.1 Component degradation

The degradation of a component *i* at time *t*, $d_i(t)$, depends on the following:

- The intrinsic (or proper) degradation of the i^{th} component, $d_{ip,k}(t)$, which is a consequence of the own degradation of the element with time due to deterioration mechanisms like corrosion and fatigue of reinforced concrete components. The subscript *k* denotes a particular degradation mechanism.
- The degradation of component *i* can be accelerated by the degradation of components *j*. For example, let us consider the two elements shown in Figure 3.1 (column and slab). The expansion of corroding steel in the slab creates tensile stresses in the concrete, which can cause cracking, delamination and spalling of the slab itself. The degradation of the column is accelerated by the degradation of the slab.

Figure 3.1: Corrosion of reinforcing steel.

The geometric position of the two components has a big influence on the degradation dependencies. Adjacent components may accelerate the degradations of each other more than distant components. Figure 3.2 shows three superstructure beams in parallel; *i*, *j* and *v*. The intrinsic degradation of each element is accelerated by the degradations of the other elements; e.i. $d_{ip}(t)$ is accelerated by $d_{jp}(t)$ and $d_{vp}(t)$ and vice-versa.

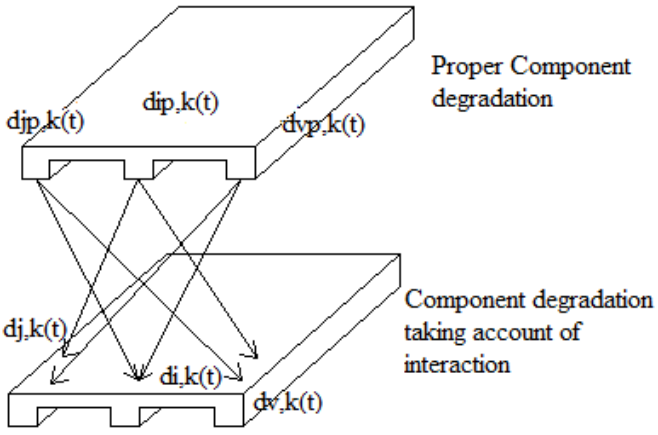

Figure 3.2: Illustration of an accelerated degradation.

In fact, the degradation of a component *i* due to a certain mechanism *k* is accelerated by other components due to all other mechanisms. To take into account this acceleration effect, let us consider two elements *i* and *j*, and two degradation mechanisms *k* and *r*. As shown in Figure

3.3, the own degradation $d_{ip,k}(t)$ of element *i* for the k^{th} degradation mechanism is accelerated by the degradation of elements *j* for the k^{th} and r^{th} degradation mechanisms, $d_{j,k}(t)$ and $d_{j,r}(t)$ respectively.

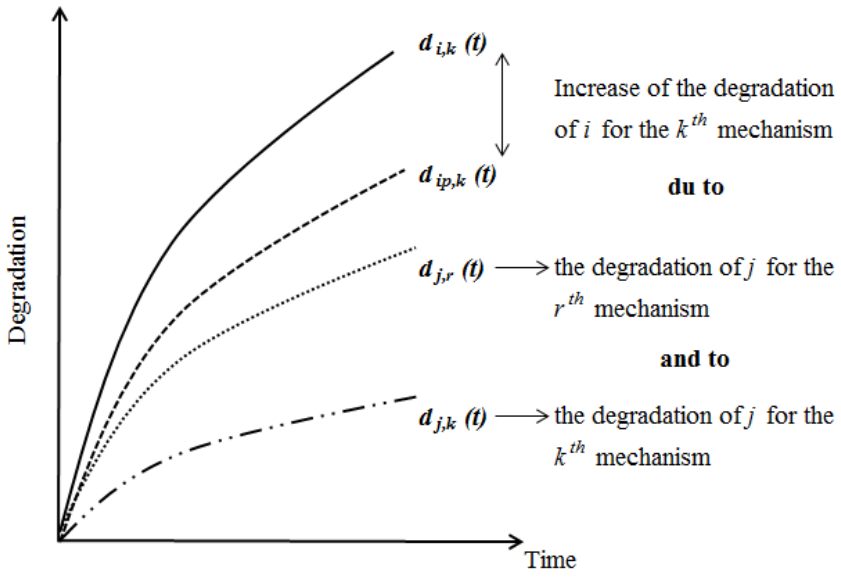

Figure 3.3: Degradation acceleration with time due to dependencies.

Therefore, the degradation of the component *i* can be expressed as following:

$$d_{i,k}(t) = d_{ip,k}(t)\left[1 + \sum_r \sum_{j \neq i} c_{1,j,r}\, e^{c_{2,j,r}\left(\frac{1}{d_{serv,j,r}} - \frac{1}{d_{j,r}(t)}\right)}\right] \tag{3.1}$$

where $d_{ip,k}(t)$ is the intrinsic degradation of the element *i* for the k^{th} degradation mechanism, $d_{serv,j,r}$ is the service limit degradation of component *j* for the r^{th} degradation mechanism, $c_{1,j,r}$ is a coefficient related to the geometrical position of *i* and *j*, and $c_{2,j,r}$ is a coefficient related to the speed of the influential degradation between the two components.

3.2.2 Component Failure

As discussed in chapter 1, the component capacity is degrading with time (section 1.5 Figures 1.4 and 1.6). Let $P_{fi}(t)$ be the cumulative failure probability of the component *i* du to its intrinsic degradation:

$$P_{fi}(t) = Pr\left[(d_{ip}(t) \geq d_{iF}) \,|d_{i0}\right] \tag{3.2}$$

where d_{i0} is the degradation of component *i* at the beginning of a maintenance cycle, or after the last intervention (i.e. inspection, preventive or corrective), and d_{iF} is the degradation limit before failing.

The intrinsic failure probability may be increased when the system's components are stochastically dependent. To clarify this idea, let us consider two elements b_1 and b_2 stochastically dependent by associated failure (AF); i.e. the failure of b_1 may induce the failure of b_2 with a probability of $P_{2|1}$ and vice-versa. Figure 3.4 shows the failure diagram for this system of two components.

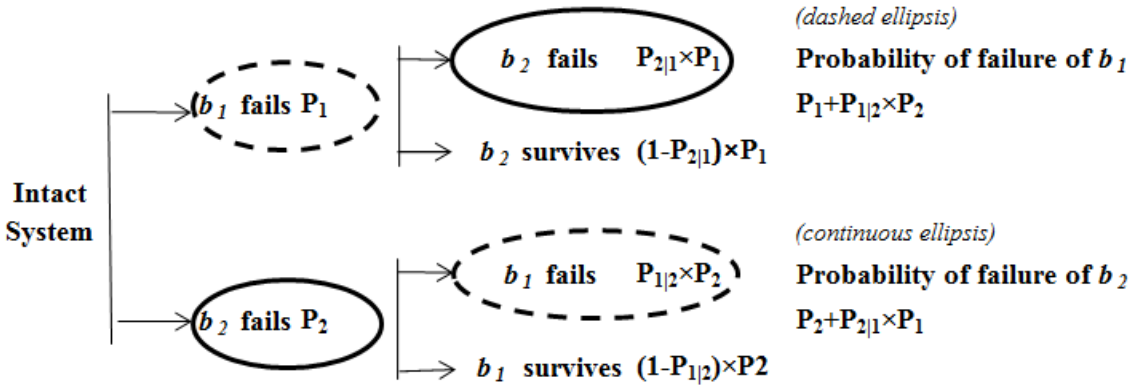

Figure 3.4: Failure diagram – two components.

Therefore, the probability of failure of a component *i*, which failure can be associated to other elements *j* in the system with a probability$P_{i|j}$, can be expressed as follows:

$$P_{fi,d}(t) = P_{fi}(t) + \sum_{j \neq i} P_{i|j}(t)\, P_j(t) \tag{3.3}$$

where $P_{fi,d}$ is the probability of failure of component *i* due to the degradation of the component itself and to all dependent components *j*. Formula 3.3 is based on the failure tree truncated at the 2nd branching level of the tree (which contains a multiple of two probabilities $P_{i|j}(t)P_j(t)$). To clarify, Figure 3.5 shows a failure diagram for a system of three components (three levels).

A more precise calculation will include the remaining levels of the tree, which are neglected in the current study for the following reasons:

- They will not significantly improve the evaluation of the probability of failure because the n^{th} level of the tree corresponds to n probability products which would be negligible compared to the first two levels.
- They will increase substantially the computation time due to all the conditional probabilities.

The above probability is not likely to have a value greater than 1 because in civil engineering the probabilities of failure are very low. Also, all conditional probabilities are multiplied by the probability of failure of the original component, which decreases further the values. Moreover, the probability of failure in equation 3.3 aims at increasing the cost expectancy related to items which have lots of dependencies. It is a notional probability and not an actuarial one and it is aimed to help decision makers to find suitable maintenance planning. Similarly, the probability of survival $P_{S,i}$: becomes:

$$P_{S,i} = 1 - \left[P_{fi}(t) + \sum_{j \neq i} P_{i|j}(t)\, P_j(t)\right] \tag{3.4}$$

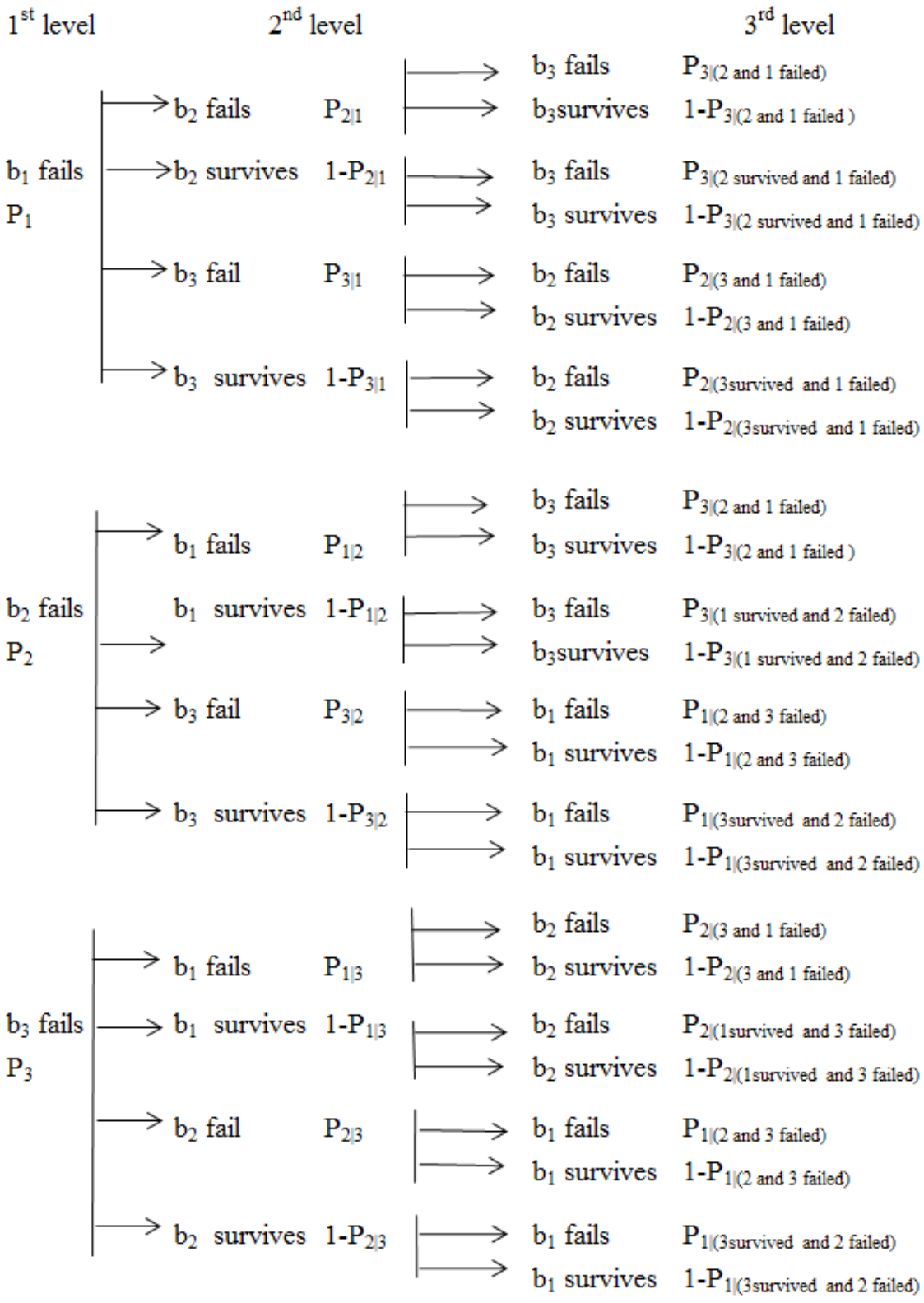

Figure 3.5: Failure diagram – three components.

3.2.3 Load redistribution

As shown in section 3.2.1, the degradation of element *i* is accelerated by the degradation of any dependent element *j*. Moreover, the degradation can be given as a function of the load $L_i(t)$ and the environment: $d_i(t) = f\,(L_i(t); Environment)$. When an element *i* is part of a system formed by interrelated degraded components, a load is transferred as follows:

$$L_i(t) = L_{i,0}(t) + \sum_{j=1}^{q} \left(\propto_{j,i} L_{j,0}(t)\right) - \sum_{j=1}^{q} \left(\propto_{i,j} L_{i,0}(t)\right)$$

$$\text{with} \qquad \sum_{i=1}^{q} L_i(t) = L_T \tag{3.5}$$

where $L_{i,0}(t)$ is the load initially supported by the element *i* before the occurrence of any degradation of other elements, $L_i(t)$ is the load supported by the element *i* after the load redistribution and L_T is the total load supported by all the elements in the system, $\sum_{j=1}^{q}\left(\propto_{j,i} \times L_{j,0}(t)\right)$ is the additional load supported by element *i* due to the degradation of element *j*, with $1 \le j \le q \;\; (j \ne i)$, $\sum_{j=1}^{q}\left(\propto_{i,j} \times L_{i,0}(t)\right)$ is the loss of load distributed to element *j* due to the degradation of element *i*, $\propto_{j,i}$ is a function of the degradation of element *j* and a geometric coefficient that indicates the amount of the transferred load between elements *i* and *j*. In this work, $\propto_{j,i}$ will be approximated as follows:

$$\propto_{j,i} = c_{i,j} \left[\frac{d_j(t)}{d_{F,j}}\right]^n \tag{3.6}$$

where $c_{i,j}$ and n can be calibrated by mechanical analysis (theory of structures, finite element, etc).

3.3 System probability of failure

The failure probability of the system $P_{f,system}$ is estimated in literature by the use of combinations of series and parallel subsystems to model the whole system. However, in case of a redundant system such as civil engineering structures, its estimation is governed among others by: (1) the complex dependencies between the different components and subsystems, (2) the different possible load paths, (3) the geometrical configuration of components, (3) the level of ductility of each component. Therefore, we propose a method to estimate the system failure probability, by the use of a redundancy factor I_{redund}, such that:

$$P_{f,system} = (1 - I_{redund})\, P_{f,series} + I_{redund}\, P_{f,parallel} \tag{3.7}$$

$$P_{f,series}(t) = 1 - \prod_i (1 - Pf_{i,d}\,(t)) \tag{3.8}$$

$$P_{f,parallel}\,(t) = \prod_i Pf_{i,d}\,(t) \tag{3.9}$$

$$\text{with} \qquad P_{fi,d}(t) = P_{fi}(t) + \sum_{j \ne i} P_{i|j}(t)\, P_j(t) \tag{3.10}$$

where $P_{fi}(t)$ is the intrinsic failure probability of component *i*, $\sum_{j \ne i} P_{i|j}(t)\, P_j(t)$ is the probability of failure of component *i* due to the failure of other components of the system,

I_{redund} is a function of the system architecture and the correlation between the system components.

In case of civil engineering structures, I_{redund} can be given as a function of the geometric coefficient $c_{i,j}$ defined in equation (3.6). The coefficient $c_{i,j}$ indicates the amount of the transferred load between elements *i* and *j*, depending on the geometrical configuration of the system, the ductility and the stiffness of each component. Therefore the coefficient $c_{i,j}$ can be estimated by the theory of structures or by finite element analysis. Let us observe this geometric coefficient for two elements *i* and *j* in case of degradation of element *j*:

- $0 \leq c_{i,j} \leq 1$
- If $c_{i,j} = 0$, then the load supported by *j* is not redistributed on *i*, which is similar to a series system configuration.
- If $c_{i,j} = 1$, then the load supported by *j* is totally redistributed on *i*, which is similar to a parallel system configuration.
- If $c_{i,j}$ increases then the redistribution of the load initially carried by *j* on the element *i* increases.

The procedure for evaluating I_{redund} consists first of computing $c_{i,j}$ for all the q components of the system. This will result in q^2 geometric coefficients (in a matrix q×q). Then I_{redund}. can be calculated as follows:

$$I_{redund} = \frac{\sum_i \sum_j c_{i,j}}{q^2} \tag{3.11}$$

3.4 Maintenance cost items

The maintenance cost of a system with dependent components is formed of many cost items. For the purpose of clarifying the function of every item, Figure 3.6 shows a diagram of all PC and CM costs applied to a single component *i.* The costs of preventive maintenance (PM) in an interdependent multi-component system are mainly formed by:

- C_d^p: the degradation consequence which spans from the time of initiation of degradation till the preventive repair time.
- C_{SD}^p : the preventive shutdown cost, which covers the direct and indirect costs suffered during the maintenance. For example, in case of bridge structures, this cost can be equal to the user costs specified according to the traffic strategy adopted. This cost is incurred during the whole duration of the maintenance action.
- C_{SU}^p : the preventive setup cost related to the common system costs, such as mobilizing repair crew, safety provisions, transportation, tools, etc.
- C_M^p : The preventive repair cost

The costs of corrective maintenance (CM) in an interdependent multi-component system are mainly formed by:

- C_d^c: the degradation consequence which spans from the time of initiation of degradation until failure.

- C_{SD}^{c} : the corrective shutdown cost which spans from the time of failure until the end of corrective repair. It is usually larger than the preventive shutdown cost because $w_i^p < w_i^c$ as explained in section 3.3.
- C_{SU}^{c} : the corrective setup cost which can be larger than the preventive one due to the fact that the sudden need for setup items costs more than a planned previously reserved one.
- C_{SU}^{c} : The corrective repair cost
- C_F : The direct and indirect failure consequences studied in chapter 2.
- The associated failure cost, which is the consequence of the failure of stochastically dependent components

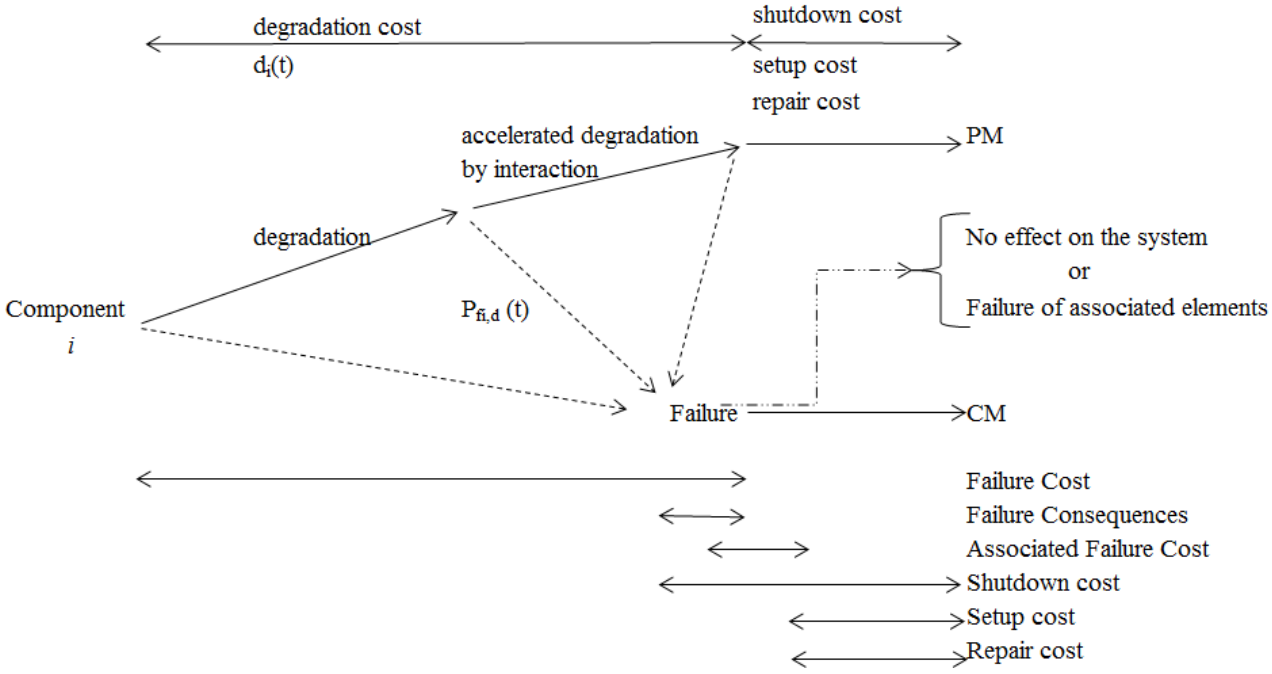

Figure 3.6: PM and CM costs of component *i*.

3.5 Cost Expectancy for individual components

The procedure to evaluate the costs explained above is detailed in this section for an individual component *i*, dependent on several components *j* of the system.

The consequence of preventive maintenance for component *i*, $C_{PM,i}$, can be formulated in terms of the degradation cost $C_{d,i}^{p}$, the setup cost $C_{SU,i}^{p}$, the preventive repair cost $C_{M,i}^{p}$ and the downtime cost $C_{SD,i}^{p}$ as follows:

$$C_{PM,i} = C_{d,i}^{p} + C_{SU,i}^{p} + C_{SD,i}^{p}\, w_i^p + C_{M,i}^{p} \tag{3.12}$$

The probability of occurrence of the preventive maintenance consequence in a time cycle between two planned interventions is related to the probability that the component *i* will not fail before the time scheduled for the preventive maintenance. It is equal to the probability of survival of *i*; $1 - P_{fi,d}(t)$, as per equation (3.4).

The cost of downtimes can be obtained by multiplying the cost of shutting down the structure (e.g. suspending a bridge structure or a corresponding lane), by the downtime needed for repair, as follows;

Downtime consequence of preventive repair: $C_{SD,i}^{p}\, w_i^{p}$ (3.13)

Downtime consequence of corrective repair: $C_{SD,i}^{c}\, w_i^{c}$ (3.14)

where $C_{SD,i}^{p}$ and $C_{SD,i}^{c}$ are respectively preventive and corrective cost per unit time incurred by the shutdown of component, and w_i^{p} and w_i^{c} are respectively the preventive and corrective non-zero maintenance downtimes. This cost is related to the time lost in the maintenance tasks.

The consequence of a corrective maintenance is more complex to evaluate, since its occurrence is related to failure, which may induce direct and indirect failure consequences, $C_{F,i}$, in addition to the shutdown, setup and repair costs. Moreover, some components are stochastically dependent on *i*, and therefore, the failure of *i* will necessitate not only the repair of *i* itself, but also the repair of all associated failures (AF). Let E_{AF} be a group of elements *j* stochastically dependent on *i*. When element *i* fails, the repair of element *j* occurs only when element *j* fails knowing that element *i* has already failed. Thus, the probability of occurrence of this event is: $P_{i|j}(t) \times P_j(t)$. The downtime needed to repair element *j* when *i* fails is accounted for in w_i^{c}, which is formulated in section 3.6.3.

The consequence of corrective maintenance can then be formulated as:

$$C_{CM,i} = C_{d,i}^{c} + C_{SU,i}^{c} + C_{SD,i}^{c}\, w_i^{c} + C_{M,i}^{c} + C_{F,i} + \sum_{j \in E_{AF}} C_{M,j}^{c}\, P_{j|i}(t) \tag{3.15}$$

The probability of occurrence of the corrective maintenance consequence in a time cycle between two planned interventions is related to the probability that the component *i* will fail before the time scheduled for the preventive maintenance; $P_{fi,d}(t)$ as per equation (3.3).

Thus, the expected cost for the maintenance of component *i* for a cycle between two replacement times can be formulated as;

$$\begin{aligned} E[C_i(t)] = {} & \left(C_{d,i}^{p} + C_{SU,i}^{p} + C_{SD,i}^{p}\, w_i^{p} + C_{M,i}^{p}\right)\left(1 - P_{fi,d}(t)\right) \\ & + \left(C_{d,i}^{c} + C_{SU,i}^{c} + C_{SD,i}^{c}\, w_i^{c} + C_{M,i}^{c} + C_{F,i} + \sum_{j,AF} C_{M,j}^{c}\, P_{j|i}(t) \right) P_{fi,d}(t) \end{aligned} \tag{3.16}$$

The expected cost per unit time is given as the expected cost on one cycle over the expected length of a cycle (Barlow and Hunter 1960).

3.6 Cost Expectancy for the maintenance of multi-components

The objective of this section is to formulate the cost function for the maintenance planning of a multi-component system taking into account stochastic, structural and economic dependency.

Due to the dependencies between the system components, the maintenance cost expectancy for multiple components is not equal to the sum of the expected maintenance costs of the individual components.

Considering simply the sum of the cost expectancies for individual elements in equation (3.16) to compute the cost expectancy of a multi-component will lead to many complications. To clarify the latter idea, let us consider a system with two dependent components b_1 and b_2

- the same setup cost may be used for the maintenance of b_1 and b_2 at the same time, and thus there is no need to consider it twice.
- the same time may be needed to repair both elements, thus the shutdown cost can be considered only one time.

To avoid considering some of the common costs several times, an approach to formulate the total cost expectancy would be to associate to each cost a probability of occurrence. Let G_{pu} be a group of components to be preventively repaired at an optimal scheduled time $t_{ku} = k_u\tau$.

The expression of the total cost per unit time requires the consideration of the involved costs along a cycle. The representative cycle is given by the expected time for replacing all the components simultaneously $K\tau$ (Gertsbakh 2000), with $K = lcm(\tau, k_1, k_2, \cdots, k_q)$, where τ is continuous and k_i are integer variables (Laggoune et al. 2009), $lcm(\cdot)$ being the least common multiplier.

The total expected cost for the system maintenance along a cycle can be formulated as follows, where the subscript T refers to the cost corresponding to the total system.

$$E[C_T(t)] = C^c_{d,T}(t) + C^p_{d,T}(t) + C^c_{M,T}(t) + C^p_{M,T}(t) + C^p_{SU,T}(t) + C^c_{SU,T}(t) + C^p_{SD,T}(t) + C^p_{SD,T}(t) + C_{F,T}(t) \tag{3.17}$$

3.6.1 Maintenance Cost

In order to evaluate the costs in equation 3.17, every cost component must be associated to a probability of occurrence. The probability of occurrence of the corrective maintenance cost $C^c_{M,i}$ of the component i during a cycle is equal to its probability of failure formulated in equation 3.3.The total corrective maintenance cost for the system components that has failed along a cycle can then be formulated as follows:

$$C^c_{M,T}(t) = \sum_i \left[C^c_{M,i} \left(P_{fi}(t) + \sum_{j \neq i} P_{i|j}(t)\, P_j(t) \right) \right]$$

$$\text{with} \quad \sum_i \left[\left(P_{fi}(t) + \sum_{j \neq i} P_{i|j}(t)\, P_j(t) \right) \right] \leq 1 \tag{3.18}$$

The total preventive maintenance cost for all components of a group G_{pu} scheduled for maintenance at time $t = k_u\tau$ can be expressed as:

$$C^p_{M,T}(t) = \sum_{i \in G_{pu}} \left[C^p_{M,i} \left(1 - P_{fi}(t) - \sum_{j \neq i} P_{i|j}(t)\, P_j(t) \right) \right] \tag{3.19}$$

3.6.2 Setup Cost

In the following section, a method is proposed for the evaluation of the total preventive and corrective setup cost, $C^{p}_{SU,T}$ and $C^{c}_{SU,T}$ respectively.

The setup cost covers the costs of the required operations to set the maintenance procedures, such as tower cranes, mobile cranes, construction machines, loaders, handlers, etc… Let $C^{c}_{SI,l}$be the cost of a setup item *l*, thus it can be a part of the total setup cost $C^{c}_{SU,T}$, and let $P_{[C^{c}_{SI,l} \subset C^{c}_{SU,i}]}$ be the probability that a setup cost item $C^{c}_{SI,l}$ be included in the setup cost of component *i*, $C^{c}_{SU,i}$. The corrective setup cost is evaluated below for a system which components may fail at any time between two scheduled replacements time. The corrective setup cost of component *i* is a consequence of the failure of component *i*, thus it should be multiplied by P_{fi} in the first row below of equation (3.20). The matrix in the (3.20) allows us to compute the set up cost for component *i* as shown in equation (3.21).

$$\begin{matrix} C^{c}_{SU,T} & 1\,(P_{f1}) & \dots & \mathrm{i}\,(P_{fi}) & \dots \end{matrix}$$

$$\begin{bmatrix} C^{c}_{SI,1} \\ \vdots \\ C^{c}_{SI,l} \\ \vdots \\ \vdots \end{bmatrix} \begin{bmatrix} P_{[C^{c}_{SI,1} \subset C^{c}_{SU,1}]} & \cdots & P_{[C^{c}_{SI,1} \subset C^{c}_{SU,i}]} & \ddots \\ \vdots & \ddots & \vdots & \ddots \\ P_{[C^{c}_{SI,l} \subset C^{c}_{SU,1}]} & \cdots & P_{[C^{c}_{SI,l} \subset C^{c}_{SU,i}]} & \ddots \\ \vdots & \ddots & \vdots & \ddots \\ \vdots & \ddots & \vdots & \ddots \end{bmatrix} \tag{3.20}$$

$$C^{c}_{SU,i} = \sum_{l} SU^{c}_{l}\, P_{[SU^{c}_{l} \subset C^{c}_{SU,i}]} \tag{3.21}$$

The probability of occurrence of a setup cost item $C^{c}_{SI,l}$ depends on the union of probabilistic events$\left[C^{c}_{SI,l} \subset C^{c}_{SU,i}\right]$, which is equal to their sum minus their intersections, as follows:

$$P\left(\bigcup_{i=1}^{q}\left[C^{c}_{SI,l} \subset C^{c}_{SU,i}\right]\right) = \sum_{i} P_{[C^{c}_{SI,l} \subset C^{c}_{SU,i}]} - P\left(\bigcap_{i=1}^{q}\left[C^{c}_{SI,l} \subset C^{c}_{SU,i}\right]\right) \tag{3.22}$$

$$P\left(\bigcap_{i=1}^{q}\left[C^{c}_{SI,l} \subset C^{c}_{SU,i}\right]\right) = \sum_{i=2}^{q}\sum_{j=1}^{i-1}\left(P_{\left(\left[C^{c}_{SI,l} \subset C^{c}_{SU,i}\right] \,|\, \left[C^{c}_{SI,l} \subset C^{c}_{SU,j}\right]\right)} P_{\left[C^{c}_{SI,l} \subset C^{c}_{SU,j}\right]}\right) \tag{3.23}$$

In fact, the principle of inclusion and exclusion for probability states that the probability of the union of *q* events in a sample space is given by:

$$P\left(\bigcup_{i=1}^{q} E_i\right) = \sum_{k=1}^{q}(-1)^{k+1} \sum_{i_1,i_2,\cdots,i_k} P(E_{i1} \cap E_{i2} \cap \cdots \cap E_{ik}) \tag{3.24}$$

All the terms subsequent to the first two terms of the Union equation (3.16) are chosen to be nil in this study; which is equivalent to applying equation 3.19 for *k=1* and *k=2*, and neglecting all *k* between *2* and *q*. In fact the second term $P\left(\bigcap_{i=1}^{q}\left[C^{c}_{SI,l} \subset C^{c}_{SU,i}\right]\right)$ contains the product of two probabilities (as shown in eq 3.17), and all subsequent terms would contain the product of three to *q* probabilities, and will therefore be neglected compared to the first two terms.

When the number of elements in the system increases, the probability that $C^{c}_{SI,l}$ is included in many setup costs of the system increases, thus this function is an increasing function of the

number of elements. The probability of occurrence of a particular setup cost SU_l^c when maintaining several components depends on the inclusion of $C_{SI,l}^c$ in the setup costs of the maintained elements.

$$P\left(\bigcup_{i=1}^{q}\left[C_{SI,l}^c \subset C_{SU,i}^c\right]\right) = \sum_{i=1}^{q} P_{\left[C_{SI,l}^c \subset C_{SU,i}^c\right]} - \sum_{i=2}^{q}\sum_{j=1}^{i-1}\left(P_{\left(\left[C_{SI,l}^c \subset C_{SU,i}^c\right] \mid \left[C_{SI,l}^c \subset C_{SU,j}^c\right]\right)} P_{\left[C_{SI,l}^c \subset C_{SU,j}^c\right]}\right) \tag{3.25}$$

Therefore, the total setup cost becomes equal to the sum of each setup component multiplied by its probability of occurrence:

$$C_{SU,T}^c = \sum_l C_{SI,l}^c \left[\sum_{i=1}^{q} P_{fi}\, P_{\left[C_{SI,l}^c \subset C_{SU,i}^c\right]} - \sum_{i=2}^{q}\sum_{j=1}^{i-1} P_{fi/j}\, P_{fj}\, \left(P_{\left(\left[C_{SI,l}^c \subset C_{SU,i}^c\right] \mid \left[C_{SI,l}^c \subset C_{SU,j}^c\right]\right)} P_{\left[C_{SI,l}^c \subset C_{SU,j}^c\right]}\right)\right] \tag{3.26}$$

Similarly, the evaluation of the preventive setup cost $C_{SU,T}^p$ can be formulated for a group of components G_{pu} scheduled for maintenance at time $t = k_u\tau$. Let q_{Gpu} be the number of components belonging to G_{pu}. By following the same procedure as the corrective setup cost, $C_{SU,T}^p$ can be expressed as following:

$$C_{SU,T}^p = \sum_l C_{SI,l}^p \left[\sum_{i=1}^{q_{Gpu}} \left(1 - P_{fi}\right) P_{\left[C_{SI,l}^p \subset C_{SU,i}^p\right]} - \sum_{i=2}^{q_{Gpu}}\sum_{j=1}^{i-1}\left(1 - P_{fi}\right)\left(1 - P_{fj}\right)\left(P_{\left[C_{SI,l}^p \subset C_{SU,i}^p\right] \mid \left[C_{SI,l}^p \subset C_{SU,j}^p\right]} \times P_{\left[C_{SI,l}^p \subset C_{SU,j}^p\right]}\right)\right] \tag{3.27}$$

3.6.3 Shutdown Costs

According to Thomas (1986), the structural dependency can be horizontal or modular. Horizontal dependency can be described as the structural connection between different items in series, in parallel, or in k-out-of-n configurations. Modular dependency means that some components have to be dismantled in order to repair another component, and thus they stop functioning for the whole time of repair.

Structural dependency can only be modeled by taking into account the downtimes needed to repair or dismantle inter-related components. Let $t_{M,i}^p$ and $t_{M,i}^c$ be respectively the downtimes needed to preventively and correctively repair component i, and $\Delta t_{MD,u|i}$ be the downtime needed to dismantle an item u which is modularly dependent (MD) on i.

Stochastic dependency may induce the failure of a component *j*, in case of failure of a component *i*. There is an Associated Failure (AF) between *j* and *i* due to stochastic dependency. Therefore, in case of corrective maintenance, in addition to the downtimes needed to repair failed elements and dismantle modularly dependent element, it is required to repair failed elements by AF. Let $t_{M,j|i}^{c.AF}$ be the time needed to repair an element *j* which has failed as a consequence of the failure of *i* due to stochastic dependency between elements.

The preventive and corrective non-zero maintenance downtimes, w_i^p and w_i^c, of component *i* can be expressed as functions of the above explained times as follows ;

$$w_i^p = f\left(t_{M,i}^p; \Delta t_{MD,u|i}\right) \tag{3.28}$$

$$w_i^c = f\left(t_{M,i}^c; t_{M,j|i}^{c.AF}; \Delta t_{MD,u|i}\right) \tag{3.29}$$

The downtimes would be higher if the action is corrective because the same maintenance action will need less time if everything is planned a priori; i.e. $w_i^p < w_i^c$. Figure 3.7 illustrates the downtimes needed for PM and CM activities, where E_{AF} is a group of elements *j* stochastically dependent on *i*, and E_{MD} is a group of elements *u* modularly dependent on *i* and *j*. In case of preventive grouping, the duration w_i^p is function of the maintenance times of all components in the group and the time needed to dismantle modularly dependent items. In case of failure, the duration w_i^c is function of the time to maintain all failed items *j* by AF and to dismantle modularly dependent items *u*.

The total preventive and corrective shut down costs can then be expressed as follows:

$$C_{SD,T}^p = C_{SD,strategy}^p \left(\bigcup_{i=1}^q w_i^p\right) \tag{3.30}$$

$$C_{SD,T}^c = C_{SD,strategy}^c \left(\bigcup_{i=1}^q w_i^c\right) \tag{3.31}$$

where $C_{SD,T}^p$ and $C_{SD,T}^c$ are respectively the preventive and corrective shutdown costs for all components of the system that have failed at any time between two successive scheduled maintenance times.

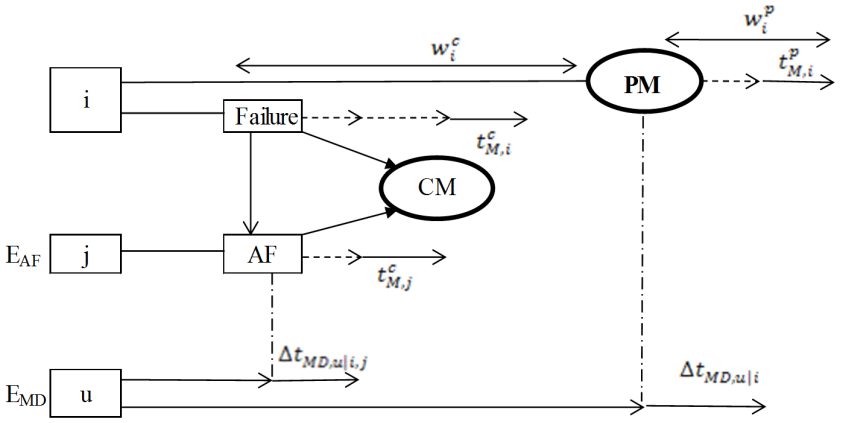

Figure 3.7: PM and CM downtimes.

3.7 Numerical applications

The above proposed model is applied to four types of structure for illustration purposes; namely, two beams in parallel, two beams in series, slab and bituminous system, and finally a bridge superstructure.

3.7.1 Two beams in parallel

The proposed model is applied on a structure formed by two beams in parallel in order to optimize the maintenance planning of the two beams by considering the dependencies between the two elements. In this example, two reinforced concrete beams (b_1 and b_2) are simply supported as shown in Figure 3.5. The beams have identical spans of 15 m. The cross-section is 40 cm wide and 90 cm deep. A 25 cm concrete slab spans between the two beams. A uniformly distributed load (UL) of 2.5 kN/m^2 is applied on the slab. The beam b_1 carries a facade load equivalent to a distributed line load of 0.05MN/m.

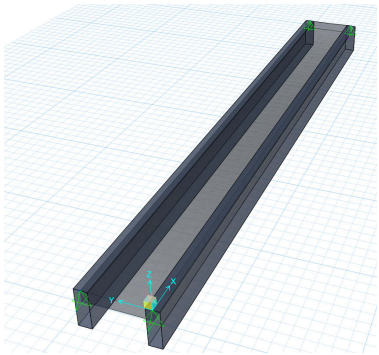

Figure 3.8: Two identical concrete beams with connecting slab.

3.7.1.1- Failure Interaction

In order to evaluate the effect of degraded or failed beam on the adjacent one, a 2D Finite Element (FE) model using SAFE V2014 (CSI 2014) is set to analyze the two structures. According to the FE model, b_1 carries 68% of the total load and b_2 carries 32% (Figure 3.5). Therefore, if M_T is the total moment carried by the two beams, the initial moments carried by each beam before any degradation are:

$$M_{1,0} = 0.68 \times M_T \quad \text{and} \quad M_{2,0} = 0.32 \times M_T \tag{3.32}$$

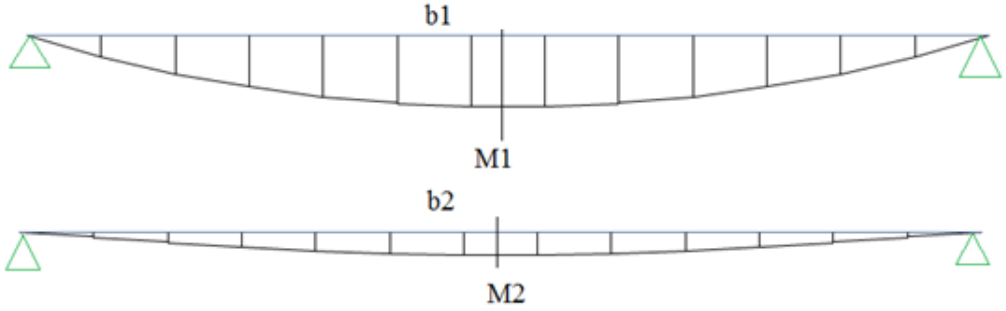

Figure 3.9: Bending moments.

The failure probability is calculated by considering the reinforcement areas: 8HA25 for b_1 and 8HA16 for b_2, which are computed according to EC2 (Code 2005). Let us consider that $M_{R,1}$ and $M_{R,2}$ are respectively the resisting moments of b_1 and b_2. Due to corrosion, the resisting moments are degraded with time. The random and deterministic variables of the problem are given in Table 3.1.

Random variables	**Symbol**	**distribution**	**mean**	**COV**	**units**
Yield strength	f_y	Lognormal	500	0.07	MPa
Deterministic parameters					
Concentration	C_{cr}		0.9		
Concentration	C_s		2.95		
Coefficient of diffusion	D_c		6.00E-12		
Cover	c		0.04		m
Concrete strength	f_c		28		MPa
Module d Young	E		25.3		GPa
Length	L		15		m
Width	B		0.4		m
Height	h		0.9		m
Load on slab	UL		2.5		kN/m^2
Load on b_1	q		50		kN/m

Table 3.1: Random and deterministic variables for the two parallel beams structure.

The probabilities of failure are calculated at discrete points of time by the first order reliability method (FORM) for each beam. FORM provides estimations of the failure probability for time increments of 0.5 years. Then, a continuous closed form of the failure probability in function of time can be approximated by a second order polynomial regression. The above approximation is intended to loosen the computational burden when applying the proposed methodology as explained in section 3.2. Other methods may also be applied to estimate a closed form of the failure probability as function of time. When applying the above, the failure probability of each beam in function of time can be estimated as follows:

$$
\begin{aligned}
&P_{fd1}(t) = P_r\left(M_{R,1}(t) - 0.68\, M_T < 0\right) = 1.59 \times 10^{-5} && if\ t \le t_i \\
&P_{fd1}(t) = 10^{\left(-4.8+7\times10^{-6}\,(t-t_i)^3-8\times10^{-4}\,(t-t_i)^2+0.0549\,(t-t_i)\right)} && if\ t > t_i \\
&P_{fd2}(t) = P_r\left(M_{R,2}(t) - 0.32 \times M_T < 0\right) = 3.045 \times 10^{-7} && if\ t \le t_i \\
&P_{fd2}(t) = 10^{\left(-6.5+9\times10^{-6}\,(t-t_i)^3-9\times10^{-4}\,(t-t_i)^2+0.0656\,(t-t_i)\right)} && if\ t > t_i
\end{aligned}
\tag{3.33}
$$

where t_i is the time of initiation of corrosion. For $t \le t_i$, the resistant moment is constant. In this application, this time is found to be $t_i = 8.25$ years.

In order to find the maintenance costs, the next step is to compute $P_{i|j}(t)$, which is the probability of failure of the element b_i knowing that element b_j has failed. The following procedure is suggested for the computation of $P_{i|j}(t)$ in this example.

- Assigning nil stiffness to b_2 in the FE model to characterize the failure of b_2. The increase $(inc_{1|2})$ in the moment of b_1 due to the failure b_2 is 47% (obtained by the FE model). Therefore $M_{1|2} = (1 + 0.47) \times 0.68\, M_T = M_T$.
- Assigning nil stiffness to b_1 in the FE model to characterize the failure of b_1. The increase $(inc_{2|1})$ in the moment of b_2 due to the failure of b_1 is 210% (obtained by the FE model). Therefore $M_{2|1} = (1 + 2.1) \times 0.32 M_T = M_T$.

The above results are predicted: when b_1 fails, the entire load is carried by b_2 until the failure of b_2 and vice-versa, therefore, $M_{1|2} = M_{2|1} = M_T$. However $P_{1|2}(t) \neq P_{2|1}(t)$ because b_1 is more reinforced than b_2, therefore $M_{R,1} > M_{R2}$. The conditional probabilities are calculated by FORM, and then they are approximated by polynomial regressions as follows:

$$\begin{aligned} P_{f1|2}(t) &= P_r\left(M_{R,1}(t) - M_T < 0\right) = 8.9 \times 10^{-4} && if\ t \le t_i \\ P_{f1|2}(t) &= 10^{\left(-3.05+6\times10^{-6}\times(t-t_i)^3-6\times10^{-4}\times(t-t_i)^2+0.042\times(t-t_i)\right)} && if\ t > t_i \\ P_{f2|1}(t) &= P_r\left(M_{R,2}(t) - M_T < 0\right) = 2.06 \times 10^{-2} && if\ t \le t_i \\ P_{f2|1}(t) &= 10^{\left(-1.69+4\times10^{-6}\times(t-t_i)^3-5\times10^{-4}\times(t-t_i)^2+0.029\times(t-t_i)\right)} && if\ t > t_i \end{aligned} \tag{3.34}$$

As explained in section 3.2.2 (eq 3.3 and Figure 3.4), the probabilities of failure of each beam due to intrinsic degradation and due to the failure of the other beam are given by:

$$\begin{aligned} P_{f1}(t) &= P_{fd1}(t) + P_{1|2}(t)\, P_{fd2}(t) \\ P_{f2}(t) &= P_{fd2}(t) + P_{2|1}(t)\, P_{fd1}(t) \end{aligned} \tag{3.35}$$

3.7.1.2- Degradation interaction

In case of degradation of beam i, the moment initially supported by this beam is transferred to the other beam. The degradation diagram is shown in Figure 3.7, where d_1 and d_2 are the degradation of beams b_1 and b_2 respectively, and d_{F1} and d_{F2} are the degradation limits that causes the beam failure, which can be equal to the beam ultimate degradation.

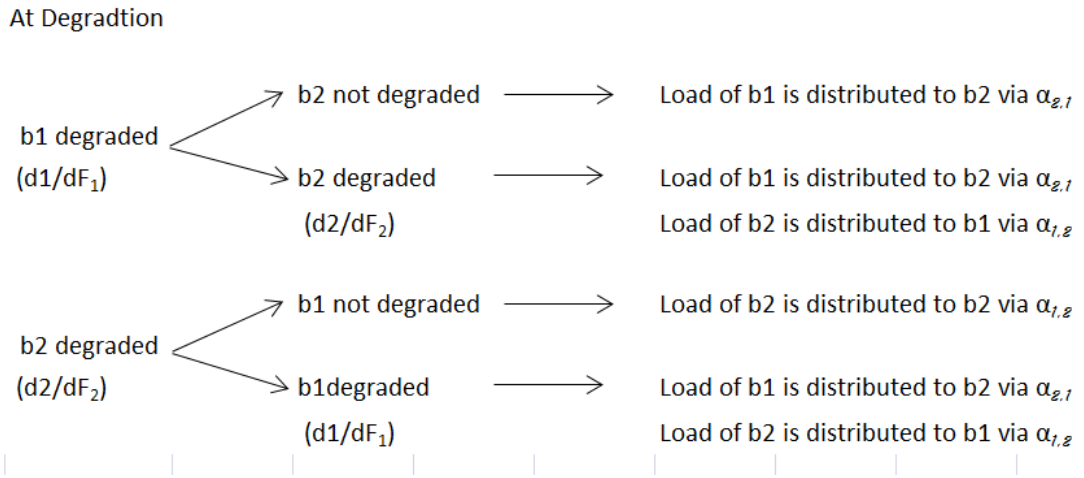

Figure 3.10: Degradation diagram.

When b_1 and/or b_2 are degraded, the moments are redistributed as follows:

$$M_1(t) = M_{1,0} - \propto_{2,1}(t) \times M_{1,0} + \propto_{1,2}(t) \times M_{2,0}$$
$$M_2(t) = M_{2,0} - \propto_{1,2}(t) \times M_{2,0} + \propto_{2,1}(t) \times M_{1,0} \quad (3.36)$$

where $\propto_{2,1}(t)$ and $\propto_{1,2}(t)$ are the moment distribution factors that are related to the degree of degradation of respectively b_1 and b_2 at time t as follows:

$$\propto_{2,1}(t) = c_{2,1}\left(\frac{d_1(t)}{dF_1}\right)^{n_{2,1}} \quad \text{and} \quad \propto_{1,2}(t) = c_{1,2}\left(\frac{d_2(t)}{dF_2}\right)^{n_{1,2}} \quad (3.37)$$

where $c_{1,2}$, $c_{2,1}$, $n_{1,2}$ and $n_{2,1}$ can be obtained by computing the moment redistributed to b_1 and/or b_2 for each stiffness value of b_2 and/or b_1 varying from 0 to 1.

In this example, $\propto_{2,1}(t) = 2.1 \times \left(\frac{d_1(t)}{dF_1}\right)^2$ and $\propto_{1,2}(t) = 0.47 \times \left(\frac{d_2(t)}{dF_2}\right)^2$ (3.38)

$$d_1(t) = 0.02 \times t \quad \text{and} \quad d_2(t) = 0.01 \times t \quad (3.39)$$

The degradation monetary consequence can be given as a function of the degrading capacities. Many factors accelerate the degradation of a system components, e.g. heavy load, corrosive environment, etc… To consider the above accelerators, the following form is considered to compute the degradation costs in this application:

$$C_{deg,1}(t) = C_{d1,fixe} \times e^{c\left(\frac{1}{M_{R,1}} - \frac{1}{M_1(t)}\right)} \quad \text{and} \quad C_{deg,2}(t) = C_{d2,fixe} \times e^{c\left(\frac{1}{M_{R,2}} - \frac{1}{M_2(t)}\right)} \quad (3.40)$$

where $M_{R,1}$ and $M_{R,2}$ are the capacity limits, c is an accelerator factor taken equal to 20 and $C_{d1,fixe} = 0.02$.

3.7.1.3- Maintenance Planning

The maintenance policy used in this application is as following:

- After a preventive maintenance action, the maintained component becomes "as good as new".
- Between two preventive maintenance actions, if a component fails, a minimal repair is immediately performed to restore the component to the "as bad as old" state.
- b_1 is maintained every $k_1\ \tau$ with $k_1 = 1$.
- b_2 is maintained every $k_2\ \tau$ with k_2 positive integer.

The total cost is calculated during a life-cycle of $K\ \tau$ with $K = lcm(k_1, k_2) = k_2$.

3.7.1.4- Economic dependency

In many previous works (Laggoune et al. 2009; Van Horenbeek and Pintelon 2013; Vu et al. 2014), the setup common cost C_{SU} was accounted for in the following way: Grouping activities yields a cost reduction such that the total setup cost is $(n-1)C_{SU}$, where n is the number of groups of preventive maintenance activities. In our application, this means that $n = 2$ if $k_1 \neq k_2$, and $n = 1$ if $k_1 = k_2$.

In the following, the new formulation, which we proposed for considering economic dependency, is applied to the two beams.

Let us consider two setup cost items: cost of allocating cranes $C_{SI,1}$ and cost of delivering special equipment $C_{SI,2}$. The philosophy of the proposed methodology yields in assigning to every possible cost a probability of occurrence. The probability of using a setup cost component when maintaining b_i $\left(P_{[C_{SI,l} \subset Mi]}\right)$ are shown in 3.2.

Name	$C_{SI,l}$ cost/unit time	$\boldsymbol{P}_{[C_{SI,l} \subset C_{SU,i}]}$	
		b_1	b_2
Cranes $(SI,1)$	0.01	0.933	0.895
special equipment $(SI,2)$	0.02	0.870	0.802

Table 3.2: Setup cost components.

If the maintenance activities of b_1 and b_2 are grouped (i.e.$k_1 \neq k_2$), then the probability that a setup cost component be used in the maintenance activity of b_1 (or b_2) knowing that it is used in the maintenance activity of b_2 (or b_1) is equal to 1 ; $P_{[C_{SI,l} \subset C_{SU,1}] | [C_{SI,l} \subset C_{SU,2}]} = 1$. The latter means that if a crane or a special equipment was brought for use in the maintenance of b_1, it will be definitely used in the maintenance of b_2 in case of grouping the two maintenance activities, and vice-versa.

- At time $K\tau$, the preventive setup cost is:

If $k_1 \neq k_2$ (i.e. there is no grouping of maintenance activities), then the preventive setup cost will be:

$$A = \frac{\left(C^p_{SI,1}\, P_{[C^p_{SI,1} \subset C^p_{SU,1}]} + C^p_{SI,2}\, P_{[C^p_{SI,2} \subset C^p_{SU,1}]}\right)\frac{K}{k_1} + \left(C^p_{SI,1}\, P_{[C^p_{SI,1} \subset C^p_{SU,2}]} + C^p_{SI,2}\, P_{[C^p_{SI,2} \subset C^p_{SU,2}]}\right)\frac{K}{k_2}}{K} \tag{3.41}$$

If $k_1 = k_2 = 1$ (i.e. the maintenance activities are grouped), then the preventive setup cost will be ; $B = A - \Delta C$, where ΔC is the cost reduction

$$\Delta C = C^p_{SI,1}\, P_{\left[C^p_{SI,2} \subset C^p_{SU,1}\right] | \left[C^p_{SI,1} \subset C^p_{SU,2}\right]}\, P_{\left[C^p_{SI,1} \subset C^p_{SU,1}\right]} + C^p_{SI,2}\, P_{\left[C^p_{SI,2} \subset C^p_{SU,2}\right] | \left[C^p_{SI,2} \subset C^p_{SU,1}\right]}\, P_{\left[C^p_{SI,2} \subset C^p_{SU,2}\right]} \tag{3.42}$$

The latter means that grouping activities yields a cost reduction proportional to the intersection of the two events: $P_{\left[\left(C^p_{SI,l} \subset C^p_{SU,1}\right) \cap \left(C^p_{SI,l} \subset C^p_{SU,2}\right)\right]}$.

- At the time of failure, the corrective setup cost becomes:

$$\begin{aligned} C = {} & \left(C^c_{SI,1}\, P_{\left[C^c_{SI,1_1} \subset C^c_{SU,1}\right]} + C^c_{SI,2}\, P_{[C^c_{SI,2} \subset C^c_{SU,1}]}\right) P_{f1}(t) + \left(C^c_{SI,1}\, P_{[C^c_{SI,1} \subset C^c_{SU,2}]} + \right. \\ & \left. C^c_{SI,2}\, P_{[C^c_{SI,2} \subset C^c_{SU,2}]}\right) P_{f2}(t) - \left(C^c_{SI,1}\, P_{[C^c_{SI,1} \subset C^c_{SU,2}] | [C^c_{SI,1} \subset C^c_{SU,1}]}\, P_{[C^c_{SI,1} \subset C^c_{SU,1}]} + \right. \\ & \left. C^c_{SI,2}\, P_{[SU_2 \subset C^c_{SU,2}] | [C^c_{SI,2} \subset C^c_{SU,1}]}\, P_{[C^c_{SI,2} \subset C^c_{SU,1}]}\right) P_{f2/1}(t)\, P_{f1}(t) \end{aligned} \tag{3.43}$$

3.7.1.5- System probability of failure

When two elements are independent, the system probability of failure is:

$$P_{f,system}(t) = I_{redund}\, P_{f,parallel}(t) + (1 - I_{redund})\, P_{f,series}(t)$$

where $I_{redund} = \frac{\sum_i \sum_j c_{ij}}{nelem^2} = \frac{0.47+2.1}{2^2} = 0.65$

$$P_{f,parallel}(t) = P_{f1}(t)\, P_{f2}(t)$$

$$P_{f,series}(t) = \left(1 - P_{f1}(t)\right)\left(1 - P_{f2}(t)\right)$$

$$P_{f1}(t) = P_{fd1}(t) + P_{1|2}(t)\, P_{fd2}(t)$$

$$P_{f2}(t) = P_{fd2}(t) + P_{2|1}(t)\, P_{fd1}(t) \qquad (3.44)$$

3.7.1.6- Effect of cost components on maintenance planning

The maintenance optimization problem is given as:

Find	k_2 and τ
minimizing	$C(k_1, k_2, \tau)$
with	$k_1 = 1$ and $\tau \geq 0$
subject to:	$P_{f,system} < P_f^T$ (3.45)

where P_f^T is the system threshold failure probability, $C(k_1, k_2, \tau)$ is the total maintenance cost and k_1, k_2 and τ are as defined in section 3.7.1.3. In the following, we will optimize the maintenance planning of the two beams by considering several formulations for the total cost, in order to study the effect of each dependency form on the maintenance scheduling. The formulations are as follows:

- Case 1: None (No dependency)

In this basic formulation, degradation cost, stochastic and economical dependencies are not considered. The Total expected cost is:

$$C(k_1, k_2, \tau) = \left[\left(C_{M1}^p + C_{M1}^c\, P_{d1}(k_1\tau)\right)\frac{K}{k_1} + \left(C_{M2}^p + C_{M2}^c\, P_{d2}(k_2\tau)\right)\frac{K}{k_2}\right] \Big/ (K\tau) \qquad (3.46)$$

The system probability of failure does not take into account the dependencies between components when computing $P_{f,parallel}$ and $P_{f,series}$.

- Case 2: Degradation (D)

In this formulation, degradation cost is considered, although stochastic and economic dependencies are not. The expected total cost is:

$$C(k_1, k_2, \tau) = \frac{\left[\left(C_{M1}^p + C_{M1}^c\, P_{d1}(k_1\tau)\right)\frac{K}{k_1} + \left(C_{M2}^p + C_{M2}^c\, P_{d2}(k_2\tau)\right)\frac{K}{k_2}\right]}{K \times \tau} + C_{deg,1} + C_{deg,2} \qquad (3.47)$$

- Case 3: Stochastic (S)

In this formulation, stochastic dependency is considered, although degradation cost and economic dependency are not. The expected total cost is:

$$C(k_1, k_2, \tau) = \left(C^c_{M,T}) + \ C^p_{M,T}\right)/(K\tau) \tag{3.48}$$

where $C^c_{M,T}(t)$ and $C^p_{M,T}(t)$ are given by:

$$C^c_{M,T}(K\,\tau) = \ \left(C^c_{M,1}\left[P_{fd1}(k_1\tau) + P_{1|2}(k_1\tau)P_{fd2}(k_1\tau)\right]\right)\frac{K}{k_1} + \left(C^c_{M,2}\left[P_{fd2}(k_2\tau) + P_{2|1}(k_2\tau)P_{fd1}(k_1\tau)\right]\right)\frac{K}{k_2}$$

$$C^p_{M,T}(K\,\tau) = C^p_{M,1}\ \frac{K}{k_1} + C^p_{M,2}\ \frac{K}{k_2} \tag{3.49}$$

The system probability of failure takes into account the dependencies between components when computing $P_{f,parallel}$ and $P_{f,series}$ as explained in section 3.7.1.5.

- Case 4: Economic (E)

In this formulation, economical dependency is considered, although degradation cost and stochastic dependency are not. The expected total cost is:

$$C(k_1, k_2, \tau) = \left(\left[C^p_{M1} + C^c_{M1}P_{f1}(k_1\tau)\right]\frac{K}{k_1} + \left[C^p_{M2} + C^c_{M2} \times P_{f2}(k_2\tau)\right]\frac{K}{k_2}\right)/K\tau + SU \tag{3.50}$$

The reliability-based optimization of equation 3.45 is performed for the four cases explained above and for a threshold system probability of failureP^T_f varying from 10^{-5} to 10^{-3}. As explained in section 3.7.1.3, b_1 is maintained every $k_1\,\tau$ and b_2 is maintained every $k_2\,\tau$. The optimum maintenance times $k_1\,\tau$ and $k_2\,\tau$ for the two elements b_1 and b_2 are shown in Figure 3.11 for the four cases distinguished by different marker types and colors, and for a system threshold failure probability of $P^T_f = 5 \times 10^{-4}$. The values of the design variables k_2 and τ are also shown in Table 3.3 for all values of P^T_f, along with the value of the probabilities of failure of the elements P_{f1} and P_{f2} with the corresponding system failure probability $P_{fsystem}$ which can equal or higher than P^T_f.

From the above results, the following observations can be drawn:

- The economic dependency induces the grouping of maintenance actions; $k_1 = k_2 = 1$ for all values of P^T_f varying from 5×10^{-5} to 10^{-3}, even though b_1 is more loaded than b_2.
- Stochastic dependency leads to smaller maintenance time intervals, and thus neglecting stochastic dependency may lead to unsafe maintenance planning; the average decrease in maintenance times is 4%.
- The degradation cost increases with time, therefore it accentuates the convex shape of the total cost formula. For all P^T_f higher than the value of Pf_{system} corresponding to the optimal unconstrained response equivalent to the lower value of the convex total cost shape, the optimization results are equal to the unconstrained results and the reliability threshold P^T_f has no effect; in this example, the unconstrained optimum correspond to a system failure probability of 1.71×10^{-4}.

- The optimum maintenance time for very low probability thresholds correspond to the time of initiation of degradation; for a threshold probability of failure of 10^{-5}, all formulations yield the same maintenance planning corresponding to a maintenance activity for b_1 every 8.24 years, which is equal to the time of initiation of corrosion.

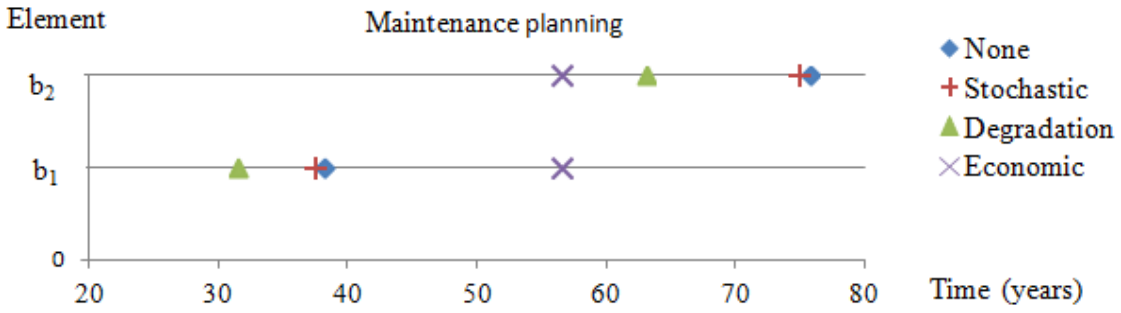

Figure 3.11: Maintenance planning for different formulations with $P_f^T = 5 \times 10^{-4}$.

NONE	P_f^T	τ	k_1	k_2	P_1	P_2	$P_{f,system}$
	1.00×10^{-3}	40.48	1	2	5.28×10^{-4}	2.33×10^{-3}	1.00×10^{-3}
	5.00×10^{-4}	37.86	1	2	4.53×10^{-4}	9.75×10^{-4}	5.00×10^{-4}
	1.00×10^{-4}	26.65	1	2	2.15×10^{-4}	7.03×10^{-5}	1.00×10^{-4}
	5.00×10^{-5}	19.70	1	2	1.22×10^{-4}	2.18×10^{-5}	5.00×10^{-5}
	1.00×10^{-5}	8.24	1	4	1.59×10^{-5}	1.27×10^{-5}	1.00×10^{-5}
Stochastic	P_f^T	τ	k_1	k_2	P_1	P_2	$P_{f,system}$
	1.00×10^{-3}	40.25	1	2	5.51×10^{-4}	2.30×10^{-3}	1.00×10^{-3}
	5.00×10^{-4}	37.47	1	2	4.53×10^{-1}	9.75E-01	5.00×10^{-4}
	1.00×10^{-4}	25.67	1	2	2.00×10^{-4}	8.65×10^{-5}	1×10^{-4}
	5.00×10^{-5}	18.83	1	2	1.12E-04	3.06×10^{-5}	5.00×10^{-5}
	1.00×10^{-5}	8.24	1	4	1.59E-04	1.42×10^{-4}	1.00×10^{-5}
Degradation	P_f^T	τ	k_1	k_2	P_1	P_2	$P_{f,system}$
	1.00×10^{-3}	31.53	1	2	3.04×10^{-4}	1.86×10^{-4}	1.71×10^{-4}
	5.00×10^{-4}	31.53	1	2	3.04×10^{-4}	1.86×10^{-4}	1.71×10^{-4}
	1.00×10^{-4}	26.65	1	2	2.15×10^{-4}	7.03×10^{-5}	1.00×10^{-4}
	5.00×10^{-5}	19.70	1	2	1.22×10^{-4}	2.18×10^{-5}	5.00×10^{-5}
	1.00×10^{-5}	8.24	1	4	1.59E-05	1.27E-05	1.00E-05
Economic	P_f^T	τ	k_1	k_2	p_1	p_2	$P_{f,system}$
	1.00×10^{-3}	66.35	1	1	2.58×10^{-3}	2.72×10^{-4}	1.00×10^{-3}
	5.00×10^{-4}	56.57	1	1	1.33×10^{-3}	9.53×10^{-5}	5.00×10^{-4}
	1.00×10^{-4}	30.09	1	1	2.76×10^{-4}	9.83×10^{-6}	1.00×10^{-4}
	5.00×10^{-5}	21.20	1	1	1.39×10^{-4}	4.11×10^{-6}	5.00×10^{-5}
	1.00×10^{-5}	8.24	1	4	1.59×10^{-5}	1.27×10^{-5}	1.00×10^{-5}

Table 3.3: Optimization results with respect to dependency type.

3.7.2 Two-span continuous beam

The proposed model is applied on a two-span continuous beam in order to optimize the maintenance planning of the two beams by considering the dependencies between the two elements. In this application, a continuous RC beam with two spans (b_1 and b_2), is simply supported as shown in Figure 3.12. The beams have identical spans of 6m. The beams cross-section is 30cm wide and 60cm depth. A uniform load (UL) of 20 kN/m (including the dead load of the beams) is applied to the beams.

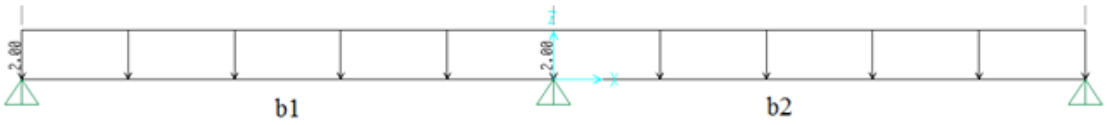

Figure 3.12: Mechanical model of the two RC beams with identical spans.

3.7.2.1- Maintenance costs

In order to evaluate the effect of a degraded or failed beam on the adjacent one, a 2D finite element model using SAP V2014 (CSI 2014) is considered to model the two beam structure. The probability of failure is the probability of violating the following bending limit state:

$$G_{M,b_i}(X) = M_R - M_i \tag{3.51}$$

where M_R is the resisting moment calculated by EC2 (Code 2005), M_i is the total moment applied to beam i. In this example, the resisting moment is degrading with time due to corrosion. The random and deterministic variables of the problem are given in Table 3.4.

Random variables	Symbol	distribution	mean	COV	units
Yield strength	f_y	Lognormal	500	0.07	Mpa
Deterministic parameters					
Concentration	C_{cr}		0.9		
Concentration	C_s		2.95		
Coefficient of diffusion	D_c		6.00×10^{-12}		
Cover	c		0.04		m
Concrete strength	f_c		28		MPa
Module d Young	E		25.3		GPa
Length	L		6		m
Width	b		0.3		m
Height	h		0.6		m
Load	UL		0.15		MN/m

Table 3.4: Random Variables and deterministic parameters of the continuous beam.

The failure probability is calculated for the positive and negative moments by considering as a reinforcement area 3HA20 for top reinforcement and 3HA16 for bottom reinforcement.

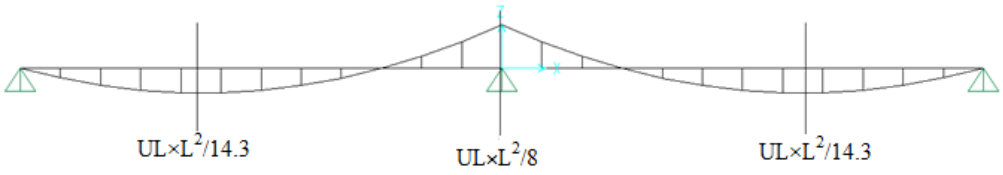

Figure 3.13 : Bending moment and studied cross-sections.

The three cross-sections shown in Figure 3.13 are to be considered: Cross-section 1 (S_1) corresponding to the maximum positive moment at mid-span of beam b_1, cross-section 2 (S_2) corresponding to the maximum negative moment at the support, and cross-section 3 (S_3) corresponding to the maximum positive moment at mid-span of beam b_2. The computation steps are as following:

- The probability of failure is obtained for the three cross-sections, which degrade with time due to corrosion.
- In the maintenance model, $P_{i|j}(t)$ is computed as the probability of failure of S_i knowing that S_j has failed. The following procedure is suggested for the computation of $P_{i|j}(t)$ in this example:
  - Assign a nil stiffness to beam j that is supposed to model the failure of cross-sections 1 or 3.
  - Create a hinge at the support between the two beams to model the failure of cross-section 2.
  - Compute the increase $inc_{i|j}$ in the moments in the beam $i \neq j$ due to the failure of beam j, such that $M_{i|j} = inc_{i|j}\, M_{bi}$
  - Calculate $P_{i|j}(t) = P_r\left[M_R - M_{i|j} \leq 0\right]$ using FORM algorithm.

$inc_{i\|j}$	1 failed	2 failed	3 failed
1	∞	1.8	1.8
2	∞	∞	∞
3	1.8	1.8	∞

Table 3.5: Moment increases in element i due to failure of element j $\left(inc_{i|j}\right)$.

i|j	Equations of $P_{i\|1}$ failed	Equations of $P_{i\|2}$ failed
1	1	$10^{(-1.29 + 2\times10^{-6}\,t3 - 6\times10^{-4}\,t2 + 4.59\times10^{-2}\,t)}$
2	1	1
3	$10^{(-1.29 + 2\times10^{-6}\,t3 - 6\times10^{-4}\,t2 + 4.59\times10^{-2}\,t)}$	$10^{(-1.29 + 2\times10^{-6}\,t3 - 6\times10^{-4}\,t2 + 4.59\times10^{-2}\,t)}$

	Equations of P_i
P_1	$10^{(-4.86 + 10^{-5}\,t3 - 1.2\times10^{-3}\,t2 + 8.70\times10^{-2}\,t)}$
P_2	$10^{(-3.38 + 10^{-5}\,t3 - 1.7\times10^{-3}\,t2 + 1.26\times10^{-1}\,t)}$
P_3	$10^{(-6.037 + 10^{-5}\,t3 - 1.2\times10^{-3}\,t2 + 8.70\times10^{-2}\,t)}$

Table 3.6: Polynomial regression of P_i and $P_{i|j}$.

The increase of the moment in section i when the cross-section j has failed is shown in Table 3.5. As the computation of $P_{i|j}(t)$ by FORM is very costly inside the optimization formula, a polynomial approximation is used for the computation of $P_{i|j}(t)$. The closed form estimations

of the failure probabilities as function of time are given in Table 3.6 where for each column *i* the approximations of $P_i(t)$ and $P_{i|j}(t)$ are given in each row *j*. The failure of a beam increases the failure rate of the adjacent beam, and leads to the failure of the common support section.

3.7.2.2- Effect of cost components on maintenance planning

The optimization problem is given by:

Find	k_2 , k_3 and τ	
minimizing	$C(k_1, k_2, k_3, \tau)$	
with	$k_1 = 1$ and $\tau \geq 0$	
subject to	$P_{f,system} < P_f^T$	(3.52)

Let us compare the following formulations in Table 3.7.

Type Description	Formulation
None Degradation cost, stochastic and economical dependencies are not considered	$E[C_T(t)] = \sum_i \left[C_{M,i}^c P_{fi}(t)\right] + + \sum_{i \in G_{pu}} \left[C_{M,i}^p \left(1 - P_{fi}(t)\right)\right]$
E Economical dependency is considered, although degradation cost and stochastic dependency are not	$E[C_T(t)] = \sum_i \left[C_{M,i}^c P_{fi}(t)\right] + \sum_{i \in G_{pu}} \left[C_{M,i}^p \left(1 - P_{fi}(t)\right)\right] + C_{SU,T}^p(t) + C_{SU,T}^c(t)$
S Stochastic dependency is considered, although degradation cost and economic dependency are not.	$E[C_T(t)] = \sum_i \left[C_{M,i}^c \left(P_{fi}(t) + \sum_{j \neq i} P_{i\|j}(t)\, P_j(t)\right)\right] + \sum_{i \in G_{pu}} \left[C_{M,i}^p \left(1 - P_{fi}(t) - \sum_{j \neq i} P_{i\|j}(t)\, P_j(t)\right)\right]$

Table 3.7: Dependency formulations.

The comparison is carried out using a threshold system probability of failure varying from 10^{-4} to 10^{-3}. The results are shown in Figures 3.14 and 3.15 and in Table 3.8.

The reliability-based optimization in equation 3.52 is performed for the three cases explained in Table 3.7 and for a threshold system probability of failure P_f^T varying from 10^{-4} to 10^{-3}. The same maintenance planning used in section 3.7.1.3 is used herein, where b_1 is maintained every $k_1\,\tau$, b_2 is maintained every $k_2\,\tau$, and b_3 is maintained every $k_3\tau$. The optimum maintenance times $k_1\,\tau$, $k_2\,\tau$ and $k_3\tau$ for the three elements corresponding to the three cross-sections are shown in Figure 3.14 and 3.15 for the three cases distinguished by different marker types and colors, and for P_f^T equal to 10^{-4} and 10^{-3} respectively. The values of the design variables k_2 , k_3 and τ are also shown in Table 3.8 for the three formulations, along with the value of the $C(k_1, k_2, k_3, , \tau)$ in cost unit.

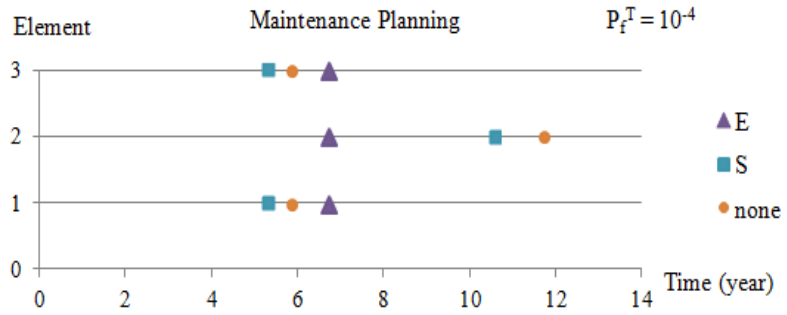

Figure 3.14: Effect of cost component on maintenance planning- P_f^T=10-4.

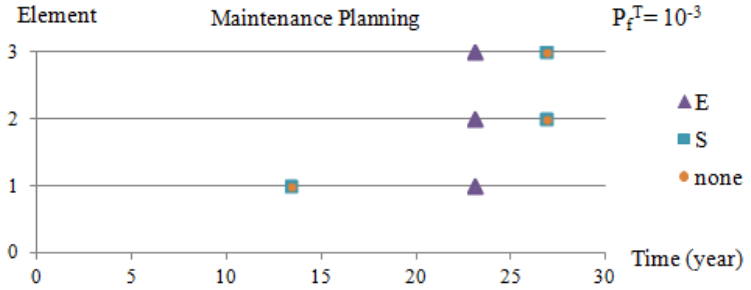

Figure 3.15: Effect of cost component on maintenance planning- P_f^T=10^{-3}.

Formulation	P_f^T	τ	k_1	k_2	k_3	$C(k_1, k_2, k_3, , \tau)$
E	1.00×10^{-3}	23.13	1	1	1	0.18
	1.00×10^{-4}	6.71	1	1	1	0.50
S	1.00×10^{-3}	13.43	1	2	2	0.30
	1.00×10^{-4}	5.30	1	2	1	0.62
None	1.00×10^{-3}	13.43	1	2	2	0.30
	1.00×10^{-4}	5.86	1	2	1	0.58

Table 3.8: Optimization results in terms of dependency type.

The following observations can be drawn from the results:

- The economic dependency induces the grouping of the maintenance actions ($k_1 = k_2 = k_3$), therefore neglecting the economic dependency leads to more costly maintenance planning.
- The stochastic dependency leads to smaller maintenance time intervals for low probabilities ($\leq 10^{-4}$), but it does not have significant effect for higher probabilities ($\geq 10^{-3}$), therefore neglecting the stochastic dependency may lead to unsafe maintenance planning.
- For high failure probabilities, the economic dependency has the biggest effect on the maintenance cost; for P_f^T=10^{-3}, the economic dependency decreases the maintenance cost by 40% compared to the cost using stochastic and non-dependent formulations.
- For low failure probabilities, the stochastic dependency has the biggest effect on the maintenance cost; for P_f^T=10^{-4}, the stochastic dependency increases the cost by 6%

compared to the cost using the non-dependent formulation, and by 20% compared to the cost using economic dependency formulation.

3.7.3 Slab and Bituminous interdependence

In this application, a slab and a bituminous coating covering the slab are considered. The objective is to optimize the maintenance planning of the slab and the bituminous coating by considering the dependencies between the two elements, in order to study the behavior of the proposed model for different types of structures.

3.7.3.1- Maintenance costs

Let us consider the following failure probabilities:

For the slab: $P_{fs} = 1 - \exp(10^{-4}\ t)$

For the bituminous: $P_{fb} = 1 - \exp(10^{-6}\ t)$ (3.53)

The failure of the slab induces the failure of the bituminous. However, the failure of the bituminous does not affect the slab performance but can increase the rate of its degradation. $P_{i|j}$ are shown in Table 3.9.

Pi/j	Slab fails	Bitume fails
slab	1	0
Bitume	1	1

Table 3.9: Conditional probabilities.

3.7.3.2- Effect of cost components on maintenance planning

The same optimization formulations applied for the example in section 3.7.2 (i.e. the continuous beam) will be applied to the slab-bituminous, using data in Table 3.7; namely, E (economic), S (stochastic) and N (none) formulations.

The comparison is applied for a threshold system probability of failure varying from 10^{-4} to 10^{-3}. The results are shown in Figures 3.16 and 3.17 and in Table 3.10, where $k_1\,\tau$ is the maintenance time for the slab and $k_2\,\tau$ is the maintenance time for the bituminous coating.

Formulation	P_f^T	τ	k_1	k_2	$C(k_1, k_2, \tau)$
E	1.00×10^{-3}	18.89	1	6	0.092
	1.00×10^{-4}	1.87	1	6	0.653
S	1.00×10^{-3}	18.53	1	6	0.100
	1.00×10^{-4}	1.83	1	6	0.679
N	1.00×10^{-3}	18.89	1	6	0.092
	1.00×10^{-4}	1.87	1	6	0.653

Table 3.10: Optimization results.

From the results, the following observations can be drawn:

- The economic dependency did not induce the grouping of maintenance actions ($k_1 \neq k_2$) because the probability of failure of the slab is by far higher than the probability of failure of the bituminous. Therefore, the "N" and the "E" formulations both yield the same results.
- The stochastic dependency leads to smaller maintenance time intervals by 2% for all the studied probabilities compared to "E" and "N" formulations, therefore neglecting this dependency may lead to unsafe maintenance planning.
- The stochastic dependency has the biggest effect on the maintenance planning and cost in this example; it increases the maintenance cost by 9% for P_f^T equal to 10^{-3} and by 4% for P_f^T equal to 10^{-4} compared to "E" and "N" formulations. This may be due to the fact that the slab failure induces automatically the bituminous failure $(P_{b|s} = 1)$.

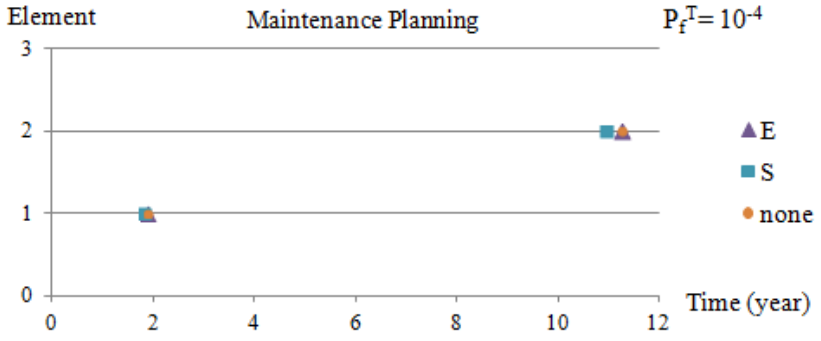

Figure 3.16: Effect of cost component on maintenance planning- P_f^T=10^{-4}.

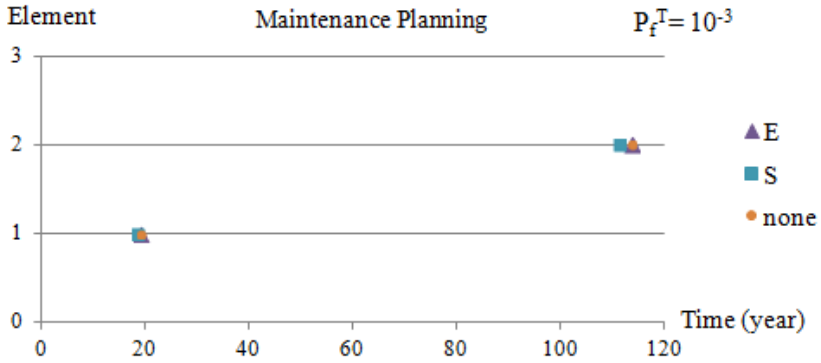

Figure 3.17: Effect of cost component on maintenance planning- P_f^T=10^{-3}.

3.7.4 Bridge Superstructure

The proposed procedure is applied herein to a RC bridge superstructure. This application is drawn from Bezih et al. (2015). The length of the bridge is 407 m and its transversal width is 9 m as shown in Figure 3.18. The objective is to optimize the maintenance planning of the bridge superstructure by considering the economic, stochastic, structural, and degradation dependencies between the structural elements, the load redistribution and the system redundancy.

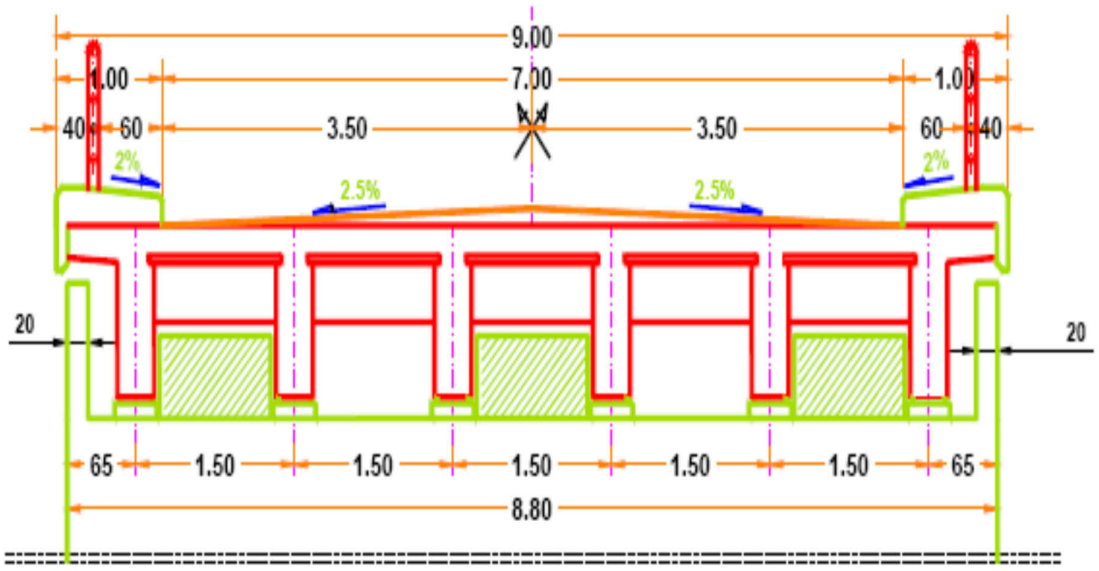

Figure 3.18: Section of the superstructure (Bezih et al. 2015).

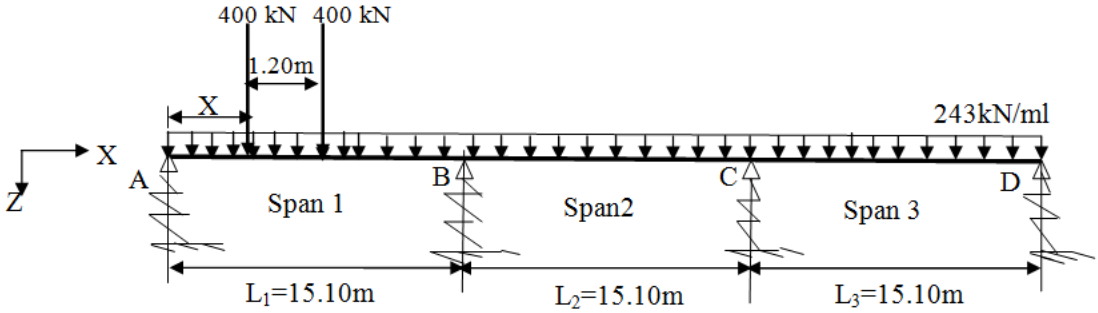

Figure 3.19: Mechanical model (Bezih et al. 2015).

A slab of 25 cm thickness is carried by 6 beams (35 cm × 90 cm). The distance between the beams is 1.5 m, and their span is 15.1 m.

Bezih et al. (2015) designed this bridge, as shown in Figure 3.18, where there is an expansion joint every 3 spans. The traffic load is represented by the load case LM1 of EC1 (CEN2003 1991), which considers simultaneously a uniformly distributed load UDL, a tandem TS on each lane, QT on sidewalks, in addition to the permanent load G. The deck is divided into 2 conventional lanes of 3 m each, and a residual area of 1m.

The aim of this application is to optimize the maintenance planning of the 6 beams ($b_1 \ldots b_6$) shown in Figure 3.18, taking into account the dependencies, as well as failure and degradation costs.

3.7.4.1- Maintenance costs

The moments on each beam, shown in Figure 3.18, are calculated using a 2D finite element model as following:

- The moment obtained by the summed load in the mechanical model is distributed on the 6 beams of the superstructure.
- The effect of degraded or failed beam on the adjacent beams is evaluated.

The load case LM1 (CEN2003 1991) gives the load values and coefficients shown in Table 3.11.

Lane	**TS Qk** (kN)	**Coefficient** αQ	**TS** (kN)	**UDL qik** (kN/m2)	**Coefficient** αq	**UDL** (kN/m2)
Lane 1	300	1	300	9	1	9
Lane 2	200	1	200	2.5	1.2	3
Residual area	0	0	0	2.5	1.2	3

Table 3.11: Load case LM1 (CEN2003 1991).

As shown in Figure 3.18, the beams b_1, b_2, and b_3 form the lane n°1, and b_3, b_4, and b_5 form the lane n°2.

By considering that the TS point loads are applied to the first span as shown in Figure 3.18, the first span maximum positive and negative moments in kNm are as shown in Table 3.12. The 3rd row shows the proportion of the moment M_i to the total positive moment.

Moment	**M_1**	**M_2**	**M_3**	**M_4**	**M_5**	**M_6**	**Units**
Positive	10880	1062.6	912.3	827.9	792.2	683.4	kNm
Negative	-1696.1	-838.3	-1055.7	-973.7	-626.8	-1074.1	kNm
α_i	0.2	0.2	0.17	0.15	0.15	0.13	

Table 3.12: Positive and negative beam moments (SAFE).

The probability of failure is the probability of violating the following bending limit state:

$$G_{M,bi}(X) = M_R - M_i \leq 0 \qquad \text{with} \qquad M_i = \alpha_i \, M_S \tag{3.54}$$

where M_R is the resisting moment calculated by EC2 (Code 2005), M_s is the total moment calculated by the mechanical model, and α_i is the ratio of the positive moment in the first span of b_i to the total moment.

We consider in this study that the two lanes are separated by a concrete barrier in the residual area. Moreover, lane 2 is dedicated to cars only, and so the bridge is not accessible for trucks in the direction of lane 2. Therefore, the load case LM1which considers that the load on lane 2 is much lighter than on lane 1 (Table 3.11), is the only load case considered in this study, which means that not all the beams b_i carry the same load. In addition, a line load q_L is applied on the first and last beams (b_1 and b_6) to take into account the massive parapet shown in Figure 3.18. With the above assumptions we can achieve the following:

- b_1 and b_2 correspond to lane 1; they are more loaded than b_5 and b_6 corresponding to lane 2.
- b_3 and b_4 are less loaded than the other beams because they correspond to the residual area.
- b_1 is more loaded than b_2 because it carries a massive parapet.
- b_6 is more loaded than b_5 because it carries a massive parapet.
- b_3 is more loaded than b_4 because it is closer to lane 1.

The above assumptions are crucial to contrive the differences between the 6 beams, and thus the example will provide richer results because the beams are not be identically loaded. The random and deterministic variables of the problem are shown in Table 3.13.

Random variables	**Symbol**	**distribution**	**mean**	**c.o.v.**	**units**
Yield strength	f_y	Lognormal	500	0.07	Mpa
Load	$TS\ P_1$	normal	400	0.15	kN
Load	$TS\ P_2$	normal	400	0.15	kN
Deterministic Parameters					
Concentration	C_{cr}		0.9		kg/m^3
Concentration	C_s		2.95		kg/m^3
Coef of diffusion	D_c		6.00×10^{-12}		m^2/s
cover	c		0.05		m
Concrete strength	f_c		30		Mpa
Load	Q		234		kN/m
Module d Young	E		30		Gpa
Length	L		15.1		m
width	b		0.35		m
height	h		0.9		m
position	P_1		6.95		m
Position	P_2		8.15		m
diameter of bar	d_0		0.025		m

Table 3.13: Random and deterministic Variables.

The probability of failure P_{fi} for the beam b_i is then calculated by FORM using MATLAB.

Despite that all the beams $b_1,\ldots,b_6$ have the same dimensions, they do not bear the same load, and thus they won't have the same reinforcement areas. Therefore, the failure probability is calculated for the 6 beams by considering different reinforcement areas. The results of the probabilities obtained by FORM are given in Appendix 3.

The probability of failure is obtained for each beam, which degrades with time due to corrosion. In order to find the expected maintenance costs $C^c_{M,T}$ and $C^p_{M,T}(t)$, we have to compute $P_{i|j}(t)$, which is the probability of failure of the beam b_i knowing that b_j has failed. The above procedure is applied for the computation of $P_{i|j}(t)$:

- Assign a nil stiffness to the beam *j* that is supposed to be failed in the FE model.
- Compute the increase factor $inc_{i/j}$ of the moments in beams $i \neq j$ due to the failure of beam *j*; such that $M_{i|j} = inc_{i|j}\, M_{bi}$ with $M_i = \alpha_i\, M_S$
- Calculate $P_{i|j}(t) = P_r\left[M_R - M_{i|j} \leq 0\right]$ using FORM.

The increases in the moment of beam *i* knowing that beam *j* has failed is given in Tables 3.14, where for every beam *i* at each row of the Table, $inc_{i|j}$ is given for every beam *j* at each column. Table 3.15 gives the proportion of the total moment carried by each beam *i* at each row given that the beam *j* at each column has failed, such that $M_{i|j} = inc_{i|j} \times \alpha_i \times M_S$.

As the computation of $P_{i|j}(t)$ by FORM is repeatedly required inside the optimization loops, a polynomial regression is proposed for the computation of $P_{i|j}(t)$. The equations are shown in Table 3.16. The computation of the following equations is detailed in Appendix 3.

$inc_{i\|j}$	1	2	3	4	5	6
1	1	1.3	1.1	1.0	1.0	1.0
2	1.6	1	1.2	1.1	1.0	1.0
3	1.3	1.3	1	1.2	1.1	1.0
4	1.1	1.1	1.2	1	1.2	1.2
5	1.0	1.1	1.1	1.2	1	1.5
6	0.9	1.0	1.1	1.2	1.4	1

Table 3.14: Moment increases in element *i* due to failure of element *j* $\left(inc_{i/j}\right)$.

$inc_{i\|j} \times \alpha_i$	1	2	3	4	5	6	nbar
1	0.19	0.247	0.209	0	0	0	8
2	0.304	0.19	0.228	0.209	0	0	8
3	0.208	0.208	0.16	0.192	0.176	0	7
4	0.176	0.176	0.192	0.16	0.192	0.192	7
5	0	0.165	0.165	0.18	0.15	0.225	7
6	0	0	0.165	0.18	0.21	0.15	7

Table 3.15: Moments proportion of the total moment.

i|j	Equations of Pi|1	Equations of Pi|2
1	1	$10^{(-0.65+3\times10^{-6}\,t^3-3\times10^{-4}\,t^2+1.66\times10^{-2}\,t)}$
2	1	1
3	$10^{(-1.12+3\times10^{-6}\,t^3-4\times10^{-4}\,t^2+2.32\times10^{-2}\,t)}$	$10^{(-1.12+3\times10^{-6}\,t^3-4\times10^{-4}\,t^2+2.32\times10^{-2}\,t)}$
4	$10^{(-4.06+3\times10^{-6}\,t^3-7\times10^{-4}\,t^2+0.05t)}$	$10^{(-4.06+3\times10^{-6}\,t^3-7\times10^{-4}\,t^2+0.05t)}$
5	0	$10^{(-5.78+8\times10^{-6}\,t^3-8\times10^{-4}\,t^2+0.061t)}$
6	0	0

i|j	Equations of Pi|3	Equations of Pi|4
1	$10^{(-3.02+5\times10^{-7}\,t^3-7\times10^{-4}\,t^2+0.043\,t)}$	0
2	$10^{(-1.53+5\times10^{-6}\,t^3-5\times10^{-4}\,t^2+0.029\,t)}$	$10^{(-3.02+5\times10^{-7}\,t^3-7\times10^{-4}\,t^2+0.043\,t)}$
3	1	$10^{(-2.27+5\times10^{-6}\,t^3-5\times10^{-4}\,t^2+0.0356\,t)}$
4	$10^{(-2.27+5\times10^{-6}\,t^3-5\times10^{-4}\,t^2+0.0356\,t)}$	1
5	$10^{(-5.78+8\times10^{-6}\,t^3-8\times10^{-4}\,t^2+0.061t)}$	$10^{(-3.54+6\times10^{-6}\,t^3-7\times10^{-4}\,t^2+0.0462\,t)}$
6	$10^{(-5.78+8\times10^{-6}\,t^3-8\times10^{-4}\,t^2+0.061t)}$	$10^{(-3.54+6\times10^{-6}\,t^3-7\times10^{-4}\,t^2+0.0462\,t)}$

i|j	Equations of Pi|5	Equations of Pi|6
1	0	0
2	0	0
3	$10^{(-4.06+3\times10^{-6}\,t^3-7\times10^{-4}\,t^2+0.05t)}$	0
4	$10^{(-2.27+5\times10^{-6}\,t^3-5\times10^{-4}\,t^2+0.0356\,t)}$	$10^{(-2.27+5\times10^{-6}\,t^3-5\times10^{-4}\,t^2+0.0356\,t)}$
5	$10^{(-8.91+9\times10^{-6}\,t^3-10^{-3}\,t^2+0.077\,t)}$	1
6	$10^{(-1.02+3\times10^{-6}\,t^3-3\times10^{-3}\,t^2+0.0218\,t)}$	1

	Equations of Pi
P1	$10^{(-5.33+9\times10^{-6}\,t^3-9\times10^{-4}\,t^2+0.0594\,t)}$
P2	$10^{(-5.33+9\times10^{-6}\,t^3-9\times10^{-4}\,t^2+0.0594\,t)}$
P3	$10^{(-6.71+8\times10^{-6}\,t^3-9\times10^{-4}\,t^2+0.0662\,t)}$
P4	$10^{(-6.71+8\times10^{-6}\,t^3-9\times10^{-4}\,t^2+0.0662\,t)}$
P5	$10^{(-8.91+9\times10^{-6}\,t^3-10^{-3}\,t^2+0.077\,t)}$
P6	$10^{(-8.91+9\times10^{-6}\,t^3-10^{-3}\,t^2+0.077\,t)}$

Table 3.16: Polynomial regression of P_i and $P_{i|j}$.

3.7.4.2- Maintenance Policy

Let q be the number of components in the system, *i* being the component number: i=1,…..,q. Let $\tau_1, \tau_2, \cdots, \tau_q$ be the time intervals between preventive replacements of components respectively (Figure 3.20). The basic maintenance time is defined as the minimum replacement time $\tau = \min_{i=1,\ldots,q} \tau_i$. The maintenance times for different components are defined by $\tau_i = k_i\tau$, where k_i are integer multipliers and τ is continuous (Figure 3.20).

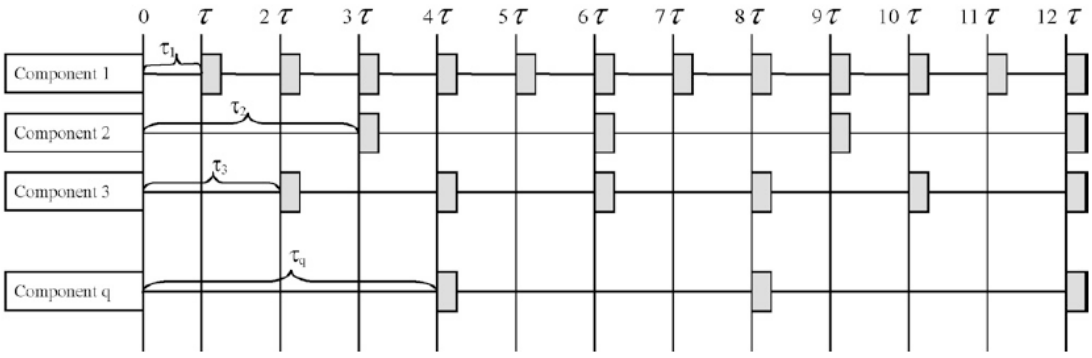

Figure 3.20: Scheduled preventive maintenance plan (Laggoune et al. 2009).

The optimization problem is given by:

Find	k_2 , k_3, k_4, k_5 , k_6, τ	
minimizing	$C(k_1, k_2, k_3, k_4, k_5, k_6, \tau)$	
with	$k_1 = 1$ and $\tau \geq 0$	
subject to	$P_{f,system} < P_f^T$	(3.55)

where $P_{f,system}$ is the system probability of failure and P_f^T is the admissible probability of failure.

The preventive intervention brings the component to the "as good as new" state. Between two preventive maintenance actions, the failed components are subject to immediate minimal repair to restore them to the "as bad as old" state. The i^{th} component is identified such as its lifetime is the lowest among all the components. In this context, the decision variables are (*τ,*

k_2, k_3…. k_q), with $\tau = min\ k_i = k_1 = 1$. The representative cycle is given by the expected time for replacing all the components simultaneously $K\tau$, with $K = lcm(k_1, k_2, k_3, k_4, k_5, k_6)$.

3.7.4.3- Stochastic dependency

The stochastic dependency means that the failure of a component may increase the failure rate of other components. Two optimization formulas for the maintenance planning of the 6 beams are proposed, according to the consideration or not of the stochastic dependency. In other words, the Stochastic Non Dependent (SND) and Stochastic Dependent (SD) cases are considered. The aim of this subsection is to analyze the effect of stochastic dependency on the maintenance planning. Let us consider the following grouping:

- Beams b_1 and b_2 are to be preventively maintained every $k_1\tau$
- Beams b_3 and b_4 are to be preventively maintained every $k_2\tau$
- Beams b_5 and b_6 are to be preventively maintained every $k_3\tau$

The maintenance cycle is given by the expected time for replacing all the components simultaneously $K\tau$, with $K = lcm(k_1, k_2, k_3)$.

The cost $C_{M,i}^{c}$ corresponds to the cost of the minimal repair added to the preventive repair in case of failure before the intended maintenance time. The system probability of failure is calculated as follows:

$$P_{f,system} = (1 - I_{redund})\, P_{f,series} + I_{redund}\, P_{f,parallel} \tag{3.56}$$

When $I_{redund} = 1$; the system is considered equivalent to a parallel system.
When $I_{redund} = 0$; the system is considered equivalent to a series system.
In the Non Dependent case (SND), the maintenance cost is:

$$C_{M,T}^{c}(t) = \sum_i \left[C_{M,i}^{c}\left(P_{fi}(t)\right) \right] \quad \text{and} \quad C_{M,T}^{p}(t) = \sum_{i \in G_{pu}} \left[C_{M,i}^{p}\left(1 - P_{fi}(t)\right) \right] \tag{3.57}$$

In the Dependent case (SD), the maintenance costs are computed as per section 3.2.2 (equations 3.3 and 3.14).

Due to the complexity of the optimization problem, a genetic algorithm is used. The initial population is evaluated by performing an element-based optimization by considering equation 3.16 as objective function and by using the nearest multiple of τ as an initial population for each element. The function and the constraint tolerances are set to 10^{-6}.

The optimization is performed for the SD and SND cases, with a redundancy factor equal 0.5, a corrective cost varying from 10 to 1000 times the preventive cost, and for an admissible probability of failure varying from 10^{-5} to 10^{-3} (e.g. 100C0-SD means that the corrective cost is taken equal to 100 times the preventive cost and the stochastically dependent formula is used). For each run, the following is computed: k_1, k_2 , k_3, τ , $C_{tot} = C(k_1, k_2, k_3, k_4, k_5, k_6, \tau)$, $P_{fi\,(i\ldots6)}$ and $P_{fsystem}$. We present in Table 3.17 the obtained values for k_2, k_3, τ and C_{tot} for different runs. Figure 3.21 shows the optimal cost for the all the runs distinguished by different mark types and colors, and for all the threshold probabilities.

The most influencing factors on the maintenance planning are:

- The high corrective cost $C_{M,i}^{c}$ compared to the preventive cost
- The admissible probability of failure of the system P_f^T.
- The stochastic dependency SD between different components of the system
- The redundancy factor I_{redund}

To better understand the influence of each factor, the following analysis is presented:

- When the reliability constraint is not active, the value of the total cost C_{tot} is equal to the unconstrained optimization value. Otherwise, C_{tot} increases when the reliability constraint is more stringent. In the range of our study $P_f^T = [10^{-5}; 10^{-3}]$, the following runs may not always be constrained:
  - When $P_f^T < 2.00 \times 10^{-4}$ the reliability constraint is not active for 1000C0-SND (corresponding to a simulation with the corrective cost equal to 1000 times the preventive cost and in stochastically not dependent case).
  - When $P_f^T < 6.45 \times 10^{-5}$ the reliability constraint is not active for 1000C0-SD
  - When $P_f^T < 1.25 \times 10^{-4}$ the reliability constraint is not active for 100C0-SD
  - When $P_f^T < 4.22 \times 10^{-4}$ the reliability constraint is not active for 10C0-SD

  These values can also be deduced from the Figure 3.21 and Table 3.17, since the maintenance planning does not change for $P_f^T <$ active value.
- When the corrective cost is equal to 10 times the preventive cost (i.e. cases 10C0-SD and 10C0-SND), the non-dependent formula SND may yield the same maintenance planning than the dependent formula SD if the reliability constraint is active (both cases yield 0.0268 unit costs when $P_f^T = 5 \times 10^{-5}$). However, the dependency formula SD requires a higher maintenance cost when the constraint is not active (0.0228 unit costs for SD compared to 0.0175 unit costs for SND when $P_f^T = 10^{-3}$ is not active). This means that not considering the stochastic dependency may lead to non-conservative maintenance planning. This danger is less seen when the constraint is active because the reliability constraint forbids the under-estimation of maintenance planning,
- When the corrective cost is equal to 100 times the preventive cost (i.e. 100C0-SD and 100C0-SND), the dependent formula SD requires a higher maintenance cost when the constraint is not active and when the SND does not reach the unconstrained minimum maintenance cost (0.0247 unit costs). When both formulas are properly constrained, they yield the same maintenance cost. The reliability constraint is not always sufficient to maintain a safe maintenance planning. Considering the dependency ensures safe results.
- When the corrective cost is equal to 100 and 1000 times the preventive cost (i.e. 100C0-SD, 100C0-SND, 1000C0-SD and 1000C0-SND), the SD cases lead always to higher costs than the SND cases. This is due to the fact that the SND formula yields maintenance cost lower than the unconstrained cost of the SD formula (0.0247 and 0.0246 unit costs respectively), even in the higher range of the constraint (10^{-5}).
- For the dependent cases SD, using 1000C0 as corrective cost yields more conservative maintenance planning than using 100C0 which yields a more conservative planning than using 10C0.

  For the non-dependent cases SND, using 1000C0 yields more conservative planning than using 100C0 or 10 C0. However, using 100C0 and 10C0 yields the same planning

(0.0268 unit cost when $P_f^T = 5 \times 10^{-5}$). This is due to the fact that the resulting planning is prescribed by the stringent threshold probability rather than by high corrective costs as in the case of 1000C0.

	P_f^T	τ	k_2	k_3	$10^{-4} \times C_{tot}$
1000C0-SD	1.00×10^{-3}	15.63	3	5	277
	5.00×10^{-4}	15.63	3	5	277
	1.00×10^{-4}	15.63	3	5	277
	5.00×10^{-5}	14.93	3	5	282
100C0-SD	1.00×10^{-3}	16.80	3	5	247
	5.00×10^{-4}	16.81	3	5	247
	1.00×10^{-4}	16.47	3	5	248
	5.00×10^{-5}	14.93	3	5	269
10C0-SD	1.00×10^{-3}	12.83	5	7	228
	5.00×10^{-4}	12.83	5	7	228
	1.00×10^{-4}	16.47	3	5	243
	5.00×10^{-5}	14.93	3	5	268
1000C0-SND	1.00×10^{-3}	17.35	3	5	246
	5.00×10^{-4}	17.35	3	5	246
	1.00×10^{-4}	16.47	3	5	251
	5.00×10^{-5}	14.93	3	5	272
100C0-SND	1.00×10^{-3}	15.28	5	6	179
	5.00×10^{-4}	18.21	3	5	220
	1.00×10^{-4}	16.47	3	5	244
	5.00×10^{-5}	14.93	3	5	268
10C0-SND	1.00×10^{-3}	15.28	5	6	175
	5.00×10^{-4}	18.21	3	5	220
	1.00×10^{-4}	11.55	5	7	247
	5.00×10^{-5}	14.93	3	5	268

Table 3.17: Planning results for SD and SND cases.

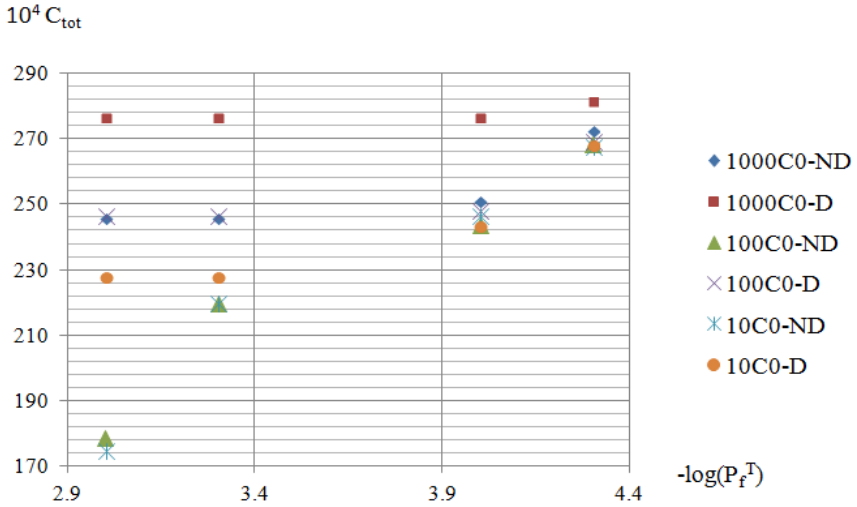

Figure 3.21: Results for stochastically dependent and non-dependent formulations.

3.7.4.4- Redundancy Factor

In this section, the influence of the system redundancy on the maintenance planning is investigated. The factor I_{redund} can be calculated as performed in the previous examples (see equation 3.11), and as explained in section 3.3. However, in order to observe the influence of this factor on the maintenance planning, the optimization is performed for different values of $I_{redund} = [0, 0.25, 0.5, 0.75, 1]$, and different values of $P_f^T = [10^{-5}, 10^{-3}]$.

The results are shown in Figure 3.22, where the following can be observed:

- When the system is fully redundant (i.e. $I_{redund} = 1$), the probability of failure of the system is very low $\left(\prod P_{fi} = 4.07 \times 10^{-22}\right)$ and consequently the optimal maintenance is independent of the constraints, leading to the same value of 0.0167 unit costs for $P_f^T = [10^{-5}, 10^{-3}]$.
- A more redundant system leads to a less costly optimal planning, whatever the reliability levels.

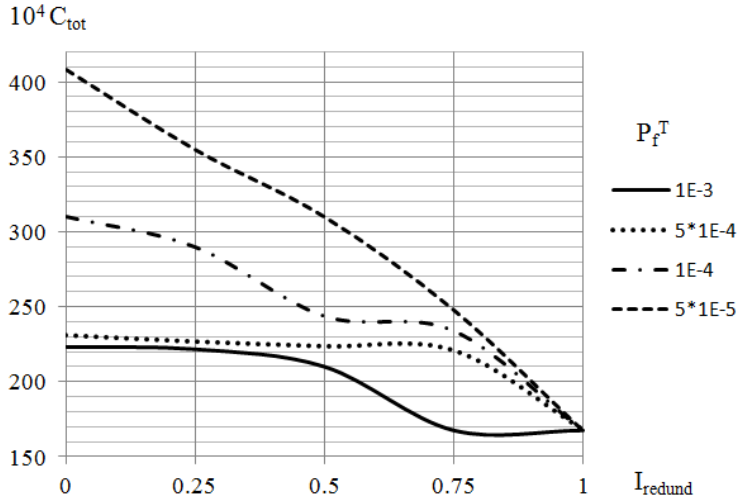

Figure 3.22: Influence of the system redundancy on maintenance planning.

3.7.4.5- Economic Dependency

Two Formulations for finding the optimal maintenance planning are investigated in this section. The first is denoted "EC" (for economic dependency), and considers the setup costs explained in section 3.6.4. The second is denoted "NO-EC" and will not consider economic dependencies. Figure 3.23a to 3.23f show a comparison between an optimal maintenance planning which considers economic dependency (EC), and another that does not (NO-EC), for different values of admissible probability of failure, varying from 10^{-3} to 10^{-5}.

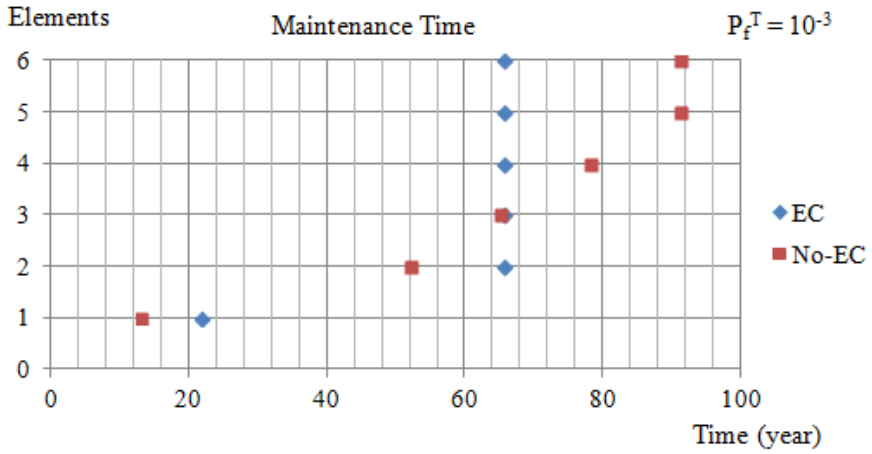

Figure 3.23a : Comparison between (EC) and (NO-EC) for a $P_f^T = 10^{-3}$.

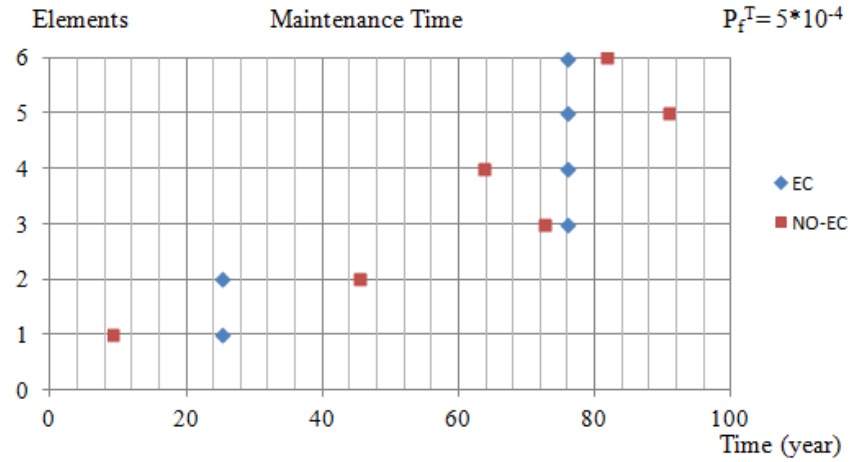

Figure 3.23b : Comparison between (EC) and (NO EC) for $P_f^T = 5\times10^{-4}$.

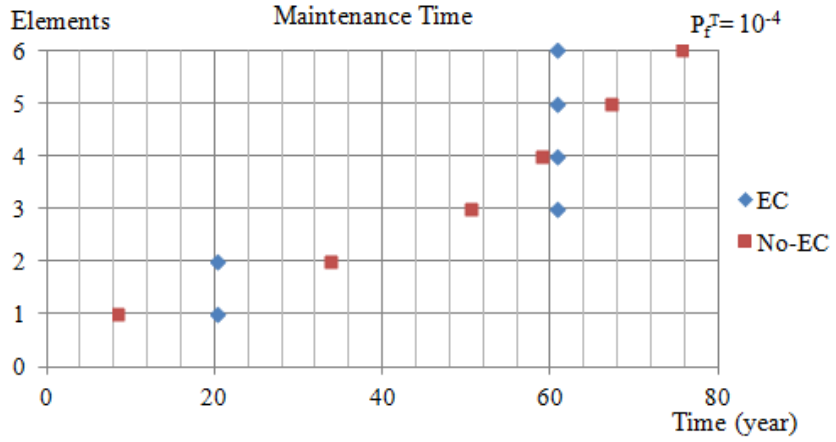

Figure 3.23c : Comparison between (EC) and (NO EC) for $P_f^T = 10^{-4}$.

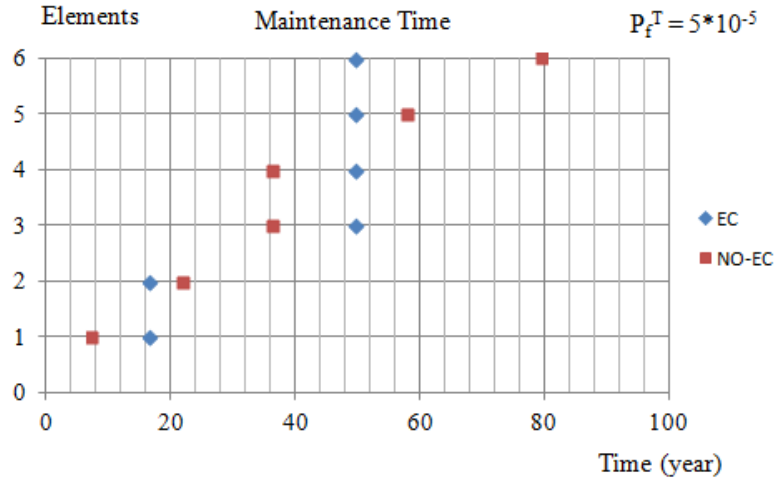

Figure 3.23d : Comparison between (EC) and (NO EC) for $P_f^T = 5\times10^{-5}$.

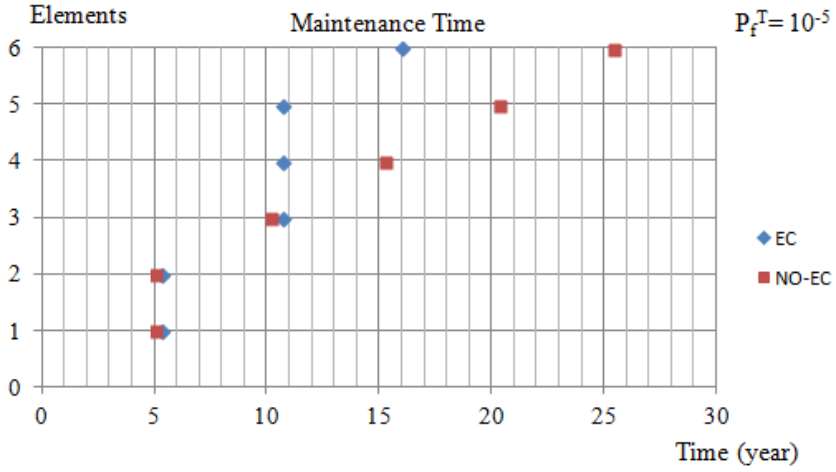

Figure 3.23e : Comparison between (ec) and (NO ec) for $P_f^T = 10^{-5}$

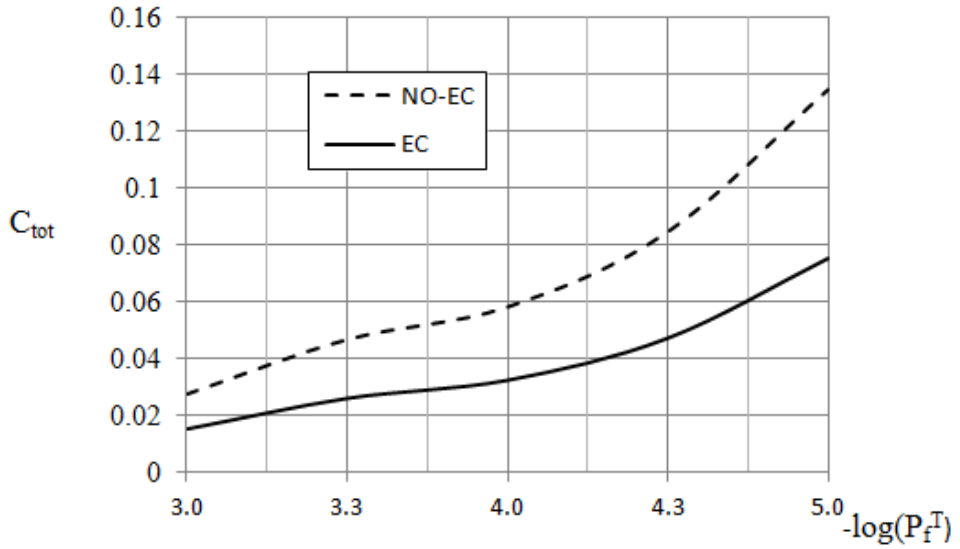

Figure 3.23f: Comparison between maintenance cost of (EC) and (NO EC) formulations.

The following observations can be drawn from the results:

- Considering the economic dependency by maintenance grouping leads to significant cost savings around 25%.
- The optimization algorithm allows rearranging the optimal individual replacement times in such a way that all component times become multiple of the smallest one, to allow for joint replacements.
- The genetic algorithm can solve the problem with reasonable computing time.

3.7.4.6- Degradation Costs

The beam degradation by corrosion of the steel reinforcement is enhanced by significant crack width. The moment of inertia of concrete is reduced when the concrete is cracked. Thus the load initially supported by the uncracked element will be distributed to adjacent elements when cracking occurs.

The load redistribution explained in section 3.2.3 is applied to this example, where $\propto_{j,i}$ is computed as in equation 3.24. The factors $c_{i,j}$ and n are estimated by the FE model. To obtain these factors, the stiffness of each beam is incrementally reduced by steps of 25% to model the degradation of the beam in the FE model. After each increment of stiffness reduction, a part of the load initially carried by the beam is redistributed to other beams. Then, the moments carried by the beams after redistributions are noted. The new moments corresponding to a redistributed load are compared to the initial moments corresponding to full stiffness. Afterward, $\propto_{i,j}$ is computed for each beam i due to each stiffness reduction assigned to j. Finally, $\propto_{i,j}$ is approximated according to equation 3.6 by the mean of $c_{i,j}$ and n based on the obtained data. Table 3.18 shows the values of $c_{i,j}$ and n for all beams combinations (i, j), and the approximated equations are shown in Table 3.19. Figure 3.24 shows a comparison between the exact values of $\propto_{1,2}$ and the values approximated by the proposed formula, which proves the goodness of the fit of the proposed formula.

Load distributed to b_i			Stiffness reduction assigned to b_j					
	$\alpha_{i,j}$		**1**	**2**	**3**	**4**	**5**	**6**
	1	$c_{1,j}$	0	0.3	0.12	0	0	0
		n	0	1.27	1.3	0	0	0
	2	$c_{2,j}$	0.59	0	0.19	0.09	0	0
		n	1.6	0	1.29	1.26	0	0
	3	$c_{3,j}$	0.33	0.28	0	0.18	0.09	0.09
		n	1.9	1.35	0	1.21	1.28	2.1
	4	$c_{4,j}$	0.15	0.13	0.22	0	0.22	0.23
		n	2	1.45	1.23	0	1.29	1.9
	5	$c_{5,j}$	0	0.05	0.13	0.22	0	0.49
		n	0	1.16	1.25	1.23	0	1.75
	6	$c_{6,j}$	0	0	0.07	0.17	0.36	0
		n	0	0	1.23	1.27	1.3	0

Table 3.18: values of values of $c_{i,j}$ and n for all beams (i,j).

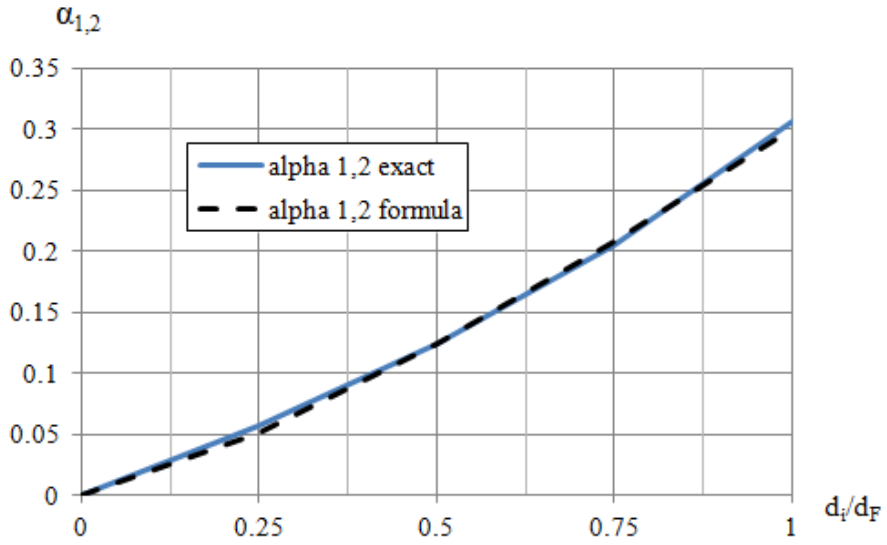

Figure 3.24: comparison between the exact and the formula values of $\propto_{1,2}$.

Load distributed to b_i	Stiffness reduction assigned to b_j						
	$\alpha_{i,j}$	**1**	**2**	**3**	**4**	**5**	**6**
	1	0	$0.3\times d^{1.27}$	$0.12\times d^{1.3}$	0	0	0
	2	$0.59\times d^{1.6}$	0	$0.19\times d^{1.29}$	$0.09\times d^{1.26}$	0	0
	3	$0.33\times d^{1.9}$	$0.28\times d^{1.35}$	0	$0.18\times d^{1.21}$	$0.09\times d^{1.28}$	$0.09\times d^{2.1}$
	4	$0.15\times d^{2}$	$0.13\times d^{1.45}$	$0.22\times d^{1.23}$	0	$0.22\times d^{1.29}$	$0.23\times d^{1.9}$
	5	0	$0.05\times d^{1.16}$	$0.13\times d^{1.25}$	$0.22\times d^{1.23}$	0	$0.49\times d^{1.75}$
	6	0	0	$0.07\times d^{1.23}$	$0.17\times d^{1.27}$	$0.36\times d^{1.3}$	0

Table 3.19: Proposed formulas for $\alpha_{i,j}$.

The monetary consequences of degradation are estimated as:

$$C_{d,T}(t) = \sum_i C_{d,i}(t) \text{ with } C_{d,i}(t) = C_{d,fixe} \times e^{c\left(\frac{1}{MS} - \frac{1}{Mi}\right)} \quad (3.58)$$

where $C_{d,fixe}$ is a fixed cost of degradation, M_s is the total moment calculated by the mechanical model, M_i is the degraded moment calculated as the equation (3.54). $C_{d,T}(t)$ is calculated at each scheduled replacement time $k_i \times \tau$. In order to estimate the redistribution factor at each replacement schedule, the degradation ratio $\frac{d_j(t)}{d_{F,j}} = 2\, a_j\, t$ is computed first.

3.7.4.7- Effect of cost components on maintenance planning

It is interesting to study the effect of each cost component on the maintenance planning using the proposed model. Let us compare the six formulations shown in Table 3.20. The comparison is applied for a threshold failure probability of the system varying from 10^{-5} to 10^{-3}. The results are shown in Figures 3.25a to 3.25e.

From the results, the following observations can be drawn:

- The economic dependency has the biggest effect on the maintenance schedule and induces the grouping of maintenance actions.
- SED is more stringent than ED and E cases. It induces the grouping of the maintenance actions, but at smaller time intervals due to the inclusion of stochastic dependency.
- ED and E yield the same results; this may be due to the fact that the effect of grouping is more pronounced than the effect of degradation.
- Stochastic dependency and degradation costs lead to smaller maintenance time intervals.
- SD and D lead to the same maintenance planning; this may be due to the fact that they have similar effects on degradation and failure.
- Neglecting stochastic dependency and degradation costs lead to unsafe maintenance planning.
- Neglecting economic dependency lead to costlier maintenance planning.

Figure 3.26 shows the cost per unit time versus the system probability of failure for each of the six formulations. The following observations can be concluded:

- For high failure probabilities, the economic dependency has the biggest effect on the maintenance cost.
- For low failure probabilities, the stochastic dependency has the biggest effect on the maintenance cost.
- Degradation cost and stochastic dependency behave in a similar manner.

Type Description	Formulation
None Degradation cost, stochastic and economical dependencies are not considered	$E[C_T(t)] = \sum_i [C^c_{M,i} P_{fi}(t)] + \sum_{i \in G_{pu}} \left[C^p_{M,i}\left(1 - P_{fi}(t)\right)\right]$
E Economical dependency is considered, although degradation cost and stochastic dependency are not	$E[C_T(t)] = \sum_i [C^c_{M,i} P_{fi}(t)] + \sum_{i \in G_{pu}} \left[C^p_{M,i}\left(1 - P_{fi}(t)\right)\right] + C^p_{SU,T}(t) + C^c_{SU,T}(t)$
ED Economical dependency and degradation cost are considered, although stochastic dependency is not	$E[C_T(t)] = C_{d,T}(t) + \sum_i [C^c_{M,i} P_{fi}(t)] + \sum_{i \in G_{pu}} \left[C^p_{M,i}\left(1 - P_{fi}(t)\right)\right] + C^p_{SU,T}(t) + C^c_{SU,T}(t)$
SD Stochastic dependency and degradation cost are considered, although economic dependency is not.	$E[C_T(t)] = C_{d,T}(t) + \sum_i \left[C^c_{M,i}\left(P_{fi}(t) + \sum_{j \neq i} P_{i\|j}(t)\, P_j(t)\right)\right] + \sum_{i \in G_{pu}} \left[C^p_{M,i}\left(1 - P_{fi}(t) - \sum_{j \neq i} P_{i\|j}(t)\, P_j(t)\right)\right]$
SED Stochastic, economic dependencies and degradation cost are considered.	$E[C_T(t)] = C_{d,T}(t) + \sum_i \left[C^c_{M,i}\left(P_{fi}(t) + \sum_{j \neq i} P_{i\|j}(t)\, P_j(t)\right)\right] + \sum_{i \in G_{pu}} \left[C^p_{M,i}\left(1 - P_{fi}(t) - \sum_{j \neq i} P_{i\|j}(t)\, P_j(t)\right)\right] + C^p_{SU,T}(t) + C^c_{SU,T}(t)$

Table 3.20: Proposed formulations.

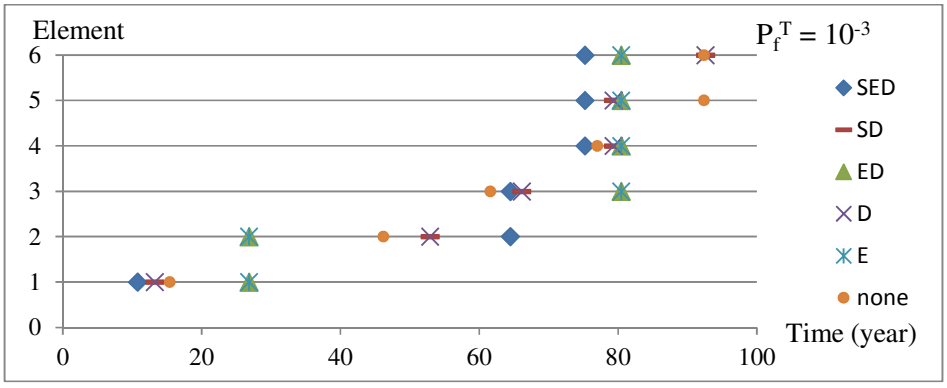

Figure 3.25a: Effect of cost component on maintenance planning- P_f^T=10^{-3}.

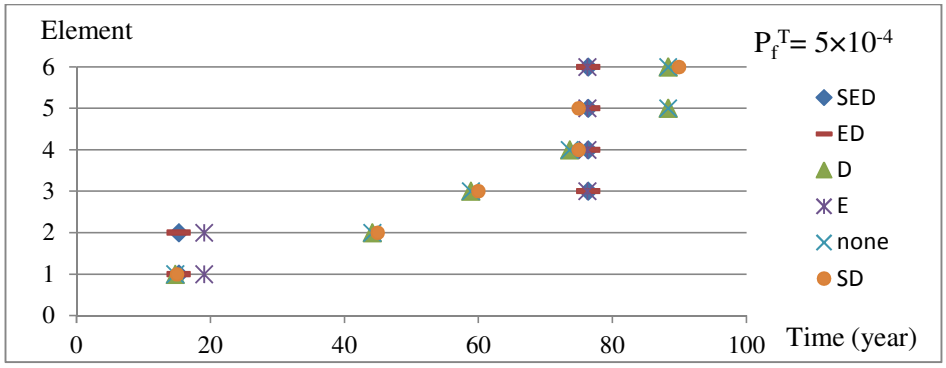

Figure 3.25b: Effect of cost component on maintenance planning- P_f^T=5×10^{-4}.

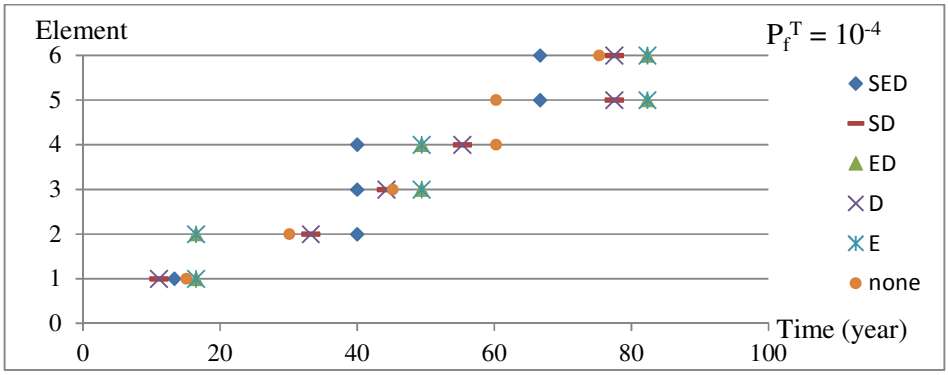

Figure 3.25c: Effect of cost component on maintenance planning- P_f^T=10^{-4}.

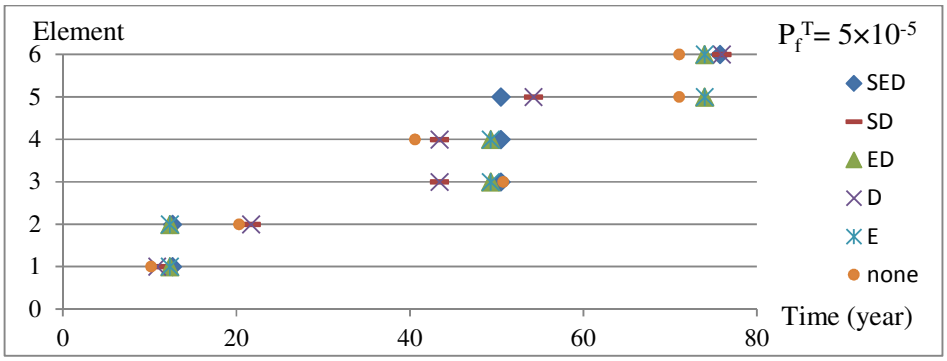

Figure 3.25d: Effect of cost component on maintenance planning- P_f^T=5×10^{-5}.

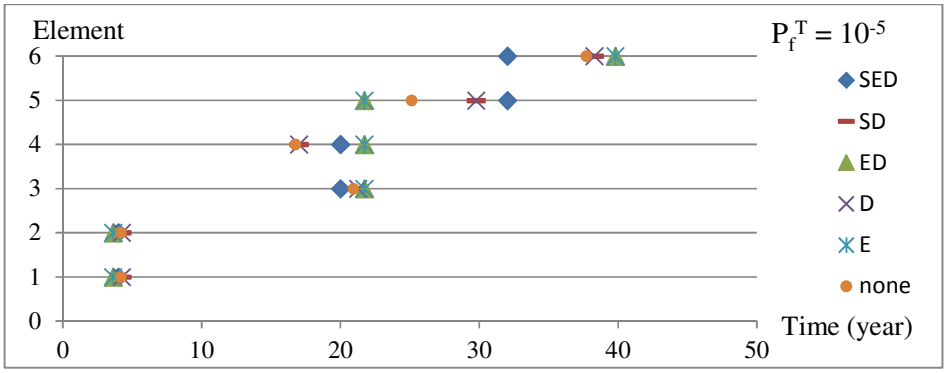

Figure 3.25e: Effect of cost component on maintenance planning- P_f^T=10^{-5}.

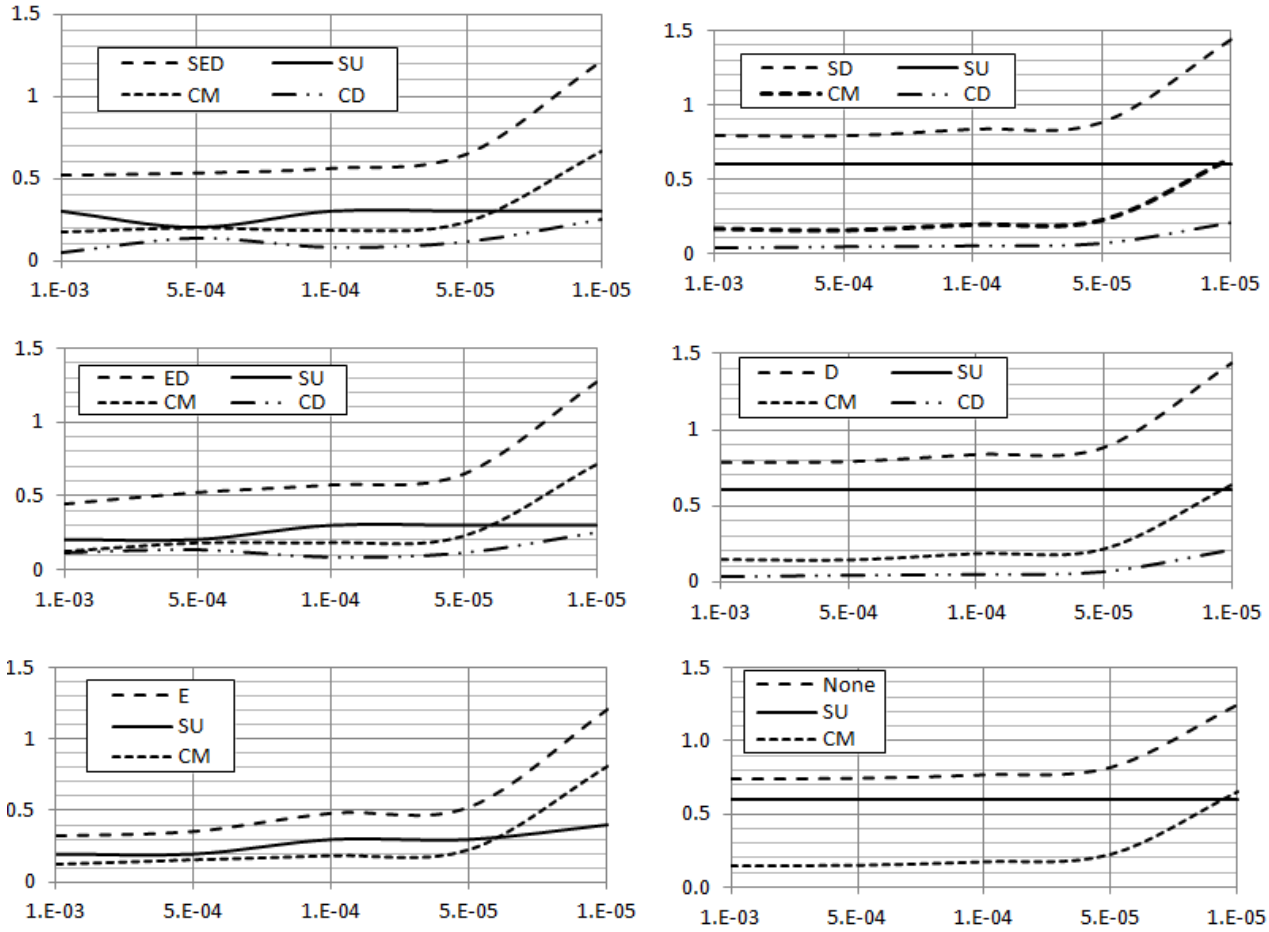

Figure 3.26: Cost per unit time versus system probability of failure for the six formulations.

3.8 Conclusion

In this chapter, a life-cycle maintenance planning for a multi-component bridge system is proposed. A procedure to model all types of failure interactions is suggested, using fault tree analysis and conditional probabilities. The economic dependency is taken into account via several interdependent common costs. Horizontal structural dependency is considered by the mean of a redundancy factor proposed, and to which a parametric analysis is performed. Modular/vertical structural dependency is modeled through the consideration of downtimes needed to dismantle modularly dependent units, and/or to repair associated failed units. Degradation dependencies between different items are modeled, and corresponding consequences are quantified by the mean of degradation costs. The load redistribution to non-failed elements in case of failure of an adjacent bridge element is also considered in the formulated model. An approach that outperforms the currently used series and/or parallel logical relationship for evaluating bridge system reliability is suggested. A solution procedure for the maintenance scheduling of a bridge system by considering all the above dependencies is detailed.

The model is validated through four numerical applications, namely two beams in parallel, two beams in series, a slab with a bituminous coating and a bridge superstructure. The applications demonstrated an important role for the dependencies between the elements of a

system when scheduling their maintenance times. The economical dependency effect is the most pronounced, because in most cases the components of a structural system have comparable failure probabilities with time, and therefore their maintenance scheduling can be grouped. The latter can save a substantial amount of funds to the managers. Stochastic dependency may lead to smaller time intervals when high system reliability is needed, and its effect can surpass the grouping effect of the economical dependency for very stringent failure thresholds or when the failure of some items leads automatically to the failure of others. However, considering both dependencies will usually result in grouping the activities at smaller time intervals, which may outcome a less costly yet safer maintenance planning. Moreover, the degradation dependency behaves similarly to the stochastic dependency by favoring a preventive policy regarding degradation and failure. However, the degradation monetary consequence directs the total cost function versus time to a more convex shape. The latter can possibly result in an optimal planning independent of the threshold reliability.

Chapter 4: Robust formulation for Reliability-based LCC optimization

4.1 Overview

Deterministic Design Optimization (DDO) is traditionally applied in structural design. Its drawback is that uncertainties are not constantly taken into account. As the uncertainties related to design variables, material properties and loads can have large impacts on the structural performance, probabilistic constraint formulations have been developed since the 1980th (Madsen et al. 1986).

In order to point out the difference between the existing optimization methods, a distinction is to be highlighted between the terms 'variability' and 'uncertainty'. In this thesis, the Van Belle's terminology (Van Belle 2011) is considered, where 'variability' refers to natural or intrinsic variation in some quantity, whereas 'uncertainty' refers to the degree of precision with which a quantity is measured. Usually, uncertainty can be probabilistically modeled, whereas variability cannot without specific assumptions; other methodologies, such as fuzzy sets and interval algebra could be appropriate for modeling variability. A more elaborated discussion over the definition of uncertainties has been given in chapter 1 (section 1.3).

Although the Reliability-Based Design Optimization (RBDO) takes into account the uncertainty in the analysis, it does not reflect the ability of the structure to adapt to variability, unforeseen actions or deterioration mechanisms. A design that is less sensitive to changes in the variable parameters can sustain greater excursions from the assumed design conditions before failing (Sandgren and Cameron 2002).

The Robust Design Optimization (RDO) implies that the objective function becomes less sensitive to random variations by reducing the variability of the structural performance while improving its mean level. Structural robust design differs from RBDO for it aims at controlling the everyday variation of the structural performance, rather than the probability of system failure under catastrophic extreme events. The conventional method of engineering robust design was proposed by Taguchi and Rafanelli (1994) with the aim of improving the quality of a product or process not only by achieving performance target, but also by minimizing the performance variation without eliminating the cause of these variations. Later on, the limitations of Taguchi methods are clarified by Parks (2001)

It has been proven in many studies that reliability-based and robust design has advantages over deterministic design (Lee and Park 2001; Sandgren and Cameron 2002; Doltsinis et al. 2005; Saydam and Frangopol 2011). However, there are still ambiguities regarding the links between the two approaches, and the domain of application in which RBDO or RDO can be recommended. Although the former uses the reliability theory and the latter uses deterministic models (Beck and de Santana Gomes, Wellison José 2012), the engineer is seeking for a consistent and adapted decision-making methodology whatever the applied procedure.

In order to combine the advantages of both optimization methods, we have developed a robust formulation for reliability-based design optimization (RRBDO). The proposed RRBDO takes account for uncertainty and variability in one mathematical formulation, which is demonstrated through applications to design of concrete and steel structures. The RRBDO formulation provides a general framework in which the link between RBDO and RDO is well established, through the definition of the application domain for each method and the

appropriate setting of the optimization constraints. The advantage of the proposed RRBDO over the existing formulation is demonstrated from both conceptual and numerical points of view.

4.2 Total Cost

The total design cost of structures has been widely studied in the literature; e.g. (Aoues and Chateauneuf 2008; Aoues and Chateauneuf 2010; Saad et al. 2015). As explained in chapter 2, the common approach in engineering practice is the design of structures which avoid failure. Hence, the total cost minimization is carried out for initial and failure costs. It can be formulated as follows:

$$C_T = C_0 + C_F \tag{4.1}$$

where C_0 is the initial cost and C_F is the expected failure cost. The initial cost covers the costs of design, material and workmanship. It includes all the costs of buying the physical asset and bringing it to operation. Let the limit state function g_j represents the structural condition that preserves the operation, away from the certain critical performance level; the subscript *j* makes reference to a given failure scenario. The probability of failure P_{fj} is the probability of having a negative limit state function (i.e. failed condition):

$$P_{fj} = P\left[g_j \leq 0\right] \tag{4.2}$$

The expected failure cost can be estimated as:

$$C_F = \sum_{j=1}^{M} C_{fj}\, P_{fj}(t) \tag{4.3}$$

where $P_{fj}(t)$ is the cumulative failure probability for the j^{th} limit state (i.e., probability that failure occurs anytime between the construction and the time *t*), *M* is the number of independent limit states *j*, and C_{fj} is the failure cost associated with the occurrence of the j^{th} limit state.

When all attributes and consequences of a decision concerning a structure can be expressed in monetary terms, an optimal decision will be met by minimizing the life-cycle cost of the structure (Val and Stewart 2003).

4.3 Deterministic design optimization

The deterministic design optimization (DDO) is described as follows (Arora 1989):

$$\begin{aligned} &\text{Find} && d, \\ &\text{minimizing} && f(d) \\ &\text{subject to} && g_j(d) \leq 0 \qquad j = 1, \cdots, m \\ & && d_L \leq d \leq d_U \end{aligned} \tag{4.4}$$

where d, d_L and d_U are vectors of design variables, lower bounds and upper bounds respectively, $f(d)$ is the objective function and $g_j(d)$ is the j^{th} constraint function among the m constraints.

4.4 Reliability-based design optimization

As the uncertainties in the design variables can give rise to large changes in performance, a probabilistic model should be considered. The probabilistic constraint formulation, described by Madsen and Krenk (1986) defines the design optimization under probabilistic constraints as a standard nonlinear programming problem:

$$\begin{aligned} &\text{Find} && d, \\ &\text{minimizing} && f(X,d) \\ &\text{subject to} && P_{fj} = P\left[g_j(X,d) \le 0\right] \le P_f^T \qquad j = 1,\cdots,m \\ & && d_L \le d \le d_U \end{aligned} \tag{4.5}$$

where X and d are the vectors of random and design variables respectively, P_{fj} is the probability of failure for the limit state function g_j , d_L and d_U are respectively the lower and upper bounds of the design variables, m is the number of independent limit states j, and P_f^T is the admissible failure probability (assumed, in this case, to be the same for all limit states). The optimality conditions for the RBDO problem are as following:

$$\begin{aligned} &\frac{\partial E[f(X,d)]}{\partial d_i} + \sum_{j=1}^{m} \kappa_j \frac{\partial\, P\left[g_j(X,d) \le 0\right]}{\partial d_i} = 0 \\ &\kappa_j\left(P\left[g_j(X,d) \le 0\right] - P_f^T\right) = 0 \end{aligned} \tag{4.6}$$

where κ_j is the Lagrange multiplier for the j^{th} constraint. Each one of the second system of equations means that either the multiplier is nil (i.e. inactive constraint) or the constraint is nil (i.e. active constraint). These optimality conditions indicate that the rate of decrease of the expected cost is balanced by the increase rate of the weighted probability sum for active constraints.

The intricate part in RBDO applications is the assessment of the probability of failure. Standard Monte-Carlo simulations and classical reliability methods have been widely used, but suffer from high computation costs.

The reliability constraint in RBDO formulation allows us to take into account the uncertainties related to structural parameters. The transmitted variation from uncontrollable variability to the objective function can result in the deterioration of product quality and can compromise the design feasibility. The effect of noise variables on the objective function can be reduced by adjusting the design values. Therefore, there are strong needs to define the values of controllable settings (such as concrete dimensions of a bridge cross-section) which minimize the negative effects of the uncontrollable phenomena (such as humidity or corrosion rate). In this context, the Robust design optimization (RDO) aims at finding the optimal settings to minimize cost by minimizing the response variation, where consistent design meets better quality.

4.5 Robust Design Optimization Formulation

Robust design is an engineering methodology for optimal design of products and process conditions, in order to make them less sensitive to system variations (Kang 2005). Robustness is also defined as the ability of a structure to sustain damage without disproportionate consequences. Robust design is achieved by the reduction of variation of a product without eliminating the causes of variations.

There is no consensus on a simple measure to quantify the robustness of structures. (De et al. 1989) defined robustness as the ability of the system to still carry some load after the brittle fracture of one or more critical components. An approach to robustness has been proposed by Saydam and Frangopol (2011) by the ratio of the failure probability of the intact structure to the failure probability of the damaged structure, for each damage case. Casas and Chambi (2014) defined a robustness coefficient which modifies a typical condition rating obtained with standard inspection procedures, to take into account structural type and configuration, based on redundancy measures. A robustness index is also proposed to measure the influence of deterioration propagation on the loss of performance. The above mentioned robustness insight is generally accompanied by redundancy insight. Frangopol and Curley (1987) defined the system redundancy as the ability of a structural system to redistribute the applied load after reaching the ultimate capacity of its main load-carrying members. In our study, robust design refers to a design that is less sensitive to changes in the variable parameters and that can sustain greater excursions from the assumed design conditions before failing (Sandgren and Cameron 2002).

The first key points in the application of robust design are as follows:

- Define the objective function, which is a performance measure of the design process.
- Identify the design parameters that affect the performance measure and that can be easily controlled.
- Identify the uncertain parameters that cause the variation of the performance function. Compute the mean and variance of the performance function.

The above key points are indicated in Figure 4.1

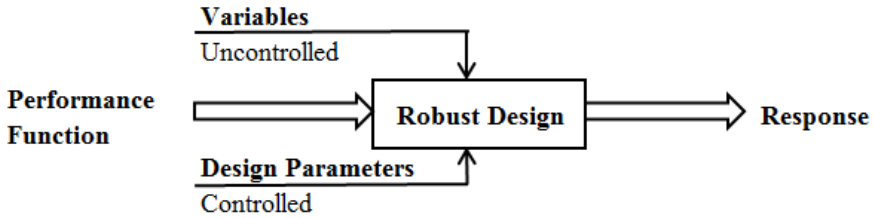

Figure 4.1: Design and uncertain parameters in robust design.

Robust design identifies the optimal combination of design parameters that makes the performance function less sensitive to the effect variability, which tends to reduce the variance and/or deviate the mean value of the performance function.

Lee and Park (2001) proposed a mathematical formulation for robust design by defining the robustness of the objective and the constraint functions as follows:

Find d,

$$\begin{aligned}
&\text{minimizing} && \tilde{f}(d,\alpha) = \frac{(1-\alpha)\mu(f(d))}{\mu_f^*} + \frac{\alpha\sigma(f(d))}{\sigma_f^*} && 0 \le \alpha \le 1 \\
&\text{subject to} && \widetilde{g_j}(d,\lambda_j) = g_j(d) + \lambda_j \sum_{i=1}^{n} \frac{|\partial g_j|}{|\partial d_i|}\Delta d_i \le 0 && j = 1,\cdots,m \\
& && d_L \le d \le d_U && (4.7)
\end{aligned}$$

where $f(.)$ is the original objective function, $\tilde{f}(.)$ is the desirability robustness objective, d is the design variable, μ_f and σ_f are respectively the mean and the standard deviation of the objective function, μ_f^* and σ_f^* are normalization factors denoting the mean value and the standard deviation of the objective function, respectively, m is the number of limit states j, α is the weighting factor and λ_j is the penalty factor. The value of the weighting factor α can be set to specify the relative weights to put on the different objective functions and therefore enables the user to investigate the trade-off between the objectives in an easy manner. To include the variations of the constraint, the revised constraint $\widetilde{g_j}(.)$ is defined by Sundaresan et al. (1995). The penalty factors λ_j are determined by the designer. The low sensitivity of the objective function to system variations is enhanced by decreasing the weighting factor α, while the low sensitivity of constraint to system variations is enhanced by increasing the penalty factor λ_j. Most of the researches, e.g. Lee and Park (2001), take into account only the variations of the design variables, while the variability of other parameters including loads are not accounted for in the formulation. They have considered robust design as a revised deterministic optimization problem, in which the weighting factor is introduced to define a compound multi-objective function and the penalty factor is introduced to account for the variation in the constraints observing the tolerance bands of design variables. Random fluctuation of structural parameters other than the design variables is not considered in their study. Doltsinis et al. (2005) used the same objective function as in equation 4.7, but developed a different constraint formulation which is able to deal with variations in both design and uncertain parameters:

$$\begin{aligned}
&\text{Find} && d, \\
&\text{minimizing} && \tilde{f} = \frac{(1-\alpha)\mu_{f(d)}}{\mu_f^*} + \frac{\alpha\sigma_{f(d)}}{\sigma_f^*}, && 0 < \alpha < 1 \\
&\text{subject to} && \frac{\mu_{g_j(d)}}{\sigma_{g_j(d)}} \le -\lambda_j && j = 1,\cdots,m \\
& && d_L \le d \le d_U && (4.8)
\end{aligned}$$

In this formulation, the designer is left with a choice of weights that will ultimately define how far from the failure surface should the mean optimum lie. The optimality conditions for the above RDO problem are as following:

$$\begin{aligned}
&\frac{(1-\alpha)}{\mu_f^*}\frac{\partial\mu_{f(d)}}{\partial d_i} + \frac{\alpha}{\sigma_f^*}\frac{\partial\sigma_{f(d)}}{\partial d_i} + \sum_{j=1}^{m}\kappa_j\left(\frac{\partial\,\mu_{g_j(d)}}{\partial d_i} + \lambda_j\frac{\partial\,\sigma_{g_j(d)}}{\partial d_i}\right) = 0 \\
&\kappa_j\left(\mu_{g_j(d)} + \lambda_j\sigma_{g_j(d)}\right) = 0 && (4.9)
\end{aligned}$$

In these optimality conditions, the weighted mean and standard deviation are balanced at the optimal solution. In addition to the Lagrange multiplier κ_j, the penalty factor λ_j plays a

significant role in the optimal design solution, as it controls the coefficient of variation of the constraint function $g_j(d)$.

Although the RDO optimization allows us to minimize the performance variance, it presents many disadvantages, among them are the following:

- RDO cannot guarantee the desired reliability level.
- The linear combination that forms the desirability function performed well in many studies (Doltsinis et al. 2005), but it may present some difficulties in cases of non-convex objective functions.
- The reduction of the variance of the structural performance in robust design is frequently achieved at the penalty of worsening its expected value. The two aspects: mean and variance can diverge, and the designer has to select a feasible structural design out of the set of optima obtained with different weighting factors for the desirability function.
- The obtained results do not exactly indicate which parameter has the highest effect on the performance characteristic value.
- RDO is a deterministic method and is not appropriate for a dynamically changing process such as simulation study or for time-variant processes (Rizzuti et al. 2009).
- The mean and variance modeling approach of robust design does not take direct advantage of the interactions between controllable and uncontrollable variables

Therefore, a reliable optimization procedure that can overcome the above disadvantages is sought, and this will be developed in section 4.7. For this purpose, we should first of all understand the behavior of reliability-based design optimization.

4.6 Behavior of RBDO formulation

Let us consider the following RBDO formulation applied to the total cost of the structure:

$$\begin{aligned} &\text{Find} && d \\ &\text{minimizing} && C_T(d) = C_0(d) + C_f P_f(d) \\ &\text{subject to} && P_f(d) \le P_f^T \\ & && d_L \le d \le d_U \end{aligned} \tag{4.10}$$

where d, P_f, g, d_L, d_U and P_f^T are defined in section 4.4.

In this formulation, the reliability constraint is not always active, as the optimal solutions may be found with failure probabilities lower than the admissible one; i.e. $P_f(d^*) < P_f^T$. Depending on the considered problem, there may be conflicting requirements between the objective function minimization and the failure probability constraint. When the admissible failure probability increases, the initial cost $C_0(d)$ decreases but the expected failure cost $C_f P_f(d)$ increases, and vice-versa, leading to the convex shape of the cost function, as shown in Figure 4.2 Let $C_{T,RBDO}$ be the optimal cost found by the application of the above RBDO formulation, and $C_{T^*_{min}}$ be the optimal cost corresponding to the unconstrained formulation. In fact, the constraint on the failure probability is not active beyond a certain value $P_f(d^*)$ corresponding to the unconstrained minimum cost $C_{T^*_{min}}$, as shown in Figure 4.2.

with $C_{T_{min}}^{*} = C_T(d^*) = C_0(d^*) + C_f P_f(d^*)$

such that $P_f^T = P_f(d^*)$ (4.11)

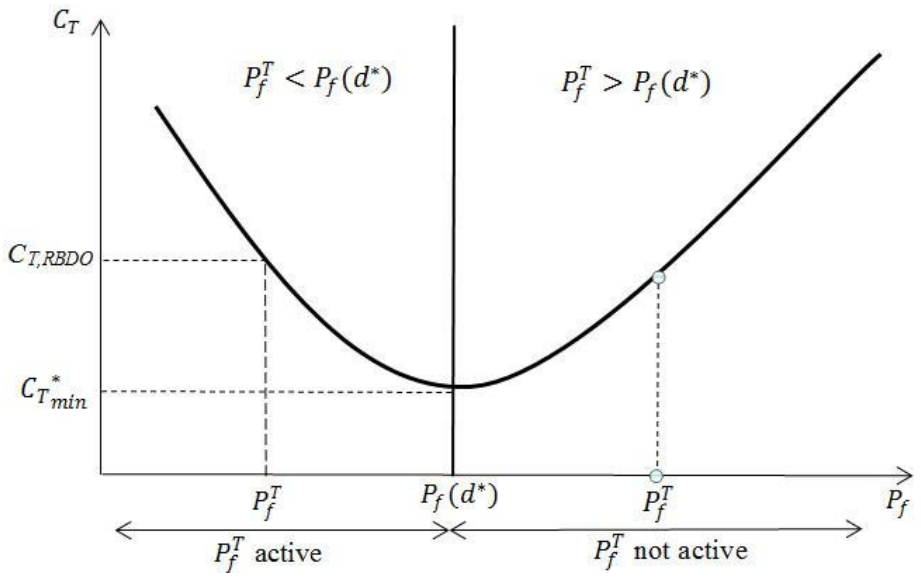

Figure 4.2. Active Reliability limit.

The constraint P_f^T is not active when: $P_f(d^*) < P_f^T < 1$

The constraint P_f^T is active when: $0 < P_f^T < P_f(d^*)$

If the RBDO constraint P_f^T is between *0* and $P_f(d^*)$, the optimal cost $C_{T,RBDO}$ will be greater than the unconstrained minimum $C_{T_{min}}^{*}$, and in this case, P_f^T is active. However, when the limit P_f^T is greater than $P_f(d^*)$, the optimal cost will be $C_{T_{min}}^{*}$, and in that case the reliability constraint is not active.

When the expected value of performance exceeds the level corresponding to the target (i.e. $P_f(d^*) < P_f^T$), the RBDO becomes insensitive to the reliability constraint. The drawback in this situation is that the wrong or large setting of the admissible failure probability, will lead to unrobust solution as it mostly corresponds to large variability. In other words, the obtained solution will satisfy the optimality conditions and the reliability constraints, but not the robustness requirements. This drawback makes the solution very sensitive to the choice of the reliability target and the probabilistic input parameters, and therefore inappropriate for practical engineering use.

Another drawback of RBDO appears when the expected total cost function is narrow, as shown in Figure 4.3; this situation is frequently observed when the failure cost is high. A narrow cost function is very sensitive to the failure probability; i.e. larger cost data points are clustered closely around the optimum $C_{T_{min}}^{*}$. In this case, inquiring optimal solutions may be skipped when applying the RBDO, since a less costly solution can be found without compromising neither the structural performance nor the safety level, if a small variation is allowed for P_f^T. Therefore, considering a target failure probability as a constraint without tolerating small amount of variation may lead to highly conservative solutions. By using P_f^T as a constraint, the

RBDO finds a solution that costs much more than the unconstrained one $C_{T_{min}}^{*}$. Knowing the various levels of uncertainties in engineering systems, this over-cost cannot be properly justified when the admissible failure probability P_f^T is close to the one corresponding to the unconstrained minimum cost $P_f(d^*)$. In this case, a better solution can be found with much less cost than for the crude RBDO solution, without compromising significantly the structural reliability.

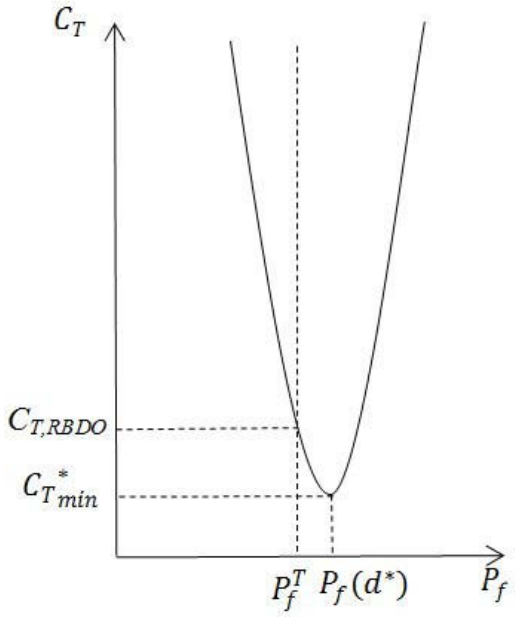

Figure 4.3. Inquiring optimal solution skipped by the use of RBDO.

The above two situations, either inappropriate setting of reliability target or narrow expected cost function, show clearly that the crude RBDO is not sufficient to provide robust solution; especially that large amount of uncertainties cannot be predicted and identified in engineering practice. Among these uncertainties, we can mention the direct and indirect failure costs which are often very difficult to estimate precisely, and the admissible failure probability which is a conventional measure depending on the precision of input data and the involved physical and probabilistic models. It is therefore necessary to develop a more consistent methodology for optimal decision-making under uncertainties.

Some authors proposed reliability-based formulations for robust optimization by keeping the robust objective function in equation 4.7, and adding a reliability constraint instead of the constraint on the performance variation (Youn et al. 2005; Lee et al. 2008; Rathod et al. 2013; Shahraki and Noorossana 2014) . This formulation can be expressed as following:

Find	d,		
minimizing	$\tilde{f} = \frac{(1-\alpha)\mu_{f(d)}}{\mu_f^*} + \frac{\alpha\sigma_{f(d)}}{\sigma_f^*}$,	$0 < \alpha < 1$	
subject to	$P_f(d) \leq P_f^T$	$j = 1, \cdots, m$	
	$d_L \leq d \leq d_U$		(4.12)

where $\tilde{f}$, μ_f^*, σ_f^*, α , P_f^T, d_L and d_U are as defined in section 4.4. The drawback of this formulation is that it cannot take account for variations in system parameters. Moreover, it suffers from the same limitations explained herein mainly caused by the fixed value of the reliability target.

It is worth to note that unconstraint formulations of robust and reliability optimization procedures were compared by (Beck et al. 2015). The following unconstraint formulations were used:

Risk formulation: $$d^* = argmin\left[f(d) + C_f P_f(d);\ \ d \in [d_L, d_U]\ \right] \tag{4.13}$$

Robust formulation: $$d^* = argmin\left[\frac{(1-\alpha)\mu_{f(d)}}{\mu_f^*} + \frac{\alpha\sigma_{f(d)}}{\sigma_f^*};\ \ d \in [d_L, d_U]\right] \tag{4.14}$$

The unconstraint risk formulation was found in their study to outperform robust formulation, mainly due to the non-convex shape of the robust objective function which leads to optimal designs determined by the variable bounds.

The available methods in the literature still need to be improved, in order to properly handle both variability and uncertainty, affecting structural performance and parameters. The main difficulties are related to the consistency of reliability and robustness objective function and constraints, on one hand, and to the arbitrary choice of the constraint bounds, on the other hand. According to the above discussion, the inconsistency of setting the reliability target in accordance with the problem context is believed to be the key feature for combining effectively the reliability and robustness considerations. In this framework, the optimization model proposed in the next section overcomes the above limitations without compromising the reliability level, by considering a robust convex objective function and a performance variation constraint.

4.7 Proposed Robust Reliability-based design optimization

As mentioned in the above sections, the RBDO solution leads to reliable design, but does not consider the performance variation. On the opposite, the RDO optimization can minimize performance variation, but cannot guarantee the desired reliability. A formulation that combines the benefits of robust and reliability design is proposed herein, by considering both: the objective function robustness and the reliability level. This method can overcome the previously discussed weaknesses of both optimization procedures. The proposed Robust Reliability-Based Design Optimization RRBDO applied to the total cost of the structure is formulated as following:

Find d,

minimizing $$\tilde{f} = \frac{(1-\alpha)\mu(C_T(X,d))}{\mu_{C_T}^*} + \frac{\alpha\sigma(C_T(X,d))}{\sigma_{C_T}^*}, \qquad 0 < \alpha < 1$$

with $$C_T(X,d) = C_0(X,d) + \sum_{j=1}^{m} C_{fj}\ P\left[g_j\ (X,d) \le 0\right],$$

subject to $$\frac{\mu(g_j(X,d))}{\sigma(g_j(X,d))} \le -\lambda_j \qquad j = 1, \cdots, m$$

$$d_L \le d \le d_U \tag{4.15}$$

As can be seen, the mean value of the limit state function g_j appears in the objective function as well as in the constraint function. Consequently, the increase in the mean value that is usually observed in robust design is limited in this formulation. The advantages of the proposed optimization method are as follows:

- The sensitivity of the objective function is lowered with respect to usual RBDO formulation,
- The effect of uncontrollable random variables on the structural performance is minimized,
- The tolerance to comply with unforeseen actions or to deterioration mechanisms is quantified and controlled,
- The prescribed reliability level is ensured.

The optimality conditions for the above RRBDO problem are as following:

$$\frac{(1-\alpha)}{\mu^*_{C_T}}\frac{\partial\mu\left(C_0(X,d)+\sum_{j=1}^{m}C_{fj}\,P_{fj}(X,d)\right)}{\partial d_i}+\frac{\alpha}{\sigma^*_{C_T}}\frac{\partial\sigma\left(C_0(X,d)+\sum_{j=1}^{m}C_{fj}\,P_{fj}(X,d)\right)}{\partial d_i}$$
$$+\sum_{j=1}^{m}\kappa_j\left(\frac{\partial\,\mu(g_j(X,d))}{\partial d_i}+\lambda_j\frac{\partial\,\sigma(g_j(X,d))}{\partial d_i}\right)=0$$
$$\kappa_j\left(\mu(g_j(X,d))+\lambda_j\sigma(g_j(X,d))\right)=0 \tag{4.16}$$

These optimality conditions aim at balancing, not only the cost function mean and standard deviation, but also the dispersion of the failure cost expectance, including failure cost and failure probability. In addition to random variable considerations, the obtained solution takes into account the possible variations in the design variables d, through their effects on both the limit state functions and the failure probabilities. As a consequence, it is expected to get more stable solution with less sensitivity to variations than in the classical formulations. This can be seen from the optimality conditions where the derivatives of the standard deviations are to be lowered. Beside the failure costs C_{fj}, the final solution is governed by two types of control parameters: the weighting factor α and the penalty factor λ_j specified for each constraint.

Let z^* refers to the optimal solution of the problem, C_T^* is the optimal total cost of the structure, μ_{Pf} and σ_{Pf} are respectively the mean and standard deviation of the failure probability, and μ_g and σ_g are respectively the mean and standard deviations of the limit state function $g(X,d)$.

For each failure scenario (i.e. limit state function), the mean and standard deviation of the failure probability are given by:

$$\mu_{Pf_j}=\int_{d_L}^{d_U}P_{f_j}(X,d)\;f_{Pf_j(X,d)}d_d \tag{4.17}$$

$$\sigma_{Pf_j}=\sqrt{\int_{d_L}^{d_U}[P_{f_j}(X,d)-\mu_{Pf_j}]^2\;f_{Pf_j(X,d)}\;d_d} \tag{4.18}$$

where $f_{Pf_j(X,d)}$ is the probability density function of $P_{f_j}(X,d)$. The mean and standard deviation of the limit state function are given by:

$$\mu_{g_j} = \int_{d_L}^{d_U} g_j(X,d)\, f_{g_j(X,d)}\, d_d \tag{4.19}$$

$$\sigma_{g_j} = \sqrt{\int_{d_L}^{d_U} [g_j(X,d) - \mu_{g_j}]^2\, f_{g_j(X,d)}\, d_d} \tag{4.20}$$

where $f_{g_j(X,d)}$ is the probability density function of $g_j(X,d)$. These parameters can be estimated by either Monte-Carlo simulations or by first order approximations.

The above formulation can be extended to time-variant problems if the limit state can be expressed as a function of time $g_j\,(X,d,T)$. This is particularly useful for structures subjected to performance degradation due to aging. A discount rate can thus be attributed to the future failure cost to convert it to its equivalent present value. By adopting annual discretization of the structure lifetime, the total cost is then expressed as follows:

$$C_T(X,d,T) = C_0(X,d) + \sum_{j=1}^{m}\sum_{\tau=0}^{T} \frac{C_{SFj}\, P[g_j\,(X,d,\tau)\leq 0]}{(1+\nu)^i} \tag{4.21}$$

where $P\left[g_j\,(X,d,\tau) \leq 0\right]$ is the annual probability of failure for the limit state j at the τ^{th} year (i.e., probability that failure will occur anytime during the year τ), and ν is the discount rate. The above time-variant extension is made possible by the existence of physical degradation models for the most influential deterioration processes, and also by the development of numerical procedures that can evaluate the failure probability of complex nonlinear problems.

4.8 Solution procedure

When robustness is considered, the solution procedure should be defined such that practical engineering problems can be handled in a reasonable computation time. This procedure can also be used for comparison between RRBDO and RBDO. The proposed procedure, illustrated in Figure 4.4, can be divided into the following steps:

- Step 1: The limit state functions g_j are evaluated.
- Step 2: The failure probability P_{f_j} associated with the limit state function g_j is evaluated. For this purpose, the First Order Reliability Method (FORM), or any other numerical procedure, can be applied to give an approximation of P_{f_j}. The uncertainties in the problem-related parameters are accounted for through their corresponding probability distributions.
- Step 3: Monte-Carlo simulations (MCS) are performed on the reliability analysis results (e.g. *FORM* results) in order to evaluate the mean and standard deviation of the failure probability (μ_{Pfj} and σ_{Pfj}).
- Step 4: The same Monte-Carlo simulations can be used to evaluate the mean and the standard deviation of the limit state functions g_j (μ_{g_j} and σ_{g_j}); in this way, no additional computation cost is considered to compute these quantities.

- Step 5: Having the mean values and standard deviations of the limit state and failure probability functions, the RRBDO can be solved using classical optimization procedures by solving problem 4.14.
- Step 6: When comparison between RBDO and RDO is required, the RBDO is performed by considering the solution of RRBDO as initial values for the design variables. In addition, the admissible failure probability used in the RBDO constraint is taken equal to the failure probability when the design variables take the values given by RRBDO solution. This procedure allows us to obtain the results of RRBDO and RBDO for the same reliability level, and thus allowing for comparison between the two optimization procedures.

The different executions of the RRBDO correspond to different values of the constraint λ, such as $\mu_{gj}/\sigma_{gj} \leq -\lambda_j$. In fact, λ_j is a constraint on the coefficient of variation of the limit state function. For simplification, the subscript j is eliminated from the notations in Figure 4.4.

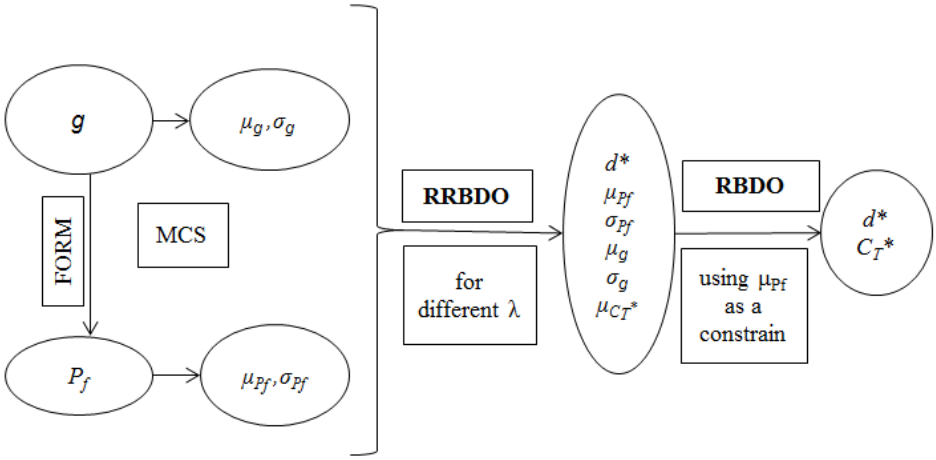

Figure 4.4. Solution procedure for RBDO problem.

The above procedure allows us to ensure the reliability level while minimizing the effect of variability on the design objectives. However, several computational challenges have to be faced:

(1) FORM has to be applied herein to evaluate the reliability index in the space of random variables, leading to two nested optimization problems (Aoues and Chateauneuf 2010). The outer problem searches for design variables to minimize the cost function, while the inner one searches for the most probable failure point in the space of random variables; when the limit state function is highly non-linear, the convergence of FORM cannot be guaranteed.

(2) MCS are applied for the limit state function and the failure probability (obtained herein by FORM analysis), in order to determine their mean values and coefficients of variation. MCS requires a large number of samples to give stable results, which is very time consuming, and cannot be always feasible, especially with FORM results.

It is important to note that, although the FORM algorithm is used in our applications, any other reliability procedure (e.g. Monte-Carlo simulations, response surfaces, stochastic expansions, etc.) can be applied to compute the failure probability. The main criteria to consider when choosing a method are the precision and the computation cost.

In order to cater for the above problems, a polynomial approximation is adopted herein to compute μ_{Pf}, σ_{Pf} , μ_g and σ_g as functions of the design variables, using least square regression on a reduced number of *MCS* samples. Beck et al. (2015) proposed a design space root finding method for efficient risk based optimization (corresponding to the herein RBDO formulation (4.10)). Their method can be extended to the above described sequence in order to overcome the computational burden of the nested optimization and reliability loops. Other authors also proposed approached based on decoupling the reliability loop from the optimization loop (Spence et al. 2015). This formulation is still in need of more accurate and performing numerical estimation methods; however, the solution procedures are beyond the scope of the present document, although the reader can refer to the work of Aoues and Chateauneuf (2010) comprehensive discussion about this issue.

4.9 Numerical Applications

Four applications are considered hereafter in order to investigate the performance of the proposed RRBDO formulation and to compare it with Reliability-Based Design Optimization. The first example aims at illustrating in details the proposed procedure and at describing the behavior of reliability-based design. In the second application, the role of time in the RRBDO formulation of a time-variant process is investigated. The third example shows the interest of RRBDO framework for system analysis, through the design of overhanged beam with variable cantilever depth. The fourth application investigates the effect of robustness objective regarding the structural topology, where several failure modes are considered. The structural applications are chosen to have different structural properties and modes of failure, in order to show the applicability of the proposed methodology on a large range of engineering problems (i.e. structural topology, number of failure modes, time-invariant and time-variant, component and system reliability, etc.)

4.9.1 Plane truss example

This application, drawn from Beck and Gomes (2012) aims at finding the optimal height and thickness of a plane truss structure, considering the yielding of steel cross-section as shown in Figure 4.5.

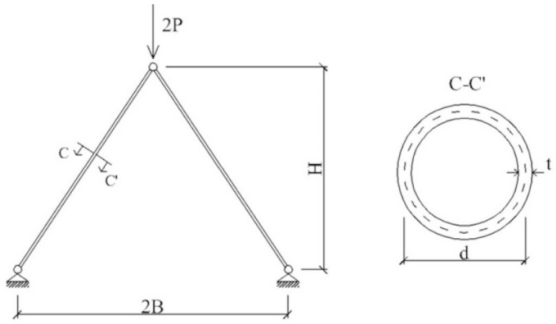

Figure 4.5. Plane truss example.

The span is fixed to $2B = 6\ m$. Table 4.1 summarizes the values and distributions of the system variable. The considered limit state function accounts for yielding, and takes the form:

$$g = f_y - \sigma = f_y - \frac{P\sqrt{B^2+H^2}}{\pi t\, Hd} \tag{4.22}$$

where σ is the compressive stress in the tubes, B and H are respectively the truss half-span and height, d and t are respectively the cross-section diameter and thickness, P is the applied load, and f_y is the yield stress. The initial cost is composed of a fixed cost of labor (taken equal to 10 unit costs), plus a term proportional to cost of materials:

$$C_0 = C_s \times [1.2\ \rho\ 2\pi\ d\ t\ \sqrt{B^2 + H^2} + 10] \tag{4.23}$$

where C_s is the cost of steel per unit weight and ρ is the material density. The total cost C_T is written as:

$$C_T = C_0 + C_f P_f \quad \text{with } P_f = P[g \leq 0] \tag{4.24}$$

In Table 4.1, the design variables are represented by the vector d= $[t, H]$. The uncertainties are characterized by their probability distributions, mean values, coefficients of variation, and they are represented by the vector X = $[P, f_y]$.

Design variables	**Deterministic parameters**		**Uncertainties (X)**			
			Random variables	**μ**	**Distribution**	**COV**
t (thickness)	d (diameter)	0.15 m	P (load)	337 kN	Normal	0.10
H (height)	B (span)	3 m	f_y (material strength)	105 MPa	Lognormal	0.07

Table 4.1. Input variables for the plane truss.

The RBDO problem of the plane truss is:

$$\begin{aligned} &\text{Find} && d = [H, t] \\ &\text{minimizing} && C_T(X, d) = C_0 + C_f \times P_f(d) \\ &\text{subject to} && P_f(d) = P[g(X, d) \leq 0] \leq P_f^T \\ & && d_L \leq d \leq d_U \end{aligned} \tag{4.25}$$

where the admissible failure probability P_f^T is taken equal to 10^{-4}. $P_f(d)$ is approximated using the first order reliability method FORM . The RBDO is applied with different values of C_f leading to the results in Table 4.2. The amplification of the failure cost C_f does not lead to significant variations in the optimal design. A rise of C_f from $10C_0$ to $10^6 C_0$ induces an increase of 16% in the optimal thickness, and 31% in the optimal cost.

C_f/C_0	H^*	t^*	$C_{T,RBDO}$	P_f (d_{RBDO})
10	3	0.0169	620	1.00×10^{-4}
100	3	0.0169	620	1.00×10^{-4}
1000	3	0.0169	621	1.00×10^{-4}
10000	3	0.0169	630	1.00×10^{-4}
100000	3	0.0178	712	6.26×10^{-5}
1000000	3	0.02	897	1.67×10^{-6}
%	0	16	31	

Table 4.2. RBDO solutions in terms of C_f for the plane truss.

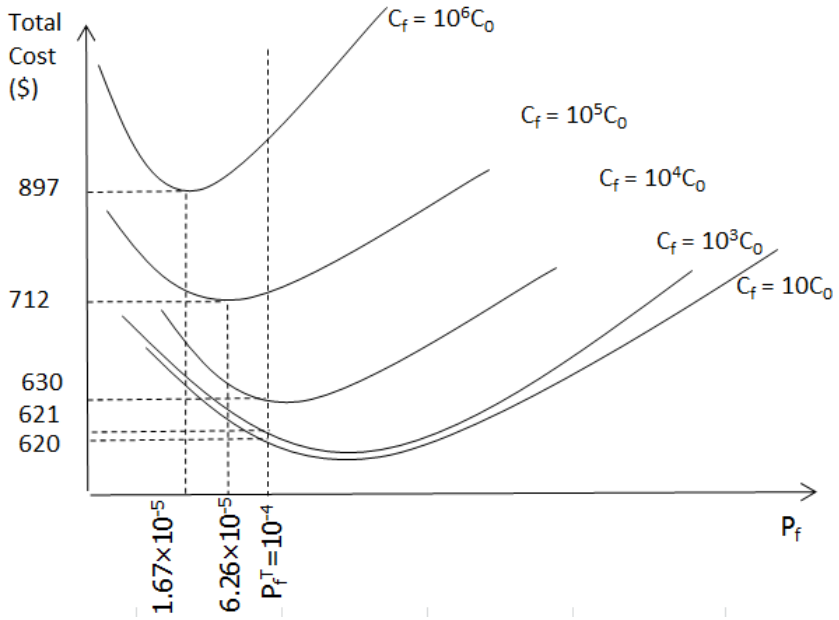

Figure 4.6. Total cost of plane truss for different values of C_f.

As a matter of fact, for all failure costs below 10^4C_0 , the reliability constraint of 10^{-4} is active, as shown in Figure 4.6. Therefore the optimal results correspond to a failure probability equal to P_f^T and an optimal cost higher than for the unconstrained case. For C_f higher than 10^4C_0, the reliability limit of 10^{-4} is not active, and the minimum cost is equal to $C_{T_{min}}^*$.

The robust formulation for reliability-based design optimization (RRBDO) applied to the plane truss example is written as follows:

$$
\begin{aligned}
&\text{Find} && d = [H, t] \\
&\text{minimizing} && \tilde{f} = \frac{(1-\alpha)\mu_{C_T(X,d)}}{\mu_{C_T}^*} + \frac{\alpha\sigma_{C_T(X,d)}}{\sigma_{C_T}^*}, && \textit{with } 0 < \alpha < 1 \\
&\text{with} && C_T(X,d) = C_0 + C_f\, P_f(d) \\
&\text{subject to} && \frac{\mu_{(g(X,d))}}{\sigma_{(g(X,d))}} \leq -\lambda \\
& && d_L \leq d \leq d_U && (4.26)
\end{aligned}
$$

where $\mu_{C_T}^*$, $\sigma_{C_T}^*$, α , λ, d_L and d_U are defined in section 4.5. The normalization factors $\mu_{C_T}^*$ and $\sigma_{C_T}^*$ are taken equal to the mean and the standard deviation of $C_T(X,d)$ when the design variables take the initial values $d_0 = [2.4m\,;\, 0.018m]$. The lower and upper limits are respectively $d_L = [1\,;\, 0.01]$ and $d_U = [3;\, 0.03]$. Figure 4.7 shows the mean values of the initial cost, the failure cost and the total cost, for decreasing values of the penalty factors λ from 5 to 0.5, with α taken equal to 0.5 and C_f equal to 10^4C_0. A larger value of λ generally requires the corresponding performance to be more robust regarding the system variability. A decrease

of the penalty factor corresponds to an increase in μ_{Pf}, leading to an increase in the mean failure cost and a decrease in the mean initial cost. This behavior is foreseen because the penalty factor is a measure of the inverse of the coefficient of variation of the limit state function, and the failure probability (thus the failure cost) increases when σ_g increases. This is a result of the fact that an increase of the optimal design values leads to an increase in the mean of the performance measure and a decrease in the coefficient of variation, as seen in Figure 4.8. In this RRBDO formulation, the objective function is directly related to the constraint function by the mean of $P[g < 0]$. Therefore, the increase of the objective function expectation that is usually seen in RDO studies is limited in the suggested RRBDO formulation.

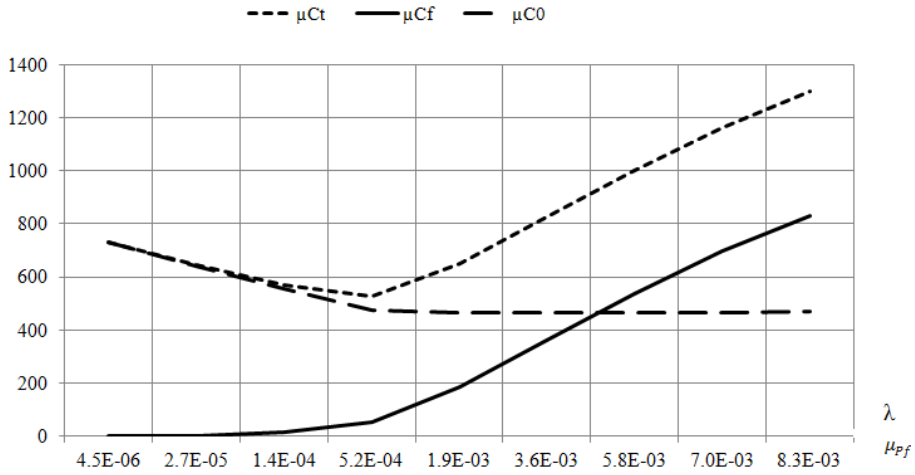

Figure 4.7. Optimal cost obtained by RRBDO - Plane truss.

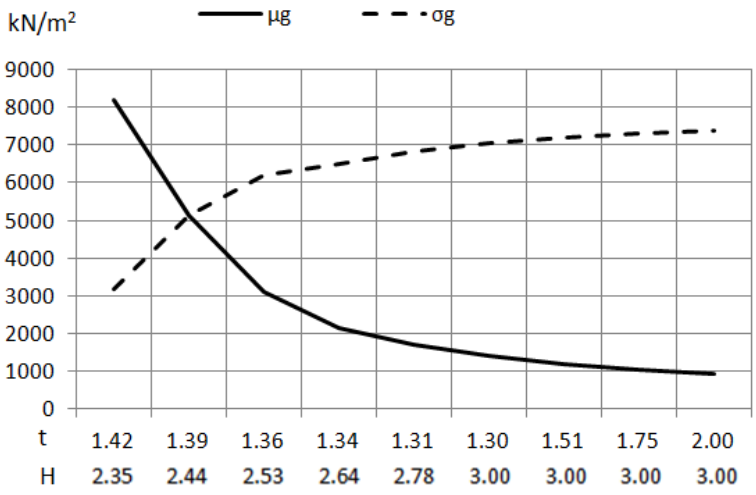

Figure 4.8. Mean and coefficient of variation of the performance function - Plane truss.

As explained above, the reliability constraint in RBDO is not active when P_f^T exceeds $P_f(d^*)$ corresponding to the unconstrained minimum cost $C_{T^*_{min}}$. Therefore, the optimal cost obtained by the use of RBDO is independent of the reliability constraint when P_f^T exceeds $P_f(d^*)$. Figure 4.9 shows the optimal costs found by the RBDO and the RRBDO for increasing values of P_f^T. For $P_f^T < P_f(d^*)$, the RRBDO solution costs 7% less than the RBDO for the same

reliability level. On the opposite, when $P_f^T > P_f(d^*)$, the reliability constraint in the RBDO is not active, although the RRBDO continues to perform properly when P_f^T is greater than $P_f(d^*)$ because the optimal cost increases with the failure probability.

The optimal design parameters are shown in Figure 4.10, in terms of the target failure probability P_f^T. For low target probability (i.e. $P_f^T < P_f(d^*)$), both procedures tend to decrease the optimal thickness and maintain a constant optimal height. For higher target probability ($P_f^T > P_f(d^*)$), the RRBDO tends to increase the optimal thickness by 10% and decrease the optimal height by 20% in order to maintain a certain level of reliability while minimizing the total cost. However, the optimal design of RBDO becomes independent of the failure probability beyond $P_f(d^*)$.

As a result, the proposed RRBDO has better behavior than the RBDO for all reliability targets, since it provides more robust and less costly optimal solutions for high reliability levels, and it continues to perform properly for low reliability levels.

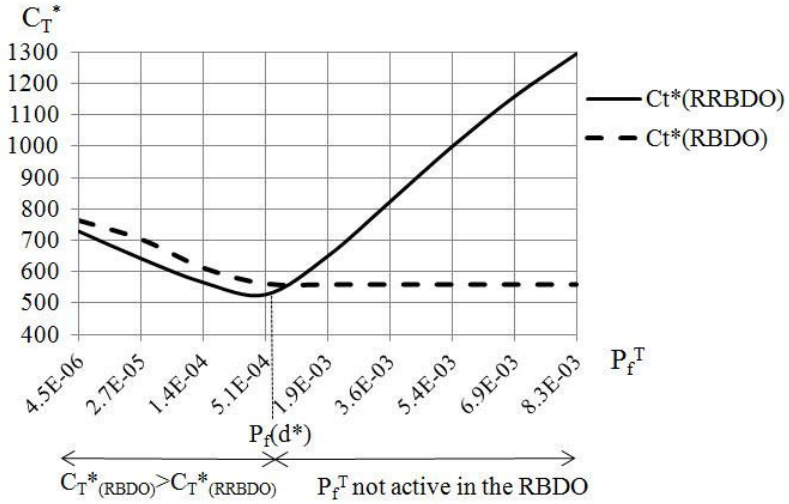

Figure 4.9. Optimal costs CT* - the plane truss.

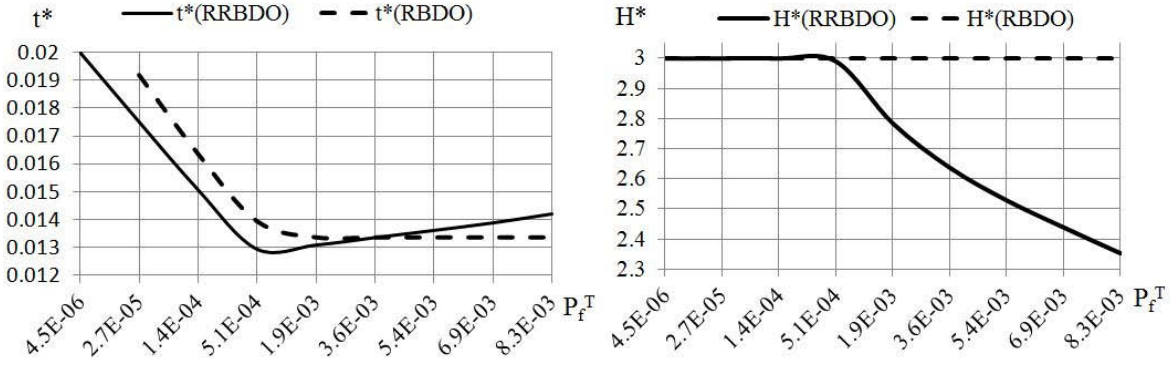

Figure 4.10. Optimal solution z* -the plane truss.

4.9.2 Bridge girder example

This application aims at finding the optimal longitudinal steel area and concrete depth of a reinforced concrete girder, considering degradation with time due to corrosion and fatigue. The coupled corrosion and fatigue deterioration process is formulated by Bastidas-Arteaga et al. (2009), and was divided into three stages. The first stage is corrosion initiation and pit nucleation. The time to corrosion initiation τ_{ini} is given by Thoft-Christensen (1998) and the time to pit nucleation τ_{pn} is given by (Stewart 2004). The second stage is pit-to-crack transition τ_{pt} obtained by equating the pit growth rate to the equivalent crack growth rate, as defined by Val et al. (1997; 1998). The third stage is the crack growth, τ_{cg} , which is reached when the crack size induces cross-section failure. The reduction of the steel reinforcement cross-section which is caused by the coupled effect of corrosion and fatigue starts after the time-to-corrosion initiation τ_{ini}. This reduction is estimated by considering pitting corrosion from τ_{ini} till τ_{pt}. After the pit-to-crack transition, the new crack size is calculated by integrating the fatigue crack growth rate. A full description of this degradation model is given in Appendix 1. The limit state considered herein is related to the bending capacity of a bridge girder:

$$g(d, X, t) = M_r(d, X, t) - M_a(d, X) \tag{4.27}$$

where M_r is the resisting moment and M_a is the applied bending moment, d and X are the vectors of design and random variables, respectively, and t is the time. The initial cost is:

$$C_0 = C_c\, \rho_c\, b\, h\, l + C_{reinf}\, \rho_{reinf}\, A_s\, l + C_{form}\, \rho_{form}\, 2(b + h)\, l\, e_{form} \tag{4.28}$$

where C_c, C_{reinf} and C_{form} are respectively the costs of concrete, reinforcement and formwork per unit weight, ρ is the material density and e_{form} is the formwork width. The cost of failure is considered as $C_{SF} = 10C_0$.

Table 4.3 summarizes the values and distributions of different variables in this problem (Bastidas-Arteaga et al. 2009; El Hassan et al. 2010).

Design variables	**Deterministic parameters**			
	Variable	**Description**	**value**	**unit**
A_s (Steel Area)	b	Width	4	m
	l	Length	10	m
	h	Depth	0.8	m
	E_s	elastic modulus of steel	210000	MPa
	wc	water cement ratio	50	mm
	i_{th}	threshold corrosion	5	μA/cm^2
	f	traffic frequency	2000	cycles/day

Uncertainties (X)					
Variable	**Description**	**Mean value μ**	**Unit**	**Distribution**	**Cefficient of variation COV**
G	dead load	26	kN/m	Normal	0.15
Q	live load	115	kN	Normal	0.25
f_y	steel strength	500	MPa	Lognormal	0.07
C_{th}	threshold chloride concentration	0.9	kg/m^3	Lognormal	0.19
C_s	chloride concentration	2.95	kg/m^3	Lognormal	0.5
D_c	coefficient of diffusion	6×10^{-12}	m^2/s	Lognormal	0.2
c	concrete cover	0.05	m	Lognormal	0.3
f_c	concrete strength	30	MPa	Lognormal	0.15

Table 4.3. Input data for the bridge girder.

The RBDO problem is given by:

$$\begin{aligned} &\text{Find} && d = [As, h] \\ &\text{minimizing} && C_T(X,d) = C_0 + C_f P_f(d) \\ &\text{subject to} && P_f(d) = P[g(X,d) \le 0] \le P_f^T \\ & && 30cm^2 \le A_s \le 50\ cm^2 \\ & && 0.5\text{m} \le \text{h} \le 1.2\ \text{m} \end{aligned} \tag{4.29}$$

and the corresponding RRBDO formulation is:

$$\begin{aligned} &\text{Find} && d = [As, h] \\ &\text{minimizing} && \tilde{f} = \frac{(1-\propto)\mu_{C_T(X,d)}}{\mu^*_{C_T}} + \frac{\alpha\sigma_{C_T(X,d)}}{\sigma^*_{C_T}}, && with\ 0 < \alpha < 1 \\ &\text{with} && C_T(X,d) = C_0 + C_f P_f(d) \\ &\text{subject to} && \frac{\mu(g(X,d))}{\sigma(g(X,d))} \le -\lambda \\ & && 30cm^2 \le A_s \le 50\ cm^2 \\ & && 0.5\text{m} \le \text{h} \le 1.2\ \text{m} \end{aligned} \tag{4.30}$$

The weighting factor α is taken equal to 0.5, and the normalization factors $\mu^*_{C_T}$ and $\sigma^*_{C_T}$ correspond to the steel area of 44 cm² and a beam depth of 0.9 m. Different values are assigned to the penalty factor λ (from 0.5 to 5) in order to parametrically study the problem.

Figures 4.11 and 4.12 shows the optimal costs and steel area respectively found by RBDO and RRBDO as functions of P_f^T. The optimal height is constant for a fixed point in time in both optimization formulations and for all reliability levels. The procedure explained in section 4.7

is applied here for a reference period of 10 years. In this example, the value of $P_f(d^*)$ is 10^{-4} as shown in Figure 4.11 and Table 4.4. The reliability constraint of RBDO is not active when $P_f(d^*) < P_f^T$ corresponding to the unconstrained minimum cost $C_{T_{min}}^*$ of 585 cost units. The optimal solution and cost obtained by RBDO are constant when P_f^T exceeds $P_f(d^*)$, with optimum reinforcement area of 48 cm^2 for all reliability constraints higher than 10^{-4}, as shown in Figure 4.11. Nevertheless, the RRBDO continues to perform properly when P_f^T is greater than $P_f(d^*)$, i.e. although the optimal costs increases by 17%, the optimal reinforcement area (and therefore the initial cost) decreases by 18% when the admissible failure probability increases from 10^{-5} to 10^{-3}. In fact, an increase of the admissible probability of failure P_f^T leads to a decrease in the penalty factor λ which increases the coefficient of variation of the limit state function. It is thus normal to have a larger optimal cost with more variation in the limit state function. Therefore, a more robust design with a constraint on the coefficient of variation leads to a structure that can better adapt to unforeseen variations.

Moreover, the procedure is executed for different points in time in order to observe the influence of time on the optimum solution. A reference performance coefficient of variation of 0.16 is adopted. As predicted, the optimal RRBDO cost increases by 4.5% when the timespan increases by 10 years (Figure 4.13). In addition, a very interesting RRBDO behavior is deducted from the results shown in Table 4.4. When time increases, the RRBDO increases the beam depth h^* in the aim of reducing the steel area A_s^*. This behavior is not present in the RBDO runs for different times. In fact, most of the degradation uncertainties are related to the steel area that becomes more corroded with time. Therefore, the RRBDO provides solutions that are less sensitive to variations, while keeping the same reliability level as the RBDO. This is achieved by the performance variation constraint in the RRBDO formulation.

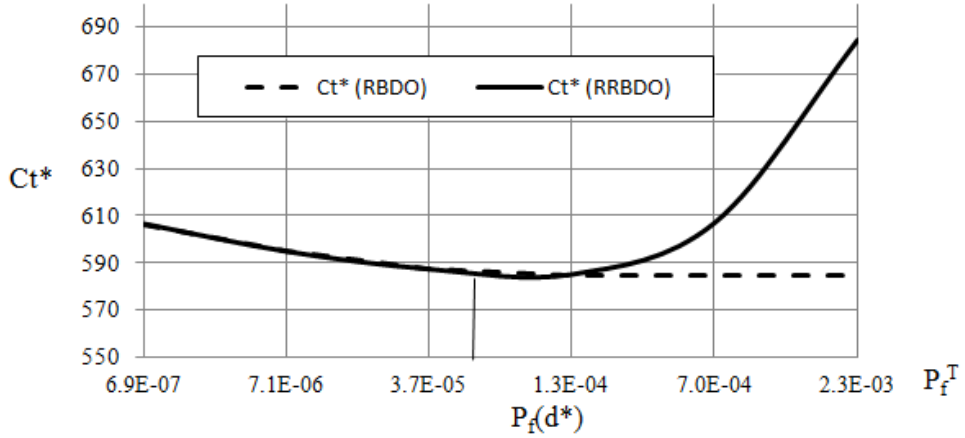

Figure 4.11. Optimal total costs C_T^* versus P_f^T for the bridge girder.

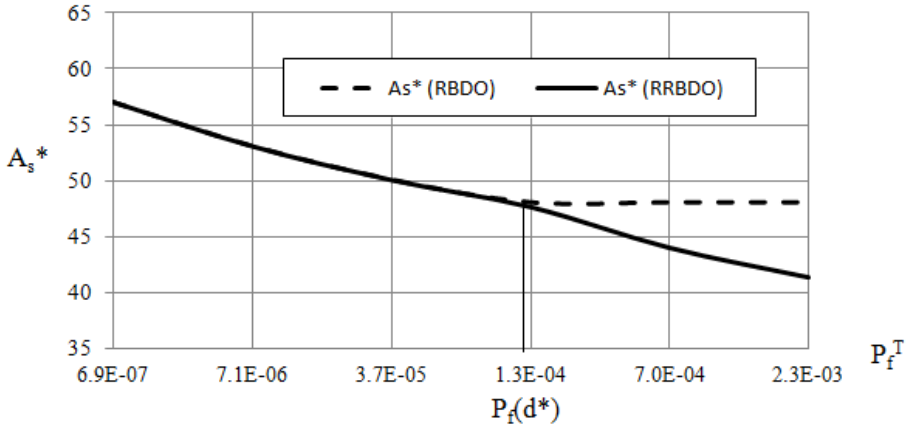

Figure 4.12. Optimal solution A_s^* for the bridge girder.

1/ λ	RRBDO			RBDO		
COV_g	P_f (RRBDO)	A_s^* (RRBDO)	C_T^* (RRBDO)	P_f (RBDO)	A_s^* (RBDO)	C_T^* (RBDO)
0.08	2.07×10^{-9}	65.77	632.91	2.07×10^{-9}	65.77	632.91
0.09	2.07×10^{-9}	65.77	632.90	2.07×10^{-9}	65.77	632.90
0.10	1.89×10^{-8}	62.63	623.30	1.89×10^{-8}	62.63	623.30
0.11	6.90×10^{-7}	57.08	606.41	6.90×10^{-7}	57.08	606.41
0.12	7.11×10^{-6}	53.13	594.70	7.11×10^{-6}	53.13	594.70
0.13	3.70×10^{-5}	50.10	587.21	3.70×10^{-5}	50.10	587.21
0.14	1.27×10^{-4}	47.69	585.01	1.00×10^{-4}	48.04	584.91
0.16	7.00×10^{-4}	44.04	606.93	1.00×10^{-4}	48.04	584.91
0.18	2.30×10^{-3}	41.38	684.29	1.00×10^{-4}	48.04	584.91
0.2	5.10×10^{-3}	39.35	835.25	1.00×10^{-4}	48.04	584.91
0.22	9.50×10^{-3}	37.73	1066.20	1.00×10^{-4}	48.04	584.91
0.23	1.22×10^{-2}	37.04	1210.70	1.00×10^{-4}	48.04	584.91
0.24	1.53×10^{-2}	36.42	1373.30	1.00×10^{-4}	48.04	584.91
0.25	1.87×10^{-2}	35.85	1552.50	1.00×10^{-4}	48.04	584.91
0.26	2.24×10^{-2}	35.32	1746.80	1.00×10^{-4}	48.04	584.91

Table 4.4. Output data for the bridge girder.

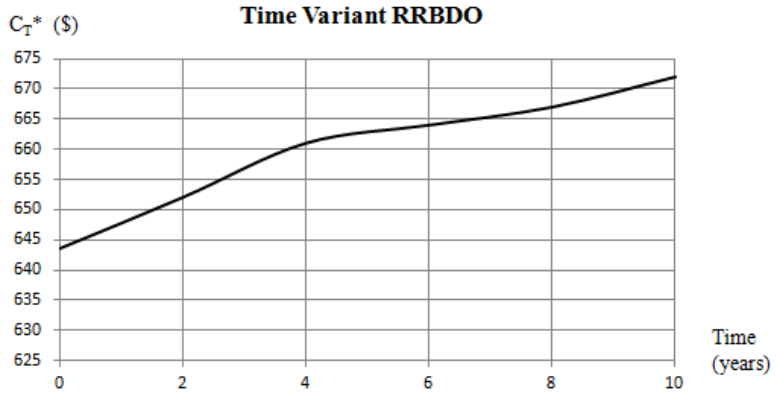

Figure 4.13. Optimal total Costs Ct* versus time for the bridge girder.

Time	RRBDO		RBDO	
years	h^* (m)	A_s^* (cm^2)	h^* (m)	A_s^* (cm^2)
0	0.800	8.556	0.800	9.729
2	0.831	8.155	0.800	9.785
4	0.893	7.446	0.800	9.819
6	0.895	7.515	0.800	10.275
8	0.909	8.806	0.800	10.492
10	0.968	8.056	0.800	10.640

Table 4.5. RRBDO and RBDO solutions versus time- bridge girder example.

4.9.3 Overhanged beam example

This application aims at finding the optimal thicknesses of a reinforced concrete overhanged beam structure with variable depths (fig 4.14), considering the bending due to uniformly distributed load and concentrated end loads. This problem is drawn from Aoues and Chateauneuf (2008).

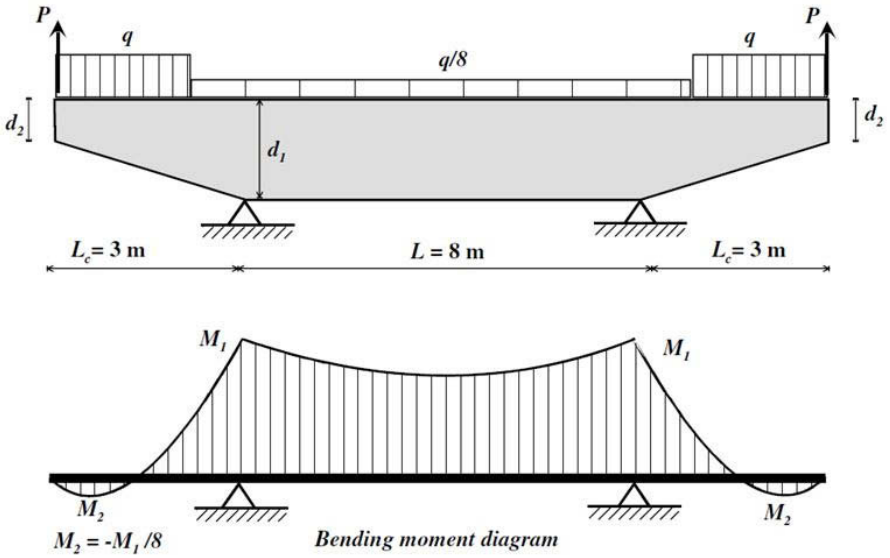

Figure 4.14. Overhanged beam with variable cantilever depth.

Design variables	Deterministic parameters			
Beam depth	**Variable**	**Description**	**Value**	**Unit**
	f_c	concrete compressive strength	25	MPa
	f_y	steel strength	200	MPa
d_1	q	distributed load	40	kN/m
d_2	P	tensile force	30	kN/m
	L_c	cantilever length	3	m
	b	beam width	0.2	m
	L	beam span	8	m

Uncertainties (X)				
Moment	**Mean Value μ**	**Unit**	**Distribution**	**cov**
M_1	90	kNm	Normal	0.2
M_2	11.2	kNm	Normal	0.2

Table 4.6. Input data for the beam.

The beam is defined by the mid-span depth d_1 and the cantilever end depth d_2. In this example, the mid-span and the cantilever are considered as two perfectly correlated components of a system. The span is $L = 8\ m$ and the cantilever length is $L_c = 3\ m$. The beam is subjected to the distributed loads q and $q/8$, as illustrated in Figure 4.13. In order to reduce the negative moments, two tension rods are acting at the cantilever ends, with tensile force P. Table 4.6 summarizes the parameters and distributions of the problem variables. Under nominal conditions, the maximum moments are M_1 = 90 kNm and M_2 = -11.25 kNm.

For a given cross-section, the limit state function is written as:

$$g_i = f_Y\, A_{si} \left(d_i - \frac{f_Y\, A_{si}}{2(0.85 f_{cu} b)}\right) - M_i \tag{4.31}$$

The reinforcement area is chosen as $A_{s1} = 12\ cm^2$ and $A_{s2} = 6\ cm^2$, leading to the following nominal values of the limit state functions:

$$g_1 = 0.24(d_1 - 0.02824) - M_1 \tag{4.32}$$

$$g_2 = 0.12\ (d_2 - 0.01412) - M_2 \tag{4.33}$$

The initial costs C_0 and the failure costs C_f are computed as in the previous example, and the design variables are d_1 and d_2.

As shown in Table 4.7, when applying the RBDO, the constraint $P[g_1 \leq 0] \leq P_{f1}^T$ is not active when it is greater than 6×10^{-3}, which is the value of $P_{f1}(d_1^*)$ for the limit state g_1. Therefore the RBDO optimal solutions for d_1 are constant beyond $P_{f1}(d_1^*)$ as shown in Figure 4.15. The optimal solution found for d_2 through the use of RRBDO and RBDO are the same, because $P_{f2}(d_2^*)$ for the limit state g_2 is not reached by the RBDO constraint P_{f2}^T (which is equal to the RRBDO solution $\mu(P_{f2})$ as explained in section 4.6). Therefore, the initial cost is similar for both optimization procedures until $P_{f1}(d_1^*)$, after which the use of RBDO does not affect d_1 and the use of RRBDO provides solutions that reduce the initial cost by continuously reducing d_1 (Figure 4.16). Since the RBDO does not allow the probability of failure to exceed $P_{f1}(d_1^*) = 6 \times 10^{-3}$, the failure costs using RBDO are also irreducible even when a greater probability of failure is allowed. The proposed formulation is therefore able to decrease the depth where cost is involved (mid-span) without compromising the structural safety of the components, as long as the performance variability limit is respected; d_1 is reduced by 3.7% for an admissible probability of failure of 10^{-2}.

It is interesting to note that (Aoues and Chateauneuf 2008) proposed a scheme for consistent RBDO of structural systems, where the component target safety is adapted in order to fulfill the overall system target. They considered the overhanged beam example to investigate the adaptive target approach. The adaptive target approach reduced d_1 by 4.7% for a reliability index of 1.645. The comparison with this result shows that the proposed RRBDO is able to handle properly the system effect in the structural optimization framework.

	RRBDO				RBDO			
1/λ	$\mu_{P_{f1}}$	$\mu_{P_{f2}}$	d_1*	d_2*	d_1*	d_2*	P_{f1}	P_{f2}
0.1	5.10×10^{-6}	4.45×10^{-5}	0.821	0.201	0.821	0.201	5.10×10^{-6}	4.45×10^{-5}
0.12	8.32×10^{-5}	3.55×10^{-4}	0.759	0.188	0.759	0.188	8.32×10^{-5}	3.55×10^{-4}
0.15	9.00×10^{-4}	2.40×10^{-3}	0.698	0.175	0.697	0.175	9.00×10^{-4}	2.40×10^{-3}
0.17	2.50×10^{-3}	5.80×10^{-3}	0.667	0.168	0.667	0.168	2.50×10^{-3}	5.80×10^{-3}
0.18	3.80×10^{-3}	8.20×10^{-3}	0.654	0.165	0.654	0.165	3.80×10^{-3}	8.20×10^{-3}
0.185	4.50×10^{-3}	9.60×10^{-3}	0.648	0.163	0.649	0.163	4.50×10^{-3}	9.60×10^{-3}
0.2	7.50×10^{-3}	1.48×10^{-2}	0.632	0.159	0.640	0.159	6.00×10^{-3}	1.48×10^{-2}
0.205	8.70×10^{-3}	1.68×10^{-2}	0.626	0.158	0.640	0.158	6.00×10^{-3}	1.68×10^{-2}
0.21	1.00×10^{-2}	1.89×10^{-2}	0.621	0.157	0.640	0.157	6.30×10^{-3}	1.89×10^{-2}
0.215	1.14×10^{-2}	2.12×10^{-2}	0.617	0.156	0.640	0.156	6.30×10^{-3}	2.12×10^{-2}

Table 4.7. Comparison of RBDO and RRBDO results for the beam.

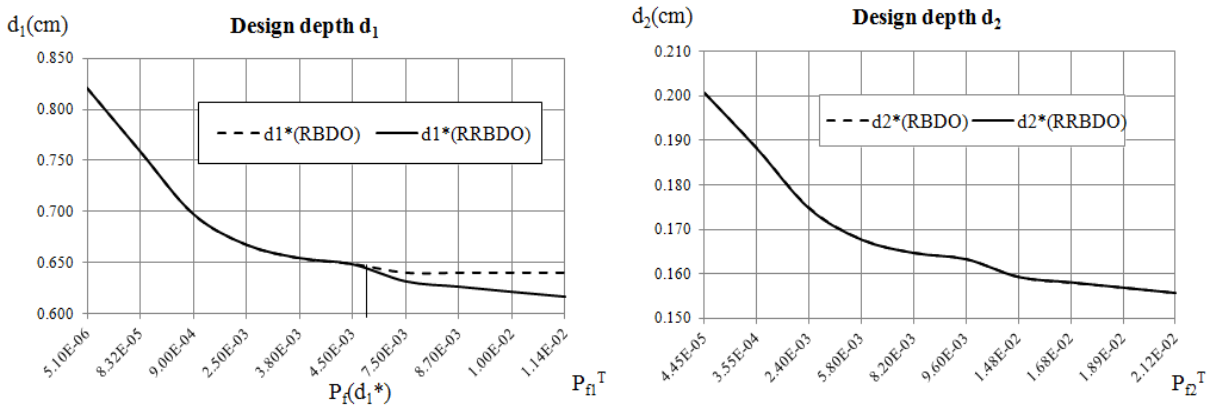

Figure 4.15. Optimal solution z* for the beam.

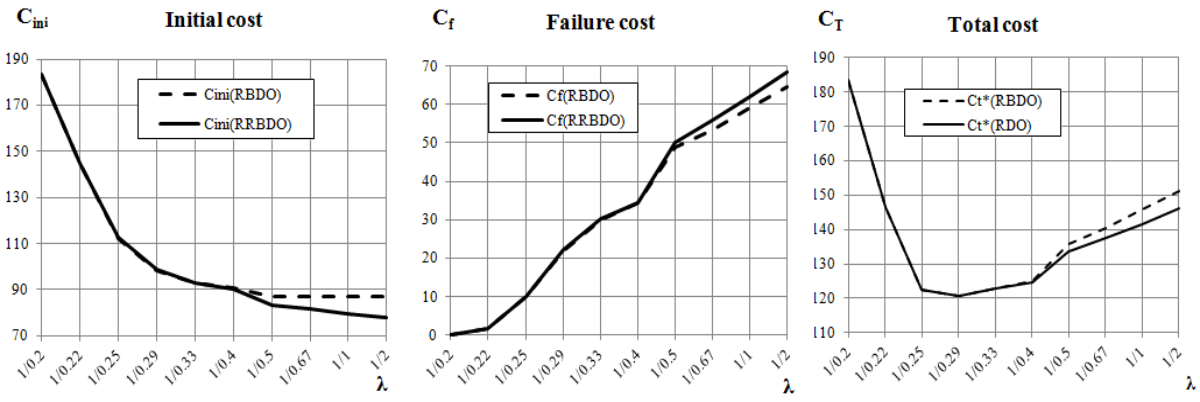

Figure 4.16. Optimal costs for the beam.

4.9.4 Built-up column example

This application aims at finding the optimum width and topology of a steel column formed of U and L cross-sections, subjected to local and global buckling due to axial load. The impact of robust design on the topology of the structure is also observed. This problem is drawn from Beck and Gomes (2012) and is illustrated in Figure 4.17.

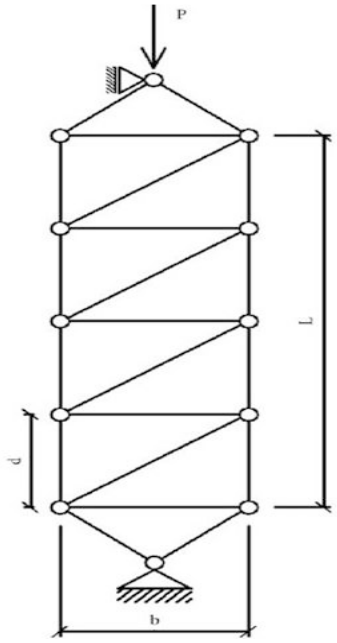

Figure 4.17. Built-up column example.

Design variables		Deterministic parameters			
Symbol	**Description**	**Variable**	**Description**	**Value**	**Unit**
b	(width)	L	length	7	m
N	(number)	λ_L	Local buckling Factor	1.875	
		λ_G	Global buckling factor	1.676	

Uncertainties (X)					
Variable	**Description**	**Mean value μ**	**Unit**	**Distribution**	**cov**
P	load	300	kN	Normal	0.15
E	Elastic modulus	210	GPa	Normal	0.03
f_y	Yield stress	250 MPa	MPa	LogNormal	0.1

Table 4.8. Input data for the built-up column.

The column is made of U-section struts (U200×75×2.65 mm), with L-section braces and battens (L30×2.25mm). The total length is *L* and the column is subject to a load *P*. The Optimization variables are the width *b* and the number of braces and battens ($N = L/d$). The input data are

summarized in Table 4.8. The limit state functions are related to local and global buckling. Local buckling of the U-shaped struts is given by:

$$g_L = \frac{\pi^2 \times E \times I_U}{d^2} - \lambda_L \times \frac{P}{2} \tag{4.34}$$

where I_U is the moment of inertia of the U-section. The global column buckling is given by:

$$g_G = \frac{\pi^2 \times E \times I_G}{L^2} - \lambda_G \times P \tag{4.35}$$

where I_G is the moment of inertia of the column cross-section, given by:

$$I_G = 2\,(I_U + A_U\,\left(\frac{b}{2}\right)^2) \tag{4.36}$$

One unit of braces and battens is considered as one horizontal and one diagonal L-shape. The total length of a brace-batten unit is:

$$L_{bb} = \sqrt{b^2 + \left(\frac{L}{N}\right)^2} + b \tag{4.37}$$

The material cost C_{mat} is:

$$C_{mat} = C_S\,\rho\,(N\,L_{bb}\,A_L + 2\,L\,A_U) \tag{4.38}$$

where C_S is the cost of steel material per unit weight and ρ is the material density. Considering a fixed reference cost of $C_{ref} = 150\,C_S$, the construction cost C_{const} contains a set up cost, a material cost, and a cost due to the number of brace-batten units:

$$C_{const} = C_{ref} + 0.2\,C_{mat} + C_{ref}\,0.025\,(N-1) \tag{4.39}$$

The initial cost is:

$$C_0 = 1.2\,C_{mat} + C_{ref}\,[1 + 0.025\,(N-1)] \tag{4.40}$$

The probabilities of local and global failures are respectively:

$$P_{fG}(X,d) = P_f[g_G(X,d) \le 0] \tag{4.41}$$

$$P_{fL}(X,d) = P_f[g_L(X,d) \le 0] \tag{4.42}$$

The cost of global failure is considered as $C_{SFG}=100C_{ref}$, and the cost of local failure is considered as $C_{SFL}=10C_{ref}$. The total cost takes the form:

$$C_T = C_0 + C_{SFG}\,P_{fG}(X,d) + C_{SFL}\,P_{fL}(X,d) \tag{4.43}$$

The weighting factor α is taken equal to 0.5 in this example, and the same values of the penalty factor λ is used for both limit states.. As shown in Table 4.9, the optimal number of braces and battens increases when the optimization robustness increases (i.e. λ increases), which means that additional members help in improving the structural robustness. The robust design increases the initial cost by increasing the number of members N and the width b, but decreases the failure cost by decreasing the failure probability. The optimum configuration found by the RRBDO has 5 brace-batten units ($N=5$), $b=13.5$ *cm*, a system failure probability of 1.45×10^{-4}, and an optimal cost of 28580 cost units. In addition, it is interesting to note that the RRBDO favors the increase of the number of members over the amplification of the width. Between the two extents of the penalty constraint values, the RRBDO solution increases the number of members by 72% and the member widths by 31% to meet the most stringent penalty function.

It can be concluded from this example that the topology plays a higher role in robustness than the member widths.

$1/\lambda$	N^*	b^* (cm)	μ_{C_T}	μ_{P_f}	cov_{P_f}
0.2	5.5	14.4	28842	1.60×10^{-6}	2.93
0.25	5.2	13.9	28683	2.09×10^{-5}	2.59
0.3	5	13.5	28580	1.45×10^{-4}	2.32
0.5	4.6	13	28711	2.20×10^{-3}	1.91
1	4.1	12.6	31869	2.43×10^{-2}	1.6

Table 4.9. Results of the RRBDO for the column example.

In this example, the RBDO constraint P_f^T is not active beyond $P_f(d^*) = 2.09 \times 10^{-5}$. Therefore, the RBDO optimal solutions for *N* and for the optimal cost are constant after $P_f(d^*)$. Whereas by the use of RRBDO, the parameters *b* and *N* as well the optimal cost continue on decreasing when the constraint λ is loosen, as shown in Table 4.9. Therefore, the RRBDO formulation delivers less costly results while satisfying the performance variability limit and without compromising the targeted safety level. Moreover, it can give solutions that are consistent with all reliability targets. The RRBDO formulation clearly outperforms the RBDO formulation for this example.

4.10 Conclusion

The proposed formulation for robust reliability-based design optimization (RRBDO) considers the total cost of structure and controls the variations in the structural parameters. The reliability-based design optimization (RBDO) is known to be sensitive to the input data and their possible variation, regarding the assumed or initial conditions. Meanwhile, a more robust structure is less likely to fail, which is particularly important for optimized systems, as no additional margin is available. A robust design may increase the mean initial cost by increasing the design variables in order to reduce the variability, leading to decrease the probability of failure. In this scope, the proposed RRBDO is able to find an optimal solution that reduces the variability of the structure.

A comparison between the RBDO and the RRBDO procedures is carried out for the design of two structural concrete and two structural steel problems. It is shown in this study that the proposed RRBDO behaves better than the RBDO for all reliability values, since it provides more robust optimal solutions for high reliability levels, and it continues to perform properly for low reliability levels. The scope of work of the RRBDO is wider than the RBDO and the DDO because more information and better assumptions can be handled by the application of RRBDO.

General conclusion

The objective of this work is to provide comprehensive LCCA and procedures that can be applied to select optimal and robust design and maintenance decisions regarding new and existing structures. The main outputs of the present study are the optimum design and consistent maintenance planning allowing fulfilling the management needs. The proposed methodologies enhance the life-cycle decision-making process and enable the effective budget allocation.

The study employed uncertainty-based optimization techniques to obtain design and maintenance decisions that can minimize the life-cycle cost and maximize the structural performance. Although multiple probabilistic performance indicators exist, the focus has been placed on estimating the structural performance in terms of reliability index. When considering the life-cycle cost components, the state-of-the-art shows large limitations in the stochastic, economic and structural dependencies between structural elements.

A probabilistic design method is considered to meet the need for an integrated and systematic approach to model coherently the deterioration processes, the increasing traffic loads, the aging, and the direct and indirect consequences of failure. An approach to evaluate the user cost and integrate it in the life cycle cost function is proposed. Several traffic disruption scenarios are considered, namely bridge degradation, rehabilitation, load suspension and, in the most extreme case, collapse. A case study in Lebanon is presented, where the model is applied to bridge elements located in various chloride-contaminated environments and subjected to different traffic frequencies. The results show that the optimal design of a reinforced concrete bridge is strongly affected by the degradation models, the different scenarios of user delay costs, the concrete cover and parameters, the failure costs considered in the LCC, and the admissible probability of failure.

The methodology is then extended to the scheduling of the maintenance actions along the life-cycle of structures under time-dependent deteriorating actions by considering economic, structural and stochastic dependencies between structural elements. The approach aims at finding the maintenance schedule of dependent elements which minimizes the total maintenance cost and keeps a targeted reliability level. Stochastic dependency is integrated in the cost function by the mean of conditional probabilities, and a process to quantify the consequences of degradation is proposed. A procedure to calculate the load redistribution to non-failed elements is also proposed and integrated in the cost formulation. The lack of system modeling approaches that take into account the interdependent structural elements motivated us to develop a new system reliability computation as a function of the structure redundancy. The approach also accounts for downtimes needed to dismantle modularly dependent elements, and to repair associated failed elements. The proposed methodology is applied to several numerical examples to prove its validity and functionality. The results show that the economic dependency leads to the grouping of maintenance actions. Moreover, considering the degradation consequences and the stochastic dependencies leads to smaller maintenance time intervals. Also, a mutual consideration of all dependencies leads to the grouping of the maintenance actions, but at smaller time intervals. Hence, neglecting stochastic dependency and degradation costs may lead to unsafe maintenance planning, and neglecting economic dependency may lead to more costly maintenance planning. Furthermore, for high failure probabilities, the economic

dependency has the biggest effect on the maintenance cost, and for low failure probabilities, the stochastic dependency has the biggest effect on the maintenance cost.

The optimization techniques are used in this study to find the optimal design and maintenance decisions. It has been observed that the existing optimization procedures focus either on the robustness of the objective function, or on maintaining a certain level of reliability. In order to address this inconsistency, a new optimization procedure is developed, taking into account the uncertainties in the analysis, and the ability of the structure to adapt to variability and unforeseen actions. It is shown in this work that the proposed formulation behaves better than the existing ones for all required reliability values, since it provides more robust optimal solutions for high reliability levels, and it continues to perform properly for low reliability levels.

The proposed approaches and formulations provide helpful assistance for decision-makers in selecting optimal and robust design and maintenance decisions for civil engineering structures, taking into account uncertainty, variability, interaction between the elements and different direct and indirect consequences of degradation, failure and maintenance.

Perspectives

The developed work has opened several research axes that can be considered for improving the structural design and management system. Many enhancements can be achieved in the future, as follows:

- The proposed design approach considers user costs as an indirect consequence arising from a bridge failure, degradation or maintenance. However, other indirect failure consequences should be included as they may affect the cost estimation, particularly social and environmental aspects.
- In this study, the reliabilities of structural elements are computed with respect to corrosion and fatigue damage. Although they are the major deterioration processes affecting reinforced concrete elements, other degradation processes should be considered, like delamination, spalling, creep, shrinkage etc.... The interaction between degradation scenarios is also an important topic.
- The performance prediction process depends to a great extent on the accuracy of the performance prediction model and the descriptors of its probabilistic parameters. However, in some cases, the accurate information on some model parameters does not exist. Therefore, future efforts to quantify these parameters are crucial. The accurate estimation of the characteristics of these parameters can be achieved by making use of the available structural inspection and monitoring results and will help improve the reliability assessment process of structures.
- The effect of maintenance on the structural performance is generally difficult to quantify, especially when using probabilistic performance indicators. In the maintenance optimization approach presented in this study, the maintenance restores the structural performance to the initial level. However, in real world situations, maintenance can yield other levels of performance restoration. Therefore, further research is needed to establish the relationship between various maintenance types and the associated performance

restoration, on one hand, and to incorporate these maintenance types into the maintenance optimization approaches, on the other hand.

- The solution procedures that were suggested and applied herein in design and maintenance optimization are very computationally expensive, and several approximations were needed to obtain results in reasonable time. The latter was mainly done to overcome the computational burden of several nested optimization loops. Efforts should be made to find more numerically performing solution procedures for the proposed approaches.

References

Ang, A. H., and Tang, W. H. (1984). *Probability concepts in engineering planning and design.* Wiley, New York.

Ang, A. H., and Tang, W. H. (2007). *Probability concepts in engineering: emphasis on applications in civil and environmental engineering.* Hoboken, New Jersey.

Aoues, Y., and Chateauneuf, A. (2010). "Benchmark study of numerical methods for reliability-based design optimization." *Structural and Multidisciplinary Optimization,* 41(2), 277-294.

Aoues, Y., and Chateauneuf, A. (2008). "Reliability-based optimization of structural systems by adaptive target safety–Application to RC frames." *Struct.Saf.,* 30(2), 144-161.

Barlow, R., and Hunter, L. (1960). "Optimum preventive maintenance policies." *Oper.Res.,* 8(1), 90-100.

Barone, G., and Frangopol, D. M. (2014). "Life-cycle maintenance of deteriorating structures by multi-objective optimization involving reliability, risk, availability, hazard and cost." *Struct.Saf.,* 48 40-50.

Bastidas-Arteaga, E., Bressolette, P., Chateauneuf, A., and Sánchez-Silva, M. (2009). "Probabilistic lifetime assessment of RC structures under coupled corrosion–fatigue deterioration processes." *Struct.Saf.,* 31(1), 84-96.

Bastidas-Arteaga, E., Chateauneuf, A., Sánchez-Silva, M., Bressolette, P., and Schoefs, F. (2011). "A comprehensive probabilistic model of chloride ingress in unsaturated concrete." *Eng.Struct.,* 33(3), 720-730.

Bastidas-Arteaga, E., Sánchez-Silva, M., Chateauneuf, A., and Silva, M. R. (2008). "Coupled reliability model of biodeterioration, chloride ingress and cracking for reinforced concrete structures." *Struct.Saf.,* 30(2), 110-129.

Beck, A. T., Gomes, W. J., Lopez, R. H., and Miguel, L. F. (2015). "A comparison between robust and risk-based optimization under uncertainty." *Structural and Multidisciplinary Optimization,* 1-14.

Beck, A. T., and de Santana Gomes, Wellison José. (2012). "A comparison of deterministic, reliability-based and risk-based structural optimization under uncertainty." *Prob.Eng.Mech.,* 28 18-29.

Berthelot, C. F., Sparks, G. A., Blomme, T., Kajner, L., and Nickeson, M. (1996). "Mechanistic-probabilistic vehicle operating cost model." *J.Transp.Eng.,* 122(5), 337-341.

Bezih, K., Chateauneuf, A., Kalla, M., and Bacconnet, C. (2015). "Effect of soil–structure interaction on the reliability of reinforced concrete bridges." *Ain Shams Engineering Journal,* 6(3), 755-766.

Biondini, F., Bontempi, F., Frangopol, D. M., and Malerba, P. G. (2006). "Probabilistic service life assessment and maintenance planning of concrete structures." *J.Struct.Eng.,* 132(5), 810-825.

Biondini, F., Camnasio, E., and Palermo, A. (2014). "Lifetime seismic performance of concrete bridges exposed to corrosion." *Structure and Infrastructure Engineering,* 10(7), 880-900.

Biondini, F., and Frangopol, D. M. (2008). "Probabilistic limit analysis and lifetime prediction of concrete structures." *Structure and Infrastructure Engineering,* 4(5), 399-412.

Casas, J. R., and Chambi, J. L. (2014). "Partial safety factors for CFRP-wrapped bridge piers: Model assessment and calibration." *Composite Structures,* 118 267-283.

Chen, D., and Mahadevan, S. (2008). "Chloride-induced reinforcement corrosion and concrete cracking simulation." *Cement and Concrete Composites,* 30(3), 227-238.

Coronelli, D., and Gambarova, P. (2004). "Structural assessment of corroded reinforced concrete beams: modeling guidelines." *J.Struct.Eng.,* 130(8), 1214-1224.

Das, P. C. (2000). "Reliability based bridge management procedures.Bridge management 4-Inspection, maintenance, assessment and repair". *TRB London*, 1-11.

Das, P. C. (1998). "New developments in bridge management methodology." *Struct.Eng.Int.,* 8(4), 299-302.

Dasgupta, A., and Pecht, M. (1991). "Material failure mechanisms and damage models." *Reliability, IEEE Transactions,* 40(5), 531-536.

De, R. S., Karamchandani, A., and Cornell, C. A. (1989). "Study of redundancy in near-ideal parallel structural systems." *Structural safety and reliability,* ASCE, 975-982.

Deby, F., Carcassès, M., and Sellier, A. (2009). "Probabilistic approach for durability design of reinforced concrete in marine environment." *Cem.Concr.Res.,* 39(5), 466-471.

Derman, C., and Veinott Jr, A. F. (1972). "Constrained Markov decision chains." *Management Science,* 19(4, part-1), 389-390.

Ditlevsen, O. (1979). "Narrow reliability bounds for structural systems." *Journal of Structural Mechanics,* 7(4), 453-472.

Ditlevsen, O., and Madsen, H. O. (1996). *Structural reliability methods.* Wiley, New York .

Dogaki, M., Furuta, H., Tsukiyama, I., and Frangopol, D. M. (2000). "Optimal maintenance planning of reinforced concrete decks on highway network." *Conference Proceedings, US-Japan Workshop on Life-Cycle Cost Analysis and Design of Civil Infrastructure Systems, ASCE, Honolulu, Hawaii*

Doltsinis, I., Kang, Z., and Cheng, G. (2005). "Robust design of non-linear structures using optimization methods." *Comput.Methods Appl.Mech.Eng.,* 194(12), 1779-1795.

Doostparast, M., Kolahan, F., and Doostparast, M. (2014). "A reliability-based approach to optimize preventive maintenance scheduling for coherent systems." *Reliab.Eng.Syst.Saf.,* 126, 98-106.

DOT, N. (2001). "Road User Cost Manual." New Jersey department of transportation.

Echard, B. (2012). *Evaluation Par Krigeage De La Fiabilité Des Structures Sollicitées En Fatigue.*PhD, Blaise Pascal University-Clermont II.

Ehlen, M. A. (1999). "Life-cycle costs of fiber-reinforced-polymer bridge decks." *J.Mater.Civ.Eng.,* 11(3), 224-230.

El Hassan, J., Bressolette, P., Chateauneuf, A., and El Tawil, K. (2010). "Reliability-based assessment of the effect of climatic conditions on the corrosion of RC structures subject to chloride ingress." *Eng.Struct.,* 32(10), 3279-3287.

Ellingwood, B., MacGregor, J. G., Galambos, T. V., and Cornell, C. A. (1982). "Probability based load criteria: load factors and load combinations." *Journal of the Structural Division,* 108(5), 978-997.

Eurocode 1 (2003). " Actions on structures-Part 2: Traffic loads on bridges." CEN- European committee for Standardization, AFNOR, Paris.

Eurocode 2 (2005). " Design of concrete structures-Part 1-1: General rules and rules for buildings." *CEN- European committee for Standardization, AFNOR, Paris.*

FHWA, U. (2011). "Work zone road user costs concepts and applications".Final report, Federal Highway Administration- US departement of transportation.

Flint, M. M., Baker, J. W., and Billington, S. L. (2014). "A modular framework for performance-based durability engineering: From exposure to impacts." *Struct.Saf.,* 50 78-93.

Frangopol, D. M. (1999). "Life-cycle cost analysis for bridges." *Bridge safety and reliability,* ASCE, 210-236.

Frangopol, D. M., and Curley, J. P. (1987). "Effects of damage and redundancy on structural reliability." *J.Struct.Eng.,* 113(7), 1533-1549.

Frangopol, D. M., Kong, J. S., and Gharaibeh, E. S. (2001). "Reliability-based life-cycle management of highway bridges." *J.Comput.Civ.Eng.,* 15(1), 27-34.

Frangopol, D. M., and Maute, K. (2003). "Life-cycle reliability-based optimization of civil and aerospace structures." *Comput.Struct.,* 81(7), 397-410.

Frangopol, D. M., and Soliman, M. (2016). "Life-cycle of structural systems: recent achievements and future directions." *Structure and Infrastructure Engineering,* 12(1), 1-20.

Frangopol, D., Iizuka, M., and Yoshida, K. (1992). "Redundancy measures for design and evaluation of structural systems." *Journal of Offshore Mechanics and Arctic Engineering,* 114(4), 285-290.

Furuta, H., Kameda, T., Nakahara, K., Takahashi, Y., and Frangopol, D. M. (2006). "Optimal bridge maintenance planning using improved multi-objective genetic algorithm." *Structure and Infrastructure Engineering,* 2(1), 33-41.

Gertsbakh, I. (2000). *Reliability theory: with applications to preventive maintenance.* Springer, Science & Business Media. New York. .

Ghosn, M., and Frangopol, D. M. (1999). "Bridge reliability: components and systems." *Bridge safety and reliability,* ASCE, 83-112.

Golmakani, H. R., and Moakedi, H. (2012). "Periodic inspection optimization model for a two-component repairable system with failure interaction." *Comput.Ind.Eng.,* 63(3), 540-545.

Gomes, W. J., Beck, A. T., and Haukaas, T. (2013). "Optimal inspection planning for onshore pipelines subject to external corrosion." *Reliab.Eng.Syst.Saf.,* 118 18-27.

González, A. (2010). *Vehicle-bridge dynamic interaction using finite element modelling.* Sciyo, Croatia.

Gould, E., Parkman, C., and Buckland, T. (2013). "The Economics of Road Maintenance." *RAC Foundation, Adept- Association of Directors of Environment, Economy, Planning and Transport* .

Guedri, M., Cogan, S., and Bouhaddi, N. (2012). "Robustness of structural reliability analyses to epistemic uncertainties." *Mechanical Systems and Signal Processing,* 28 458-469.

Hansen, I. (2001). "Determination and evaluation of traffic congestion costs." *European Journal of Transport and Infrastructure Research EJTIR,* 1,(1),61-72 .

Hasofer, A. M., and Lind, N. C. (1974). "Exact and invariant second-moment code format." *Journal of the Engineering Mechanics Division,* 100(1), 111-121.

Hawk, H., and Small, E. P. (1998). "The BRIDGIT bridge management system." *Struct.Eng.Int.,* 8(4), 309-314.

Hearn, G. (1998). "Condition data and bridge management systems." *Struct.Eng.Int.,* 8(3), 221-225.

Hmaidan, W. M. 2002. National Land transport strategy options for Lebanon. Green Line association. The campaign for sustainable transport report. Ministry of public works and transport, Lebanon.

Huang, Y., and Huang, H. (2012). "A model for concurrent maintenance of bridge elements." *Autom.Constr.,* 21, 74-80.

Hudson, S., Carmichael III, R., Moser, L., Hudson, W., and Wilkes, W. (1987). "Bridge management systems." *NCHRP Report,* (300), project 12-28(2).

IDAL, Invest In Lebanon. 2015. Distribution of Labor force by economic activity. Guardianship Authority. Presidency of the Council of Minister In Accordance With Investment Law No.360.

ILO (1996), International Classification of jobs and professions 3rd ed. known as ISCO-88 - ILO (International Labor Organization). Geneva-22.

Islam, H., Jollands, M., Setunge, S., Haque, N., and Bhuiyan, M. A. (2015). "Life cycle assessment and life cycle cost implications for roofing and floor designs in residential buildings." *Energy Build.,* 104 250-263.

Kagho-Gouadjio, N., Orcesi, A., Cremona, C., and Marcotte, C. (2015). "Quantification of structural robustness: application to the study of a prestressed concrete beam." *Mechanics & Industry,* 16(1), 104.

Kang, Y., and Wen, Y. (2000). "Minimum Life-Cycle Cost Design Criteria Under Multiple Loads." *Session Tc311, Paper PMC2000-146 at the 8th ASCE Specialty Conference on Probabilistic Mechanics and Structural Reliability.*

Kang, Z. (2005). "Robust design optimization of structures under uncertainties." PhD.-Institute of Statics and Dynamics of Aerospace Structures, Stuttgart.

Kari, O. (2011). "8.14 Modelling the durability of concrete for nuclear waste disposal facilities." *KYT2010 Finnish Research Programme on Nuclear Waste Management 2006–2010,* 72.

Kaysi, I., and Salvucci, F. (1993). "Passenger transportation options for a revitalized Beirut. AUB." A Report on Year 1 Activities", AUB/MIT Collaborative Research Program on Science, Technology, and Development.

Kendall, A., Keoleian, G. A., and Helfand, G. E. (2008). "Integrated life-cycle assessment and life-cycle cost analysis model for concrete bridge deck applications." *J Infrastruct Syst,14(3),* 214-222 .

Khodakarami, V., and Abdi, A. (2014). "Project cost risk analysis: A Bayesian networks approach for modeling dependencies between cost items." *Int.J.Project Manage.,* 32(7), 1233-1245.

Kong, J. S., and Frangopol, D. M. (2003). "Life-cycle reliability-based maintenance cost optimization of deteriorating structures with emphasis on bridges." *J.Struct.Eng.,* 129(6), 818-828.

Laggoune, R., Chateauneuf, A., and Aissani, D. (2009). "Opportunistic policy for optimal preventive maintenance of a multi-component system in continuous operating units." *Comput.Chem.Eng.,* 33(9), 1499-1510.

Lai, M., and Chen, Y. (2008). "Optimal replacement period of a two-unit system with failure rate interaction and external shocks." *Int.J.Syst.Sci.,* 39(1), 71-79.

Lauridsen, J., Bjerrum, J., Andersen, N. H., and Lassen, B. (1998). "Creating a bridge management system." *Struct.Eng.Int.,* 8(3), 216-220.

Lee, I., Choi, K., Du, L., and Gorsich, D. (2008). "Dimension reduction method for reliability-based robust design optimization." *Comput.Struct.,* 86(13), 1550-1562.

Lee, K., Cho, H., and Choi, Y. (2004). "Life-cycle cost-effective optimum design of steel bridges." *Journal of Constructional Steel Research,* 60(11), 1585-1613.

Lee, K., and Park, G. (2001). "Robust optimization considering tolerances of design variables." *Comput.Struct.,* 79(1), 77-86.

Liberati, E. A., Nogueira, C. G., Leonel, E. D., and Chateauneuf, A. (2014). "Nonlinear formulation based on FEM, Mazars damage criterion and Fick's law applied to failure assessment of reinforced concrete structures subjected to chloride ingress and reinforcements corrosion." *Eng.Failure Anal.,* 46, 247-268.

Liu, M., and Frangopol, D. M. (2006). "Optimizing bridge network maintenance management under uncertainty with conflicting criteria: Life-cycle maintenance, failure, and user costs." *J.Struct.Eng.,* 132(11), 1835-1845.

Madsen, H., and Krenk, Lind S. (1986)." Methods of Structural Safety." . Englewood Cliff, Dover publications, United States.

Meeker, W. Q., Escobar, L. A., and Lu, C. J. (1998). "Accelerated degradation tests: modeling and analysis." *Technometrics,* 40(2), 89-99.

Mitropoulou, C. C., Lagaros, N. D., and Papadrakakis, M. (2011). "Life-cycle cost assessment of optimally designed reinforced concrete buildings under seismic actions." *Reliab.Eng.Syst.Saf.,* 96(10), 1311-1331.

Mori, Y., and Ellingwood, B. R. (1993). "Reliability-based service-life assessment of aging concrete structures." *J.Struct.Eng.,* 119(5), 1600-1621.

Moses, F. (1999). "Bridge evaluation, bridge safety and reliability." *ASCE, SEI,* 136.

Moses, F., and Ghosn, M. (1985). *A comprehensive study of bridge loads and reliability.* Case Western Reserve University.

Murthy, D., and Nguyen, D. (1985). "Study of a multi-component system with failure interaction." *Eur.J.Oper.Res.,* 21(3), 330-338.

Nicolai, R. P., and Dekker, R. (2008). *Optimal maintenance of multi-component systems: a review.* Springer. Rotterdam.

Nielsen, J. S., and Sørensen, J. D. (2015). "Risk-based decision making for deterioration processes using POMDP." *Proceedings of 12th International Conference on Applications of Statistics and Probability in Civil Engineering. Civil Engineering Risk and Reliability Association*, Vancouver.

Nowak, A. S. (1995). "Calibration of LRFD bridge code." *J.Struct.Eng,* 121(8), 1245-1251.

Nowak, A. S. (1989). "Probabilistic basis for bridge design codes." *Structural Safety and Reliability,* ASCE, 2019-2026.

Orcesi, A. D. (2015). "Gestion des ouvrages d'art sur leur cycle de vie". HDR- Université de Nantes.

Orcesi, A. D., and Cremona, C. F. (2010). "A bridge network maintenance framework for Pareto optimization of stakeholders/users costs." *Reliab.Eng.Syst.Saf.,* 95(11), 1230-1243.

Orcesi, A. D., and Frangopol, D. M. (2011). "Optimization of bridge maintenance strategies based on structural health monitoring information." *Struct.Saf.,* 33(1), 26-41.

Orcesi, A. D., Frangopol, D. M., and Kim, S. (2010). "Optimization of bridge maintenance strategies based on multiple limit states and monitoring." *Eng.Struct.,* 32(3), 627-640.

Parks, J. (2001). "On stochastic optimization: Taguchi Methods™ demystified; its limitations and fallacy clarified." *Prob.Eng.Mech.,* 16(1), 87-101.

Pendola, M. (2000). *Fiabilité Des Structures En Contexte D'Incertitudes Statistiques Et D'Écarts De Modélisation.* PhD- Blaise Pascal University.

Pendola, M., Mohamed, A., Lemaire, M., and Hornet, P. (2000). "Combination of finite element and reliability methods in nonlinear fracture mechanics." *Reliab.Eng.Syst.Saf.,* 70(1), 15-27.

Rackwitz, R., Lentz, A., and Faber, M. (2005). "Socio-economically sustainable civil engineering infrastructures by optimization." *Struct.Saf.,* 27(3), 187-229.

Radner, R., and Jorgenson, D. W. (1962). *Optimal replacement and inspection of stochastically failing equipment.* Stanford University Press, Stanford, California.

Rathod, V., Yadav, O. P., Rathore, A., and Jain, R. (2013). "Optimizing reliability-based robust design model using multi-objective genetic algorithm." *Comput.Ind.Eng.,* 66(2), 301-310.

Rizzuti, S., De Napoli, L., Giampà, F., and Lofranco, F. (2009). "Axiomatic design as a means to find contradiction in an integrated approach for product design." *Fifth International Conference on Axiomatic Design, ICAD,* 25-27.

Rocha, M., and Brühwiler, E. (2012). "Prediction of fatigue life of reinforced concrete bridges using Fracture Mechanics." *Proceedings bridge maintenance, safety, management, resilience and sustainability,* CRC Press/Balkema, 3755-3761.

Saad, L., Aissani, A., Chateauneuf, A., and Raphael, W. (2016). "Reliability-based optimization of direct and indirect LCC of RC bridge elements under coupled fatigue-corrosion deterioration processes." *Eng.Failure Anal.* 58, 570-587

Saad, L., Aissani, A., Chateauneuf, A., and Raphael, W. (2013). "Life-cycle cost optimization of reinforced concrete structures under coupled fatigue-corrosion deterioration". Icossar Conference, New York.

Sabatino, S., Frangopol, D. M., and Dong, Y. (2015a). "Life cycle utility-informed maintenance planning based on lifetime functions: optimum balancing of cost, failure consequences and performance benefit." *Structure and Infrastructure Engineering*, 1-18.

Sabatino, S., Frangopol, D. M., and Dong, Y. (2015b). "Sustainability-informed maintenance optimization of highway bridges considering multi-attribute utility and risk attitude." *Eng.Struct.,* 102 310-321.

Sadasivam, S., and Mallela, J. (2015). "Application of work zone road user costs in determining schedule related incentives and disincentives- A conceptual 2 Framework 3" *Transportation Research Board 94th Annual Meeting. No. 15-6037*.

Sahraoui, Y., Khelif, R., and Chateauneuf, A. (2013). "Maintenance planning under imperfect inspections of corroded pipelines." *Int.J.Pressure Vessels Piping,* 104 76-82.

Sandgren, E., and Cameron, T. (2002). "Robust design optimization of structures through consideration of variation." *Comput.Struct.,* 80(20), 1605-1613.

Sasieni, M. W. (1956). "A Markov chain process in industrial replacement." *OR,* 7(4), 148-155.

Saydam, D., and Frangopol, D. M. (2011). "Time-dependent performance indicators of damaged bridge superstructures." *Eng.Struct.,* 33(9), 2458-2471.

Schrank, D., and Lomax, T. (2003). "The 2003 annual urban mobility report." *Texas Transportation Institute, the Texas A&M University System*.

Shahraki, A. F., and Noorossana, R. (2014). "Reliability-based robust design optimization: A general methodology using genetic algorithm." *Comput.Ind.Eng.,* 74 199-207.

Singh, D., and Tiong, R. L. (2005). "Development of life cycle costing framework for highway bridges in Myanmar." *Int.J.Project Manage.,* 23(1), 37-44.

Söderqvist, M., and Veijola, M. (1998). "The Finnish bridge management system." *Struct.Eng.Int.,* 8(4), 315-319.

Soliman, M. (2015). "Life-Cycle Management of Civil and Marine Structures under Fatigue and Corrosion Effects." PhD-Lehigh University.

Spence, S. M., Gioffrè, M., and Kareem, A. (2015). "An efficient framework for the reliability-based design optimization of large-scale uncertain and stochastic linear systems." *Prob.Eng.Mech*.

Stewart, M. G. (2004). "Spatial variability of pitting corrosion and its influence on structural fragility and reliability of RC beams in flexure." *Struct.Saf.,* 26(4), 453-470.

Stewart, M. G., and Al-Harthy, A. (2008). "Pitting corrosion and structural reliability of corroding RC structures: Experimental data and probabilistic analysis." *Reliab.Eng.Syst.Saf.,* 93(3), 373-382.

Sundaresan, S., Ishii, K., and Houser, D. R. (1995). "A robust optimization procedure with variations on design variables and constraints." *Engineering Optimization A35,* 24(2), 101-117.

Taguchi, G., and Rafanelli, A. J. (1994). *Taguchi on Robust Technology Development: Bringing Quality Engineering Upstream*.

Tamaki, H., Mukai, T., Kawakami, K., and Araki, M. (1998). "Genetic algorithm approach to multi-objective scheduling problem in plastics forming plant." *Advances in Production Management Systems,* Springer, 435-444.

Taylor, H. M. (1975). "Optimal replacement under additive damage and other failure models." *Naval Research Logistics Quarterly,* 22(1), 1-18.

Thoft-Christensen, P. (1998). "Assessment of the reliability profiles for concrete bridges." *Eng.Struct.,* 20(11), 1004-1009.

Thomas, L. (1986). "A survey of maintenance and replacement models for maintainability and reliability of multi-item systems." *Reliability Engineering,* 16(4), 297-309.

Thompson, P., and Shepard, R. (1994). "Pontis." *Transportation Research Circular* (423).

Tighe, S., Lee, T., McKim, R., and Haas, R. (1999). "Traffic delay cost savings associated with trenchless technology." *J Infrastruct Syst,* 5(2), 45-51.

Tovo, R. (2001). "On the fatigue reliability evaluation of structural components under service loading." *Int.J.Fatigue,* 23(7), 587-598.

Tsompanakis, Yannis, Nikos D. Lagaros, and Manolis Papadrakakis, (2008) eds. Structural Design Optimization Considering Uncertainties: Structures & Infrastructures Book, Vol. 1, Series, Series Editor: Dan M. Frangopol. CRC Press.

Val, D. V., and Melchers, R. E. (1997). "Reliability of deteriorating RC slab bridges." *J.Struct.Eng.,* 123(12), 1638-1644.

Val, D. V., and Stewart, M. G. (2003). "Life-cycle cost analysis of reinforced concrete structures in marine environments." *Struct.Saf.,* 25(4), 343-362.

Val, D. V., Stewart, M. G., and Melchers, R. E. (1998). "Effect of reinforcement corrosion on reliability of highway bridges." *Eng.Struct.,* 20(11), 1010-1019.

Van Belle, G. (2011). *Statistical rules of thumb.* John Wiley & Sons.

Van Horenbeek, A., and Pintelon, L. (2013). "A dynamic predictive maintenance policy for complex multi-component systems." *Reliab.Eng.Syst.Saf.,* 120 39-50.

van Noortwijk, J. M., and Frangopol, D. M. (2004). "Two probabilistic life-cycle maintenance models for deteriorating civil infrastructures." *Prob.Eng.Mech.,* 19(4), 345-359.

Vidal, T., Castel, A., and Francois, R. (2004). "Analyzing crack width to predict corrosion in reinforced concrete." *Cem.Concr.Res.,* 34(1), 165-174.

Vu, H. C., Do, P., Barros, A., and Bérenguer, C. (2014). "Maintenance grouping strategy for multi-component systems with dynamic contexts." *Reliab.Eng.Syst.Saf.,* 132 233-249.

Vu, K. A. T., and Stewart, M. G. (2000). "Structural reliability of concrete bridges including improved chloride-induced corrosion models." *Struct.Saf.,* 22(4), 313-333.

Vu, K., Stewart, M. G., and Mullard, J. (2005). "Corrosion-induced cracking: experimental data and predictive models." *ACI Struct.J.,* 102(5), 719.

Wang, R., Ma, L., Yan, C., and Mathew, J. (2012). "Condition deterioration prediction of bridge elements using Dynamic Bayesian Networks (DBNs)." *Quality, Reliability, Risk, Maintenance, and Safety Engineering (ICQR2MSE), 2012 International Conference on,* IEEE, 566-571.

Woodward, D. G. (1997). "Life cycle costing—theory, information acquisition and application." *Int.J.Project Manage.,* 15(6), 335-344.

Yang, S., Frangopol, D. M., and Neves, L. C. (2004). "Service life prediction of structural systems using lifetime functions with emphasis on bridges." *Reliab.Eng.Syst.Saf.,* 86(1), 39-51.

Youn, B. D., Choi, K. K., and Yi, K. (2005). "Performance moment integration (PMI) method for quality assessment in reliability-based robust design optimization." *Mechanics Based Design of Structures and Machines,* 33(2), 185-213.

Yu, W., and Lo, S. (2005). "Time-dependent construction social costs model." *Constr.Manage.Econ.,* 23(3), 327-337.

Appendixes

Appendix 1: Uniform corrosion degradation model

Uniform corrosion consists of approximately uniform loss of metal over the whole exposed surface of a reinforcing bar, as shown in Figure A.1.

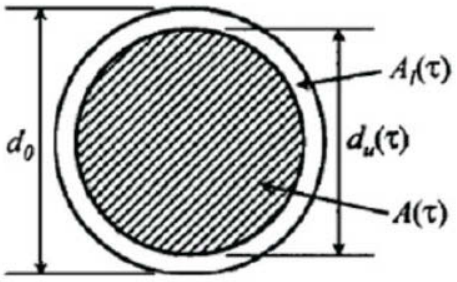

Figure A.1: Uniform Corrosion.

In this case, Faraday's law indicates that a corrosion current density of $i_{corr} = 1\ \mu A cm^{-2}$ corresponds to a uniform corrosion penetration of 11.6 $\mu m year^{-1}$. Thus, the reduction of the diameter of a corroding bar, Δd, at time T, can be estimated directly (in mm) from i_{corr} as:

$$\Delta d(T) = 0.0232 \int_{\tau_{ini}}^{T} i_{corr}(t)\ dt \tag{A.1}$$

where τ_{ini} is the time to corrosion initiation estimated by using the classical solution of Fick's law:

$$\tau_{ini} = \frac{e^2}{4\,D_c}\left[\text{erf}^{-1}\left(1 - \frac{C_{th}}{C_s}\right)\right]^{-2} \tag{A.2}$$

where *c* is the concrete cover, D_c is the coefficient of diffusion, and C_{th} and C_s are respectively the threshold and surface chloride concentrations. The corrosion ratio is calculated using the following empirical expression:

$$i_{corr} = \frac{37.8(1-wc)^{-1.64}}{c} \tag{A.3}$$

where *wc* is the water/cement ratio and *c* is the concrete cover. The net cross-sectional area of a reinforcing bar, A_{pit}, at time t, is then equal to:

$$A_{pit}(t) = \begin{cases} \frac{\pi d_0^2}{4}, for\ t \le \tau_{ini} \\ \frac{\pi[d_0 - \Delta d(T)]^2}{4}, for\ t > \tau_{ini} \end{cases} \tag{A.4}$$

where d_0 is the initial diameter of the reinforcing bar (in mm).

Appendix 2: Coupled corrosion fatigue degradation model

Time-dependent structural deterioration processes, such as corrosion and fatigue lead to continuous aging of bridge structures. Corrosion is the main cause of damage in reinforced

concrete structures (Deby et al. 2009). Severe cracking of concrete cover may be caused by corrosion in aggressive environment. Also, a reinforced concrete bridge may experience up to 7×10^8 stress cycles during the course of its lifespan (Rocha and Brühwiler 2012). It is thus important to be able to assess the corrosion and fatigue performance of such structures.

A.2.1 Rate Competition criteria

Improved corrosion models were developed by (Vu and Stewart 2000; Val and Stewart 2003) in the aim of calculating the failure probabilities, based on which (Bastidas-Arteaga et al. 2008) presented a model of *RC* deterioration due to corrosion and fatigue. Bastidas' model computes the reduction of the area of steel reinforcement in order to assess the change of structural capacity with time. A coupled corrosion-fatigue deterioration process is basically divided into three stages (Bastidas-Arteaga et al. 2009): the first stage is the corrosion initiation and pit nucleation τ_{cp}, the second is the pit-to-crack transition τ_{pt}, and the third is the fatigue crack growth τ_{cg}.

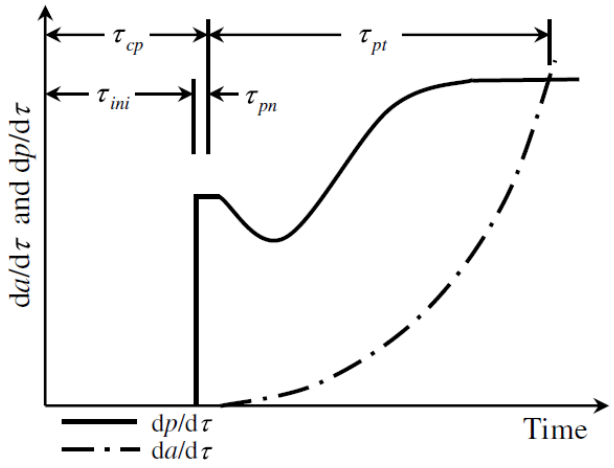

Timespan and depths

Figure A.2: Rate Competition criteria - (Bastidas-Arteaga et al. 2009; Val and Stewart 2003).

A.2.2 Reduction of steel cross-section

The reduction of the reinforcement steel cross-section which is caused by the coupled effect of corrosion and fatigue starts after the time to corrosion initiation τ_{ini} estimated by using the classical solution of Fick's law as in equation A.2. Fick's law considers that the penetration of chlorides in concrete is only controlled by the diffusion process, and that concrete is a homogeneous, isotropic and inert material. Moreover, equation 3.24 assumes that the coefficient of diffusion is independent of time, the chloride concentration and the location. In fact, Fick's law is not fully appropriate because concrete is not homogeneous and not saturated media, the coefficient of diffusion changes with time and chloride ions penetrate in concrete not only by diffusion. However, Fick's law is often used because of its simplicity. Moreover, in many cases the diffusion equation provides good approximation to laboratory or field data (Nogeuira and Leonel 2013).

The time-to-pit nucleation is given by Stewart (2004) as:

$$\tau_{pn} = \frac{2.281\ \mathrm{cp0}}{\alpha}\ (1 - \mathrm{wc})^{1.64} \qquad \text{(A.5)}$$

The reduction of the steel cross-section is estimated by considering pitting corrosion from τ_{ini} to τ_{pt}. The pit depth can be computed as follows (Melchers 1997, Stewart 2004):

$$p(t) = 0.0116\ \alpha \int_{t_{ini}}^{t} i_{corr}(t)dt \tag{A.6}$$

where α is the ratio between pitting and uniform corrosion depths, and $i_{corr}(t)$ is the time-variant corrosion rate. For simplicity, a spherical form of pits is assumed. The pit configuration shown in Figure A.3 is used to predict the cross-sectional area of the pit A_{pit}, as follows:

$$A_{pit}(t) = \begin{cases} A_1 + A_2, & \text{for } p(t) \le \frac{d_0}{\sqrt{2}} \\ \frac{\pi d_0^2}{4} - A_1 + A_2, & \text{for } \frac{d_0}{\sqrt{2}} < p(t) < d_0 \\ \frac{\pi {d_0}^2}{4}, & \text{for } p(t) > d_0 \end{cases}$$

with

$$A_1 = 0.5\ [\theta_1 \left(\frac{d_0}{2}\right)^2 - b_p \left|\frac{d_0}{2} - \frac{p(t)^2}{d_0}\right|]$$

$$A_2 = 0.5\ [\theta_2 p(t)^2 - b_p \frac{p(t)^2}{d_0}]$$

$$\theta_1 = 2\ \arcsin\left(\frac{b_p}{d_0}\right)$$

$$\theta_2 = 2\ \arcsin\left(\frac{b_p}{2p(t)}\right)$$

$$b_p = 2p(t)\sqrt{1 - \left(\frac{p(t)}{d_0}\right)^2} \tag{A.7}$$

where d_0 is the diameter of the intact reinforcement bar.

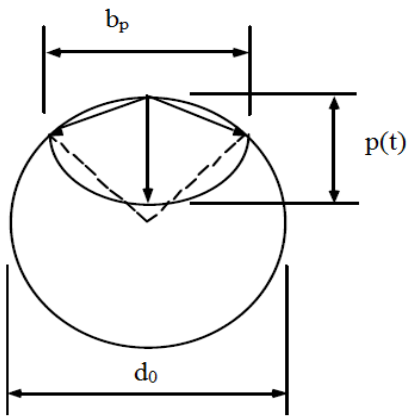

Figure A.3 : Pit configuration (Stewart 2004).

The remaining area of the steel cross-section becomes:

$$A_p^{st}(t) = n\ \pi\ \frac{{d_0}^2}{4} - A_{pit}(t) \tag{A.8}$$

where n is the number of steel bars.

During the period corresponding to the initial corrosion age, the corrosion rate i_{ini} is estimated on the basis of empirical results as (Vu & Stewart 2000):

$$\mathrm{i_{ini}}(\tau) = \begin{cases} \frac{37.8\left(1-\frac{\mathrm{E}}{\mathrm{C}}\right)^{-1.64}}{\mathrm{e}}, & \text{for } \tau_{\mathrm{ini}} + 1 \geq \tau > \tau_{\mathrm{ini}} \\ \frac{32.13\left(1-\frac{\mathrm{E}}{\mathrm{C}}\right)^{-1.64}}{\mathrm{e}}(\tau - \tau_{\mathrm{ini}})^{-0.3}, & \text{for } \tau > \tau_{\mathrm{ini}} + 1 \end{cases} \quad \text{(A.9)}$$

where τ is the time in years and *wc* is the water/cement ratio. During the period corresponding to the active corrosion age, the time-variant corrosion rate considering concrete cracking and environmental aggressiveness takes the following form (Bastidas et. al 2008)):

$$i_{corr}(\tau) = \frac{\mu_{ini}(\tau)\, i_{ini}(\tau) + \mu_{ac}(\tau)\, i_{th}(\tau)}{\mu_{ini}(\tau) + \mu_{ac}(\tau)} \quad \text{(A.10)}$$

and

$$\mu_{\mathrm{age}}(\tau, \mathrm{a}, \mathrm{b}) = \frac{1}{1+\exp^{-\mathrm{a}(\tau-\mathrm{b})}} \quad \text{(A.11)}$$

where i_{th} is the threshold corrosion rate, μ_{ini} and μ_{ac} are the initial and active membership functions respectively, *a* and *b* are constants that define the function shape, drawn from Bastidas et al. (2008). After the pit-to-crack transition, the new crack size is calculated by integrating the fatigue crack growth rate using Paris law (1961):

$$\frac{\mathrm{da}}{\mathrm{dN}} = \begin{cases} 3.83 \times 10^{-29}(\Delta \mathrm{K})^{20.863}, & \text{if } \Delta \mathrm{K} \leq 9\mathrm{MPa}\sqrt{\mathrm{m}} \\ 3.16 \times 10^{-12}(\Delta \mathrm{K})^{3.143}, & \text{otherwise} \end{cases} \quad \text{(A.12)}$$

where ΔK is the stress intensity factor range. The time of pit-to-crack transition τ_{pt} is reached when equating the pit growth rate with the equivalent crack growth rate: $\frac{dp}{dt} = \frac{da}{dt}$.

After the pit-to-crack transition, the new crack size is calculated by integrating the fatigue crack growth rate with the initial condition $a(\tau_{pt}) = p(\tau_{pt})$. The fatigue life corresponding to the crack growth, τ_{cg} is reached when the crack size induces the RC cross-section failure.

$$\tau_{\mathrm{cg}} = \begin{cases} \frac{1}{\mathrm{f}}\left(\int_{\mathrm{a0}}^{\mathrm{a1}} \frac{\mathrm{da}}{3.83\times10^{-29}(\Delta \mathrm{K})^{20.863}} + \int_{\mathrm{a1}}^{\mathrm{ac}} \frac{\mathrm{da}}{3.16\times10^{-12}(\Delta \mathrm{K})^{3.143}}\right), & \text{for a0} < a1 \\ \int_{\mathrm{a0}}^{\mathrm{ac}} \frac{\mathrm{da}}{3.16\times10^{-12}(\Delta \mathrm{K})^{3.143}}, & \text{otherwise} \end{cases} \quad \text{(A.13)}$$

where a_0 is the pit depth at the time of transition from pit to crack τ_{pt}, a_1 is the crack size at the critical stress intensity factor estimated by $9MPa\sqrt{m}$ (Salah el Din and Lovegrove 1982), *m* is a material constant and a_c is the critical crack or pit size corresponding to structural failure.

In the above model, it is assumed that the mechanical properties of reinforcing steel such as the modulus of elasticity, the yield stress and ultimate tensile strength, are unaffected by corrosion; this assumption corresponds to available experimental data (Val et. al 1998). Moreover, perfect bond is assumed between concrete and steel.

The resisting bending moment is calculated by:

$$M_r = A_{s0}(1 - 0.4\,\alpha)\, d\, f_y$$

with $A_{s0} = n\,\pi\,\frac{{d_0}^2}{4}$ *for* $t \le \tau_{ini}$

$A_{s0} = n\,\pi\,\frac{{d_0}^2}{4} - A_{pit}(t)$ *for* $t > \tau_{ini}$ (A.14)

where $A_{pit}(t)$ is calculated using the pit depth at time t for $t \in [\tau_{ini}, \tau_{pt}]$.

After the pit-to-crack transition time τ_{pt}, the crack size is calculated by integrating the fatigue crack growth rate.

Appendix 3: Polynomial regression of the failure probabilities obtained by FORM

The following Table shows the results of the first order reliability method applied to the elements of the bridge superstructure example treated in chapter 3. The failure probability is calculated for the 6 beams by considering different reinforcement areas. The probability of failure is obtained for each beam, which degrades with time due to corrosion. Also, the conditional probability $P_{i|j}(t)$ is computed for each beam, which is the probability of failure of the beam b_i knowing that b_j has failed.

n	8	8	8	8	8
α_i*$inc_{i/j}$	0.304	0.247	0.228	0.209	0.19
t/i	$P_{2/1}$	$P_{1/2}$	$P_{2/3}$	$P_{2/4}$	P_1 & P_2
1	1.000	1.644×10^{-1}	1.785×10^{-2}	4.524×10^{-4}	1.667×10^{-6}
2	1.000	1.644×10^{-1}	1.785×10^{-2}	4.524×10^{-4}	1.667×10^{-6}
3	1.000	1.644×10^{-1}	1.785×10^{-2}	4.524×10^{-4}	1.667×10^{-6}
4	1.000	1.644×10^{-1}	1.785×10^{-2}	4.524×10^{-4}	1.667×10^{-6}
5	1.000	1.644×10^{-1}	1.785×10^{-2}	4.524×10^{-4}	1.667×10^{-6}
6	1.000	1.644×10^{-1}	1.785×10^{-2}	4.524×10^{-4}	1.667×10^{-6}
7	1.000	1.644×10^{-1}	1.785×10^{-2}	4.524×10^{-4}	1.667×10^{-6}
8	1.000	1.644×10^{-1}	1.785×10^{-2}	4.524×10^{-4}	1.667×10^{-6}
9	1.000	2.210×10^{-1}	2.922×10^{-2}	9.347×10^{-4}	4.489×10^{-6}
10	1.000	2.311×10^{-1}	3.154×10^{-2}	1.048×10^{-3}	5.258×10^{-6}
11	1.000	2.407×10^{-1}	3.383×10^{-2}	1.164×10^{-3}	6.077×10^{-6}
12	1.000	2.498×10^{-1}	3.609×10^{-2}	1.283×10^{-3}	6.956×10^{-6}
13	1.000	2.587×10^{-1}	3.835×10^{-2}	1.407×10^{-3}	7.903×10^{-6}
14	1.000	2.674×10^{-1}	4.062×10^{-2}	1.535×10^{-3}	8.922×10^{-6}
15	1.000	2.759×10^{-1}	4.291×10^{-2}	1.668×10^{-3}	1.002×10^{-5}
16	1.000	2.842×10^{-1}	4.523×10^{-2}	1.807×10^{-3}	1.121×10^{-5}
17	1.000	2.924×10^{-1}	4.756×10^{-2}	1.952×10^{-3}	1.248×10^{-5}
18	1.000	3.005×10^{-1}	4.993×10^{-2}	2.103×10^{-3}	1.386×10^{-5}
19	1.000	3.084×10^{-1}	5.233×10^{-2}	2.260×10^{-3}	1.533×10^{-5}
20	1.000	3.163×10^{-1}	5.477×10^{-2}	2.424×10^{-3}	1.692×10^{-5}
21	1.000	3.241×10^{-1}	5.723×10^{-2}	2.595×10^{-3}	1.863×10^{-5}
22	1.000	3.318×10^{-1}	5.974×10^{-2}	2.774×10^{-3}	2.046×10^{-5}
23	1.000	3.395×10^{-1}	6.228×10^{-2}	2.959×10^{-3}	2.242×10^{-5}
24	1.000	3.470×10^{-1}	6.486×10^{-2}	3.153×10^{-3}	2.453×10^{-5}
25	1.000	3.546×10^{-1}	6.748×10^{-2}	3.354×10^{-3}	2.678×10^{-5}
26	1.000	3.620×10^{-1}	7.014×10^{-2}	3.564×10^{-3}	2.918×10^{-5}
27	1.000	3.694×10^{-1}	7.284×10^{-2}	3.782×10^{-3}	3.175×10^{-5}
28	1.000	3.768×10^{-1}	7.558×10^{-2}	4.008×10^{-3}	3.450×10^{-5}
29	1.000	3.841×10^{-1}	7.836×10^{-2}	4.244×10^{-3}	3.743×10^{-5}
30	1.000	3.913×10^{-1}	8.118×10^{-2}	4.488×10^{-3}	4.055×10^{-5}
31	1.000	3.985×10^{-1}	8.404×10^{-2}	4.742×10^{-3}	4.388×10^{-5}
32	1.000	4.057×10^{-1}	8.694×10^{-2}	5.006×10^{-3}	4.742×10^{-5}
33	1.000	4.128×10^{-1}	8.989×10^{-2}	5.279×10^{-3}	5.118×10^{-5}
34	1.000	4.199×10^{-1}	9.287×10^{-2}	5.563×10^{-3}	5.518×10^{-5}

35	1.000	4.269×10^{-1}	9.590×10^{-2}	5.857×10^{-3}	5.944×10^{-5}
36	1.000	4.339×10^{-1}	9.897×10^{-2}	6.161×10^{-3}	6.395×10^{-5}
37	1.000	4.408×10^{-1}	1.021×10^{-1}	6.477×10^{-3}	6.874×10^{-5}
38	1.000	4.477×10^{-1}	1.052×10^{-1}	6.804×10^{-3}	7.381×10^{-5}
39	1.000	4.545×10^{-1}	1.084×10^{-1}	7.142×10^{-3}	7.919×10^{-5}
40	1.000	4.613×10^{-1}	1.117×10^{-1}	7.491×10^{-3}	8.488×10^{-5}
41	1.000	4.680×10^{-1}	1.149×10^{-1}	7.853×10^{-3}	9.091×10^{-5}
42	1.000	4.748×10^{-1}	1.182×10^{-1}	8.227×10^{-3}	9.728×10^{-5}
43	1.000	4.814×10^{-1}	1.216×10^{-1}	8.613×10^{-3}	1.040×10^{-4}
44	1.000	4.880×10^{-1}	1.250×10^{-1}	9.013×10^{-3}	1.111×10^{-4}
45	1.000	4.946×10^{-1}	1.284×10^{-1}	9.425×10^{-3}	1.187×10^{-4}
46	1.000	4.989×10^{-1}	1.319×10^{-1}	9.850×10^{-3}	1.266×10^{-4}
47	1.000	4.924×10^{-1}	1.354×10^{-1}	1.029×10^{-2}	1.350×10^{-4}
48	1.000	4.860×10^{-1}	1.390×10^{-1}	1.074×10^{-2}	1.438×10^{-4}
49	1.000	4.796×10^{-1}	1.426×10^{-1}	1.121×10^{-2}	1.531×10^{-4}
50	1.000	4.733×10^{-1}	1.462×10^{-1}	1.169×10^{-2}	1.629×10^{-4}

Table A.1: Conditional probability data obtained by FORM for 50 years, for for $P_{1/2}$, $P_{2/3}$, $P_{2/4}$, P_1 and P_2.

n	7	7	7	7
$\alpha_i*inc_{i/j}$	0.208	0.192	0.176	0.16
t/i	$P_{3/1}$	$P_{3/4}$	$P_{3/5}$	P_3
1	4.876×10^{-2}	2.815×10^{-3}	3.526×10^{-5}	6.021×10^{-8}
2	4.876×10^{-2}	2.815×10^{-3}	3.526×10^{-5}	6.021×10^{-8}
3	4.876×10^{-2}	2.815×10^{-3}	3.526×10^{-5}	6.021×10^{-8}
4	4.876×10^{-2}	2.815×10^{-3}	3.526×10^{-5}	6.021×10^{-8}
5	4.876×10^{-2}	2.815×10^{-3}	3.526×10^{-5}	6.021×10^{-8}
6	4.876×10^{-2}	2.815×10^{-3}	3.526×10^{-5}	6.021×10^{-8}
7	4.876×10^{-2}	2.815×10^{-3}	3.526×10^{-5}	6.021×10^{-8}
8	4.876×10^{-2}	2.815×10^{-3}	3.526×10^{-5}	6.021×10^{-8}
9	7.359×10^{-2}	5.222×10^{-3}	8.282×10^{-5}	1.845×10^{-7}
10	7.843×10^{-2}	5.756×10^{-3}	9.489×10^{-5}	2.208×10^{-7}
11	8.311×10^{-2}	6.291×10^{-3}	1.075×10^{-4}	2.604×10^{-7}
12	8.770×10^{-2}	6.833×10^{-3}	1.207×10^{-4}	3.037×10^{-7}
13	9.222×10^{-2}	7.385×10^{-3}	1.347×10^{-4}	3.513×10^{-7}
14	9.671×10^{-2}	7.950×10^{-3}	1.494×10^{-4}	4.034×10^{-7}
15	1.010×10^{-1}	8.529×10^{-3}	1.651×10^{-4}	4.607×10^{-7}
16	1.060×10^{-1}	9.125×10^{-3}	1.817×10^{-4}	5.234×10^{-7}
17	1.100×10^{-1}	9.737×10^{-3}	1.992×10^{-4}	5.920×10^{-7}
18	1.150×10^{-1}	1.037×10^{-2}	2.178×10^{-4}	6.671×10^{-7}
19	1.190×10^{-1}	1.102×10^{-2}	2.375×10^{-4}	7.492×10^{-7}
20	1.240×10^{-1}	1.168×10^{-2}	2.584×10^{-4}	8.387×10^{-7}
21	1.280×10^{-1}	1.237×10^{-2}	2.804×10^{-4}	9.363×10^{-7}
22	1.330×10^{-1}	1.308×10^{-2}	3.037×10^{-4}	1.042×10^{-6}
23	1.370×10^{-1}	1.381×10^{-2}	3.284×10^{-4}	1.158×10^{-6}
24	1.420×10^{-1}	1.456×10^{-2}	3.544×10^{-4}	1.283×10^{-6}

25	1.460×10^{-1}	1.533×10^{-2}	3.819×10^{-4}	1.419×10^{-6}
26	1.510×10^{-1}	1.612×10^{-2}	4.109×10^{-4}	1.567×10^{-6}
27	1.560×10^{-1}	1.694×10^{-2}	4.414×10^{-4}	1.727×10^{-6}
28	1.610×10^{-1}	1.778×10^{-2}	4.736×10^{-4}	1.899×10^{-6}
29	1.650×10^{-1}	1.865×10^{-2}	5.074×10^{-4}	2.086×10^{-6}
30	1.700×10^{-1}	1.954×10^{-2}	5.431×10^{-4}	2.288×10^{-6}
31	1.750×10^{-1}	2.045×10^{-2}	5.806×10^{-4}	2.505×10^{-6}
32	1.800×10^{-1}	2.139×10^{-2}	6.200×10^{-4}	2.739×10^{-6}
33	1.850×10^{-1}	2.235×10^{-2}	6.613×10^{-4}	2.991×10^{-6}
34	1.890×10^{-1}	2.334×10^{-2}	7.048×10^{-4}	3.263×10^{-6}
35	1.940×10^{-1}	2.436×10^{-2}	7.503×10^{-4}	3.555×10^{-6}
36	1.990×10^{-1}	2.540×10^{-2}	7.981×10^{-4}	3.868×10^{-6}
37	2.040×10^{-1}	2.647×10^{-2}	8.482×10^{-4}	4.204×10^{-6}
38	2.090×10^{-1}	2.756×10^{-2}	9.007×10^{-4}	4.565×10^{-6}
39	2.140×10^{-1}	2.868×10^{-2}	9.556×10^{-4}	4.952×10^{-6}
40	2.190×10^{-1}	2.984×10^{-2}	1.013×10^{-3}	5.366×10^{-6}
41	2.240×10^{-1}	3.101×10^{-2}	1.073×10^{-3}	5.809×10^{-6}
42	2.300×10^{-1}	3.222×10^{-2}	1.136×10^{-3}	6.284×10^{-6}
43	2.350×10^{-1}	3.346×10^{-2}	1.202×10^{-3}	6.791×10^{-6}
44	2.400×10^{-1}	3.472×10^{-2}	1.271×10^{-3}	7.332×10^{-6}
45	2.450×10^{-1}	3.602×10^{-2}	1.342×10^{-3}	7.910×10^{-6}
46	2.500×10^{-1}	3.734×10^{-2}	1.417×10^{-3}	8.527×10^{-6}
47	2.550×10^{-1}	3.869×10^{-2}	1.495×10^{-3}	9.185×10^{-6}
48	2.610×10^{-1}	4.008×10^{-2}	1.577×10^{-3}	9.886×10^{-6}
49	2.660×10^{-1}	4.149×10^{-2}	1.661×10^{-3}	1.063×10^{-5}
50	2.710×10^{-1}	4.294×10^{-2}	1.750×10^{-3}	1.143×10^{-5}

Table A.2: Conditional probability data obtained by FORM for 50 years, for $P_{3/1}$, $P_{3/4}$, $P_{3/5}$ and P_3.

n	7	7	7	7
$\alpha_i*inc_{i/j}$	0.21	0.18	0.165	0.15
t/i	$P_{6/5}$	$P_{5/4}$	$P_{5/3}$	P_5
1	6.376×10^{-2}	1.245×10^{-4}	5.650×10^{-7}	3.122×10^{-10}
2	6.376×10^{-2}	1.245×10^{-4}	5.650×10^{-7}	3.122×10^{-10}
3	6.376×10^{-2}	1.245×10^{-4}	5.650×10^{-7}	3.122×10^{-10}
4	6.376×10^{-2}	1.245×10^{-4}	5.650×10^{-7}	3.122×10^{-10}
5	6.376×10^{-2}	1.245×10^{-4}	5.650×10^{-7}	3.122×10^{-10}
6	6.376×10^{-2}	1.245×10^{-4}	5.650×10^{-7}	3.122×10^{-10}
7	6.376×10^{-2}	1.245×10^{-4}	5.650×10^{-7}	3.122×10^{-10}
8	6.376×10^{-2}	1.245×10^{-4}	5.650×10^{-7}	3.122×10^{-10}
9	9.399×10^{-2}	2.749×10^{-4}	1.588×10^{-6}	1.148×10^{-9}
10	9.980×10^{-2}	3.118×10^{-4}	1.874×10^{-6}	1.416×10^{-9}
11	1.054×10^{-1}	3.499×10^{-4}	2.181×10^{-6}	1.717×10^{-9}
12	1.108×10^{-1}	3.895×10^{-4}	2.513×10^{-6}	2.056×10^{-9}
13	1.162×10^{-1}	4.310×10^{-4}	2.873×10^{-6}	2.437×10^{-9}
14	1.215×10^{-1}	4.745×10^{-4}	3.262×10^{-6}	2.866×10^{-9}

15	1.267×10^{-1}	5.201×10^{-4}	3.685×10^{-6}	3.348×10^{-9}
16	1.320×10^{-1}	5.681×10^{-4}	4.144×10^{-6}	3.888×10^{-9}
17	1.372×10^{-1}	6.186×10^{-4}	4.640×10^{-6}	4.493×10^{-9}
18	1.424×10^{-1}	6.716×10^{-4}	5.178×10^{-6}	5.170×10^{-9}
19	1.476×10^{-1}	7.274×10^{-4}	5.759×10^{-6}	5.925×10^{-9}
20	1.528×10^{-1}	7.860×10^{-4}	6.387×10^{-6}	6.765×10^{-9}
21	1.580×10^{-1}	8.476×10^{-4}	7.065×10^{-6}	7.700×10^{-9}
22	1.633×10^{-1}	9.123×10^{-4}	7.796×10^{-6}	8.738×10^{-9}
23	1.685×10^{-1}	9.801×10^{-4}	8.584×10^{-6}	9.889×10^{-9}
24	1.738×10^{-1}	1.051×10^{-3}	9.432×10^{-6}	1.116×10^{-8}
25	1.791×10^{-1}	1.126×10^{-3}	1.034×10^{-5}	1.257×10^{-8}
26	1.844×10^{-1}	1.204×10^{-3}	1.132×10^{-5}	1.413×10^{-8}
27	1.897×10^{-1}	1.286×10^{-3}	1.237×10^{-5}	1.584×10^{-8}
28	1.950×10^{-1}	1.372×10^{-3}	1.350×10^{-5}	1.773×10^{-8}
29	2.004×10^{-1}	1.462×10^{-3}	1.471×10^{-5}	1.981×10^{-8}
30	2.058×10^{-1}	1.556×10^{-3}	1.600×10^{-5}	2.209×10^{-8}
31	2.111×10^{-1}	1.654×10^{-3}	1.739×10^{-5}	2.459×10^{-8}
32	2.166×10^{-1}	1.757×10^{-3}	1.887×10^{-5}	2.734×10^{-8}
33	2.220×10^{-1}	1.864×10^{-3}	2.045×10^{-5}	3.034×10^{-8}
34	2.274×10^{-1}	1.975×10^{-3}	2.213×10^{-5}	3.363×10^{-8}
35	2.329×10^{-1}	2.092×10^{-3}	2.393×10^{-5}	3.722×10^{-8}
36	2.384×10^{-1}	2.214×10^{-3}	2.585×10^{-5}	4.115×10^{-8}
37	2.439×10^{-1}	2.340×10^{-3}	2.789×10^{-5}	4.543×10^{-8}
38	2.494×10^{-1}	2.473×10^{-3}	3.007×10^{-5}	5.009×10^{-8}
39	2.550×10^{-1}	2.610×10^{-3}	3.238×10^{-5}	5.517×10^{-8}
40	2.605×10^{-1}	2.753×10^{-3}	3.484×10^{-5}	6.070×10^{-8}
41	2.661×10^{-1}	2.902×10^{-3}	3.745×10^{-5}	6.671×10^{-8}
42	2.717×10^{-1}	3.057×10^{-3}	4.022×10^{-5}	7.324×10^{-8}
43	2.772×10^{-1}	3.218×10^{-3}	4.316×10^{-5}	8.033×10^{-8}
44	2.829×10^{-1}	3.385×10^{-3}	4.629×10^{-5}	8.802×10^{-8}
45	2.885×10^{-1}	3.559×10^{-3}	4.959×10^{-5}	9.635×10^{-8}
46	2.941×10^{-1}	3.739×10^{-3}	5.310×10^{-5}	1.054×10^{-7}
47	2.998×10^{-1}	3.927×10^{-3}	5.681×10^{-5}	1.151×10^{-7}
48	3.054×10^{-1}	4.121×10^{-3}	6.074×10^{-5}	1.257×10^{-7}
49	3.111×10^{-1}	4.322×10^{-3}	6.489×10^{-5}	1.371×10^{-7}
50	3.167×10^{-1}	4.531×10^{-3}	6.928×10^{-5}	1.495×10^{-7}

Table A.3: Conditional probability data obtained by FORM for 50 years, for $P_{6/5}$, $P_{5/4}$, $P_{5/3}$ and P_5.

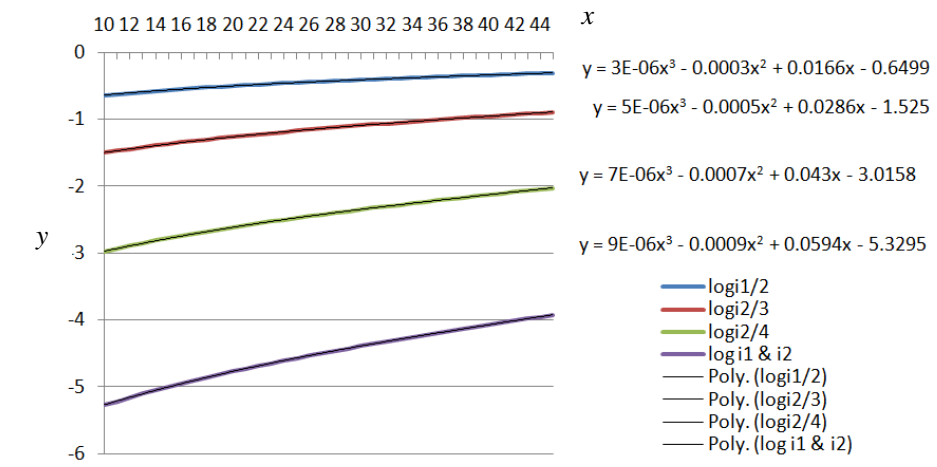

Figure A.4: Regression formula for $P_{1/2}$, $P_{2/3}$, $P2_{/4}$, P_1 and P_2.

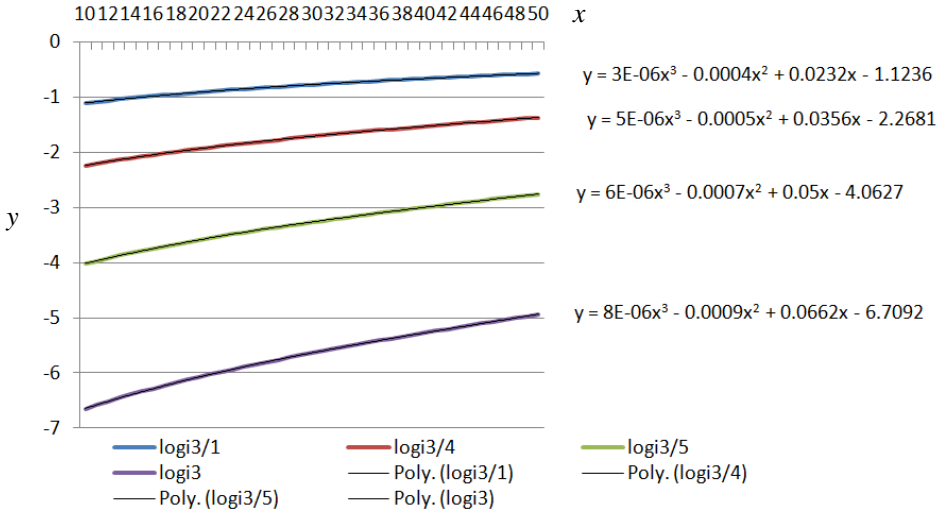

Figure A.5: Regression formula for $P_{3/1}$, $P_{3/4}$, $P_{3/5}$ and P_3.

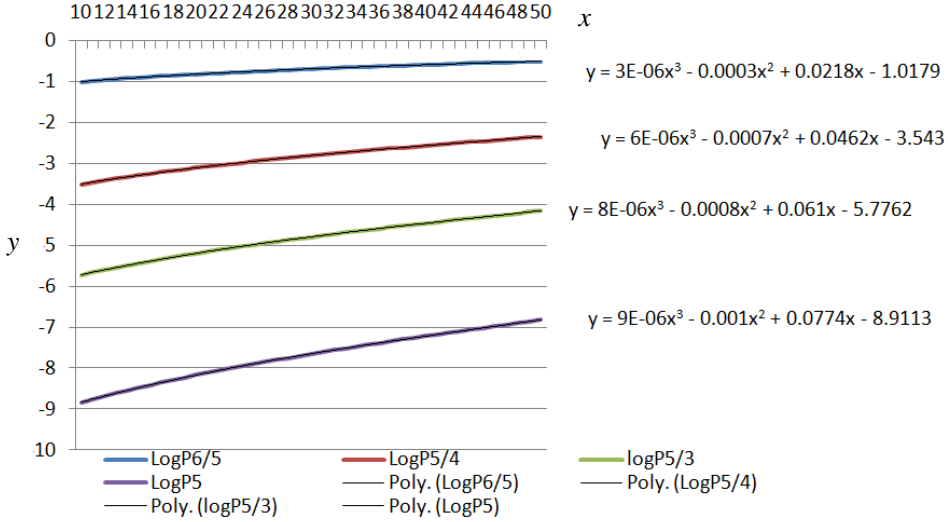

Figure A.6 : Regression formula for $P_{6/5}$, $P_{5/4}$, $P_{5/3}$ and P_5.